Vol. 109 No. 1, August 1, 1979

ISSN 0003-2670

ANALYTICA CHIMICA ACTA

International journal devoted to all branches of analytical chemistry

ELSEVIER SCIENTIFIC PUBLISHING COMPANY

ANALYTICA CHIMICA ACTA

International journal devoted to all branches of analytical chemistry
Revue internationale consacrée à tous les domaines de la chimie analytique
Internationale Zeitschrift für alle Gebiete der analytischen Chemie

PUBLICATION SCHEDULE FOR 1979 (incorporating the section on Computer Techniques and Optimization).

	J	F	M	A	M	J	J	A	S	O	N	D
Analytica Chimica Acta	104/1	104/2	105	106/1	106/2	107	108	109/1	109/2	110/1	110/2	111
Section on Computer Techniques and Optimization			112/1			112/2			112/3			112/4

Scope. *Analytica Chimica Acta* publishes original papers, short communications, and reviews dealing with every aspect of modern chemical analysis, both fundamental and applied. The section on *Computer Techniques and Optimization* is devoted to new developments in chemical analysis by the application of computer techniques and by interdisciplinary approaches, including statistics, systems theory and operation research. The section deals with the following topics: Computerized acquisition, processing and evaluation of data. Computerized methods for the interpretation of analytical data including chemometrics, cluster analysis, and pattern recognition. Storage and retrieval systems. Optimization procedures and their application. Automated analysis for industrial processes and quality control. Organizational problems.

Submission of Papers. Manuscripts (three copies) should be submitted to:
for *Analytica Chimica Acta:* Dr. A. M. G. Macdonald, Department of Chemistry, The University, P.O. Box 363, Birmingham B15 2TT, England;
for the section on *Computer Techniques and Optimization:* Dr. J. T. Clerc, Universität Bern, Pharmazeutisches Institut, Sahlistrasse 10, CH-3012 Bern, Switzerland.

Information for Authors. Papers in English, French and German are published. There are no page charges. Manuscripts should conform in layout and style to the papers published in this Volume. Authors should consult Vol. 102, p. 253 for detailed information. Reprints of this information are available from the Editors or from: Elsevier Editorial Services Ltd., Mayfield House, 256 Banbury Road, Oxford OX2 7DE (Great Britain).

Reprints. Fifty reprints will be supplied free of charge. Additional reprints (minimum 100) can be ordered. An order form containing price quotations will be sent to the authors together with the proofs of their article.

Advertisements. Advertisement rates are available from the publisher.

Subscriptions. Subscriptions should be sent to: Elsevier Scientific Publishing Company, P.O. Box 211, 1000 AE Amsterdam, The Netherlands. The section on *Computer Techniques and Optimization* can be subscribed to separately.

Publication. *Analytica Chimica Acta* (including the section on *Computer Techniques and Optimization*) appears in 9 volumes in 1979. The subscription for 1979 (Vols. 104–112) is Dfl. 1179.00 plus Dfl. 135.00 (postage) (total approx. U.S. $641.00). The subscription for the *Computer Techniques and Optimization* section only (Vol. 112) is Dfl. 131.00 plus Dfl. 15.00 (postage) (total approx. U.S. $71.00). Journals are sent automatically by air mail to the U.S.A. and Canada at no extra cost and to Japan, Australia and New Zealand for a small additional postal charge. All earlier volumes (Vols. 1–95) except Vols. 23 and 28 are available at Dfl. 144.00 (U.S. $70.00), plus Dfl. 10.00 (U.S. $5.00) postage and handling, per volume.

Claims for issues not received should be made within three months of publication of the issue, otherwise they cannot be honoured free of charge.

Customers in the U.S.A. and Canada who wish to obtain additional bibliographic information on this and other Elsevier journals should contact Elsevier/North Holland Inc., Journal Information Center, 52 Vanderbilt Avenue, New York, NY 10017. Tel: (212) 867-9040.

ANALYTICA CHIMICA ACTA
VOL. 109 (1979)

ANALYTICA CHIMICA ACTA

International journal devoted to all branches of analytical chemistry

ELSEVIER SCIENTIFIC PUBLISHING COMPANY

Anal. Chim. Acta, Vol. 109 (1979)

Printed in The Netherlands

Analytica Chimica Acta, 109 (1979) 1—24

INJECTION TECHNIQUES IN DYNAMIC FLOW-THROUGH ANALYSIS WITH ELECTROANALYTICAL SENSORS

ERNŐ PUNGOR*, ZSÓFIA FEHÉR, GÉZA NAGY, KLÁRA TÓTH, GYÖRGY HORVAI and MIKLÓS GRATZL

Institute for General and Analytical Chemistry, Technical University, H-1111 Budapest (Hungary)

(Received 15th January 1979)

SUMMARY

The theoretical and practical aspects of injection techniques used in flow-through systems with ion-selective electrodes and voltammetric detectors are discussed. Mathematical descriptions of the measuring systems based on the use of mixing chambers in the analytical channel are briefly outlined. The effects of different parameters on the analytical signals are described theoretically and experimentally. The methods developed for the evaluation of the analytical signals are presented in detail.

Applications of electroanalytical detectors in flowing systems are not new, but have recently achieved special importance. Numerous important analytical tasks can easily be done by measurements in streaming solution. Thus, for example, in monitors or monitoring systems, recycling or by-pass circuits are often used to ensure continuous sampling, and measurements can be simplified in various fields of analytical chemistry. Undoubtedly, the general introduction of flow-through analytical methods has been promoted by the fact that modern instruments widely used for serial analyses are mostly based on the flow-through channel principle. The predominant position of high-performance flow-through analyzers incorporating electroanalytical detectors is not jeopardized by the appearance of serial analyzers based on other principles (e.g., centrifugal analyzers), which offer remarkable advantages in some respects, as these systems generally cannot be equipped with electroanalytical detectors.

The adaptation of electroanalytical techniques to flowing systems offers special advantages, but may also involve special difficulties. In particular, with potentiometric and voltammetric detectors, the signal developed results from a heterogeneous reaction at the solution—electrode interface which involves certain transport processes. Obviously, the relative movement of the electrode and the solution affects the transport, and thus, may also influence the behaviour of the electrode.

The use of potentiometric detectors in flowing solutions offers the following main advantages. First, as the sample in contact with the electrode surface is moving continuously, the electrode does not influence the sample concen-

tration. Secondly, as the diffusion layer established at the electrode surface is thinner owing to the convection, the response time and the sensitivity of the electrode are often improved. Thirdly, the reference electrode is usually placed downstream from the indicator electrode, so that the ionic species of the reference electrode do not influence the response of the indicator. Finally, reference electrodes with flowing inner solutions can easily be employed to overcome problems arising from alterations of the liquid junction potential. The formation of the potentiometric signal is based, in general, on dynamic equilibrium reactions, thus the magnitude of the signal is independent of the rate of the transport process. Accordingly, the flow rate affects only the transient signal produced at rapid concentration changes. The use of potentiometric sensors in flow-through analysis is greatly facilitated by the fact that electrodes can be produced in widely different sizes and shapes. Simple flow-through measuring cells can easily be constructed for use with commercially available electrodes, such as micro-capillary and flow-through cap electrodes. Difficulties may arise in the case of narrow conduits: insufficient conductivity may cause a significant streaming potential which leads to errors in the potential measurements especially in the case of non-uniform flow (e.g. with peristaltic pumps).

With voltammetric sensors, the signal, i.e. the current intensity, depends on the rate of mass transport to the electrode surface; thus, under suitable hydrodynamic conditions, the signals in streaming solutions may reach considerably higher values than in stationary solutions, giving a remarkable increase in sensitivity. A further advantage is that the noise is smaller under the conditions of convective diffusion. In voltammetry in streaming solution, the current is usually measured at constant potential, thus not only is there a reduction in the interfering effect of the residual current, which is due to time-dependent surface reactions and the charging current of the surface double layer, but measurements of the current and the electrical or electrochemical compensation of the residual current are simplified. Because of all these factors, the lower limit of detection can be decreased remarkably. The sensitivity of hydrodynamic voltammetry as a measuring technique in streaming solutions at constant electrode potential can be compared with that of the most sensitive electroanalytical techniques.

The advantages offered by the conditions of convective diffusion are, of course, often utilized in voltammetry in stationary solutions, e.g. at rotating disc electrodes. One of the most critical problems in the use of voltammetric sensors in flowing systems is that constancy of the active electrode surface must be ensured if reproducible results are to be obtained; reproducible renewal of the electrode surface is more difficult in a flow-through channel than under stationary conditions. Another important point is that the conditions of convective diffusion at the electrode surface must be kept strictly constant if signals are to be reproducible, as the signal depends on the rate of mass transport.

The general scheme of a serial analyzer based on the flow-through principle is as follows. The sample is carried to the detector by a carrier solution streamed at constant rate. The analysis channel contains facilities for sample

introduction, sample transport, sample treatment and detection. The carrier solution not only enables samples of small volumes to be analyzed, but can be used to adjust the sample to appropriate physical and chemical condition. Analyses can be based on two different principles: (a) steady-state signals produced after the sample and the carrier solution have been mixed and possible reactions have taken place, or (b) dynamic signals as in the case of continuous flow techniques with sample injection.

Where dynamic signals are to be related to analyte concentrations, a well-defined, reproducible concentration profile at the detector cell is essential, and this can be achieved in different ways. The most important condition for reliability is that the concentration profile set up in the analysis channel after sample introduction should depend solely on the amount or concentration of the analyte in the sample. Among the most important factors influencing the concentration profile are viscosity, specific gravity and temperature.

Several workers have found that the concentration profile produced by injecting the sample into the carrier solution depends on the viscosity of the sample. To eliminate the resulting errors, Betteridge and Růžička [19] suggested the use of standards with viscosities equal to those of the samples. The problem here is that the suggestion is difficult to realize in practice, as it is not easy to determine the viscosity of very small samples. Moreover, there may be differences in the viscosities of the samples.

With samples of different origin, the specific gravity may also differ, in certain types of analysis channel, this may cause differences in the dispersion profile. This effect can become important if the specific gravity of the samples differs markedly from that of the carrier solution, and if the conduit of the carrier stream is of small internal diameter. Finally, the effects of temperature are complex, but temperature differences can certainly change concentration profiles.

If the concentration profile prevailing in the detector cell is to provide unambiguous information on the analyte concentration, a suitable means of sample introduction is needed. This can be ensured by using either a unit that gives a constant rate of sample introduction, or a system in which the sample mass flow is not strictly constant but the effect of differences in sample introduction is eliminated or reduced by suitable construction of the analysis channel. Obviously, well-defined reproducible concentration profiles in the carrier stream can be expected only if the hydrodynamic conditions remain constant within experimental error during the time of analysis. The main problem here arises from inconstancy of flow rate.

The concentration profile formed in the analysis channel is followed by a suitable detector, the characteristics of which may make special demands on the nature of the profile. If an integrating detector (e.g. spectrophotometric) is used, the homogeneity of the solution in the direction perpendicular to the flow is not very important. With a non-integrating detector which follows the concentration profile at a single point in the channel, the profile must also be reproducible in the direction perpendicular to the flow. This is most easily done by ensuring homogeneity of the solution in the cross-section of the detector cell. The signals from voltammetric and potentiometric detectors are

determined solely by the analyte concentration in the solution layer in contact with the electrode, i.e. these sensors are non-integrating. Accordingly, the proper dimensioning, construction and positioning of electroanalytical detectors in flow-through channels is important; experience gained with spectrophotometric detectors is essentially irrelevant in this respect. For example, whereas a flow-through spectrophotometric cell has a certain averaging capacity, potentiometric sensors give a mixed potential which is not characteristic of the average concentration of the solution if different points of the electrode surface are in contact with solutions of different ion activities [2]. Accordingly, it is advisable to use detectors whose surface area is small in the direction of the flow. Moreover, reproducible signals will be obtained only if the electroanalytical cell is constructed in such a way that the concentration profile in the channel is unaffected.

FLOW-THROUGH-SYSTEM DEVELOPED FOR INJECTION ANALYSIS

The apparatus developed about ten years ago in these laboratories [1] is simple in construction and is suitable for serial analysis of small volumes of samples. Various potentiometric and voltammetric sensors have been incorporated into the system for numerous applications [3—13]. A diagram of a

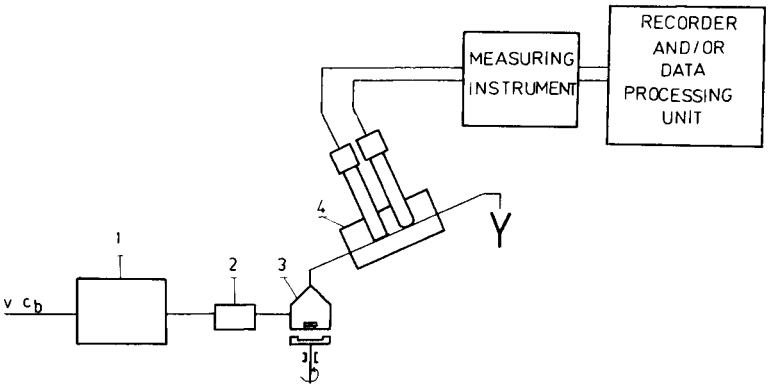

Fig. 1. Flow-through system for carrying out injection measurements. (1) Peristaltic pump; (2) injector section; (3) mixing chamber; (4) detector cell.

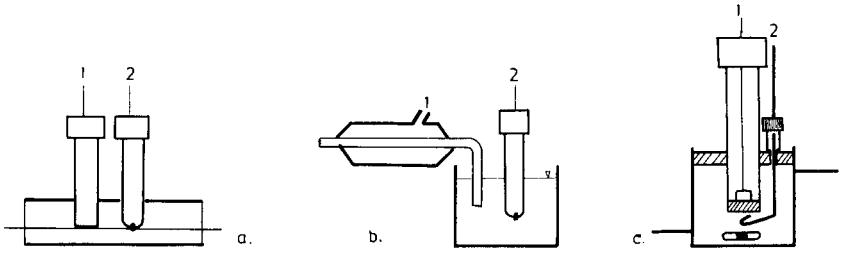

Fig. 2. Different flow-through detectors employed. (a) Flow-through tube cell incorporating the indicator and reference electrodes; (b) micro-capillary indicator electrode (Radelkis) with reference electrode placed downstream; (c) indicator electrode (sensitized electrode) placed in the mixing chamber.

representative apparatus is shown in Fig. 1. A solution of suitable composition is continuously pumped through the analysis channel at a constant rate by a peristaltic pump. The solution reaches the injector section, where samples are introduced, and then passes through a mixing chamber and a potentiometric or voltammetric flow-through detector, the electrodes of which are connected to an appropriate measuring instrument and a recorder. Figure 2 shows some typical detector cells. Samples can be injected into the carrier stream by Hamilton syringes through rubber caps or septa or introduced by constant-volume or variable-volume valves in the now conventional manner. Different sizes and forms of the general apparatus can be constructed for particular analytical purposes.

The mixing chamber is an important feature of the general construction of the apparatus. Various flow-through systems have been constructed in other laboratories [14—21] which differ from the system described here. Most of these do not include a mixing chamber with mechanical stirring. The favourable experience reported with these devices, as well as the fact that the mixing chamber has a hold-up effect and other unfavourable properties, makes inclusion of the mixing chamber questionable. However, these chambers offer distinct advantages, despite some suggestions and experimental findings which favour their elimination. The mixing rod, driven externally, homogenizes the solution in the mixing chamber. The intensity of stirring is such that the concentration profile in the analysis channel is basically determined by the dispersion produced in the mixing chamber. This offers a number of advantages. For example, in the case of samples with different viscosities, the small differences in dispersion in the channel are leveled by the stirrer; at suitable stirring rates, the dispersion conditions in the mixer are independent of the viscosity of the solution entering the mixer. Similarly, the effects of differences in specific gravity, temperature, detergent content, etc., of the samples on the concentration profile can be remarkably reduced.

The effects of differences in the viscosity of samples on the shape of signal obtained after sample injection for apparatus without and with a mixing chamber are shown in Fig. 3. For these tests, equal volumes of a potassium chloride solution were injected and the e.m.f. of the measuring cell incorporating a chloride-selective electrode was recorded. Differences in viscosity were produced by adding glycerol. Figure 3 clearly shows that the peaks are markedly affected by as little as 2% glycerol if no mixing is employed, whereas if a 1-ml mixing chamber is inserted, there is no appreciable difference between the peaks for samples with and without glycerol. Similar effects can be seen in Fig. 4 for the addition of a surfactant (Brij 35).

An additional advantage offered by mixing chambers is that differences in signals caused by variations in injection rates are reduced. Thus even manual injection can be used, and there is no need for sophisticated injection devices to provide adequate accuracy and reproducibility.

The solution leaving the mixing chamber is homogeneous in the direction perpendicular to the flow, which is of basic importance from the point of view of electroanalytical detection.

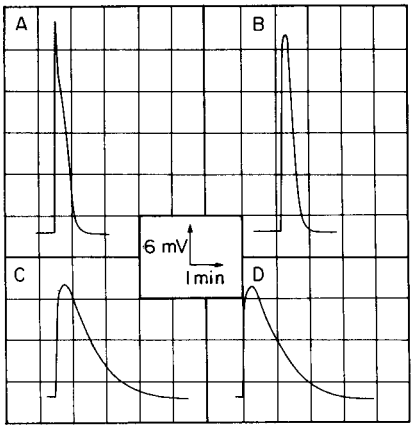

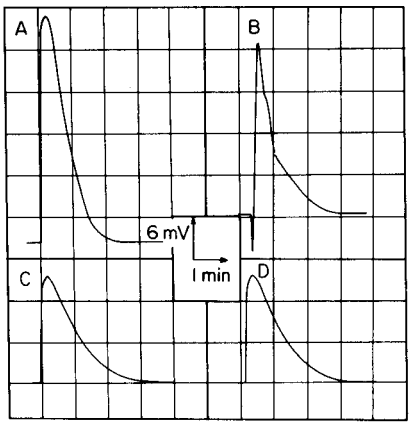

Fig. 3. Injection peaks obtained with samples of different viscosities. Peaks A and C are for 10^{-2} M KCl—2% glycerol, and peaks B and D for 10^{-2} M KCl. A and B, without mixing chamber; C and D with mixing chamber.

Fig. 4. Injection peaks obtained with 10^{-2} M KCl samples in the absence (peaks A and C) and presence (peaks B and D) of a surfactant (2% Brij 35) without (peaks A and B) and with (peaks C and D) a mixing chamber.

The composition of the flowing solution is of great importance, for the concentration profile reflects any changes in the ratio of the volume of the carrier solution to that of the sample. If the carrier contains components important from the point of view of the detection, this volume ratio should not be changed appreciably in favour of the sample at any point. A mixing chamber of appropriate volume inserted in the flow system allows well-defined control of the mixing ratio. Moreover, mixing with a pH- and ionic strength-adjusting buffer, background electrolyte or reagent in a defined controllable ratio is ensured. Appropriate choice of the volume of the mixing chamber makes it possible to adjust the concentration profile to an optimal configuration for measurement. Dilution of the sample is often advantageous, so as to reduce the concentration of interfering components or insoluble particles.

Changing the volume of the mixing chamber makes it possible to adjust the time of contact of the sample with the detector, so that even electrodes with slow response (enzyme electrodes, membrane-covered gas electrodes) can be used as detectors. The results of ammonia determinations by the injection technique with an ammonia gas electrode with and without insertion of a mixing chamber are shown in Fig. 5; otherwise the apparatus and sample were identical. It can be seen that the signals obtained with the mixing chamber are much greater, although the maximum concentration within the profile must obviously be much higher when the mixing chamber is omitted.

After this survey of the obvious advantages afforded by the use of mixing chambers, it should be noted that systems without these chambers are also of value for certain analytical tasks, especially if an integrating-type detector

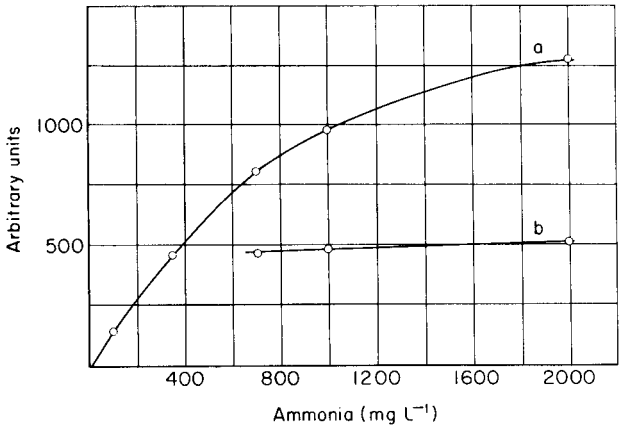

Fig. 5. Calibration curves for an ammonia probe (EIL) obtained by injecting samples into a flow-through system: (a) with mixing chamber; (b) without mixing chamber. Flowing solution, 2.5 mg NH_4Cl l^{-1}—10^{-1} M NaOH; flow rate, 2.8 ml min^{-1}; chamber volume, 1.4 ml.

is used. However, the introduction of a mixing chamber remarkably simplifies the construction of an apparatus for injection analysis, without detriment to the required accuracy and reproducibility. Obviously, these systems allow a lower rate of analysis, but analysis of very similar samples (equal viscosity, specific gravity, etc.) at a rate of 400 analyses per hour is relatively rarely needed in an analytical laboratory.

THEORETICAL BACKGROUND

In all these measurements, small volumes of sample are introduced plug-like into the carrier solution streaming at a constant rate. The concentration profile established in the flow stream can be described on the basis of the concentration conditions prevailing in the mixing chamber, provided that the dispersion characteristics of the system are basically determined by the mixing chamber, i.e., there is no concentration gradient in the direction of flow within the plug of solution injected, and the sample and carrier solution are homogenized in the mixing chamber instantaneously and completely. Accordingly, the concentration of a substance in the mixing chamber, under suitable conditions in the analysis channel, can be described as a function of time by

$$d\Delta c_t/dt = (V/W)\,[\Delta(c_s)_t - \Delta c_t] \qquad (1)$$

if $\Delta(c_s)_t = M/V\tau$ at $t \leqslant \tau$ and $\Delta(c_s)_t = 0$ at $t > \tau$. Here, t is the time (s) from the moment of injection; $\Delta c_t = c_t - c_0$; c_t is the actual analyte concentration at time t; $(c_s)_t$ is the concentration difference between the carrier stream and the solution carrying the injected sample, on entry into the mixing chamber; c_0 is the analyte concentration in the carrier stream before injection of solution; V is the flow rate (ml min^{-1}); W is the volume of the

mixing chamber; M is the mass of sample injected (i.e., the product of the concentration and volume of the sample); and τ is the time needed by the plug of injected solution to pass through the entrance of the mixing chamber. If dispersion in the flow stream to that point is negligible, this time is equal to the time taken for the actual injection.

From eqn. (1), the concentration change in the carrier stream at any moment after sample injection can be expressed by the following equations:

$$\Delta c_t = (M/V\tau)\,[1 - \exp(-Vt/W)] \text{ at } 0 \leqslant t < \tau \tag{2}$$

$$\Delta c_t = (M/V\tau)\,[1 - \exp(-V\tau/W)]\exp(-V(t-\tau)/W)\,] \text{ at } t \geqslant \tau \tag{3}$$

The detector signal can readily be expressed if the response time is small, provided that the signal vs. concentration relationship is known. For example, for potentiometric detection with an ion-selective electrode sensitive to the substance injected, the change in the electrode potential as a function of time can be described at time $0 \leqslant t < \tau$ by

$$\Delta E_t = S \ln \left\{1 + [M/V\tau]\,[1 - \exp(-Vt/W)]/\left[c_0 + \sum_{i=0}^{n} K_i c_i\right]\right\} \tag{4}$$

and at time $t \geqslant \tau$ by

$$\Delta E_t = S \ln \left\{1 + [M/V\tau]\,[1 - \exp(-V\tau/W)]\exp(-V(t-\tau)/W)/\left[c_0 + \sum_{i=1}^{n} K_i c_i\right]\right\} \tag{5}$$

where K_i is the selectivity coefficient and c_i is the concentration of an interfering ion in the carrier solution.

When a voltammetric detector cell is used, the concentration of the component injected is followed by measuring the voltammetric current at a suitable constant electrode potential. For the voltammetric detector used here, the relationship between the current measured at constant potential and the concentration is linear. The actual form of the equation describing this relationship depends on the hydrodynamic conditions prevailing in the cell. For a disc electrode with a surface area of a few mm^2 placed in the stream parallel to the direction of flow, the current can be described at time $0 \leqslant t < \tau$ by

$$i_t = (KM/V\tau)\,[a + V^{1/2}]\,[1 - \exp(-Vt/W)] \tag{6}$$

and at time $t \geqslant \tau$ by

$$i_t = (KM/V\tau)\,[a + V^{1/2}]\,[1 - \exp(-V\tau/W)]\,[\exp(-V(t-\tau)/W)] \tag{7}$$

where K and a are constants involving the electrochemical and hydrodynamic parameters of the system.

The validity of the potential and current equations derived has been checked in two ways [22]. First, experimental electrode potential vs. time and current vs. time curves were compared with the corresponding theoretical curves, which were calculated by inserting the parameters determined in separate experiments into eqns. (4) and (5) or (6) and (7) (Figs. 6 and 7). Secondly,

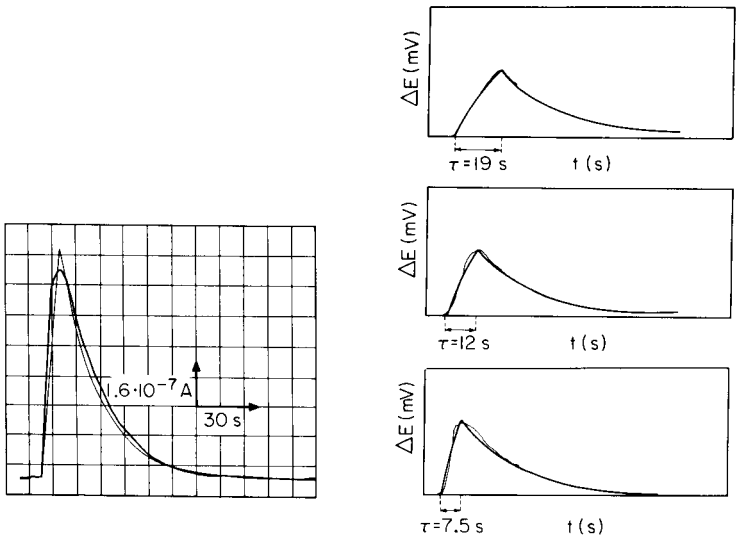

Fig. 6. Voltammetric injection peaks obtained by calculation from the model expressed by eqns. (1—3), indicated by the thin smooth line, and by experiment (thicker line). W = 3.2 ml; V = 0.2 ml s^{-1}; τ = 9 s; K = 2.88; $M = 5 \times 10^{-6}$ mol; a = 0.20. Carrier solution 0.5 M KCl; solution injected $K_4Fe(CN)_6$; applied potential +0.7 V.

Fig. 7. Potentiometric injection peaks obtained by calculation from the model expressed by eqns. (1—3) indicated by thick smooth lines, and by experiment (thin lines) for different values of τ. $c_0 = 10^{-4}$ M $AgNO_3$—10^{-1} M KNO_3; $M = 6.75 \times 10^{-8}$ mol Ag^+; S = 58 mV; V = 0.13 ml s^{-1}; W = 2.7 ml.

the dependence of the characteristic parameters (see later) of the potentiometric and voltammetric peak signals on the factors included in the equations (flow rate, volume of mixing chamber, time of injection, concentration) was studied theoretically and experimentally. The relationship between the peak current and time of injection, and the dependence of the potentiometric peak height on the flow rate, are shown in Figs. 8 and 9 as examples.

In general, the agreement of the theoretical and experimental curves was good, which indicates that the assumptions used in deriving the theoretical equations approach reality closely. In comparing the experimental and theoretical curves, better agreement was generally obtained if not the geometric volume of the mixing chamber (W) but a value slightly exceeding it (W_{eff}) was used in the calculations. The reason for this might be that the stirring is not restricted to the mixing chamber but extends to the preceding and succeeding portions of the channel. Experimental curves are compared with theoretical ones obtained by fitting with respect to the volume of mixing chamber in Fig. 10.

The simple model and the corresponding equations gradually lapse if the time of sample introduction is reduced below about 3 s or if the tubing be-

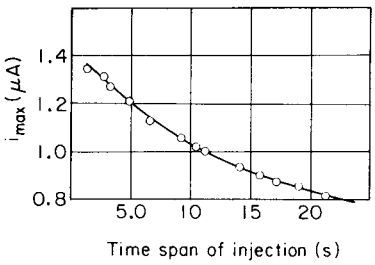

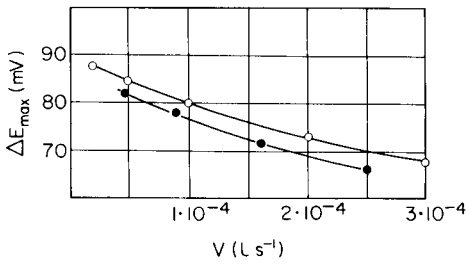

Fig. 8. Relationship between voltammetric peak heights and the time span of the injection. $M = 5 \times 10^{-6}$ mol; $V = 0.09$ ml s^{-1}. Carrier solution 0.5 M KCl; solution injected $K_4[Fe(CN)_6]$; applied potential +0.7 V.

Fig. 9. Relationship between the potentiometric peak height and the flow rate of the carrier solution. The conditions were as described in Fig. 7 apart from flow rate and mixer volume (2.1 ml). (○) Calculated; (•) measured.

tween the mixing chamber and detector is longer than about 2 cm. The simple model is not valid when the tube length between the mixing chamber and the point of detection exceeds 20 cm. As this may occur in practice, it was considered necessary to modify the above relationships to take into account any dispersion of the sample plug in the channel under the conditions mentioned. The derivation was started with eqn. (1), as in the previous case, with the difference that the generator function $\Delta(c_s)_t$ in differential eqn. (1) was replaced by a more complicated term to include dispersion effects. As dispersion is not solely due to molecular diffusion of the component injected, but also to longitudinal mixing, the relationship for $\Delta(c_s)_t$ cannot be derived simply from Fick's second law. This law can be applied only if the molecular diffusion coefficient is replaced by an effective diffusion coefficient (D_{eff}, dispersion coefficient) as in modelling chemical reactors [23].

If a sharp concentration profile is assumed, at the point of injection, the following relationship can be deduced from Fick's second law [24]:

$$\Delta(c_s)_t = \frac{M}{2\pi(D_{eff}t)^{1/2}} \exp\left[-\frac{1}{4D_{eff}}\left(\frac{L}{t^{1/2}} - \frac{Vt^{1/2}}{q}\right)^2\right] \tag{8}$$

where L is the length of tubing between the points of injection and detection, and q is the cross-section of the tube.

By inserting eqn. (8) into differential equation (1), the following relationship is obtained:

$$\frac{d\Delta c_t}{dt} = \frac{V}{W}\left\{\frac{M}{2q(\pi D_{eff}t)^{1/2}} \exp\left[-\frac{1}{4D_{eff}}\left(\frac{L}{t^{1/2}} - \frac{Vt^{1/2}}{q}\right)^2\right] - \Delta c(t)\right\} \tag{9}$$

Equation (9) cannot be solved for Δc_t by the standard methods of mathematical analysis, but there are several numerical methods for the computerized calculation of Δc_t. The simplest integration procedure is that of Euler [25], which can be applied to the present problem in the following form: $\Delta c_{t_0} = \Delta c_{t_1} = 0$ and for $i = 2, 3 \ldots n$

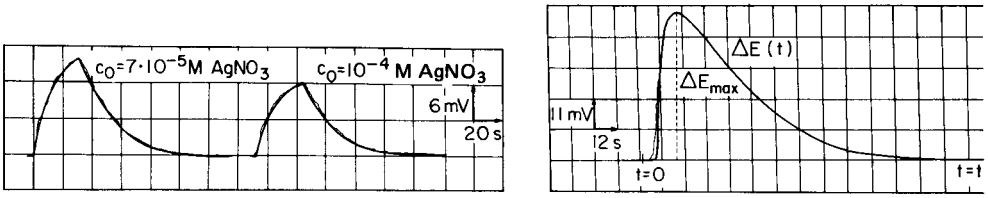

Fig. 10. Injection peaks obtained experimentally (—) and by calculation (—), fitting the volume of the mixing chamber for W_{eff} = 2.7 ml.

Fig. 11. Potentiometric injection peak obtained by calculation (—) and experimentally (—). $c_0 = 10^{-4}$ M KI; $M = 3 \times 10^{-6}$ mol; S = 58 mV; V = 0.13 ml s^{-1}; W = 2.7 ml; $D_{eff} = 3 \times 10^{-4}$ m^2 s^{-1}.

$$\Delta c_{t_i} = [(V/W)\ (c_s)_{t_{(i-1)}} + (1 - V/W)\ \Delta c_{t_{(i-1)}}]\ \Delta t_i \qquad (10)$$

where $\Delta t_i = t_i - t_{(i-1)}$.

The function $\Delta(c_s)_t$ is described by eqn. (8). At $t = t_n$, $\Delta c_{t_n} \cong 0$, which means that the concentration vs. time curve returns to the base line after the sample plug has passed through the detector. The Δc_t function can thus be obtained. The detector signal vs. time curve in which sample dispersion in the channel is taken into account can be calculated by inserting the Δc_t function into the equation describing the response of the detector.

A difficulty in the application of this model is that D_{eff} is not a simple physical constant defined by one process only, but a parameter which describes the simultaneous effects of several processes, such as molecular diffusion, convection, etc., and which depends on various factors, such as the cross-section of the analysis channel, flow rate and the microscopic properties of the injected and streaming solution. The easiest way of determining D_{eff} is to fit the model described by eqn. (9) to the experimental detector signal vs. time curves.

In Fig. 11, an experimental electrode potential vs. time curve is compared with the theoretical curve calculated for the model described by eqn. (9). In the experiment, a 20-cm tube (2.5 mm internal diameter) was inserted between the point of injection and the mixing chamber; a 50-µl sample was injected by means of a Hamilton syringe in about 1 s. The D_{eff} value used in the calculations was 3×10^{-4} m^2 s^{-1}. As shown by the fairly good agreement of the curves, the model can be used for describing the phenomena under the given experimental conditions.

ANALYTICAL ASPECTS OF THE INJECTION TECHNIQUE

Evaluation of the signals measured

The methods of evaluation of the signals will be treated separately for the voltammetric sensors giving linear response and the potentiometric sensors with logarithmic signal conversion. As can be seen from eqns. (4, 5) and (6, 7),

respectively, each point of the peak-type signal gives information about the amount of material injected into the flow stream. However, for such signals, the important characteristics for quantitative evaluation are the peak height and the peak area.

The appropriate correlations for the peak height when potentiometric and voltammetric sensors are used can easily be obtained from eqns. (4) and (6), since $\Delta E_t = \Delta E_{max}$ and $i_t = i_{max}$ for $t = \tau$. The area under the detector signal-time curve (T), i.e., the integral of the detector signal with time, can be derived simply for voltammetric detection:

$$T = (KM/V)\,(a + V^{1/2}) \tag{11}$$

With potentiometric detection, this cannot be obtained in an explicit form, but the peak area can still be used for determination of concentrations; a calibration technique or the result of a numerical iteration is used in this case.

If the injection peak is detected voltammetrically, then the peak height and the peak area are linear functions of the amount of material injected, and either can be used to quantify the results with the help of a calibration line or a numerical comparison, obtained by injection of appropriate standard solutions. Peak height is more easily measured than peak area, which requires integration of the signal, but electronic integrators and microprocessors simplify the area measurements. The higher costs are overcompensated by the advantage that the peak area — as opposed to peak height — is independent of the volume of the mixing chamber and of the duration of the injection process (eqns. 6 and 11). Small variations in the injection and the mixing process exert practically no influence on the peak area.

If the injection peak is detected by a potentiometric sensor, several methods of evaluation are available. The most important methods are as follows. Quantification can be based on peak height or peak area; the potentiometric signal can be used either as it was measured or after Gran transformation. Further, the potentiometric signal measured can be used for evaluation either relative to the signal measured in the background solution, i.e. relative to the base line, or relative to the instrument zero. Some of the techniques for evaluation discussed below require the plotting of a calibration line based on measurements with appropriate standards. In most cases, however, calibration with only one or two standards will suffice if the relationships discussed above are linearized.

The following discussion of evaluation is based on the equations:

$$\Delta E_t = S \log (c_0 + \Delta c_t)/c_0 \tag{12α}$$

if $c_0 \neq 0$, whereas if $c_0 = 0$ is also allowed, then

$$E_t = E^0 + S \log c_t \tag{12β}$$

These equations represent a more general form of eqns. (4) and (5) by applying the general expressions Δc_t and c_t, respectively, to describe the concentration peak caused by injection. Equation (12β) can be used if the signal is related

to the instrument zero, while eqn. (12α) is used if the signal is related to that measured in a carrier solution of concentration c_0; in the latter case, Δc_t is defined as $c_t - c_0$. These equations are, of course, valid only if the detector can promptly follow the changes in concentration. Further discussion will deal only with case α (signal measured relative to the base line); for case β the derivation is very similar, so that separate treatment is unnecessary.

Methods based on peak height (ΔE_{max}) measurement

ΔE_{max} is the maximum (or minimum) voltage measured relative to the base line, and depends on Δc_{max}, by analogy with eqn. (12α):

$$\Delta E_{max} = S \log (c_0 + \Delta c_{max})/c_0 \tag{13}$$

On the basis of the models discussed above, the sample amount injected (M) and Δc_{max} can be related by $\Delta c_{max} = kM$. The proportionality constant k is determined by the geometry of the experimental setup and the streaming conditions.

Direct calibration method. In order to obtain the correlation between ΔE_{max} and the amount of sample injected, $\Delta c_{max} = kM$ is inserted into eqn. (13) to give

$$\Delta E_{max} = S \log (c_0 + kM)/c_0 = S \log (1 + kM/c_0) \tag{14}$$

This can be linearized if $1 \ll kM/c_0$:

$$\Delta E_{max} \cong S \log kM/c_0 = S \log k/c_0 + S \log M \tag{15}$$

Thus a ΔE_{max} vs. log M plot will be linear if proper experimental conditions have been selected.

Methods based on Gran transformation

Gran transformation of eqn. (14) gives

$$10^{\Delta E_{max}/S} - 1 = kM/c_0 \tag{16}$$

Since M is directly proportional to the left-hand side of eqn. (16), either a linear calibration curve can be made, or a singlepoint calibration, i.e. calibration by a single standard injection becomes possible. If the amounts of standard and sample solutions injected are denoted by M_{st} and M_s, respectively, and the corresponding potential peak heights are denoted by $E_{max,\,st}$ and $E_{max,\,s}$, then eqn. (16) can be written for both standard and sample, and combination of these equations gives

$$M_s = M_{st} (10^{\Delta E_{max,\,s}/S} - 1)/(10^{\Delta E_{max,\,st}/S} - 1) \tag{17}$$

Thus, if S is known, M can be calculated. If k is also known, then no standard is needed, because M can be calculated directly from eqn. (16) after the obvious rearrangement. If k is known but S is not, then M can be calculated from eqn. (16) written for standard and sample injections, by an iteration procedure [26]. This means that the electrode need not be calibrated before the actual measurement is taken in the sample provided that all experimental conditions are correctly controlled.

Methods based on peak area measurement

Although peak area measurements require more sophisticated equipment, they are used quite often. The inherent advantages of peak area determination have already been indicated in the case of voltammetric detection. If potentiometric detection is used, somewhat different aspects have to be considered.

Evaluation based on the potentiometric peak area. The area under the potentiometric peak can be calculated from eqn. (12α) by integrating it over the time period 0 to t_n:

$$\int_0^{t_n} \Delta E_t \, dt = S \int_0^{t_n} \log [(c_0 + \Delta c_t)/c_0] \, dt \tag{18}$$

where t_n is the time span during which the concentration peak passes the detector. The relation between the amount of sample M and the function Δc_t is given by the generalized form $\Delta c_t = k_t M$, where k_t denotes a time function determined by the experimental setup which is independent of M. Combination of this equation with eqn. (18) does not yield a linear relationship between the potentiometric peak area — the left-hand side of eqn. (18) — and the amount of sample, M, or between any simple derived quantities of these components. Hence, only non-linear calibration curves can be plotted.

It may be realized that the model equations discussed earlier can be used to calculate M from eqn. (18) without calibration if all relevant conditions are properly controlled.

Evaluation based on the area of the Gran-transform of the potentiometric peak. Application of the Gran transformation to eqn. (12α) gives the following equation after integration:

$$\int_0^{t_n} 10^{\Delta E_t/S} \, dt = (1/c_0) \int_0^{t_n} \Delta c_t \, dt + t_n \tag{19}$$

The mass balance is expressed by

$$M = c_0 V \int_0^{t_n} \Delta c_t \, dt \tag{20}$$

and combination of these equations gives

$$\int_0^{t_n} 10^{\Delta E_t/S} \, dt = (M/Vc_0) + t_n \tag{21}$$

This equation means that there is a linear relationship between M and the area under the Gran-transformed peak. Thus, linear calibration curves can be plotted, in contrast to the case when the area under the potential peak is used.

Calibration lines need not be drawn if the values of S, V, c_0 and t_n in eqn. (21) are known with sufficient accuracy, because M can then be easily calculated from the equation

$$M = Vc_0 \left[\int_0^{t_n} 10^{\Delta E_t/S} \, dt - t_n \right] \tag{22}$$

In this case, a standard solution need not be injected. If S cannot be considered constant during a long series of measurements, then a standard solution must be injected into the carrier stream from time to time. In this case, M can be calculated by applying eqn. (22) to both sample and standard and using an iterative procedure to solve these equations [26].

Comparison of the methods used for evaluation of the potentiometric peaks

Evaluation on the basis of peak height is technically very simple and this is its great advantage. Peak area measurements require more sophisticated instrumentation, but they utilize the complete measured signal instead of using only a single point of the peak, so that errors arising from the noise superimposed on the signal are decreased.

The Gran transformation seems to be most advantageous not only because the calibration curve becomes linear but because the result is independent of the shape of the concentration peak and even of its reproducibility. Figure 12 shows a potentiometric peak and its Gran transform.

As stated above, the potentiometric signal can be measured relative to the base line or the instrument zero. The decision between these two possibilities will be dictated by the characteristics of the sensor. The potential measured relative to the base line, ΔE, is independent of E^0, so that this method should be applied if E^0 is not stable enough. If the potential is measured relative to the instrument zero, E^0 must be stable (or frequently checked), since the calculations are based on the constancy of E^0. In this case, however, it is not necessary to wait until the base line is accurately reached. This is an important factor, because the potential of most potentiometric sensors stabilizes quite slowly in dilute solutions (background solution). Thus the techniques based

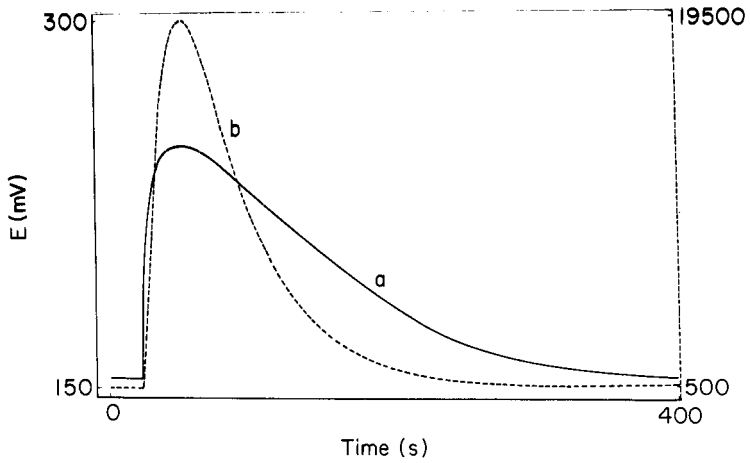

Fig. 12. Comparison of the potentiometric peak (a) and its Gran transform (b). Streaming solution, 10^{-4} M KI—10^{-1} M KCl; solution injected, 200 μl 10^{-1} M KI; V = 2.5 ml min^{-1}; W = 1.4 ml.

on the measurement of potential relative to the instrument zero rather than to the base line allow an increased speed of analysis.

These points may be illustrated by an example. Let us assume that the concentration of the background solution is 10^{-5} M and that the maximum of the concentration peak corresponds to the value 10^{-3} M. To achieve a 1% accuracy when the potential is measured relative to the base line, the base line must be restored within at least 0.25 mV (see eqn. 15) for S = 59 mV; this usually requires quite a long time. It should be noted that 0.25 mV is about 0.2% of the potentiometric peak height, while the accuracy of the concentration measurement is only 1%.

Potential applications of the injection technique

Quite generally, injection techniques allow numerous analytical tasks to be solved in a simple and convenient way. Obviously, the general technique is most advantageous when serial analyses of samples of more or less similar composition are required. When it is considered that the wide range of concentration sensitivity and the high selectivity of potentiometric detectors avoid, in many cases, any requirement for sample pretreatment, the direct injection of microliter samples into a carrier stream combined with electroanalytical detectors becomes very attractive for many analytical applications. Mechanization of potentiometric and voltammetric determinations offers a simple fast technique for analysis.

Further advantages are as follows. First, as the detector electrode is in contact with the carrier solution of constant composition during the time elapsed between the passage of each sample, it is conditioned; thus measuring problems that may arise from changes in the active electrode surface often decrease dramatically. The continuous flow of the carrier solution gives some regeneration of the electrode surface state. Secondly, recalibration of the detectors is fast and simple; thus, even electrodes of changeable electrochemical properties can give fairly reliable results with frequent recalibration. For example, in the case of enzyme electrodes, regular recalibration with injecting standards is essential, the frequency of recalibration depending mainly on the stability of the reaction layer of the enzyme sensor. Other useful aspects are presented by the favourable signal-to-noise ratios given by the difference signals, and the speed of analysis available from the dynamic signal-time recordings.

If the species to be determined cannot be sensed directly by the detector employed, it may be possible to select appropriate chemical reactions between the analyte and the carrier solution to produce a detectable concentration change. Thus, without any complicated flow patterns, a wide range of inactive species becomes determinable.

The varieties of the injection technique employing chemical reactions can be classified as follows.

(1) Analysis of samples containing species not detectable by the sensor employed (inactive sample analysis). Two methods can be used in this case. (a) The carrier solution contains a component detectable by the sensor which reacts with the analyte as well as components required for the de-

tection (e.g. supporting electrolyte, ionic strength adjusting buffer, pH buffer, etc.). The concentration of the detectable material decreases as the reaction proceeds. (b) The streamed solution contains an inactive material which reacts with the sample solution to give an electroactive reaction product. Naturally the solution must also contain any other important components required for the chemical reaction and detection.

(2) Analysis of continuously streaming sample solution containing a component not detectable with the detector employed (inactive species analysis in the flow stream). In this case a suitable reagent solution is injected. If the reagent is sensed by the detector, then the consumption of the reagent is followed. If the reagent is not sensed, then the product of the chemical reaction must be electroactive and its appearance is monitored. Obviously, the terms "electroactive", "inactive", "sensed", "not detectable" depend on the nature of the sensor and on the experimental conditions.

The two "indirect" injection methods described above can be considered as complementary. The choice of whether the reagent is streamed or injected will depend on the analytical problem, as well as on the volume of sample available and on its concentration. In this last aspect, it may be noted that with more concentrated samples, sample injection gives more satisfactory results than reagent injection, whereas with diluted samples the situation is reversed.

It becomes clear then, that the indirect techniques are applicable to almost all determinations which can be solved by potentiometric or amperometric titrations.

In applications of potentiometric detection — owing to the non-linear signal-conversion character of the sensor — the reagent injection technique offers a possibility for determining the concentration of a streaming sample solution by standard addition or subtraction (see below).

The reagent can often be prepared advantageously by electrolytic generation. This has widespread application, especially when the reagent is the injected solution, however, the reagent can easily be produced in the streaming solution also by a continuous electrolysis process.

The apparatus shown schematically in Fig. 13 can be employed for injection

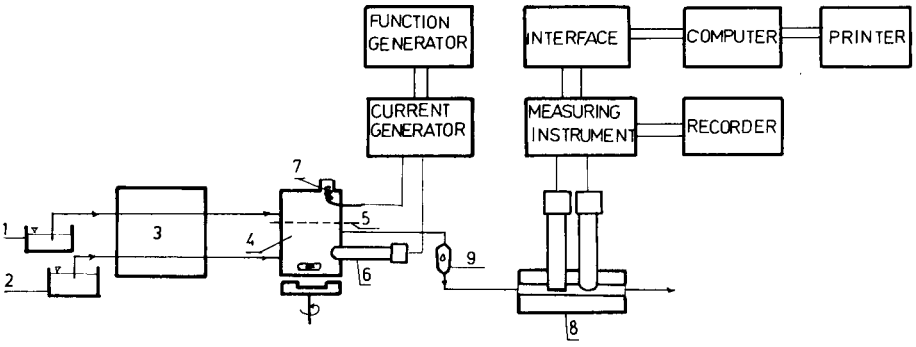

Fig. 13. Experimental set-up used for injection measurements employing electrically generated reagent. (Details see in text.)

analysis with in situ electrolytic reagent generation [12]. The generation of different reagents has been successfully solved with the arrangement designed. The sample solution (1) containing also the reagent precursor and the auxiliary solution (2) pumped with a multichannel peristaltic pump (3) flow through a two-compartment electrolysis cell (4); the two compartments are separated by a dialysis membrane (5) and contain the appropriate generating (6) and auxiliary (7) electrodes. The generator compartment also serves as a mixing chamber. The generating and the detector units (8) are separated electrically from each other by a drip vessel (9). The reagent injection is done by controlled current electrolysis employing square-wave current pulses of adjustable intensity and length. The signal—time curve is recorded and/or evaluated with the help of a suitable data processing unit.

The peak-type signals provided by potentiometric detectors depend on the primary ion activity of both the injected and the streaming solutions. Thus a particular attribute of the potentiometric injection technique is that continuously streamed samples can be analyzed simply by standard addition or subtraction. Signals obtained by volumetric or electrolytic injection of the primary ion standard (addition) or of a suitable reagent (subtraction) are evaluated by calibration or numerically (see above, *Evaluation of signals*).

The special feature of the voltammetric injection technique is mainly related to the advantages of the hydrodynamic conditions involved. The effects of convection and the favourable signal-to-noise ratio with the constant-potential measurements ensure a sensitivity as high as can be obtained with far more sophisticated voltammetric techniques, e.g., a.c., differential pulse methods.

The most important characteristics of injection analysis such as accuracy, sensitivity and rate of analysis depend largely on the type of the sensor, on the hydrodynamic conditions and the geometry of the injection setup, as well as on the evaluation method used. It is, therefore, difficult to characterize briefly these features of the many types of injection analysis studied so far. Some data concerning typical accuracies with voltammetric detection are, however, listed in Table 2. When potentiometric detectors were employed, relative errors of 3—6%, 1—3% and 1—5% were obtained for the same measuring setup when evaluation was based on peak area, peak shape and peak height measurements, respectively, by the numerical iteration procedures mentioned earlier. A typical rate of analysis is 40—60 samples per hour.

SELECTION OF OPTIMAL PARAMETERS FOR INJECTION MEASUREMENTS

The choice of the optimal conditions is assisted by the relationships discussed in earlier sections. These relationships are useful for direct determinations as well as for indirect determinations if the reaction involved can be regarded as instantaneous. If the chemical reactions are slow, the reaction rates must also be considered. It has to be realized that all the parameters involved in the potential and current equations describing the dynamic signal

TABLE 1

Potential analytical applications of the injection technique
(M, sample solution; R, reagent; P, reaction product; A, "electroactive"; I, "electroinactive"; S, streaming; J, injected.
The figures show detected peaks with sample concentrations increasing from left to right.

Direct sample injection $M_A^J + R_I^S \rightarrow M_A$	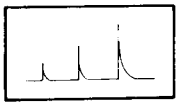
Indirect sample injection 1(a) $M_I^J + R_A^S \rightarrow R_A^S - P$	
(b) $M_I^J + R_I^S \rightarrow P_A$	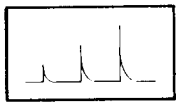
2(a) $M_I^S + R_A^J \rightarrow R_A^S - P$	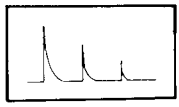
(b) $M_I^S + R_I^J \rightarrow P_A$	

TABLE 2

Some reproducibility data obtained by the voltammetric manual injection method [22] (Concentration range studied, 10^{-1}—10^{-3} M; volume injected, 100 μl; evaluation by peak area measurements.)

Indicator electrode	Material	Relative standard deviation (%)
Silicone rubber-based graphite electrode	$K_4[Fe(CN)_6]$	0.6
	Chlorpromazine	0.7
	Amidopyrin	1.0
Dropping mercury electrode	Cadmium	0.8
	Calcium (indirect)	1.3
Membrane-covered mercury electrode [10]	EDTA	1.2
	No-spa[a]	1.8
	Diazepam[b]	1.5

[a] 1-Benzoyl-3',4',6,7-tetraethoxy-1,2,3,4-tetrahydro-isoquinoline hydrochloride.
[b] 7-Chloro-1,3-dihydro-1-methyl-5-phenyl-2H-1,4-benzodiazepine-2-one.

play a role in determining the course of the respective signal—time curves. However, the relative importance of each parameter is discussed below.

Flow rate

The dependence of the signals on the flow rate can be assessed from eqns. (4), (6) and (11) if slow chemical reactions are absent. As the flow rate increases, the voltammetric peak height increases (Fig. 14) while the peak area (i.e. the charge passed through the detector cell as a result of the injection) at the same time decreases (Fig. 15). At small flow rates (0.5—1.0 ml min^{-1} for 2 mm i.d. tubes), the effect of a unit change in the flow rate on i_{max} and T is much higher than at higher flow rates.

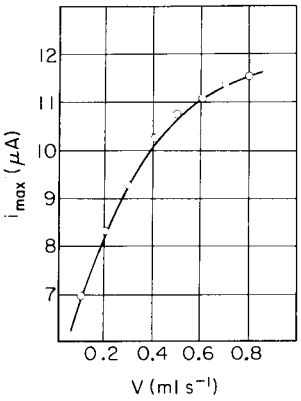

Fig. 14. Relationship between the voltammetric peak height and the flow rate of the carrier solution. Carrier solution, 0.5 M KCl; solution injected, $K_4[Fe(CN)_6]$; M = 10^{-6} mol; K = 1.85; a = 0.104. Applied potential, +0.7 V. The line is calculated and the symbols indicate the measured values.

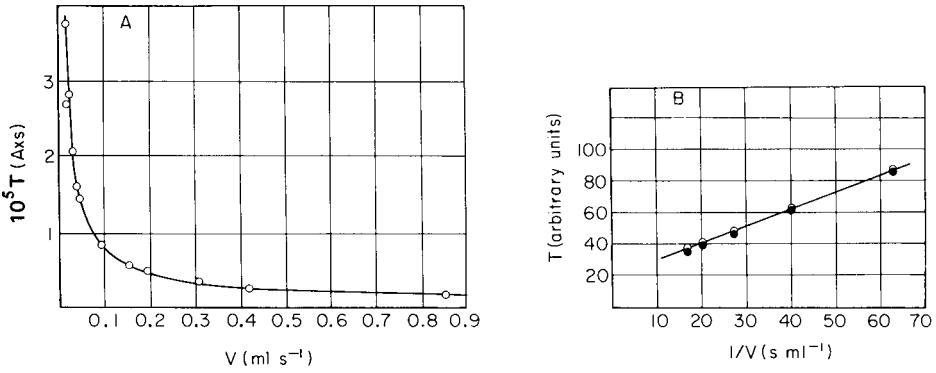

Fig. 15. Relationship between the area under the voltammetric peak and (A) the flow rate of the carrier solution; (B) the area under the potentiometric peak and the reciprocal value of the flow rate. Conditions for (A) as for Fig. 14 for (B) as for Fig. 9. Open and filled symbols indicate different experiments.

It is well known that the analysis time is determined primarily by the flow rate prevailing in the analysis channel. High analysis rates require high flow rate, but this can have adverse effects. The peak area, which is generally used for evaluation of the results, especially for voltammetric methods, will decrease as the flow rate increases and so the accuracy and precision of the measurement may suffer. Another important effect which has to be considered is that increasing the flow rate may make the rate of mass transfer to the electrode surface approach the rate of charge transfer — especially for reactions of analytically important organic molecules on solid electrodes. This renders the calibration line non-linear and may even make the measured signal almost independent of sample concentration. The flow rate should be chosen by considering all these effects. In this work, good results were obtained by applying flow rates of 4—5 ml min^{-1} with 2 mm i.d. conduits.

The peak height obtained with a potentiometric sensor will be much less dependent on flow rate than that obtained with a voltammetric detector. On increasing the flow rate, ΔE_{max} decreases as shown in Fig. 9; the points of the curve were calculated by using the simple model (eqns. 1—3) which neglects dispersion in the analysis channel. Naturally, the peak area decreases on increasing the flow rate (Fig. 15B).

The characteristics of the electrodes used should also be considered when setting the flow rate. Electrodes of high response time (e.g. enzyme electrodes or gas probes) will show decreased sensitivity if the flow rate is increased, i.e. if the time during which the sample is in contact with the electrode is decreased.

For indirect measurements based on reactions which cannot be regarded as instantaneous, the time available for the reaction to proceed will depend on the flow rate inter alia. A general discussion of this case, however, is beyond the scope of this work.

Volume of the mixing chamber

The choice of this volume is influenced by several factors. If slow chemical reactions are not involved, the voltammetric peak height decreases with increased chamber volume because the sample will become more diluted in this way (eqns. 2 and 3); the peak area, however, is practically independent of the chamber volume (Table 3). If potentiometric detection is used, both the peak height and the peak area depend on the volume of the mixing chamber (Fig. 16), whereas the area of the Gran-transformed peak is independent of it.

Other important factors are the required mixing ratio of the sample and the reagent or solutions added to adjust conditions such as pH, ionic strength, etc., the time required for the chemical reactions to proceed, the time during which the sample and the electrode must be in contact and the specific gravity, viscosity and surface tension of the samples.

Time span of injection

The peak shape is affected by the duration of the injection (eqns. 4—7). Good reproducibility of the flow pattern and of the signal measured can be

TABLE 3

The area under the voltammetric peak (electric charge passing through the detector cell as a result of injection; μCb) with mixing chambers of different volumes

W (ml)	Area of peak for different sample amounts (mol)				
	2×10^{-7}	4×10^{-7}	6×10^{-7}	8×10^{-7}	1×10^{-6}
0.3	1.09	1.93	3.03	3.97	5.05
1.7	1.12	1.83	3.05	3.98	5.21
3.2	1.17	1.89	3.12	3.89	5.03

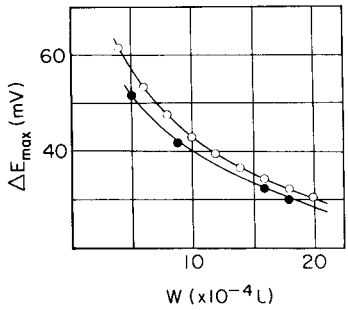

Fig. 16. Comparison of the calculated (from eqn. 4 written for ΔE_{max}) and measured potentiometric peak heights obtained with mixing chamber of different volumes. τ = 5 s; $V = 2.10^{-5}$ l s^{-1}. (○) Calculated; (●) measured.

achieved by applying short injection times and small sample volumes. The injection time is reproducible enough if an injector valve is used; with manual injection, however, it may vary from sample to sample and this necessitates the use of evaluation methods which are insensitive to variations in the peak shape, e.g. peak area measurements for voltammetric detection, and the Gran-transform area method for potentiometric sensors.

Composition of the carrier solution

Attention must be paid to the particular analytical problem. If direct voltammetric detection is used, the supporting electrolyte can be used as the carrier solution; the peaks then rise from the background current measured in the supporting electrolyte at the potential applied for detection.

If the indirect voltammetric method is used, then the concentration of the reagent should be chosen in such a way that the measured signal, which is due to the electroactive reagent or the reaction products, will be in an unambiguous, well-defined correlation with the concentration of the component detected over the whole concentration range in question.

In selecting the proper concentration of the reagent, it should be remem-

bered that the reagent must always be in excess in the mixing chamber. The optimal ratio of reagent to sample always depends on the analytical problem. As in any other type of analysis, if the reaction is not instantaneous, then decreasing the excess of reagent will decrease the reaction rate, whereas if the reagent concentration is too high, the relative change in its concentration caused by the sample will be small and accuracy and precision will decrease.

The background solution used for potentiometric injection generally incorporates the components required for ensuring the optimal working conditions (pH, ionic strength, etc.) of the indicator electrode. The problems connected with the use of primary ion in the carrier solution have been discussed under *Evaluation of signals.* It must be emphasized that the concentration of the primary ion — if used at all — should be relatively low compared to that of the sample injected. It is necessary to ensure not only a reasonable change in concentration by the injection but also a background signal in the linear range of the response function of the appropriate electrode.

Additionally, voltammetric detection requires a proper choice of the applied potential. Obviously, the rules governing selection are the same as in any other amperometric measurement, if optimal selectivity is required.

The interplay of all these factors must be considered in optimizing performance for any analytical problem. The injection measuring technique has been used for more than ten years in these laboratories for solving various practical problems, usually with voltammetric and ion-selective electrodes as detectors. In the course of this work, numerous analytical methods and some laboratory instruments have been developed based on injection techniques [8, 10, 12, 13, 22, 27].

The authors thank E. Lindner, Dr. A. Hrabéczy-Páll, G. Forgách and J. Szamek for their contribution to the preparation of this work.

REFERENCES

1 G. Nagy, Zs. Fehér and E. Pungor, Anal. Chim. Acta, 52 (1970) 47.
2 E. Lindner, K. Tóth and E. Pungor, Anal. Chem., 48 (1976) 1071.
3 Zs. Fehér, G. Nagy, K.Tóth and E. Pungor, Analyst, 99 (1974) 699.
4 K. Tóth, G. Nagy, Zs. Fehér and E. Pungor, Fresenius Z. Anal. Chem., 282 (1976) 379.
5 E. Pungor and K. Tóth, in W. Husmann (Ed.), Vom Wasser, Verlag Chemie, Weinheim, 1974, p. 43.
6 E. Pungor, K. Tóth and G. Nagy, Hung. Sci. Instrum., 35 (1975) 1.
7 Zs. Fehér and E. Pungor, Anal. Chim. Acta, 71 (1974) 425.
8 G. Nagy and E. Pungor, Hung. Sci. Instrum., 32 (1975) 1.
9 E. Pungor, Zs. Fehér and G. Nagy, Pure Appl. Chem., 44 (1975) 595.
10 E. Pungor, G. Nagy and Zs. Fehér, J. Electroanal. Chem., 75 (1977) 241.
11 E. Pungor, K. Tóth, G. Nagy and Zs. Fehér, in E. Pungor (Ed.), Ion-Selective Electrodes, Akadémiai Kiadó, Budapest, 1977, p. 67.
12 Zs. Fehér, G. Nagy, K. Tóth and E. Pungor, Anal. Chim. Acta, 98 (1978) 193.
13 K. Tóth, Zs. Fehér, G. Nagy, E. Lindner and E. Pungor, Magyar Kém. Lapja, 34 (1979) 17; 34 (1979) 77.
14 V. V. S. Eswara Dutt and H. A. Mottola, Anal. Chem., 47 (1975) 357.

15 J. Růžička and E. H. Hansen, Anal. Chim. Acta, 78 (1975) 145.
16 J. Růžička, E. H. Hansen and E. A. Zagatto, Anal. Chim. Acta, 88 (1977) 1.
17 K. K. Stewart, G. R. Belcher and F. Hare, Anal. Biochem., 70 (1976) 167.
18 B. Watson and M. H. Keyes, Anal. Lett., 9 (1976) 713.
19 D. Betteridge and J. Růžička, Talanta, 23 (1976) 409.
20 E. H. Hansen, A. K. Ghose and J. Růžička, Analyst, 102 (1977) 705.
21 J. Růžička and E. H. Hansen, Anal. Chim. Acta, 99 (1978) 37.
22 Zs. Fehér, Voltammetric Measurements in Flow-through Systems, Candidate's thesis, Budapest, 1975.
23 W. Treybal, Mass Transfer Operations, McGraw-Hill, New York, 1970.
24 J. Crank, The Mathematics of Diffusion, Clarendon Press, Oxford, 1975.
25 W. K. Giloi, Principles of Continuous System Simulation, B. G. Teubner, Stuttgart, 1975.
26 M. Gratzl, G. Horvai, K. Tóth and E. Pungor, unpublished results.
27 Zs. Fehér, G. Nagy, L. Bezúr, J. Szovik, K. Tóth and E. Pungor, Hung. Sci. Instrum., in print.

Analytica Chimica Acta, 109 (1979) 25—31

POTENTIOMETRIC ELECTRODE MEASUREMENT OF SERUM ANTIBODIES BASED ON THE COMPLEMENT FIXATION TEST

PAUL D'ORAZIO and G. A. RECHNITZ*

Department of Chemistry, University of Delaware, Newark, Delaware 19711 (U.S.A.)

(Received 20th February 1979)

SUMMARY

Trimethylphenylammonium-selective electrodes are used in the measurement of serum antibodies to bovine serum albumin, with serum complement and sensitized, marker-loaded sheep red blood cell ghosts as mediators. The result is a sensitive and reproducible assay system for the antibody in the presence of its antigen. In addition, the method described is shown to be valuable for basic studies of immune complex—complement interactions.

The development of immunoassay procedures involving potentiometric electrodes is based on coupling an immune reaction to an appropriate potentiometric sensor with mediators designed to produce a measurable response on stimulation by the immuno-system. In the present paper, a novel measurement of serum antibodies is described: the complement fixation test [1] is coupled to an electrode selective for the cation trimethylphenylammonium ($TMPA^+$). The bovine serum albumin (BSA)—anti-BSA system has been chosen as a model for the application of this analytical concept.

The use of marker-loaded sheep erythrocyte ghosts as mediators between the $TMPA^+$ electrode and serum complement was described recently [2]. The release of $TMPA^+$ marker from red blood cell ghosts was monitored and related to the level of hemolytic complement present (CH_{50} units). This novel assay procedure for complement proved advantageous over existing methods. The ability to use electrodes directly in suspensions of cell ghosts without the separation steps required in spectrophotometry, permits a "dipstick" assay procedure for hemolytic complement with a minimum of sample handling. In addition, the equipment used is simple to operate and may be designed and constructed in the laboratory.

Complement, as well as lysing sensitized erythrocyte ghosts, can be fixed by many antigen—antibody complexes. Through use of the cell ghost lysis phenomenon as an indicator system, free complement can be measured after a known level has been exposed to a soluble or insoluble antigen and its antibody. The amount of free complement remaining is inversely proportional to the amount of immune complex present. Moreover, the system can be made quantitative with respect to antibody if excesses of antigen and complement

are present. Calibration curves can be constructed and unknown determinations run to confirm the presence of antibody-producing disorders in living systems. Likewise, antigen may be assayed in the presence of excesses of antibody and complement.

The BSA—anti-BSA model system described provides a valid and practical test of the indicator system. The quantitative measurement of antibodies to BSA opens the way for assay of other antibodies or antigens directly in physiological fluids by the proposed method. In addition, the usefulness of ion-selective electrodes for fundamental studies of immune complex—complement interactions is demonstrated.

EXPERIMENTAL

Equipment

Potentiometric measurements were made on a Corning Model 12 Research pH meter in conjunction with a Heath-Schlumberger Model SR-204 strip-chart recorder. Measurements were made in a 15-ml glass, water-jacketed cell with circulation and thermostating provided by a Haake Model FS water bath/circulator. All measurements were taken at 37°C.

The indicator electrode used is of the polymer matrix type [3] and is highly selective for $TMPA^+$ over other monovalent cations, e.g., Na^+, K^+, and Li^+. Miniaturization of this electrode permits its use, together with a miniature saturated calomel reference electrode, in sample volumes as small as 0.60 ml [4]. The lifetime of the $TMPA^+$ sensor is dramatically extended if it is stored dry when not in use. A brief period of soaking in the relevant buffer is required prior to operation. Since these electrodes can be produced rapidly and inexpensively in the laboratory, they are discarded when their response characteristics deteriorate.

Reagents

Lyophilized rabbit antisera to bovine serum albumin were obtained from Miles Laboratories Inc., Elkhart, Ind. (lots R148, R259, and R270). Titers expressed as mg of antibody per ml of serum were supplied with the product. Rabbit antisheep hemolysin (lyophilized) and lyophilized guinea pig serum (as a source of complement) were from Grand Island Biological Co., Grand Island, NY. The complement titer of the guinea pig serum employed was 1:100. Hemolytic complement is expressed in CH_{50} units, one unit denoting the amount of complement activity required to lyse 50% of a fixed number of sensitized sheep red blood cells under the specified conditions of assay [5].

Sheep blood was obtained from the Department of Animal Science and Agricultural Biochemistry, University of Delaware, as an 87% (v/v) suspension of whole blood from the animal in acid citrate—dextrose anticoagulant. A volume of blood could be stored and remained usable for approximately one month.

Other materials used were triethanolamine and bovine serum albumin

(lyophilized, Cohn Fraction V) from Sigma Chemical Co., and trimethylphenylammonium chloride from Eastman Kodak Co. Reagents used for preparation of buffers and other solutions were of analytical grade.

Triethanolamine-buffered saline (TBS) was prepared at pH 7.3—7.4 and contained 5.0×10^{-4} M Mg^{2+} and 1.5×10^{-4} M Ca^{2+}. This buffer is recommended for use in complement fixation studies [6]. Because of the slight Na^+ interference of the $TMPA^+$ electrode, lithium chloride was substituted for sodium chloride in TBS and the buffer was used as standard diluent for all work decribed here.

Procedures

The process of preparing sheep red blood cell ghosts for use was as described [2] with the following changes in the hemolytic and resealing steps. To increase the stability of cell ghosts, 1×10^{-5} M $CaCl_2$ was added to the lysing medium [7]. In addition, ghosts were sensitized in bulk following the 37°C resealing step with a 1:750 decomplemented anti-sheep hemolysin dilution. The advantages gained by these changes are discussed below.

Complement fixation experiments were carried out by mixing antigen, antibody, or antigen plus antibody with 11.2 CH_{50} units in a total volume of 160 μl. The reaction mixture was stored at 2—4°C for 20 h. Following the incubation period, the mixtures were placed in ice water until ready for use [1].

Experiments to determine free or unfixed complement activity were done as follows. The sensitized ghost suspension (400 μl) was diluted to 710 μl with TBS. The electrodes were immersed in this stirred mixture and the resulting equilibrium potential was noted. The test reaction mixture (40 μl) was added and the resulting potential designated as E_1. The potential after a reaction time of 15 min was recorded as E_2. ΔE_{15} values were computed ($E_2 - E_1$) and recorded.

Stock antiserum to BSA was reconstituted with distilled water and decomplemented by heating at 56°C for 30 min. Dilutions of the antiserum were prepared in TBS in the following concentrations: 1.0, 0.83, 0.67, 0.50, 0.33, 0.17, and 0.04 mg ml^{-1}. Constant aliquots of each dilution containing varying amounts of antibody from 1 μg upwards were used to establish the upper limit of the test. An optimum level of antigen and 11.2 CH_{50} units were added to each aliquot followed by mixing and incubation. A series of ΔE_{15} values resulting from free complement activity was thus obtained. These values were plotted as a function of the amount of antibody in a 25% aliquot of the initial mixture.

Complement titration curves [2] were run after the antibody calibrations to obtain a quantitative estimate of the CH_{50} units fixed at various points on the antibody calibration curve. Complement dilutions as well as antibody dilutions were prepared just before use.

RESULTS AND DISCUSSION

The model system employed in this study is: BSA + rabbit anti-BSA + complement.

After a specified reaction time, unfixed complement is assayed and related to variation in antibody or antigen level, the other components being present in constant, predetermined amounts. To quantify the antibody, it is necessary to optimize not only the antigen level but also the amount of complement employed. For good sensitivity, a level of complement was chosen which lyses close to 100% of a specified cell suspension while avoiding a large excess. Based on past results [2], a value of 2.8 CH_{50} units was used. Greater accuracy in pipetting was achieved by initially mixing 11.2 CH_{50} units with the antigen—antibody mixture. A 25% aliquot thus corresponds to 2.8 CH_{50} units if the complement activity remains constant. Fixation of complement below this level by immune complex or by either component alone results in a very sensitive assay system. The method closely resembles that of Stein and Van Ngu [8] since excess of complement is not employed and the reaction mixture is added without dilution directly to the sensitized cells.

The interference of impurities in the antisera, in terms of complement-fixing ability, was investigated. It was found that an amount of antiserum corresponding to 24 μg of antibody could be used in the presence of 11.2 CH_{50} units with no fixation of complement. Similarly, 24 μg of the bovine serum albumin preparations showed no complement fixation under these conditions. This corresponds to 6 μg of antibody and 6 μg of BSA in the presence of 2.8 CH_{50} units involved in actual determinations. ΔE_{15} values obtained were equal, within experimental error, to those obtained when 2.8 units of fresh complement were added to the indicator system.

Development of an assay system for antibody involved optimization of the antigen level to be used with 24 μg of rabbit antibody. Maximum fixation of complement, i.e. a minimum ΔE_{15} value, as a function of antibody to antigen ratio was sought. Antibody calibration curves could then be constructed by decreasing antibody added from the maximum value to values approaching zero in the presence of an optimum amount of BSA. A large slope over the range tested would be desirable to increase the sensitivity of the system. A typical result is shown in Fig. 1. Antibody to antigen ratio is varied from 1:1 to 10:1 by weight for a constant 24 μg of antibody. The minimum ΔE_{15} value occurred at an antibody: antigen ratio of approximately 3:1. This value corresponds to the equivalence point as defined by precipitin analysis, in that the maximum amount of immune complex fixes more complement than is fixed in the zones of antibody or antigen excess [1].

The amount of BSA chosen for antibody calibration was 7.2 μg per total reaction mixture. An antibody calibration curve is shown in Fig. 2. Variation of antibody from 1 to 24 μg initially, produced the values shown on the abscissa when a one-fourth aliquot was used in actual determinations. Since the potential change at the lowest antibody value tested closely corresponds

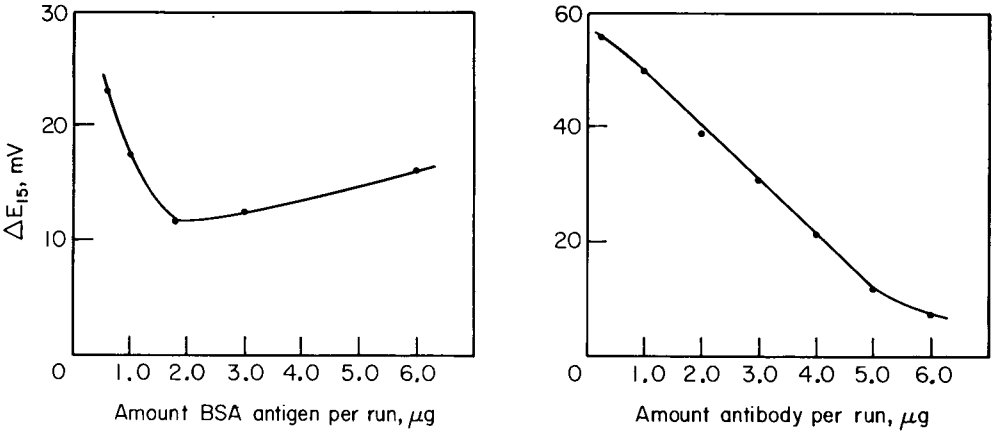

Fig. 1. Determination of antibody to antigen ratio at the point of maximum complement fixation; 24 μg of antibody and 11.2 complement units used per total reaction mixture.

Fig. 2. Calibration curve for rabbit anti-BSA; 7.2 μg of antigen and 11.2 complement units used per total reaction mixture.

to the ΔE obtained upon addition of 2.8 units of fresh complement, the full range of complement fixation has been exploited under the assay conditions used. A quantitative estimate of complement units fixed at points on the calibration curve is possible by constructing a complement titration curve immediately following antibody calibration. In this way, characteristics of the system, e.g., level of marker trapped within cell ghosts, amount of background ion, etc., remain constant. Millivolt values from the antibody calibration curve can be read as free CH_{50} units on the complement curve. These values subtracted from 2.8 result in complement units fixed under the specified conditions. Table 1 shows these results obtained for the calibration curve of Fig. 2. Owing to the low slope of the complement titration curve at the high complement end, an accurate value could not be determined at the 0.25-μg antibody level.

To evalute the accuracy and precision of the method, each of two lots of antisera other than that used as the standard were run at three different points on the antibody calibration curve. Results obtained are shown in Table 2. Excellent agreement with known values is obtained along with the reproducibility necessary for quantitative analysis.

Improvements in the preparation of erythrocyte ghosts have increased the practicality of using such vesicles as reagents in analytical systems. Addition of calcium ions in low concentration to the lysing medium (approximately 10^{-5} M) increases the proportion of usable cell ghosts [7]. Likewise, bulk sensitization of a batch of erythrocyte ghosts immediately after reforming dramatically increases the lifetime of the ghosts. The method of storing unsensitized ghosts and mixing only the desired aliquot with the hemolysin anti-

TABLE 1

Complement units fixed by varying amounts of antibody in the presence of BSA antigen[a]

Amount antibody (μg)	0.25	1.0	2.0	3.0	4.0	5.0	6.0
CH_{50} units fixed[b]	n.d.	1.8	2.1	2.2	2.3	2.4	2.4

[a]7.2 μg BSA per total reaction mixture.
[b]Out of possible 2.8 units. Each value represents the mean of three determinations with a standard deviation of ±0.1.

TABLE 2

Potentiometric determination of antibody in commercial antisera

Antiserum lot	Known value (mg Ab ml^{-1})	Value obtained[a] (mg Ab ml^{-1})
R270	2.5	2.6
R148	2.4	2.5

[a]Values represent the mean of three determinations with a standard deviation of ±0.2.

body prior to use resulted in such high rates of leakage that cells were not usable after two or three days. Under the new conditions, ghosts could be stored and remained viable for periods as long as two weeks. Refrigerated dialysis of the ghosts, when not in use, assures low background levels of ion marker. Procedures for lyophilization of modified erythrocytes [9] without damage to cell membranes upon reconstitution may also be applied to cell ghosts. This would provide convenient storage of the loaded vesicles until ready for use.

The versatility and ease of operation of ion-selective electrodes have made them readily applicable to measurements in biological systems. Their usefulness in immunochemistry has now been extended through the use of sheep red blood cell ghosts and complement as mediators to a method for determination of serum antibodies to bovine serum albumin. The application of the principles described may lead to sensitive immunoassays for various other antibodies and antigens as well as providing a system for use in basic immunochemical studies.

We gratefully acknowledge the support of a grant from the National Institutes of Health.

REFERENCES

1 E. A. Kabat and M. M. Mayer, Experimental Immunochemistry, 2nd edn., C. C. Thomas, Springfield, Ill., 1961, Chapter 4.
2 Paul D'Orazio and G. A. Rechnitz, Anal. Chem., 49 (1977) 2083.
3 G. J. Moody, R. B. Oke and J. D. R. Thomas, Analyst, 95 (1970) 910.

4 Paul D'Orazio, M. E. Meyerhoff and G. A. Rechnitz, Anal. Chem., 50 (1978) 1531.
5 Standard Complement Fixation Method and Adaptation to the Micro Test, Public Health Monograph No. 74, U.S. Department of Health, Education, and Welfare, 1965.
6 N. Rose, P. Bigazzi, W. Bartholomew and R. Zarco in N. Rose and P. Bigazzi (Eds.), Methods in Immunodiagnosis, J. Wiley, New York, 1973, p. 209.
7 G. Schwoch and H. Passow, Mol. Cell. Biochem., 2 (1973) 197.
8 G. J. Stein and J. Van Ngu, J. Immunol., 65 (1950) 17.
9 J. Spona and M. Topert, U.S. Patent 3987159 (1976).

Analytica Chimica Acta, 109 (1979) 33—38

AMPEROMETRIC DETERMINATION OF ACETIC ACID WITH IMMOBILIZED *Trichosporon brassicae*

MOTOHIKO HIKUMA, TATSURU KUBO and TAKEO YASUDA

Central Research Laboratories, Ajinomoto Co. Inc., 1 Suzuki-cho, Kawasaki-ku, Kawasaki 210 (Japan)

ISAO KARUBE* and SHUICHI SUZUKI

Research Laboratory of Resources Utilization, Tokyo Institute of Technology, Nagatsuta-cho, Midori-ku, Yokohama, 227 (Japan)

(Received 5th February 1979)

SUMMARY

A microbial sensor consisting of immobilized *Trichosporon brassicae*, a gas-permeable Teflon membrane and an oxygen electrode is suitable for the continuous determination of acetic acid in fermentation broths. When an acetic acid solution is pumped through the flow system, the current decreases to a steady state with a response time of 8 min; shorter pumping times give peaks which can also be measured. The relationship between the current decrease and the acetic acid concentration is linear up to 54 mg l^{-1}, with a relative standard deviation of about 6% at the higher concentrations. Selectivity is satisfactory. Results obtained with this sensor and by gas chromatography for a glutamic acid fermentation broth were in good agreement (regression coefficient 1.04). The sensor was stable for more than 3 weeks and 1500 assays.

On-line measurement of acetic acid concentrations is required in fermentation processes. In the cultivation of microorganisms with acetic acid as the carbon source, acetic acid inhibits growth above a certain concentration, so that the optimal concentration should be maintained by on-line measurements. Gas chromatography can be used but is unsuitable for on-line measurements.

Recently, many techniques have been developed for the immobilization of living whole cells [1—4]. These immobilized cells have been used in the electrochemical sensors known as microbial sensors. Such sensors have been developed for estimations of BOD [5—7], antibiotics [8], alcohol [9] and vitamins [10], based on oxygen electrodes, fuel cell electrodes and combined glass electrodes. As previously reported [5—8], assimilation of organic compounds by microorganisms can be determined from the respiration activity of the microorganisms, which can be measured directly with an oxygen electrode.

In this paper, a microbial sensor consisting of immobilized yeasts, a gas-permeable Teflon membrane and an oxygen electrode is described for the determination of acetic acid. Application to the continuous determination of acetic acid in fermentation broth is reported.

EXPERIMENTAL

Materials

The materials used were malt extract (Difco Laboratories), polypeptone and yeast extract (Takeda Yakuhin Kogyo Co.) and acetic acid (Junsei Chemical Co.). Laboratory-grade chemicals were used.

Preparation of the sensor

Culture and immobilization. Trichosporon brassicae CBS 6382 was cultured on 8 ml of a suitable medium in a test tube (15 mm i.d., 16 cm high) at 30°C for 2 days. The medium contained 0.3% malt extract, 0.3% yeast extract, 0.3% polypeptone, 1.0% glucose and 2.0% agar, adjusted to pH 6.0. The microorganisms (0.3 g wet weight) were suspended in 5 ml of sterilized water, and 3 ml of the suspension was dripped onto a porous acetylcellulose membrane (Millipore type HA, 0.45-μm pore size, 47-mm diameter, 150 μm thick), with slight suction.

The microbial sensor is illustrated in Fig. 1A. The oxygen electrode (Model C-3021, Denki Kagaku Keiki Co.) consisted of a Teflon membrane (50μm thick), a platinum cathode, an aluminum anode and a saturated potassium chloride electrolyte. The porous membrane with the immobilized microorganisms was cut into a circle (1.4-cm diameter) and fixed on the surface of this Teflon membrane. This was covered with a gas-permeable Teflon membrane (Millipore type FH, 0.5-μm pore size) or a silicone rubber membrane (Radiometer

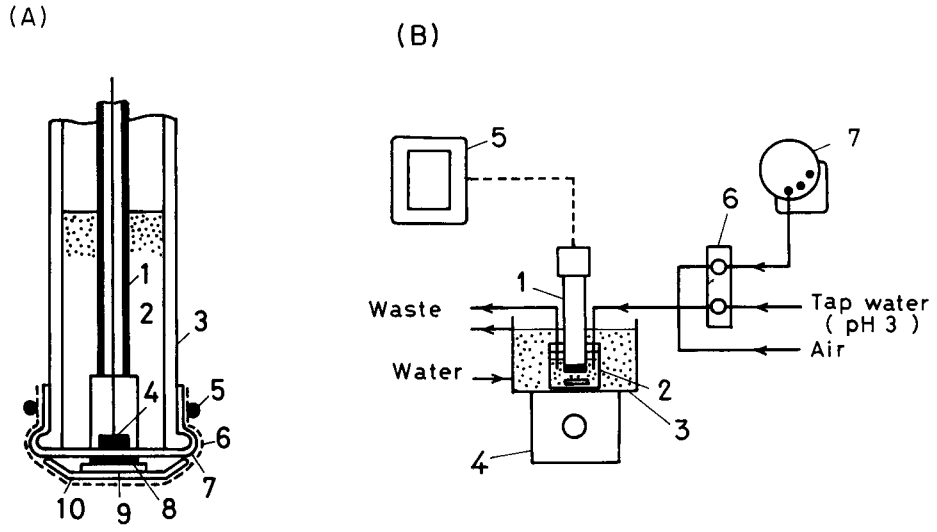

Fig. 1. (A) The microbial sensor for acetic acid: (1) aluminum anode; (2) electrolyte; (3) insulator; (4) platinum cathode; (5) rubber ring; (6) nylon net; (7) Teflon membrane; (8) microorganisms; (9) acetylcellulose membrane; (10) porous Teflon membrane. (B) The sensor system: (1) microbial electrode; (2) flow cell; (3) jacket; (4) magnetic stirrer; (5) recorder; (6) peristaltic pump; (7) sampler.

type D 606), the whole arrangement being held together with a nylon net. Thus the microorganisms were trapped between the two porous membranes.

Apparatus

The system (Fig. 1B) consisted of a jacketed flow cell (3-cm diameter, 2.7-cm high, 19-ml capacity), a magnetic stirrer (1000 rpm), a peristaltic pump (Technicon Model I), an automatic sampler (Tokyo Kagaku Sangyo Co.) and a current recorder (Yokogawa Electric Co. Model ERB-6-10 or LER-12A).

Procedure

The temperature of the flow cell was maintained at 30 ± 0.1°C by warm water passed through the jacket. Tap water was adjusted to pH 3 with 0.05 M sulfuric acid and saturated with air. Then, it was transferred to the flow cell at a rate of 1.4 ml min^{-1} together with air at a flow rate of 200 ml min^{-1}. When the output current of the sensor became constant, a sample was passed into the system at a rate of 0.8 ml min^{-1} for 3 min, 10 min or 15 min.

RESULTS AND DISCUSSION

Response of the electrode

Figure 2 shows typical response curves of the sensor based on immobilized *Trichosporon brassicae* for acetic acid. The current at time zero was obtained with the tap water saturated with oxygen; this current corresponds to the endogenous respiration level of the immobilized microorganisms. When the

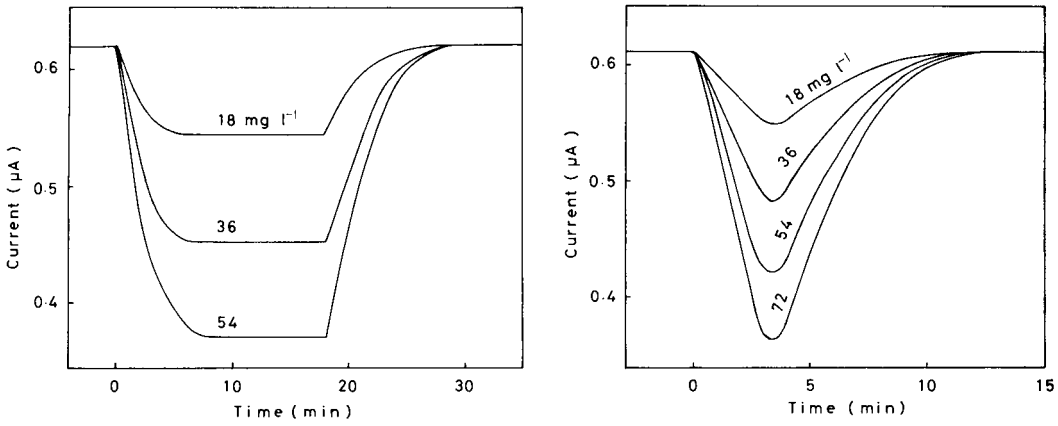

Fig. 2. Response curves of the microbial sensor for sample solutions (12 ml) containing various amounts of acetic acid passed into the system as described under Procedure.

Fig. 3. Response curve of the sensor with a gas-permeable Teflon membrane by the shorter method. Sample solution (2.4 ml) was passed into the flow cell for 3 min, as described under Procedure.

sample solution containing acetic acid entered the system, acetic acid permeated through the gas-permeable membrane and was assimilated by the microorganisms. Oxygen was then consumed by the microorganisms so that the concentration of dissolved oxygen around the membranes decreased. The current decreased until it reached a steady state, which indicated that the consumption of oxygen by the microorganisms and the diffusion of oxygen from the sample solution to the membrane were in equilibrium.

The steady-state current depended on the concentration of acetic acid. When tap water was again passed through the flow cell, the current of the sensor returned to its initial level. The pH of the solution had to be kept sufficiently below the pK value for acetic acid (4.75 at 30°C), because acetate ions cannot pass through the gas-permeable membrane.

Porous Teflon, silicone rubber, polybutadiene and polyethylene membranes were tested for covering the surface of the microbial sensor. The 90% response time (i.e. the time required to obtain 90% of the maximum current decrease) and the sensitivity (the ratio of current decrease to concentration of acetic acid) were examined for each electrode. Porous Teflon or silicone rubber membranes proved to be suitable. The 90% response times and the sensitivities of the sensor were 3.5 min and 5.0×10^{-3} μA l mg^{-1} with porous Teflon membranes, and 7.5 min and 1.8×10^{-4} μA l mg^{-1} with silicone rubber membranes, respectively. Porous Teflon membranes were employed for further work.

The time required for the determination of acetic acid is long by the steady-state method, therefore samples were passed into the flow cell for only 3 min. Figure 3 shows the response curves obtained for acetic acid concentrations of 18, 36, 54 and 72 mg l^{-1} by this method under the same conditions as those described in Fig. 2 except for the sample volume and time (3 min) involved. In this case, the maximum current decrease was only 75% of that obtained by the steady-state method, but the measurement could be done within 4 min. The total time required for an assay of acetic acid was 30 min by the steady-state method and 15 min by the shorter method. The latter method was, therefore, employed for assay.

Calibration

The calibration graphs obtained (Fig. 4) showed linear relationships between the current decrease and the concentration of acetic acid up to 54 mg l^{-1} by the steady-state method and up to 72 mg l^{-1} by the shorter method. The minimum concentration for determination was 5 mg of acetic acid per liter. The reproducibility of the current difference was examined using the same sample. The current difference was reproducible within ±6% for an acetic acid sample containing 54 mg l^{-1}. The standard deviation was 1.6 mg l^{-1} in 20 experiments.

Selectivity of the microbial sensor

The selectivity of the microbial electrode for acetic acid was examined with

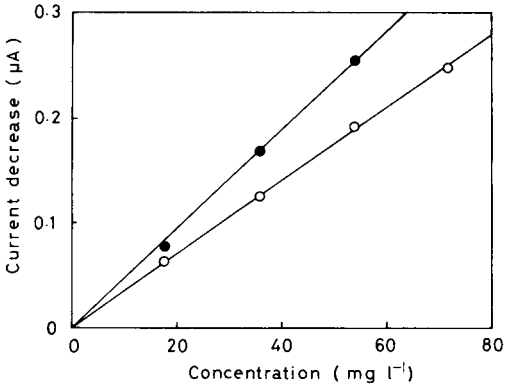

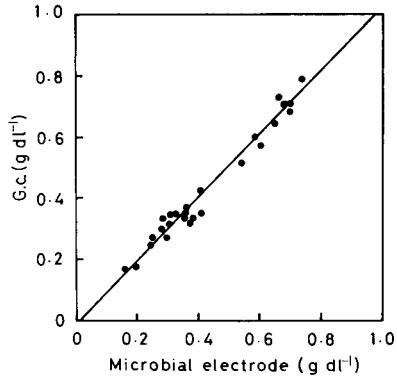

Fig. 4. Calibration plots for the sensor by the steady-state method (•) and by the shorter method (○). The experimental conditions were the same as those described in Figs. 2 and 3, respectively.

Fig. 5. Comparison between concentrations determined by the microbial electrode sensor and those determined by gas chromatography. The determination by the microbial sensor was carried out under the standard conditions except that the sample was pumped for 10 min and was diluted 170 times. The fermentation broth was diluted and pumped automatically into the system.

TABLE 1

Response of the microbial sensor to various compounds by the steady-state method (15 min)

Compound	Concentration[a] (mg l^{-1})	Current decrease (μA)	Compound	Concentration[a] (mg l^{-1})	Current decrease (μA)
Acetic acid	100	0.18	Tartaric acid	100	0
Formic acid	100	0	Methanol	40	0
Propionic acid	100	0.17	Ethanol	40	0.21
n-Butyric acid	100	0.21	Glucose	1000	0
Lactic acid	100	0	KH_2PO_4	5000	0
Succinic acid	100	0			

[a]Original concentration (diluted 2.8 times in the flow cell).

the results presented in Table 1. The sensor did not respond to volatile compounds such as formic acid and methanol or to involatile nutrients such as glucose and phosphate ions. As the microbial electrode was covered with a gas-permeable membrane, only volatile compounds could penetrate through the membrane. The response to organic compounds depends on the assimilability by the immobilized microorganisms. *Trichosporon brassicae*, which utilizes acetic acid, did not assimilate formic acid or methanol, but utilized propionic acid, n-butyric acid and ethanol. Fortunately, the latter three compounds are not generally present in fermentation broths.

Application and long-term stability of the microbial sensor

The microbial sensor for acetic acid was applied to a fermentation broth of glutamic acid. The concentration of acetic acid was determined by the microbial electrode and by a gas chromatographic method. As shown in Fig. 5, good agreement was obtained; the regression coefficient was 1.04 for 26 experiments. Whole cells in the broth did not affect the electrochemical determination of acetic acid.

The long-term stability of the microbial electrode was examined for acetic acid solutions (72 mg l^{-1}). The current output (0.29—0.25 μA) of the electrode was constant (within ±10% of the original values) for more than 3 weeks and 1500 assays. Therefore, the yeasts in the electrode survived remarkably well. In conclusion, the microbial sensor appears to be quite promising and very attractive for the determination of acetic acid in fermentation broths.

The authors are grateful to Mr. T. Kiya and Dr. K. Mitsugi, Central Research Laboratories, Ajinomoto Co., Inc., for their helpful advice and encouragement, and to Mr. T. Shirakawa for his assistance.

REFERENCES

1 I. Karube, T. Matsunaga, S. Tsuru and S. Suzuki, Biochim. Biophys. Acta, 444 (1976) 338.
2 M. Kierstan and C. Buche, Biotechnol. Bioeng., 19 (1977) 387.
3 J. F. Kennedy, S. A. Barker and J. D. Humphreys, Nature, 261 (1976) 242.
4 T. Kokubu, I. Karube and S. Suzuki, Eur. J. Appl. Microbiol. Biotechnol., 5 (1978) 233.
5 I. Karube, T. Matsunaga, S. Mitsuda and S. Suzuki, Biotechnol. Bioeng., 19 (1977) 1535.
6 I. Karube, S. Mitsuda, T. Matsunaga and S. Suzuki, J. Ferment. Technol., 55 (1977) 243.
7 I. Karube, T. Matsunaga and S. Suzuki, J. Solid-Phase Biochem., 2 (1977) 97.
8 K. Matsumoto, H. Seijo, T. Watanabe, I. Karube and S. Suzuki, Anal. Chim. Acta, 105 (1979) 429.
9 M. Hikuma, T. Kubo, T. Yasuda, I. Karube and S. Suzuki, Biotechnol. Bioeng., in press.
10 T. Matsunaga, I. Karube and S. Suzuki, Anal. Chim. Acta, 99 (1978) 233.

Analytica Chimica Acta, 109 (1979) 39—44

MICROBIOASSAY OF NYSTATIN WITH A YEAST ELECTRODE

ISAO KARUBE*, TADASHI MATSUNAGA and SHUICHI SUZUKI

Research Laboratory of Resources Utilization, Tokyo Institute of Technology, Nagatsuta-cho, Midori-ku, Yokohama 227 (Japan)

(Received 17th January 1979)

SUMMARY

Microbioassay of nystatin is achieved with an electrode composed of a yeast membrane and an oxygen electrode, based on the inhibitory action of the antibiotic on the respiration of the yeast. A linear relationship is obtained between the rate of current increase and the potency of nystatin. The minimum measurable nystatin concentration is 0.5 unit ml^{-1}. The assay takes less than 1 h; the standard deviation is 1.2 unit ml^{-1} at the 27 USP unit ml^{-1} level.

Many polyene antibiotics have been isolated from the culture broth of *Streptomyces* species. These antibiotics are active against fungi, yeast and other organisms. However, most are too toxic for clinical use. Only nystatin and some other polyene antibiotics are useful for clinical applications [1].

The agar diffusion method [2, 3] used for the microbioassay of the polyene antifungal antibiotics presents difficulties owing to the nature of the antibiotics. They consist of heterogeneous mixtures of closely related compounds which are poorly soluble in aqueous diluents, diffuse poorly in agar gel, are unstable in bright sunlight, and produce zones of inhibition that may be neither clear nor proportional in size to the logarithm of the antibiotic concentration [4]. Therefore, simple and rapid methods are required for determinations of polyene antifungal antibiotics.

The present authors have developed a number of microbial electrodes consisting of immobilized micro-organisms and electrochemical devices [5—8], which have been applied to microbioassays [9, 10].

The polyenes are believed to bind with the sterol present in the membranes of sensitive cells leading to the formation of pores. The subsequent death of the micro-organisms is preceded by the leakage of cellular materials [1]. The death of the micro-organisms can be detected with an oxygen electrode. Therefore, an electrode consisting of the micro-organisms and an oxygen electrode should be applicable to the microbioassay of polyene antifungal antibiotics. In this paper, a yeast electrode composed of a yeast membrane and an oxygen electrode is described, and applied to the determination of nystatin.

EXPERIMENTAL

Materials

Nystatin (5780 USP units mg^{-1}; Sigma Chemical Co.) was stored in a desiccator at −20°C. Collagen was obtained from steer hide and was purified as described previously [11]. Collagen membranes (50 μm thick) were prepared by casting a suspension on a Teflon plate; the membrane was then treated in 0.001% glutaraldehyde solution for 5 min and dried. Yeast membranes were prepared as follows: a portion (0.1 g) of yeast cells was suspended in 10 ml of physiological saline and yeast solution (50 μl containing 4.6×10^7 cells) was dropped onto a filter paper (diameter 2 cm, thickness 70 μm).

Saccharomyces cerevisiae was purchased from the Oriental Yeast Co. Deionized water was used in all procedures.

Construction of the yeast electrode

A diagram of the yeast electrode is shown in Fig. 1. The electrode contains a collagen membrane and an immobilized yeast membrane attached to an oxygen electrode (Ishikawa Seisakujo Co., Model A; diameter 1.7 cm, height 7.2 cm; PVC casing). The collagen membrane is used to prevent leakage of yeast cells.

Assay procedure

Nystatin was dissolved in dimethyl formamide (DMF) and diluted to the appropriate concentration with 0.05 M phthalate buffer (pH 4.5) containing glucose (500 mg l^{-1}). The concentration of DMF in the sample solution was kept below 0.66%. The yeast electrode was inserted into the sample solution which was saturated with dissolved oxygen by magnetic stirring. The electrode current was displayed continuously on a recorder (TOA, Electronics Ltd., Model EPR-200 A) and the rate of current increase calculated from the linear

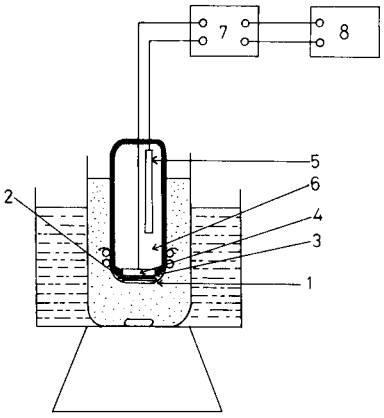

Fig. 1. The yeast electrode; (1) collagen membrane; (2) yeast membrane; (3) Teflon membrane; (4) cathode (Pt); (5) anode (Pb); (6) electrolyte (NaOH); (7) amplifier; (8) recorder.

portion of the response curve (see Fig. 4) at the middle point of the sigmoid curve.

RESULTS

Basic studies of the yeast electrode

The respiration of immobilized micro-organisms can be determined by the oxygen electrode, as described previously [5]. However, nutrients (e.g. glucose) in the sample solution affect the respiration of yeast cells, and such effects must be avoided. If sufficient nutrients are present in the solution, the electrode current is not affected by changes in nutrient concentration. Figure 2 shows the effect of glucose concentration on the steady-state current of the electrode; it takes 10 min to reach the steady state. The steady-state current decreases linearly with increasing glucose concentration, and becomes constant at concentrations exceeding 300 mg l^{-1}. The rate of metabolism in the yeast cells may be rate-determining in this range. The current depends on the total respiration activity of the yeast cells. Thereafter, a buffer solution containing 500 mg l^{-1} of glucose was employed.

The total respiration activity of yeast and therefore the current is affected by the number of yeast cells in the membrane. Figure 3 shows the relationship between the steady-state current and the number of yeast cells in the electrode membrane. The current decreased with increasing number of cells but a linear relationship was obtained for 1×10^7—4.6×10^7 yeast cells. Consequently, a membrane containing 4.6×10^7 cells was used thereafter for the electrode.

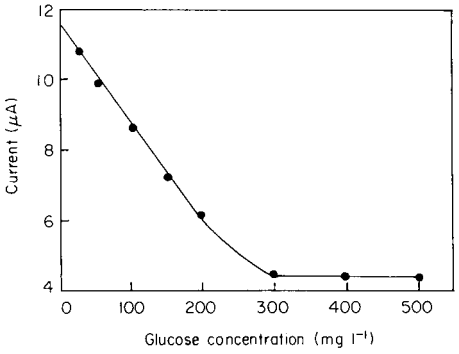

Fig. 2. Effect of glucose concentration on the steady-state current. The electrode contained 4.6×10^7 yeast cells and was inserted into the glucose—0.1 M phosphate pH 7.0 buffer solution at 30°C.

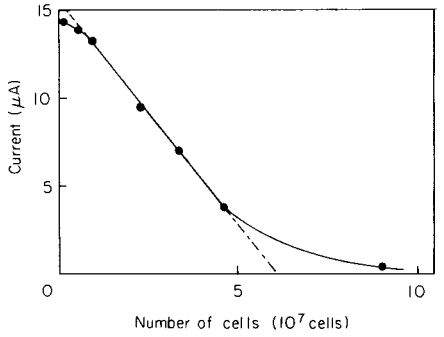

Fig. 3. Relationship between the steady-state current and the number of yeast cells in the electrode membrane, for a 0.1 M phosphate (pH 7.0) buffer containing glucose (500 mg l^{-1}) at 30°C.

Response to nystatin

The time course of the reaction (response curve) is shown in Fig. 4. When the yeast electrode was inserted into the glucose-buffer solution containing nystatin, a steady-state current was obtained and then the current began to increase giving a sigmoidal curve. When the electrode was inserted into the glucose-buffer solution not containing nystatin, no current increase was observed. In the presence of nystatin, the electrode current ultimately reached the level of the electrode in the absence of yeast. The rate of current increase is a measure of the nystatin concentration, and is most easily measured as the linear slope at the mid-point of the sigmoidal curve.

The yeast membrane used in the above experiments was suspended in physiological saline (10 ml), and the number of cells leached into the solution was counted by a hemocytometer (Kayagaki Rika Kogyo Co. Ltd.) and microscope. The total number of living yeast cells on the filter paper had decreased to below 1.0×10^6, indicating that the cell walls of the yeast were disrupted by nystatin.

The relationship between the response time and the nystatin concentration (Fig. 5) showed decreasing response times for increasing amounts of nystatin. As nystatin ($C_{47}H_{75}O_{17}$) is a large molecule (molecular weight 926), it diffuses only very slowly through the collagen membrane. Therefore, several minutes are required to initiate the current increase. Acetylcellulose and nitrocellulose membranes (both 50 μm thick) were also used to cover the yeast membrane, but the response time of the electrode was then longer (>30 min) than that of the collagen membrane. It is possible to determine nystatin on the basis of the response time.

Figure 6 shows that the rate of current increase decreased with increasing pH. However, the response time of the electrode decreased with decreasing pH. The yeast electrode was more sensitive to nystatin at a lower pH, but experiments showed that yeast cells were inactivated at pH 4.0. In the lower

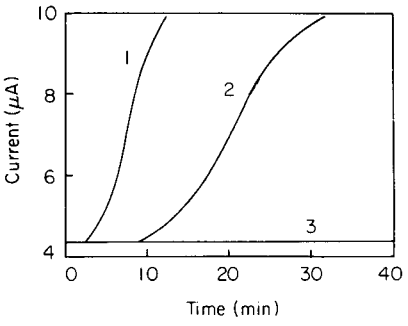

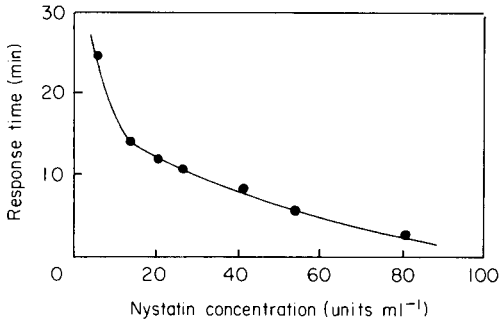

Fig. 4. Response curves obtained under the recommended conditions. The nystatin concentrations were: (1) 81 USP units ml^{-1}; (2) 27 USP units ml^{-1}; (3) zero.

Fig. 5. Relationship between response time and nystatin concentration under the recommended conditions.

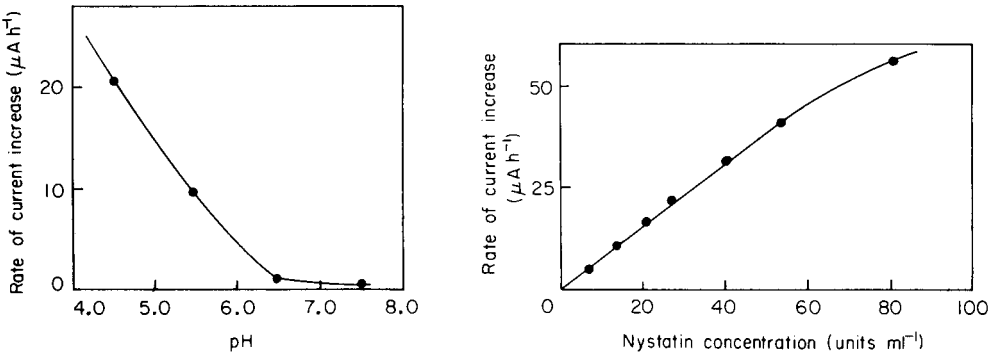

Fig. 6. Effect of pH on rate of current increase, under the recommended conditions except for pH [0.1 M acetate buffer (pH 4.5 and 5.5), 0.1 M phosphate buffer (pH 6.5 and 7.5)]. The solution contained 27 units of nystatin.

Fig. 7. Calibration curve obtained under the recommended conditions.

pH range, mitochondria and glycolytic enzymes easily lose their activities after disruption of the cell wall. Also, no response of the electrode to nystatin was observed at pH 7.5, although mitochondria and glycolytic enzymes retained their activities after disruption of the cell wall under neutral pH conditions. Therefore, pH 4.5 is most suitable for nystatin determination with the yeast electrode.

Figure 7 shows that the relationship between the rate of current increase and the nystatin concentration is linear below 54 units ml^{-1}. The rate of current increase had a standard deviation of 1.2 units ml^{-1} when a sample solution containing 27 units ml^{-1} of nystatin was analysed (30 experiments).

DISCUSSION

Nystatin is active against yeast and fungi, but is ineffective against bacteria and viruses. Therefore, a yeast electrode seemed appropriate for the microbioassay of nystatin.

As shown in Fig. 3, the relationship between the current (I μA) and the number of intact cells (N) in the membrane is given by $I = 11.5 - 2.5 \times 10^{-7} N$. The rate of current increase (in $\mu A\ h^{-1}$) is found by differentiating this equation, so that $dI/dt = -2.5 \times 10^{-7}\ dN/dt$. The rate of cell number decrease is proportional to the nystatin concentration when there is a large number of cells in the membrane, i.e., $-dN/dt = kP$, where P is the nystatin concentration (units ml^{-1}) and k is a constant. Therefore, $dI/dt = 2.5 \times 10^{-7}\ kP\ \mu A\ h^{-1}$, showing a linear relationship between the rate of current increase and the nystatin concentration, as verified experimentally (Fig. 7) where the constant ($2.5 \times 10^{-7}\ k$) was 1.6 $\mu A\ h^{-1}$ $units^{-1}$ ml.

When yeast was entrapped in polymeric matrices such as collagen, poly-

(acrylamide) and agar, the cells were not inactivated by nystatin and did not lose their respiration activity. However, when *Saccharomyces cerevisiae* cells were adsorbed on a filter paper and the paper was covered with a collagen membrane, this prevented the loss of yeast cells without impairing their inactivation by nystatin.

Yeast cells are destroyed by nystatin. Therefore a new yeast membrane is needed for each analysis; but the preparation and exchange of a yeast membrane are very easy and replacement takes only 1 min. Moreover, the yeast cell suspension can be stored for 20 days at 5°C. The electrode current was reproducible to within 5% (in the buffer solution containing 500 mg l^{-1} of glucose) when the yeast membrane used for analysis was replaced with a new membrane prepared from the stored suspension.

The yeast electrode method is different in principle from the conventional diffusion method. Inhibition of growth is measured by the conventional method, whereas inhibition of respiration activity is measured by the electrochemical method. As the respiration of yeast cells is converted immediately to an electrical signal, the microbioassay of nystatin with the yeast electrode can be completed within 1 h. Furthermore, the yeast electrode method employs a homogeneous suspension. Consequently the sensitivity of the yeast electrode is higher than that of the diffusion method; the minimum measurable inhibition concentration is 0.5 unit ml^{-1} by the yeast electrode method and 20 units ml^{-1} by the conventional method. As shown in Fig. 7, the electrode method does not exploit a logarithmic relationship; this generally improves the reproducibility of the results.

The yeast electrode method could well be extended. It could be applicable to the other polyene antifungal antibiotics such as amphterichin, candicidin, filipin and lucensomycin, and antibiotics such as antimycin, oligomycin and rutamycin. If bacteria are used instead of yeasts, the microbioassay of peptide antibiotics such as polymyxin and colistin should also be possible.

REFERENCES

1 J. M. T. Hamilton-Miller, Bacteriol. Rev., 37 (1973) 166.
2 A. I. Laskin and H. A. Lechevalier, Handbook of Microbiology, CRC Press, Ohio, 1973, p. 1026.
3 A. D. Russell and A. Morris, Method in Microbiology, Academic Press, New York, 1969, Vol. VIII, p. 96.
4 A. H. Thomas and S. D. Peters, Analyst, 102 (1977) 333.
5 I. Karube, T. Matsunaga, S. Mitsuda and S. Suzuki, Biotechnol. Bioeng., 19 (1977) 1535.
6 I. Karube, T. Matsunaga and S. Suzuki, J. Solid-Phase Biochem., 2 (1977) 97.
7 I. Karube, S. Mitsuda, T Matsunaga and S. Suzuki, J. Ferment. Technol., 55 (1977) 243.
8 K. Matsumoto, H. Seijo, T. Watanabe, I. Karube and S. Suzuki, Anal. Chim. Acta, 105 (1979) 429.
9 T. Matsunaga, I. Karube and S. Suzuki, Anal. Chim. Acta, 98 (1978) 25.
10 T. Matsunaga, I. Karube and S. Suzuki, Anal. Chim. Acta, 99 (1978) 233.
11 I. Karube, S. Suzuki, S. Kinoshita and J. Mizuguchi, Ind. Eng. Chem. Prod. Res. Develop., 10 (1971) 160.

Analytica Chimica Acta, 109 (1979) 45—54

ISOTHERMAL DISTILLATION IN FLOW INJECTION ANALYSIS
Determination of Total Nitrogen in Plant Material

E. A. G. ZAGATTO, B. F. REIS, H. BERGAMIN Fº* and F. J. KRUG
Centro de Energia Nuclear na Agricultura, CEP 13400 Piracicaba, S. Paulo (Brasil)
(Received 12th March 1979)

SUMMARY

An isothermal distillation unit is incorporated in flow injection systems. The influence of surfactant, flow rates, alkalinity, ionic strength, collector stream pH, reagent concentration and sample volume in ammonia distillation are discussed. A method for the determination of total nitgrogen in plant digests employing Nessler reagent is proposed. This method, based on merging zones approach, is characterized by a sampling rate of 100 samples per hour, a precision better than 3%, a reagent consumption of only 100 μl per sample and virtually no base-line drift. The results agree with those obtained with the indophenol blue colorimetric method. The incorporation of isothermal distillation in flow systems with potentiometric measurement is also described.

Distillation is often used in analytical chemistry, but its incorporation in automated systems is cumbersome. It has been utilized, with temperature gradients, in some of the air-segmented continuous flow analyzers. Isothermal distillation is a slow process and, despite its simplicity, cannot be incorporated in continuous flow analytical systems where a steady state is required. However, analysis by flow injection [1, 2] does not necessarily require the attainment of a steady state. Methods based on incomplete chemical reactions [3], incomplete extractions [4] or even incomplete detection [5] have been already adapted to this methodology.

The aim of this paper is to investigate the feasibility of isothermal distillation in a flow injection system. Some of the factors related to the distillation of ammonia are studied, in order to develop an automated system to analyze for total nitrogen in plant material. Distillation is followed by optical or potentiometric measurement.

The merging zones approach [5—7] is employed to add Nessler reagent in a discrete way so as to avoid base-line drift, which happens when this reagent is added continuously [8], and to diminish reagent consumption.

THEORETICAL CONSIDERATIONS

Some analytical procedures for the determination of ammonium, urea, sulphite and carbonate [9—12] require conversion of the chemical species to

be determined to a gaseous form, and diffusion of this gas towards the detection system. When the gas produced is collected in another liquid phase at the same temperature, the entire process is really an isothermal distillation. This process can be incorporated in flow-injection analytical (f.i.a.) systems by having two separated parallel streams flowing close together.

The donor stream contains the sample zone [1] where the gas has already been produced. As the partial pressure of the gas in this stream is higher than in the surrounding air, it will evaporate. The difference in the partial pressures of the gas in the two streams causes the gas to diffuse towards the stream with the lower partial pressure, where it can be collected. The process is accelerated by keeping the surface of these streams as large as possible and the gap as small as possible. The evaporation becomes faster when the partial pressure of the gas in the donor stream is higher, being accelerated with increase of temperature of this stream, ionic strength, or any physicochemical parameter which increases the partial pressure. Collection is favoured when the partial pressure of the gas is kept as small as possible in the collector stream.

Theoretical discussions about analytical procedures for ammonium and other ions with ion-selective electrodes, in which a steady state is reached, have already been published [13—15]. Those considerations apply only partly to flow injection procedures where a fraction of the species is distilled, and steady states are not reached.

EXPERIMENTAL

Apparatus

A Technicon AAII peristaltic pump furnished with Tygon pumping tubes was employed. The manifold was made from polyethylene tubing (i.d. 0.8 mm) supported by a perspex baseplate, together with a multiple proportional injector [5] and perspex connectors.

The distillation unit (Fig. 1) is a closed chamber and consists of two silicone rubber sheets supported by parallel perspex plates. The distance between the sheets can be adjusted by the screws near the ends of the plates. The exposed width of the silicone rubber strips is 10 mm. The stream containing the sample enters through inlet A, and spreads along one silicone rubber sheet, producing a thin film which passes the entire length of the rubber before going to waste (W). During this transport, the species of interest evaporates and the gas diffuses through the space between the two sheets, being collected in the receptor stream. This receptor stream enters at point B and also produces a thin film, which clings to the rubber sheet by liquid-solid adhesion and is then directed to the measurement unit. In cases where the addition of another reagent is required it is added in a chamber, at point C, and the mixture is aspirated to the detection unit.

For spectrophotometric measurements, a Beckman model 25 double-beam spectrophotometer and a Beckman 24-25 ACC recorder were used. The flow-through cuvette was a 178 Hellma cell (optical path 10 mm, volume 80 μl). The wavelength was set at 410 nm.

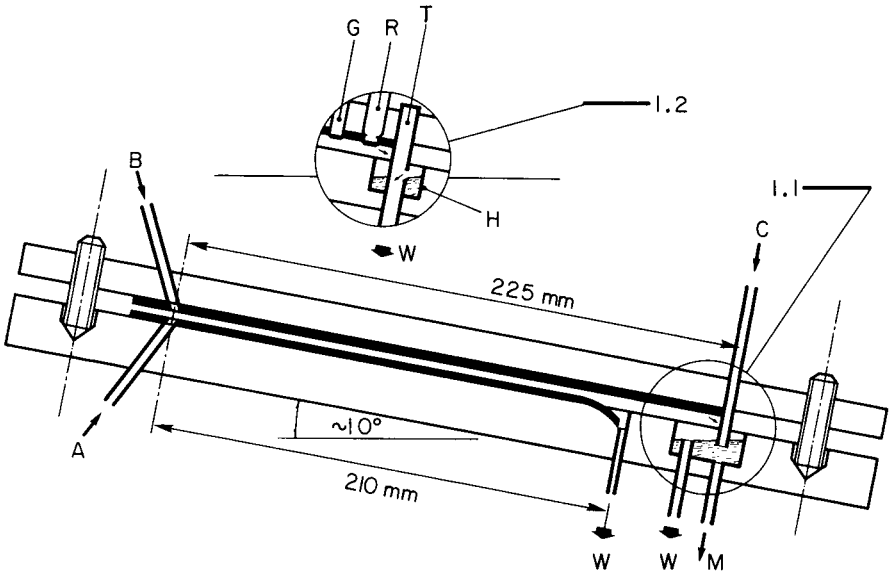

Fig. 1. Cross-section (not to scale) of the distillation units used for spectrophotometry (1.1) or potentiometry (1.2). A, B and C are the inlets for the donor stream, the receptor stream and the reagent, respectively; M is the output to coil C_2 (Fig. 2); W denotes waste; G and R are the glass and reference electrodes; T is a tube closed at one end with a lateral hole, H, of 6 mm diameter. The two heavy black traces represent the silicone rubber sheets (2 × 10 × 225 and 2 × 10 × 210 mm) held by two perspex plates. The distance between the two rubber sheets (ca 1.5 mm) can be adjusted by the screws near the ends of the perspex plates. For details, see text.

For potentiometric measurements a Radiometer assembly was used, consisting of a model 63 pH meter connected to a REC 61 Servograph with a REA 112 high-sensitivity unit, a flat glass electrode and a K401 saturated calomel electrode.

Flow diagrams

The use of isothermal distillation in conjunction with f.i.a. was studied with the systems shown in Fig. 2. The samples were injected at point S, the necessary mixing and addition of alkali was done in coil C_1 and the ammonia produced was partially distilled in unit D. The pumping rates were fixed in order to permit a sampling rate of about 100 samples per hour, with small sample dilution by the confluent streams. The spectrophotometric measurement was made after Nesslerization in coil C_2. Potentiometric measurements were made with a pH electrode, which measured the pH change caused in the collector stream by the collection of ammonia.

Effects of surfactants, flow rates, alkalinity, ionic strength and pH of the collector stream were investigated with the system shown in Fig. 2A. In all cases, 50 μl of a 100-ppm ammonium standard were injected.

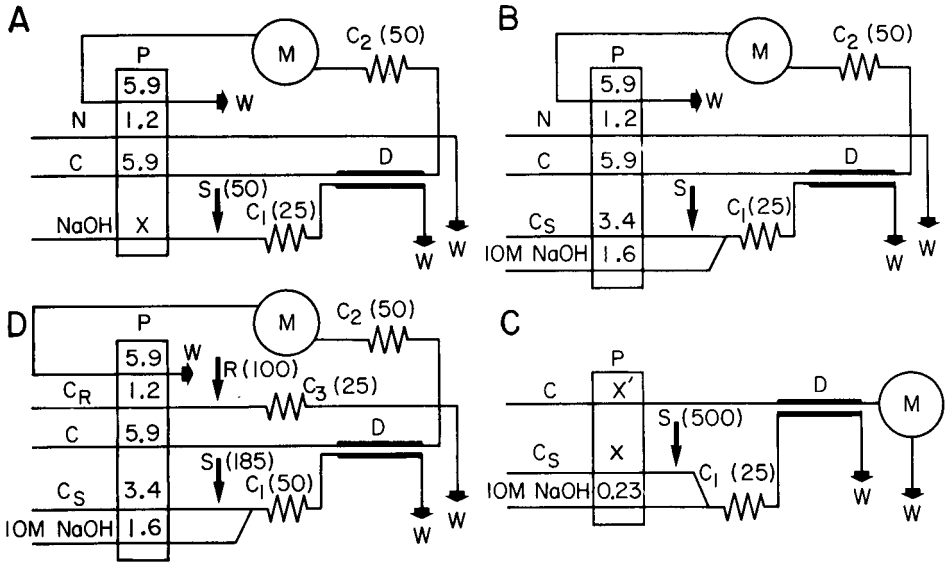

Fig. 2. Flow diagrams of the systems used. P is the peristaltic pump with indication of flow rates, in ml min^{-1}; D is the distillation unit; M is the measurement unit; C_i are coils with lengths (in cm) indicated in parentheses; S and R are the sample and reagent injection ports, with the injected volumes (in μl) indicated; W denotes waste; N is the Nessler reagent; C is the collector stream (10^{-3} M sulfuric acid for spectrophotometry or 1 M KCl for potentiometry); C_S is the sample carrier stream (water) and C_R is the reagent carrier stream (1 M NaOH). For details, see text.

The influence of surfactant was investigated with the collector stream kept at pH 6.0. The sample carrier stream, consisting of 1 M sodium hydroxide solution containing surfactant (0.01%), was pumped at 5.9 ml min^{-1}. Flow rates of the sample carrier stream (1, 2, 3, 4, and 5.9 ml min^{-1}) were investigated with the same system, wetting agent (0.01%) being added to all streams. The concentration of the sample carrier stream (0.0001, 0.0002, 0.0004, 0.001, 0.01, 0.1, 1, 2, 4 and 10 M NaOH) was investigated by pumping this stream at a rate of 5.9 ml min^{-1}. The effect of ionic strength was studied with the latter system; the 0.1 M sodium hydroxide solution was saturated with solid potassium chloride. Finally, the influence of the pH of the collector stream was studied with this system, the sample carrier stream being a 1 M sodium hydroxide solution. The pH variation (1.7, 2.3, 3.4, 4.1, 5.3, 6.3, 7.1, 8.1, 9.4 and 10.9) was done with 1 M sulfuric acid or sodium hydroxide solutions.

The system shown in Fig. 2B was employed in investigations of the effect of injected volume (30, 50, 90, 125, 185 and 250 μl) and reagent concentration (1:2, 1:4 and 1:10 dilutions of Nessler reagent with a 1 M sodium hydroxide solution). The confluence configuration was chosen in order to allow larger volumes to be injected [4]. For each situation, a calibration curve involving the routine plant standards was made.

To calculate the dispersion factor [2], the carrier stream was replaced by the smallest plant routine standard and the absorbance measured was compared with the absorbance corresponding to the injection of 185 μl of the same standard.

The percentage recoveries from distillation were obtained by replacing the sample carrier stream by a standard solution (10 ppm ammonium) and later replacing the collector stream by the same solution. The recovery corresponds to the ratio between the two measured absorbances.

The samples were analyzed with the system shown in Fig. 2D based on the merging zones approach, which requires simultaneous injection of both sample (185 μl) and reagent (100 μl), as indicated in Fig. 3. A delay coil C_3 was necessary for synchronization, and a larger mixing coil C_2 (50 cm long) was used to improve the reproducibility. The reagent carrier stream (C_R) was 1 M sodium hydroxide.

The possibility of using potentiometric measurements after distillation was investigated with the system shown in Fig. 2C. Two situations were tested: (a) the collector stream and the sample carrier stream flowed at similar speeds; and (b) the collector stream was pumped at a much lower rate than the sample carrier stream.

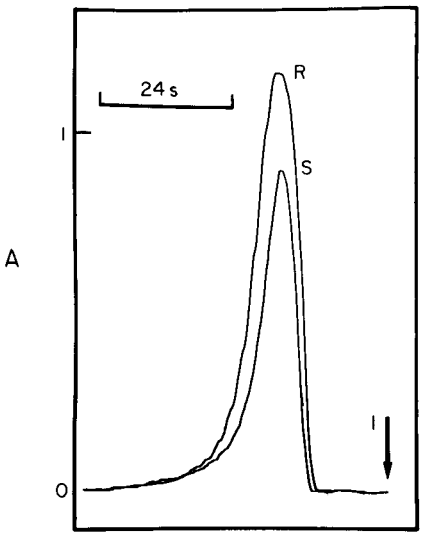

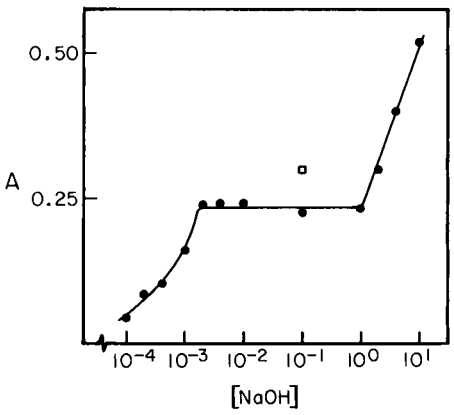

Fig. 3. Recorded peak profiles of sample (S) and reagent (R), injected at instant I in system 2D. For the sample peak, a 5% N-NH_4 standard was employed and the reagent was added continuously. The reagent signal was obtained by replacing the sample carrier stream by a 1% N-NH_4 standard and injecting the Nessler reagent.

Fig. 4. Influence of the sodium hydroxide concentration on the measured signal. Point □ was obtained with addition of solid potassium chloride to the sample carrier stream.

Reagents, samples, standards

All chemicals used were analytical grade. Freshly deionized-distilled water was used. The wetting agent was a household detergent with a very low ammonium content.

Nessler reagent was prepared by dissolving 14 g of potassium iodide in about 40 ml of water with dropwise addition of a 4% (w/v) mercury(II) chloride solution until a slight red precipitate was formed; 100 ml of 10 M sodium hydroxide solution was then added and the volume was made up to 1 l with water. After addition of more mercury(II) chloride, to give a permanent turbidity, the mixture was left for at least one day, decanted and stored in an amber glass bottle.

Plant digests were obtained by sulfuric digestion of foliar material from *Sorghum* spp. in a Technicon BD 40 digester block [16].

The standard stock solution contained 6.288 g of ammonium sulfate per liter (1715 ppm ammonium). Routine plant standards were prepared to correspond to 0, 1, 2, 3, 4 and 5% $N\text{-}NH_4^+$-in the plant material by diluting 0, 1, 2, 3, 4 and 5 ml of the stock solution with water, adding 2.2 ml of concentrated sulfuric acid and making the volume up to 50 ml with water.

RESULTS AND DISCUSSION

The addition of surfactant increased the measured signal by 27%. This increase, which was independent of the amount of the wetting agent (between 0.01 and 1.0%), occurred mainly because of better spreading on the silicone rubber sheets with consequent increase in the exposed surface. The flow rate of the sample carrier stream exerts little influence on the measured signal; for example, when the flow rate was increased from 1.0 to 6.0 ml min^{-1}, the absorbance signal decreased only from 0.240 to 0.205. This is due mainly to two conflicting factors: the available time of distillation and the dilution factor caused by differences between the pumping rates of the streams. A sample carrier stream flowing at 5.9 ml min^{-1} was chosen, since lower fluxes would decrease the sampling rate. More detailed studies on flow rates and injected volumes are now in progress, to establish a method for the analysis of natural waters and soil extracts with low ammonium contents.

The influence of sodium hydroxide concentration on the measured signal is shown in Fig. 4. When the sodium hydroxide concentration is not high enough to provide total conversion of ammonium ion to ammonia, the signal must depend on this concentration. However, if sodium hydroxide concentration is very high, the signal again depends on this concentration, because of the effect of ionic strength. This was confirmed by an increase of 30% in the signal obtained after addition of solid potassium chloride to the sample carrier stream. This increase is due to the decreased solubility of ammonia in the liquid phase on increasing the ionic strength.

Table 1 shows that the pH of the collector stream has a marked influence on the measured signal. When the pH decreases, the chemical equilibrium

TABLE 1

Influence of pH of the collector stream on the measured signal

pH	1.7	2.3	3.4	4.1	5.3	6.3	7.1	8.1	9.4	10.9
A	0.120	0.284	0.280	0.230	0.212	0.200	0.204	0.204	0.152	0.080

favors the conversion of ammonia to ammonium ion, i.e. gas collection is improved. The abrupt decrease in the signal under the more acidic conditions happened because the quantity of sulfuric acid was large enough to decrease significantly the alkalinity of the Nessler reagent, resulting in a loss of sensitivity [8]. It is interesting that even when the pH of the collector stream is higher than the pK value of the ammonia/ammonium system (pK = 9.2), distillation occurs. Preliminary experiments have indicated that the collector stream can be replaced by the Nessler reagent or even by alkaline sodium phenolate solution [17].

The influence of sample volume and reagent concentration on the calibration curves are shown in Fig. 5. When the injected volume was too small or when Nessler reagent concentration was too low, signals were not detected. The linearity of the calibration curve increases with concentration of Nessler

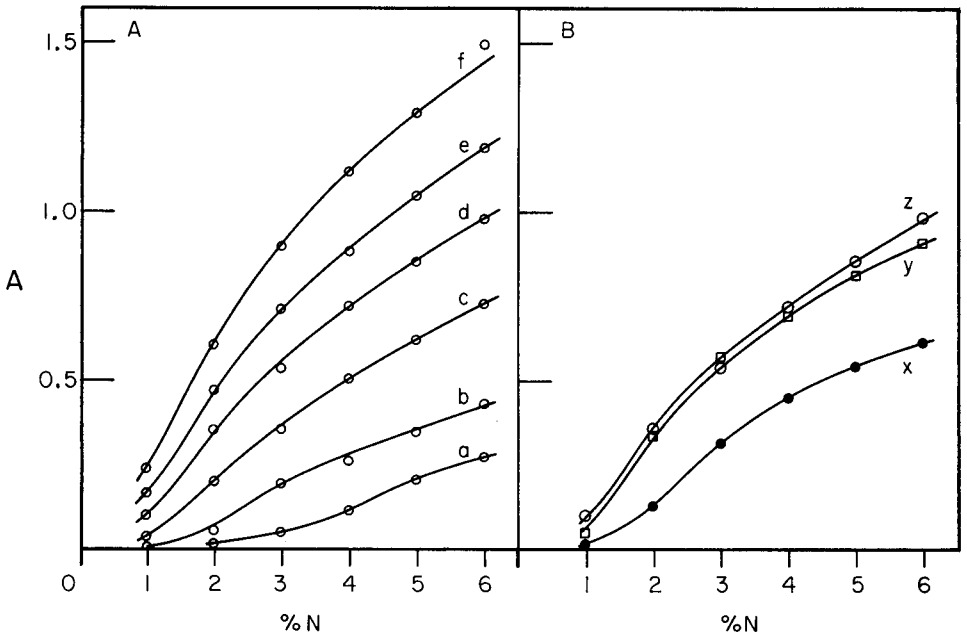

Fig. 5. Influence of sample volume (A) and reagent concentration (B) on the calibration curves. The curves shown in A were obtained with a 1:2 reagent dilution; curves a—f correspond to injected volumes of 30, 50, 90, 125, 185 and 250 μl, respectively. The curves shown in B were obtained with an injected volume of 125 μl; curves x, y and z correspond to reagent dilutions of 1:10, 1:4 and 1:2, respectively. For details, see text.

reagent and sample volume. As a compromise between linearity and convenience, a volume of 185 μl and a 1:2 dilution of the reagent were chosen. In order to utilize the merging zones approach, a more concentrated reagent must be employed, because some dilution always occurs; in this case, the normal Nessler stock solution was used.

The percentage recovery obtained in the distillation was only 11%. Although this is low, it proved adequate for routine analysis because the reproducibility was good; for example, 20 repeated runs of 100 ppm N-NH_4 standard gave a relative standard deviation of only 3% for system 2D. The dispersion factor was 0.16, indicating that better sensitivity could be easily achieved by increasing the sample volume.

Figures 6 and 7 show the feasibility of potentiometric measurement in connection with the proposed technique. Higher sensitivity is achieved when the collector stream is pumped at a very slow speed, which gives concentration of the distilled species in a smaller volume. A similar situation was found earlier in the air-gap electrode design [9].

Figure 8 shows the recording of a routine run for total nitrogen in plant material with the proposed method, and indicates that 100 samples per hour can be analysed with good precision. Table 2 shows a comparison of the results obtained by the proposed method and those obtained by the standard procedure for automatic analysis of ammonia in plant digests [18]. No statistical difference was found at the 1% level.

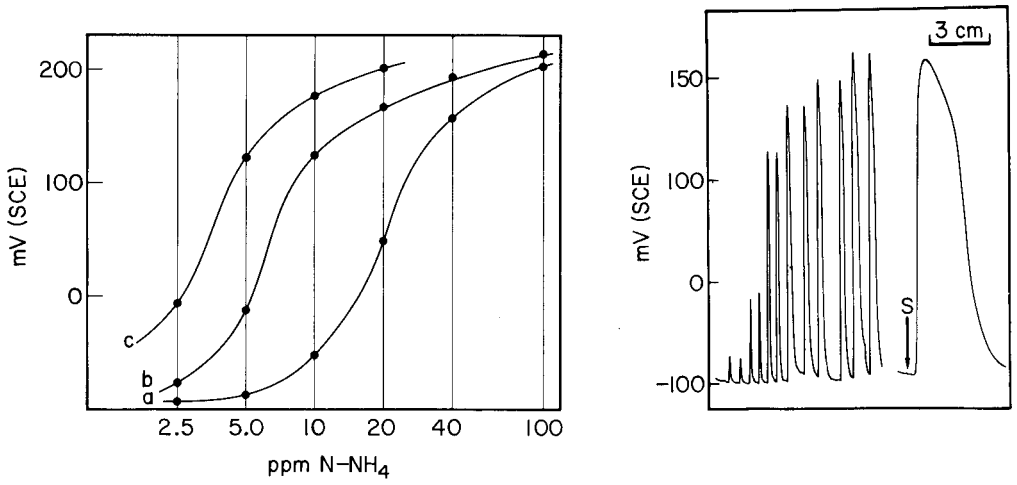

Fig. 6. Calibration curves obtained with the system 2C, and the following pumping rates: (a) $x = x' = 3.0$ ml min^{-1}; (b) $x = 3.0$ and $x' = 0.23$ ml min^{-1}; (c) $x = 0.8$ and $x' = 0.23$ ml min^{-1}.

Fig. 7. Calibration graph obtained with system 2C for the situation indicated in Fig. 6, curve b. From left to right, standards injected in duplicate containing 2.5, 5.0, 10.0, 20.0, 40 and 100 ppm N-NH_4 with a chart speed of 0.5 cm min^{-1}, followed by a recording of the 100 ppm N-NH_4 standard at a paper speed of 2 cm min^{-1}.

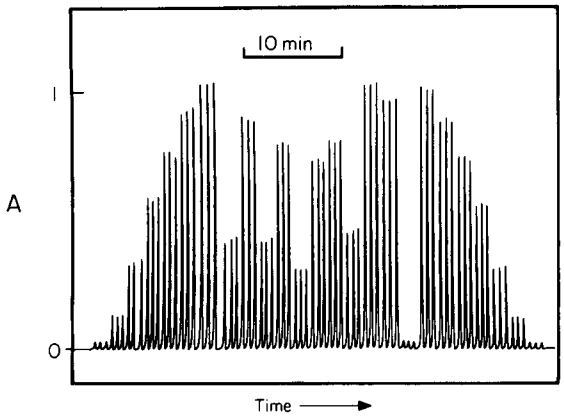

Fig. 8. Routine analysis of digested plant samples, at an average sampling rate of 100 injections per hour. From left to right, a blank, 6 ammonium standards corresponding to (0.5, 1, 2, 3, 4 and 5% N-NH_4 in dry matter), 10 samples, a blank, and the calibration again. All measurements are made in triplicate.

TABLE 2

Results obtained for total nitrogen in *Sorghum* spp by the proposed method (system 2D) and the indophenol blue colorimetric method [18]. Data obtained from triplicate measurements.

Sample	% N (dry weight)		Sample	% N (dry weight)	
	Auto Analyzer	System 2D		Auto Analyzer	System 2D
1	0.80	0.90	7	1.20	1.15
2	2.80	2.80	8	3.90	3.85
3	3.20	3.20	9	5.20	4.90
4	3.45	3.55	10	1.95	2.00
5	1.00	1.00	11	1.10	1.00
6	4.70	4.85	12	4.70	4.75

Partial support of this project by FINEP (Financiadora de Estudos e Projetos, Brasil) is greatly appreciated. The authors thank Otavio Minoru Matsumoto for helping to set up the system, and P. B. Vose for assistance in preparing the manuscript.

REFERENCES

1 J. Růžička and E. H. Hansen, Anal. Chim. Acta, 78 (1975) 145.
2 J. Růžička and E. H. Hansen, Anal. Chim. Acta, 99 (1978) 37.
3 J. Růžička and J. W. B. Stewart, Anal. Chim. Acta, 79 (1975) 79.
4 H. Bergamin F°, J. X. Medeiros, B. F. Reis and E. A. G. Zagatto, Anal. Chim. Acta, 101 (1978) 9.
5 H. Bergamin F°, E. A. G. Zagatto, B. F. Reis and F. J. Krug, Anal. Chim. Acta, 101 (1978) 17.

6 E. A. G. Zagatto, F. J. Krug, H. Bergamin Fº, S. S. Jørgensen and B. F. Reis, Anal. Chim. Acta, 104 (1979) 279.
7 B. F. Reis, H. Bergamin Fº, E. A. G. Zagatto and F. J. Krug, Anal. Chim. Acta, 107 (1979) 309.
8 F. J. Krug, J. Růžička and E. H. Hansen, Analyst, 104 (1979) 47.
9 J. Růžička and E. H. Hansen, Anal. Chim. Acta, 69 (1974) 129.
10 E. H. Hansen and J. Růžička, Anal. Chim. Acta, 72 (1974) 353.
11 E. H. Hansen, H. Bergamin Fº and J. Růžička, Anal. Chim. Acta, 71 (1974) 225.
12 U. Fiedler, E. H. Hansen and J. Růžička, Anal. Chim. Acta, 74 (1975) 423.
13 E. H. Hansen and N. R. Larsen, Anal. Chim. Acta, 78 (1975) 459.
14 M. Mascini and C. Cremisini, Anal. Chim. Acta, 97 (1978) 237.
15 F. van der Pol, Anal. Chim. Acta, 97 (1978) 245.
16 TECHNICON Industrial Method No. 369-75A, 1977.
17 E. H. Hansen, F. J. Krug, A. K. Ghose and J. Růžička, Analyst, 102 (1977) 714.
18 TECHNICON Industrial Method No. 218-72A, 1972.

Analytica Chimica Acta, 109 (1979) 55—60

BIOCHEMICAL CELL FOR THE DETERMINATION OF LACTATE

J. J. KULYS* and G.-J. S. ŠVIRMICKAS

Institute of Biochemistry, Lithuanian Academy of Sciences, Vilnius (U.S.S.R.)

(Received 25th January 1979)

SUMMARY

In the biochemical cell reported, lactate is oxidized by potassium hexacyanoferrate(III) in the presence of cytochrome b_2 as catalyst. The dependence of the steady-state current on the logarithm of the lactate concentration is linear over the range 5×10^{-6}—4×10^{-3} M. The action of the cell is explained in terms of the anolyte equilibrium.

Biochemical cells based on enzymes, multienzyme systems and microorganisms are well known [1—7]. They have found application in the determination of enzyme activity [8—10]. The high selectivity of enzymes also makes it possible to use biochemical cells for the determination of biologically important compounds.

L(+)-lactate is a metabolic product, the concentration of which indicates a certain pathological state in certain organisms. NAD-dependent lactate dehydrogenase [11, 12] and cytochrome b_2 [13] have been used in the construction of amperometric enzyme electrodes for lactate determinations in biochemical solutions. However, the sensitivity of these electrodes is low because their action is governed by steady-state requirements [14].

The present paper describes a biochemical cell based on cytochrome b_2 for L(+)-lactate determination. The system is 100 times more sensitive than that described by Racine et al. [13].

EXPERIMENTAL

Cell preparation

A biochemical cell was constructed from two glass cylinders (14 mm diameter, 60 mm high). The top of each cylinder was capped with a Teflon plug having apertures for a salt bridge, electrodes, and capillaries for gas bubbling and introduction of reagents. The salt bridge was made from a glass tube (1.0 mm i.d.) filled with a gel of 20% gelatin in the buffer solution. A platinum electrode (P-101; surface area 56.2 mm^2; Radiometer, Denmark) was placed in each chamber. The volume of solution in each chamber was 7.0 ml. The anolyte consisted of the buffer, lactate, potassium hexacyanoferrate(III) and enzyme; the catholyte was potassium hexacyanoferrate(III) in the same

buffer. Both solutions were stirred by bubbling nitrogen. The cell was thermostatted at 25 ± 0.10°C in a water bath.

Apparatus and procedure

The cell current was measured with a polarograph (LP-7, Czechoslovakia) at zero potential applied between the electrodes. During the experiment the resistance of the external circuit was 3.25 kohm. At the beginning of the experiment, buffer solution containing hexacyanoferrate(III) was poured into both chambers and allowed to stand for 5 min. Enzyme solution (0.13 ml) was added to the anolyte and a constant current was allowed to establish itself. The reaction was then initiated by the introduction of the lactate solution (0.15 ml) into the anolyte.

The lactate concentrations quoted below refer to the solution in the cell.

Materials

Cytochrome b_2 was prepared (at the All-Union Research Institute of Applied Enzymology, Vilnius), from *Hansenula anomala* [15] with an activity of 50—70 unit mg^{-1}; 1 unit of enzyme activity corresponds to the initial rate of reduction of 1 mmol hexacyanoferrate(III) at pH 7.2. The other stock solutions were a 0.1 M phosphate buffer (pH 7.2), a 1 mM potassium hexacyanoferrate(III) solution in the buffer, and a 10 mM solution of lithium L(+)-lactate (from the G.D.R. collection) in the buffer.

RESULTS

On the introduction of cytochrome b_2 into the anolyte containing hexacyanoferrate(III), a small current flows in the external circuit which quickly becomes constant (Fig. 1). Subsequent addition of lactate to the anolyte leads to a further increase in the current which reaches its maximal value after 3—15 min. The maximal value is retained for a longer time when the hexacyanoferrate(III) concentration exceeds 0.5 mM, than at lower hexacyanoferrate(III) concentrations. The lower the hexacyanoferrate(III) concentration, the quicker the decrease of the current (Fig. 1).

Above 0.5 mM hexacyanoferrate(III) there is a linear dependence of the constant maximal current on the initial lactate concentration when plotted in semilogarithmic coordinates (Fig. 2). The sensitivity is better than 5 μM lactate. Changes in enzyme concentration over the range 0.07—0.7 unit ml^{-1} do not alter the steady-state value of the current. On changing the concentration of hexacyanoferrate(III) in the anolyte and catholyte from 74 μM to 6.9 mM, the steady-state current passes through a maximum (Fig. 3) at 0.3 mM hexacyanoferrate(III) in the presence of 0.21 mM lactate in the anolyte.

The rate of cell current change shows a complex dependency on enzyme and hexacyanoferrate(III) concentrations (Figs. 4, 5). Increase of enzyme concentration increases the rate of increase of the cell current (Fig. 4). However, the rate declines sharply when the concentration of hexacyanoferrate(III)

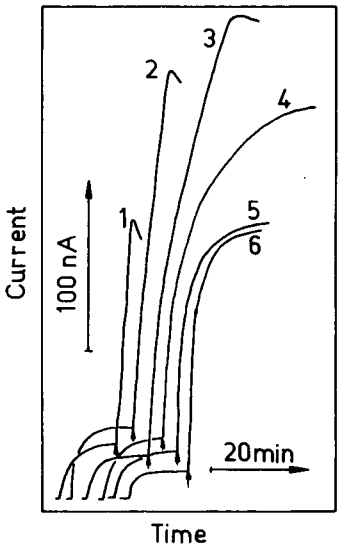

Fig. 1. Variation of biochemical cell current with time. Potassium hexacyanoferrate(III) concentrations in the anolyte and catholyte: (1) 7.4×10^{-5} M, (2) 1.4×10^{-4} M, (3) 2.9×10^{-4} M, (4) 5.7×10^{-4} M, (5) 1.1×10^{-3} M, (6) 6.9×10^{-3} M. Lactate, 2.1×10^{-4} M, enzyme, 0.06 units ml^{-1}. The arrows indicate the time of lactate introduction.

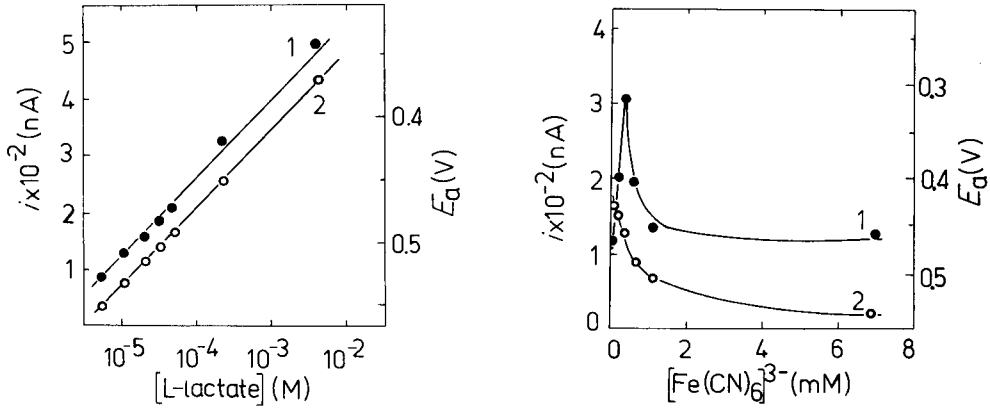

Fig. 2. Dependence of (1) maximal current and (2) calculated anode equilibrium potential on lactate concentration. Potassium hexacyanoferrate(III) in the anolyte: (1) 6.9×10^{-5} M, (2) 2×10^{-2} M, and in the catholyte, 6.9×10^{-3} M. Enzyme, 0.06 units ml^{-1}.

Fig. 3. Variation of (1) maximal current and (2) calculated anode equilibrium potential with hexacyanoferrate(III) concentration in the anolyte and catholyte. Experimental conditions for curve (1) are as in Fig. 1; for curve (2), 2×10^{-6} M lactate is present.

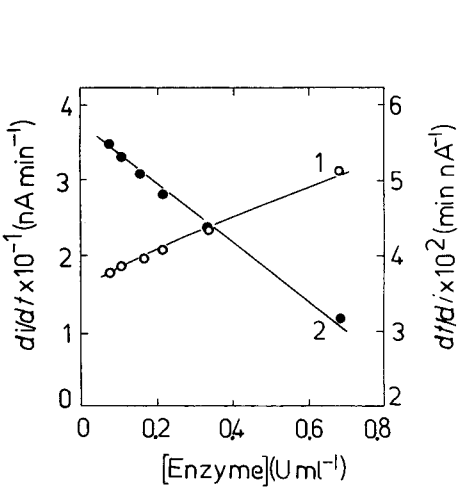

Fig. 4. Dependence of (1) the rate of cell current change and (2) its reciprocal value on enzyme concentration in the anolyte. 1.4×10^{-3} M potassium hexacyanoferrate(III) in the anolyte and catholyte; 2.1×10^{-4} M lactate. The rate is determined at the end of the first minute after introduction of lactate.

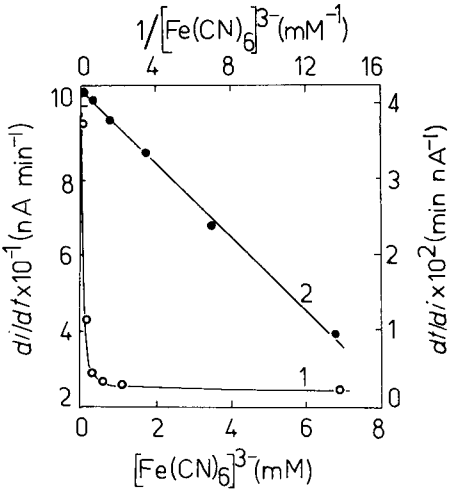

Fig. 5. (1) Dependence of the rate of cell current change on potassium hexacyanoferrate(III) concentration in the anolyte (and catholyte) and (2) linearization of data in inverse coordinates; 2.1×10^{-4} M lactate; 0.06 unit ml^{-1} enzyme. The rate of the cell current change is determined as in Fig. 4.

is raised from 74 to 570 μM; at high concentrations ($\geqslant$1 mM) it becomes steady (Fig. 5).

DISCUSSION

Cytochrome b_2 catalyzes the oxidation of L(+)-lactate by electron acceptors [15]. For hexacyanoferrate(III), the reaction can be expressed as

$$CH_3CH(OH)COO^- + 2Fe(CN)_6^{3-} \rightleftharpoons CH_3COCOO^- + 2Fe(CN)_6^{4-} + 2H^+$$

The equilibrium lies far towards pyruvate formation, since the standard redox potentials for the lactate and hexacyanoferrate system are -0.19 and 0.36 V, respectively, at pH 7.0 and 25°C [10, 16].

Hexacyanoferrate(II) formed in the anolyte is oxidized electrochemically at the anode; the electrochemical reduction of hexacyanoferrate(III) takes place at the cathode. Estimation of the enzymatic reaction rate in the anolyte indicates that at lactate concentrations above K_m (K_m = 1.3 mM [15]), 0.4—5 μmol of hexacyanoferrate(III) is reduced per minute. The highest values of the cell current do not exceed 0.5 μA which corresponds to the conversion of 0.31 neq min^{-1} of the acceptor. It follows that the rate of the enzymatic reaction considerably exceeds the rate of the electrochemical process. Conse-

quently, the constant cell current is determined by the anode equilibrium potential. Since the hexacyanoferrate couple is a reversible redox system having a high exchange current [17], it can be assumed that the anode and cathode do not polarize at low external currents. The value of the current (i_m) therefore depends on the difference of the electrode potentials and the cell resistance (r), i.e., $i_m = (E_c - E_a)/r$.

When the steady-state current is measured at high hexacyanoferrate(III) concentrations in the catholyte, E_c is constant; thus the value of the constant current and the rate of current change are determined by the anode potential. This is supported by the fact that the constant current does not depend on the enzyme concentration. It is also confirmed by the logarithmic dependence of the calculated anode potential on the initial concentration of lactate, thus obeying the Nernst equation (Fig. 2).

The dependence of the maximal constant current on the hexacyanoferrate(III) concentration is also determined by the anode equilibrium potential. The decrease in the initial hexacyanoferrate(III) concentration in the anolyte must result in a more negative equilibrium potential of the anode and in a greater external current. This conclusion is in agreement with the calculated values of anode equilibrium potentials at different hexacyanoferrate(III) concentrations in the anolyte (Fig. 3).

To explain the dependence of the rate of current change on enzyme and hexacyanoferrate(III) concentrations, the Nernst equation for the anode equilibrium potential must be differentiated:

$$-dE_a/dt = [RTF^{-1}]\,[b_0/(b_0 - X)X]\,dX/dt$$

where b_0 is the initial hexacyanoferrate(III) concentration, X is the hexacyanoferrate(II) and t is the time. At low degrees of substrate conversion and when $b_0 > K'_m$ (K'_m = 5—10 μM [18] for hexacyanoferrate(III)) the formation of hexacyanoferrate(II) may be expressed by the simplified Michaelis—Menten equation $X = k_c e_0 t$ where k_c and e_0 are the catalytic constant and total enzyme concentration, respectively. From the two previous equations, the dependence of anode potential change on the concentration of enzyme and ferricyanide is given by

$$V = -dE_a/dt = [RT/Ft]\,[b_0/(b_0 - k_c e_0 t)] = di_m/rdt$$

(This equation cannot be used when $X = k_c e_0 t \to 0$ because of the uncertainty of the potential in the Nernst equation.) Thus the reciprocal of the rate of current change at the fixed initial time is directly proportional to the enzyme activity and inversely proportional to the initial hexacyanoferrate(III) concentration, i.e. $V_{rel}^{-1} = 1 - k_c e_0 t/b_0$, where $V_{rel} = -(Ft/RT) \cdot (dE_a/dt)$.

Experimental data concerning the dependence of the rate of current change on the enzyme concentration fit the last equation well (Fig. 4). If the initial hexacyanoferrate(III) is changed, the experimental data still obey this equation (Fig. 5).

The small current that appears in the absence of substrate on the intro-

duction of enzyme into the hexacyanoferrate(III) solution (Fig. 1) is not due to lactate impurity. This was checked by dialysis of the enzyme solution and by repeated precipitation of cytochrome b_2 with ammonium sulphate. Calculations showed that this current might be due to the oxidation of active sites of reduced cytochrome b_2, usually isolated in such a form to increase stability. Consequently, with cytochrome b_2 in the oxidized form the lower sensitivity limit of the cell may reach 10^{-7}—10^{-8} M lactate.

REFERENCES

1 L. Siesler, New Scientist, 256 (1964) 110.
2 M. Cenek, Chem. Listy, 62 (1968) 927.
3 L. B. Wingard, C. C. Liu and N. L. Nagda, Biotechnol. Bioeng., 13 (1971) 629.
4 H. A. Videla and A. J. Arvia, Biotechnol. Bioeng., 17 (1975) 1529.
5 M. K. Weibel and C. Dodge, Arch. Biochem. Biophys., 169 (1975) 146.
6 S. D. Varfolomeev, A. I. Yaropolov, I. V. Berezin, M. R. Tarasevich and V. A. Bogdanovskaya, Bioelectroch. Bioenergetics, 4 (1977) 314.
7 J. J. Kulys and K. B. Kadziauskienė, Dokl. Akad. Nauk SSSR, 239 (1978) 636.
8 T. Yagi, M. Goto, K. Nakano, K. Kimura and M. Inokuchi, J. Biochem., 78 (1975) 443.
9 K. Nakano, K. Kimura, M. Inokuchi and T. Yagi, J. Biochem., 78 (1975) 1347.
10 T. C. Wallace and R. W. Coughlin, Biotechnol. Bioeng., 20 (1978) 1407.
11 W. J. Blaedel and R. A. Jenkins, Anal. Chem., 48 (1976) 1240.
12 A. Malinauskas and J. J. Kulys, Anal. Chim. Acta, 98 (1978) 31.
13 Ph. Racine, H.-O. Klenk and K. Kochsiek, Z. Klin. Chem. Klin. Biochem., 13 (1975) 533.
14 L. D. Mell and J. T. Maloy, Anal. Chem., 47 (1975) 299.
15 A. Baudras and A. Spyridakis, Biochimie, 53 (1971) 943.
16 F. Labeyrie, L. Naslin, A. Curdel and R. Wurmser, Biochim. Biophys. Acta, 41 (1960) 509.
17 J. E. B. Randles and K. W. Somerton, Trans. Faraday Soc., 48 (1952) 937.
18 M. Iwatsubo, M. Mével-Ninio and F. Labeyrie, Biochemistry, 16 (1977) 3558.

Analytica Chimica Acta, 109 (1979) 61—66

NAPHTHYLDIAZOALKANES AS DERIVATIZING AGENTS FOR THE HIGH-PERFORMANCE LIQUID CHROMATOGRAPHIC DETECTION OF FATTY ACIDS†

DUANE P. MATTHEES

Organic Analytical Research Division, National Bureau of Standards, Washington, D.C. 20234 (U.S.A.)

WILLIAM C. PURDY*

Department of Chemistry, McGill University, Montreal, Quebec H3A 2K6 (Canada)

(Received 2nd February 1979)

SUMMARY

The use of naphthyldiazoalkanes as derivatizing agents in the h.p.l.c. separation of fatty acids from C_{10} to C_{18} is described. Esterification is relatively rapid under mild conditions, and the progress of the reaction can be monitored by the color changes. Derivatization by 1-naphthyldiazomethane or 1-(2-naphthyl)-diazoethane is recommended; 1-(4-biphenylyl)-diazoethane shows some promise in the separation of short-chain fatty acids. The fatty acid profiles of butterfat, margarine, and castor oil are reported.

In recent years there has been a revival of interest in the analytical separation of fatty acids by liquid chromatography. Reversed-phase high-performance liquid chromatography (h.p.l.c.) is eminently suited for the separation of fatty acids, and the only real problem has been the detection of the eluting compounds. The most widely adopted method of detection is derivatization of the fatty acid with a strongly absorbing chromophore, followed by column separation and ultraviolet absorbance detection. The derivatizing agents used for this purpose have included arylacyl halides [1—3], methoxyaniline [4], tolyltriazine reagents [5], and substituted isoureas [6]. While these reagents are sufficiently reactive to give good yields, most of the procedures require heating for complete reaction. Moreover, there is no easy way of determining whether enough derivatizing agent has been added if the amount of fatty acid in a sample is unknown.

Diazomethane is a valuable reagent for the synthesis of methyl esters in high yield under mild conditions [7]. In an attempt to combine the advantage of diazomethane with suitable u.v. chromophores, several aryldiazoalkanes were examined as derivatizing agents for fatty acids. The aryldiazoalkanes are relatively easy to synthesize from readily available compounds, they react quickly at room temperature to give high yields of the corresponding esters, they are

†Taken in part from the Ph.D. Dissertation of D. P. Matthees, University of Maryland, 1978.

compatible with many organic solvents, and anhydrous reaction conditions are not necessary. Moreover, these compounds are intensely colored but become light yellow on reaction with acids, thus giving an indication of the extent of reaction and of the presence of sufficient reagent.

EXPERIMENTAL

Apparatus, reagents and solvents

The chromatographic equipment used included a Model 6000A pump, U6K injector, and Model 440 ultraviolet absorbance detector (254 nm) (Waters Associates, Milford, Mass.). A variable wavelength detector (Spectroflow; Schoeffel Instrument Division, Westwood, N.J.) was also used. The column packing was C_{18} μBondapak (30 cm long; Waters Associates).

The fatty acids were obtained from Applied Science Laboratories (State College, Pa.); other organic compounds and the solvents were obtained from the Fisher Scientific Company, Mallinckrodt, Inc., and Aldrich Chemical Company. Solvents were analytical-reagent grade, redistilled in glass, the first and last 10% being discarded. Water was twice-distilled, an all-glass apparatus being used for the second distillation. All solvents were filtered through 0.45-μm filters before use.

Aryldiazoalkane synthesis

Both 1-naphthyldiazomethane and 1-(2-naphthyl)-diazoethane were found to be suitable derivatizing agents because of the ease of synthesis and good chromophoric properties. These were made from the hydrazones of 1-naphthaldehyde and 2-acetonaphthone, respectively, as described by Miller [8] and Nakaya et al. [9]. A typical aryldiazoalkane preparation involved the oxidation of 2—5 g of hydrazone to the corresponding aryldiazoalkane. The solution was concentrated to about 5—15% diazoalkane in the desired solvent, so that a preparation amounted to 10—40 ml of reagent depending on the amount of starting material. Solutions of the naphthyldiazoalkanes in hexane or ether solvent are stable for several days. Old solutions can be purified by evaporation of solvent, extraction of the diazoalkane with hexane (which leaves most impurities behind), and concentration of the hexane solution.

1-(4-Biphenylyl)diazoethane was prepared from the hydrazone of 4-acetylbiphenyl by the methods described above. It was hoped that this reagent would be particularly suitable for certain applications, such as the short-chain acids, but it proved to be difficult to obtain in good yield.

Derivatization

The fatty acids (glycerides and salts do not react with the diazoalkanes under these conditions) were dissolved in hexane, chloroform, or ether (1—3 mg in about 0.5 ml of solvent) and the solutions were mixed with several drops of an ether or hexane solution of the naphthyldiazoalkane at room temperature in a graduated glass-stoppered tube (usually 1 ml). Nitrogen evolved, and

if the reddish color of the naphthyldiazoalkane disappeared, more was added so that the solution remained red for at least 1 h; this ensured complete reaction. After derivatization, the solution was diluted to the mark with the relevant solvent. An aliquot (2—5 μl) of the solution was injected directly into the liquid chromatograph without further treatment.

Chromatographic conditions

Both aqueous acetonitrile and aqueous methanol were used for elution of the fatty acid derivatives. With the C_{18} μBondapak column employed, 85:15 mixtures of acetonitrile—water and methanol—water were suitable for elution of the derivatives of the fatty acids containing 10—18 carbon atoms, i.e. the most important fatty acids. For a wider range of chain lengths, gradient elution would be desirable. A flow rate of 1.5 ml min^{-1} was used in nearly all instances.

RESULTS AND DISCUSSION

In the following discussion, fatty acids will be abbreviated by two numbers, the first designating the number of carbon atoms and the second the number of double bonds. Thus, lauric (dodecanoic) acid is referred to as $C_{12:0}$, and linoleic (octadecadienoic) acid as $C_{18:2}$.

Figures 1 and 2 show the separation of a mixture of saturated and unsaturated fatty acid derivatives with an aqueous acetonitrile eluent and an aqueous methanol eluent, respectively. (In these Figures, increasing amounts of the fatty acids were used to maintain similar peak heights despite the changing molecular weight.) Sharper, narrower peaks are obtained with aqueous acetonitrile, but there is an overlap of $C_{16:0}$ and $C_{18:1}$. If aqueous methanol is used, this pair resolves, but $C_{14:0}$ overlaps $C_{18:3}$. Both the 1-naphthyldiazomethane and the 1-(2-naphthyl)-diazoethane derivatives give essentially the same chromatographic results. Unfortunately, the peaks related to excess of reagent and decomposition products tend to obscure the short-chain acid derivatives. This difficulty can be partially solved by derivatization of these acids with 1-(4-biphenylyl)diazoethane in hexane. Under these conditions, much of the interfering material precipitates and the derivatives are retained for long enough so that fatty acids as short as $C_{4:0}$ can be detected (Fig. 3). This reagent should prove to be quite useful for fatty acid analysis when conditions for its synthesis have been optimized.

The naphthyl derivatives permit the detection of ca. 10 ng (30—40 pmol) of fatty acid, when the fixed wavelength detector and a column of about 3000 theoretical plates are used. Since all derivatives possess the same chromophore, the peak area is proportional to the number of moles of acid reacted.

Figures 4—6 show the fatty acid profiles of samples of butterfat, a margarine, and castor oil, respectively. These samples were saponified by the method of Christie [10], except that the unsaponifiable matter, which would be expected only in minute amounts in these samples, was not removed. The saponification mixture was then acidified and the free fatty acids extracted

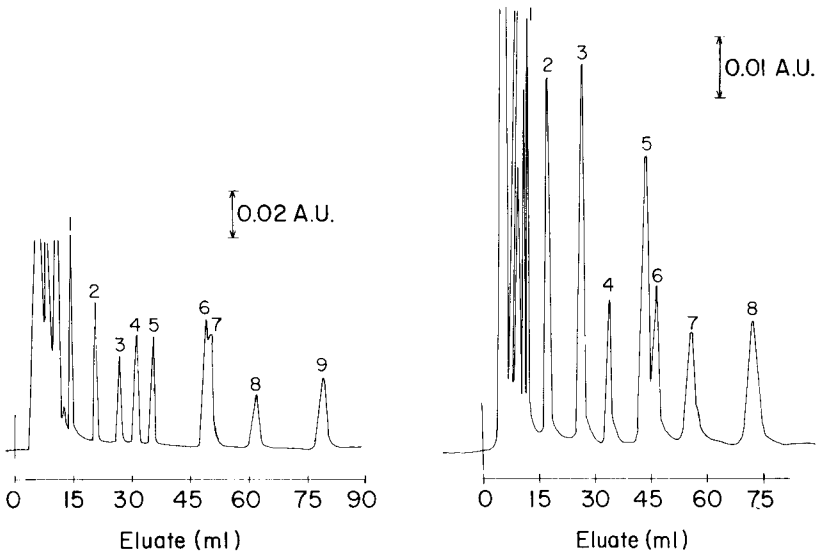

Fig. 1. Separation of the 1-(2-naphthyl)-diazoethane derivatives of a fatty acid mixture. About 4—8 μg of each acid was derivatized. Mobile phase, 85:15 acetonitrile—water; flow rate, 1.5 ml min^{-1}; detection at 254 nm (Waters). Fatty acids corresponding to numbered peaks: (1) 10:0, (2) 12:0, (3) 18:3, (4) 14:0, (5) 18:2, (6) 16:0, (7) 18:1, (8) 17:0, (9) 18:0.

Fig. 2. Separation of the 1-naphthyldiazomethane derivatives of the same fatty acids as above. About 5—12 μg of each acid was derivatized. Mobile phase, 85:15 methanol—water; flow rate, 1.5 ml min^{-1}; detection at 260 nm (Schoeffel). Fatty acids corresponding to numbered peaks: (1) 10:0, (2) 12:0, (3) 14:0 and 18:3, (4) 18:2, (5) 16:0, (6) 18:1, (7) 17:0, (8) 18:0.

with hexane, chlororform, or ether. Excess of mineral acid was removed by a water wash prior to derivatization of the fatty acids. The fatty acids in these samples were identified by comparison of the retention times of the derivatives with authentic standard fatty acid derivatives. The separation of the *cis* and *trans* isomers of $C_{18:1}$ in Fig. 5 is noteworthy; the *trans* isomer is an artifact of catalytic hydrogenation of vegetable oils. Figure 6 illustrates the marked effect of polar functional groups on the retention of fatty acids. Ricinoleic acid, the major constituent of castor oil, is an hydroxylated $C_{18:1}$ acid, and although it has a relatively long carbon chain, it elutes before any of the other acids in that mixture.

Since the aryldiazoalkanes may be synthesized from a variety of readily available aryl aldehydes and ketones, there is considerable flexibility in the type of derivatizing agent that can be prepared. The type of substituent groups introduced affects not only the absorption maximum and molar absorptivity, but also the reactivity and stability of the diazoalkane.

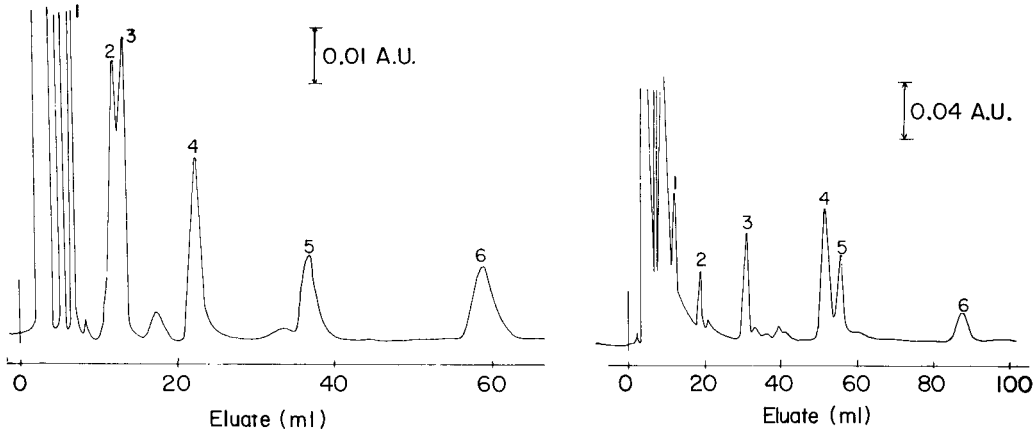

Fig. 3. Separation of 1-(4-biphenylyl)diazoethane derivatives of short-chain fatty acids. About 6 μg of each acid was derivatized. Mobile phase, 75:25 methanol—water; flow rate, 1.5 ml min^{-1}; detection at 254 nm (Waters). Fatty acids corresponding to numbered peaks: (1) n-4:0, (2) iso-5:0, (3) n-5:0, (4) n-6:0, (5) n-7:0, (6) n-8:0.

Fig. 4. Fatty acid profile of butterfat. Mobile phase, 85:15 methanol—water; flow rate, 1.5 ml min^{-1}; detection at 254 nm (Schoeffel). Fatty acids corresponding to numbered peaks: (1) 10:0, (2) 12:0, (3) 14:0 and 18:3, (4) 16:0, (5) 18:1, (6) 18:0. Injection of 5 μl corresponding to 100 μg of butterfat.

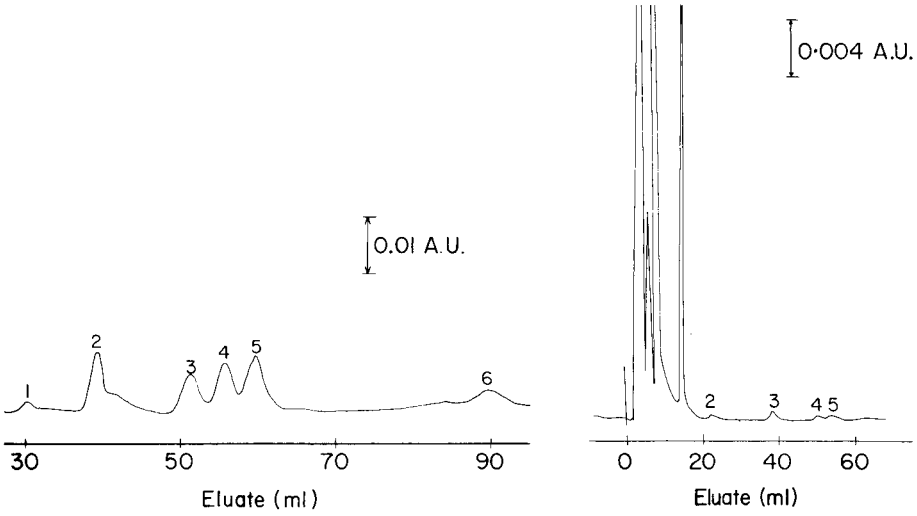

Fig. 5. Fatty acid profile of a margarine. Mobile phase, 90:10 methanol—water; flow rate, 1.5 ml min^{-1}; detection at 254 nm (Waters). Peaks: (1) 14:0 and 18:3, (2) 18:2, (3) 16:0, (4) 18:1, *cis*, (5) 18:1, *trans*, (6) 18:0. Injection of 1 μl corresponding to 50 μg of margarine.

Fig. 6. Fatty acid profile of castor oil. Mobile phase 85:15 methanol—water; flow rate, 1.5 ml min^{-1}; detection at 254 nm (Schoeffel). Fatty acids corresponding to numbered peaks: (1) ricinoleic, (2) 12:0, (3) 18:2, (4) 16:0, (5) 18:1. Injection of 2 μl corresponding to 20 μg of castor oil.

REFERENCES

1 M. J. Cooper and M. W. Anders, Anal. Chem., 46 (1974) 1849.
2 H. D. Durst, M. Milano, E. J. Kitka, Jr., S. A. Connelly and E. Grushka, Anal. Chem., 47 (1975) 1797.
3 R. F. Borch, Anal. Chem., 47 (1975) 2437.
4 N. E. Hoffman and J. C. Liao, Anal. Chem., 48 (1976) 1104.
5 I. R. Politzer, G. W. Griffin, B. J. Dowty and J. L. Laseter, Anal. Lett., 6 (1973) 539.
6 D. R. Knapp and S. Krueger, Anal. Lett., 8 (1975) 603.
7 K. Blau and G. S. King (Eds.), Handbook of Derivatives for Chromatography, Heyden, London, 1978, p. 49.
8 J. B. Miller, J. Org. Chem., 24 (1959) 560.
9 T. Nakaya, T. Tomomoto and M. Imoto, Bull. Chem. Soc. Jpn., 40 (1967) 691.
10 W. W. Christie, Lipid Analysis, Pergamon Press, Oxford, 1973, p. 86.

Analytica Chimica Acta, 109 (1979) 67—72

ANALYTICAL APPLICATIONS OF TRIETHYLENETETRAMINEHEXAACETIC ACID
Part 3**. Amperometric Determination of Calcium in Alkali Metal Salts

STANISŁAW RUBEL* and MAREK WOJCIECHOWSKI

Institute of Fundamental Problems in Chemistry, University of Warsaw, Warszawa (Poland)

(Received 25th January 1979)

SUMMARY

Triethylenetetraminehexaacetic acid (TTHA) is proposed for the amperometric titration of small amounts of calcium in strongly alkaline medium. The reduction current of added lead(II) ions serves to indicate end-points; at pH 13 the Ca—TTHA complex is more stable than Pb—TTHA. Oxygen need not be removed when square-wave polarography is used to measure the indicator current. More than 10^{-4}% of calcium can be determined in NaOH, KOH, $NaClO_4$ and $LiClO_4$ (analytical grade) with good precision. Atomic absorption spectrometry was used to obtain comparative results, but the amperometric method was more satisfactory.

The determination of calcium in chemicals is an important aspect in their purity control. Direct determination of traces of calcium in the presence of large amounts (10^4—10^6) of sodium or potassium ions is rather difficult. Spectrography [1], fluorimetric titration (for $>10^{-3}$% Ca) [2], atomic absorption spectrometry [3—5] and amperometric titration with EDTA [6, 7] have been suggested.

In this paper, TTHA as titrant is recommended for the amperometric titration of small amounts of calcium. The reduction current of lead(II) ions in strongly alkaline medium was used as the indicator current; this has advantages over the reduction current of Zn(II) ions.

EXPERIMENTAL

Apparatus

A d.c. polarograph (Model LP-60a, Laboratorni Pristroje) and a square-wave (s.w.) polarograph (Model OH-104, Radelkis) were used. The dropping mercury electrode had the following characteristics: m = 2.98 mg Hg s^{-1}, t = 3.2 s in 0.1 M KCl without applied voltage for h = 70 cm. The indicator current in amperometric titrations was measured by d.c. polarography with a d.m.e.—s.c.e. electrode system; and by s.w. polarography with a d.m.e.—s.c.e.—Pt electrode system.

**Part 2: Anal. Chim. Acta, 104 (1979) 215.

A Perkin-Elmer model 306 atomic absorption spectrometer was also used.

Reagents

A 1.0×10^{-2} M solution of triethylenetetraaminehexaacetic acid (Fluka) and 1.0×10^{-2} M solutions of calcium(II), lead(II) and zinc(II) nitrates, were prepared. The hydrochloric acid was purified by isopiestic distillation.

All reagents were of analytical grade (POCh) and water was triple-distilled from quartz apparatus.

Preliminary tests

A comparison of the stability constants of the Ca(II), Zn(II) and Pb(II) complexes with TTHA (Fig. 1) shows that the calcium complex is more stable than those of lead and zinc at pH 13. Thus during titrations of Ca—Pb or Ca—Zn mixtures with TTHA the calcium complex is formed first in 0.1 M NaOH solutions. The curves of the changes in the Pb(II) or Zn(II) reduction current during titration confirm this order of stability. Addition of TTHA to a mixture of calcium and lead ions in 0.1 M NaOH does not change the lead current until calcium has completely reacted; lead then forms the TTHA complex and the current decreases. The titration curve (Fig. 2) shows two inflections, the first corresponding to the end-point of the calcium titration and the second to the total amount of calcium and lead.

The reduction current of zinc(II), changes similarly, during titration of calcium and zinc mixtures in 0.1 M NaOH; thus either lead(II) or zinc(II) can serve as the indicator. The concentration of added indicator ion depends on

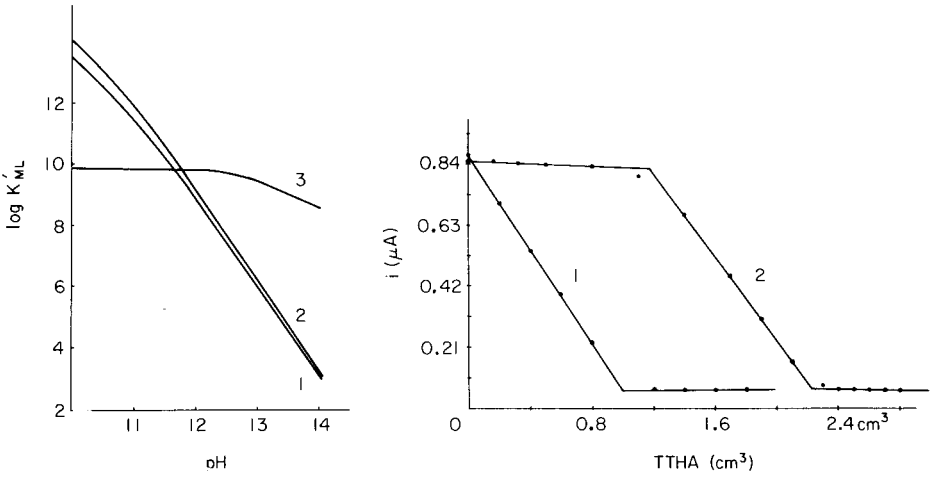

Fig. 1. Dependence of conditional stability constants of the Zn—TTHA (curve 1), Pb—TTHA (curve 2) and Ca—TTHA (curve 3) complexes on pH.

Fig. 2. Titration curves of lead(II) (curve 1) and lead(II) and calcium(II) (curve 2) in 0.1 M NaOH by TTHA; d.c. detection.

the calcium(II) and titrant concentrations and on the polarographic technique used.

Lead(II) is a better indicator than zinc(II), because surfactants are unnecessary, and because the high sensitivity of the s.w. peak of lead(II) enables small amounts of indicator and dilute solutions of TTHA to be used. Even 5×10^{-6} M calcium(II) solutions can be titrated. Moreover titrations can be done without deaeration; the presence of oxygen changes the shape of the peak but does not influence the shape of the titration curve or the final result. All metals which in 0.1 M NaOH form TTHA complexes more stable than Pb—TTHA interfere, being titrated simultaneously with calcium(II).

The method recommended here is more sensitive than the procedure based on the anodic current of TTHA [8]. The results shown in Table 1 indicate that the use of lead as the indicator provides better precision. The presence of equivalent amounts of magnesium has no significant effect.

Procedure for calcium in alkali metal hydroxides

The following procedure is recommended for 0.5×10^{-3}—1.5×10^{-3}% calcium. Place the weighed sample (50 g) in a 250-cm^3 volumetric flask, dissolve in a little water, cool and dilute to the mark. Transfer to a polyethylene bottle. Measure a 10-cm^3 aliquot into a 50-cm^3 volumetric flask and neutralize the hydroxide by adding 5 M HCl to give a final 0.1 M hydroxide concentration. Add lead nitrate solution to give a concentration of about 1×10^{-5} M and dilute with water to the mark. Place a 10-cm^3 aliquot of this solution in the amperometric cell and titrate with standard 1×10^{-4} M TTHA solution in 0.2-cm^3 portions. After each addition of TTHA, stir the solution magnetically for 30 s and record the s.w. peak of free lead(II) ions (E_p = —0.70 V). After

TABLE 1

Results of amperometric titration (d.c. detection) of Ca(II)—Zn(II) and Ca(II)—Pb(II) mixtures in 0.1 M NaOH with TTHA solution

Soln.	Sample (μmol)			Ca found (μmol)	Error (%)	Soln.	Sample (μmol)			Ca found (μmol)	Error (%)
	Ca	Mg	Zn				Ca	Mg	Pb		
1	1.25	—	0.99	1.09	—12.8	1	1.25	—	0.48	1.30	4.0
				0.99	—20.8					1.17	—6.4
2	1.25	—	1.98	1.14	—8.8	2	2.50	—	0.48	2.32	—7.2
				1.07	—14.4					2.38	—4.8
3	2.50	—	0.99	2.07	—17.2	3	1.25	—	0.96	1.32	5.6
				2.54	1.6					1.29	3.2
4	2.50	—	0.40	2.09	—16.4	4	2.50	—	0.96	2.44	—2.4
				2.20	—12.0					2.26	—9.6
5	1.25	1.01	0.99	1.15	—8.0	5	1.25	1.01	0.96	1.25	0.0
				1.21	—3.2					1.21	—3.2
6	1.25	2.02	0.99	1.25	0.0	6	1.25	2.02	0.96	1.24	—0.8
				1.29	3.2					1.27	1.6

the end-point, indicated by the decrease of the peak, add four portions of 0.2 cm^3 of TTHA. Correct the measured peak heights for volume changes. Estimate the end-point from the titration curve or by extrapolation of the linear portions of the curve after calculating the best fit by the method of least squares.

When the content of calcium is below 5×10^{-4}%, the procedure is slightly different. After addition of hydroxide, acid and lead(II) to the 50-cm^3 volumetric flask, about 2.5×10^{-4} mmol Ca is added. This simplifies estimation of the end-point; the equivalent volume of TTHA for the calcium addition is subtracted from the final result.

Procedure for calcium in alkali metal perchlorates, nitrates etc.

The procedure is similar to the above method except for sample preparation. Dissolve the weighed sample (50 g) in water in a 250-cm^3 volumetric flask and dilute to the mark. Transfer a 10-cm^3 aliquot to a 50-cm^3 measuring flask and add 5 cm^3 of 1.0 M NaOH; previously determine the calcium content of the sodium hydroxide by the above procedure. Next, add lead nitrate solution to give a concentration of 1×10^{-5} M and dilute the solution to the mark with

TABLE 2

Amperometric determination of calcium in alkali metal salts
(The results given are the mean for 2 or 3 titrations of the diluted sample solutions, x, the mean result for two separate samples of the same salt, $\bar{x}$, the standard deviation, s, and the standard deviation at a 95% confidence limit.)

Reagent	Sample solution	Ca found ($\times 10^{-3}$) (%)				A.a.s. result
		x	$\bar{x}$	s	$s(t_{0.95})$	
NaOH I	1/1	1.00	1.03	0.020	±0.051	—
	1/2	1.07				
	2/1	0.97	0.96	0.031	±0.080	—
	2/2	0.95				
NaOH II	1/1	0.71	0.73	0.010	±0.026	0.57
	1/2	0.74				
	2/1	0.66	0.67	0.009	±0.023	0.55
	2/2	0.67				
KOH	1/1	1.20	1.21	0.018	±0.057	—
	1/2	1.22				
$NaClO_4$	1/1	0.81	0.81	0.009	±0.023	0.77
	1/2	0.80				
	2/1	0.83	0.83	0.006	±0.015	0.73
	2/2	0.83				
$LiClO_4$	1/1	0.17	0.17	0.007	±0.022	—
	1/2	0.16				

water. Then proceed exactly as described above. Deduct the blank arising from the sodium hydroxide.

RESULTS AND DISCUSSION

The preliminary investigations were done with sodium hydroxide samples containing no more than 3×10^{-3}% Ca (POCh certificate). For a 0.5 M NaOH solution, the calcium concentration would be about 5×10^{-6} mol dm^{-3}. In this range titration based on the anodic current of TTHA is useless, but procedures can be based on: (a) amperometric titration of calcium with TTHA and lead(II) indicator (s.w. polarography); or (b) s.w. polarography of lead(II) displaced by calcium(II) from the Pb—TTHA complex.

The limiting current of lead(II) in d.c. polarography in the absence of TTHA is independent of the NaOH concentration in the range 0.08—0.50 M. The height of the lead(II) s.w. peak increases only slightly as the NaOH concentration increases from 0.08 to 0.12 M whereas the increase is about 40% for 0.50 M NaOH. Thus when concentrated NaOH solutions (e.g., 0.5 M) are titrated, the accompanying dilution of the sample spoils the shape of the titration curve obtained from measurements of the lead peak. To avoid this effect, the concentration of the NaOH solution should be about 0.1 M. When higher concentrations of sodium hydroxide are necessary because of low calcium contents, the excess of hydroxide must be neutralized.

In the determination of small amounts of calcium in strongly alkaline solutions, the prolonged storage in ordinary glassware must be avoided, because calcium ions are eluted from the glass after a few hours. The solutions should therefore be kept in quartz or polyethylene vessels.

The procedures recommended above for alkali metal salts were applied to samples of NaOH, KOH, $NaClO_4$ and $LiClO_4$ (analytical grade). The results are presented in Table 2; for each sample two preliminary solutions were prepared and from each preliminary solution two titration solutions were prepared. The titration curves were similar to those shown in Fig. 2 (curve 2).

Comparative determination of calcium by atomic absorption spectrometry

As a comparative method, atomic absorption spectrometry (a.a.s.) was used. Because of the influence of significant sodium concentrations on the absorbance of calcium, as well as difficulty of obtaining reagents devoid of calcium, a standard addition procedure was chosen. When a graphite furnace was used, a large scatter was observed in the results regardless of the wavelength used (422.7 nm or 393.4 nm). Atomization in a nitrous oxide—acetylene flame and absorbance measurements at 422.7 nm gave more reproducible results. The slopes of the calibration graphs obtained for the range 0—80 μg Ca in 0.2 M NaOH solutions were only about half those obtained for 0.1 M NaOH solutions, in accordance with earlier reports [4, 5]. For the determination of calcium, the best concentration of sodium hydroxide and sodium perchlorate was 4%, but at such salt concentrations the burner often became clogged;

thus the burner was frequently cleaned and washed with 0.1 M HCl and distilled water. Solutions were prepared similarly to the amperometric method, the pH being adjusted to 2 with 5 M HCl before the standard addition of calcium and final dilution. The mean results obtained for some samples are shown in the final column of Table 2.

Comparison of the results in Table 2 indicates that there is a significant negative error in the a.a.s. results in relation to the amperometric method. The presence of Al(III), Fe(III), Mg(II), Zn(II) and Pb(II) in equimolar amounts to calcium does not influence the amperometric results whereas Cu(II), Cd(II) and Ni(II) cause positive errors. The s.w. polarographic curve for 5 M NaOH solution indicated the presence of iron (1×10^{-5} M) and lead (1×10^{-7} M) but Cu, Cd, Ni and Zn were not detected. Accordingly, the amperometric results appear to be correct, and the low a.a.s. results for calcium must be ascribed to errors from the large amount of sodium.

For the determination of calcium in the alkali metal salts, the amperometric method is the more convenient because only one sample solution is needed and standard addition is not required.

REFERENCES

1 M. Růžička and A. Matrani, Chem. Zvesti, 22 (1968) 690.
2 R. L. Olsen, H. Diehl, P. F. Collins and R. B. Ellestad, Talanta, 7 (1961) 187.
3 S. Skurnik-Sarig, A. Glasner, M. Zidon and D. Weiss, Talanta, 16 (1969) 1488.
4 W. Rutkowski and M. Kupiński, Chem. Anal., 21 (1976) 707.
5 J. Ramirez-Munoz, Anal. Chem., 42 (1970) 517.
6 J. Tranka, Chem. Listy, 51 (1957) 1378.
7 M. L. Richardson, Talanta, 10 (1963) 103.
8 S. Rubel and M. Wojciechowski, Anal. Chim. Acta, in press.

Analytica Chimica Acta, 109 (1979) 73—83

AN INJECTION METHOD FOR THE SEQUENTIAL DETERMINATION OF BORON AND SEVERAL METALS IN WASTE-WATER SAMPLES BY INDUCTIVELY-COUPLED PLASMA ATOMIC EMISSION SPECTROMETRY

J. A. C. BROEKAERT* and F. LEIS

Institut für Spektrochemie und angewandte Spektroskopie, Postfach 778, 46 Dortmund (Bundesrepublik Deutschland)

(Received 12th February 1979)

SUMMARY

Boron and nine metals (Ba, Cd, Cu, Fe, Mn, Mo, Ni, Zn) can be determined in waste waters of medium and high salt concentration by inductively-coupled plasma atomic emission spectrometry. An injection method was applied in order to achieve analysis times of about 1 min per determination, and to allow trace analysis in solutions having salt concentrations up to 20 mg ml^{-1}, when a Meinhard nebulizer is used with a low-power argon plasma. When 500-μl aliquots are injected and the peak heights of the amplified photomultiplier signals are measured, the detection limits for the elements tested range from 0.05 to 0.4 μg ml^{-1}. Matrix effects caused by sodium nitrate (20 mg ml^{-1}) are less than 20%, provided that a peristaltic pump is used for feeding the nebulizer. Matrix effects can be decreased by using simultaneous background measurement. The plasma—injection method is applicable to boron and metals in the range 0.05—20 μg ml^{-1}.

Monitoring of the concentrations of a series of metals and other toxic elements in waste waters has become essential from an ecological point of view. This necessitates the development of methods that allow sequential or simultaneous determinations in solutions of very different compositions. Inductively-coupled plasma (i.c.p.) excitation is suitable for this purpose because it is characterized by high sensitivity for most elements, by large dynamic ranges and by rather low matrix effects [1—5].

In the work described here, a sequential i.c.p. procedure was applied in conjunction with an injection method, and the amplified photomultiplier current was used as the analytical signal. Injection procedures have already been applied in atomic absorption and flame atomic emission spectrometry (a.e.s.) [6] and also in i.c.p.-a.e.s. [7, 8]. The main aim then was the analysis of samples of small volume, e.g., in clinical analysis and after pre-enrichment procedures. In this work the objectives were different: to allow reproducible operation of the pneumatic nebulizer in analyses of samples of high salt concentrations; and to increase the speed of analysis compared to continuous sample feeding and integration of the measured signal. The i.c.p.—injection method developed is an extension of the injection method reported by

Sebastiani et al. [9] for flame atomic absorption spectrometry, with similar objectives.

The development of the i.c.p.—injection technique comprised three stages. First, its power of detection was compared to that obtained by continuous sample feeding. Secondly, the matrix effects caused by high sodium concentrations, which were present in the waste waters, were studied and procedures for decreasing these effects were investigated. Finally, applications to the sequential determination of boron and several metals in waste waters of varying salt contents were examined.

EXPERIMENTAL

Apparatus

The i.c.p. system and the working conditions have been described [10]; they are summarized in Table 1.

The radiation emitted by the i.c.p. is measured photoelectrically. The 0.5-m monochromator (Fig. 1) is equipped with a quartz refractor plate in front of the first exit slit; this allows accurate measurement of the analytical line intensities and of the adjacent spectral background alternatively, as has been applied in a continuous method [11]. A supplementary measuring channel is obtained by reflecting part of the emission at a wavelength adjacent to that

TABLE 1

Instrumental data and working conditions

Plasma generator	Labtest (maximum power 2 kW; frequency 27.12 MHz, crystal-controlled)
forward power	900 W
reflected power	50 W
Plasma burner	Two gas-flow type [1]
observation zone	4 mm × 4 mm, located 4—8 mm above the coil
plasma gas flow	Argon (10 l min^{-1})
Nebulizer	Meinhard concentric glass nebulizer
aerosol gas flow	0.4—0.6 l min^{-1} at an argon pressure of 3 bar
sample uptake	2.0 ml min^{-1}
peristaltic pump	"Gilson", pumping rate adjustable from 0.2 to 5 ml min^{-1}
spray chamber	As described by Scott et al. [5]
Spectral observation	0.5-m monochromator (Jarrell-Ash)
grating	60 mm × 60 mm; grating constant a = 1/2442.4 mm
curved slits	Entrance slit width 6 μm, height 10 mm; exit slits, 10 μm wide
Potentiometric recorder	Linseis (3 channels)
Photomultipliers	EMI type 9781A
Measuring modes	Two measuring cycles, each consisting of integrating intensities, 10 s on line, 10 s on background left, 10 s on line, 10 s on background right (one channel); direct signals on chart drive after amplification (measurement in two channels possible)

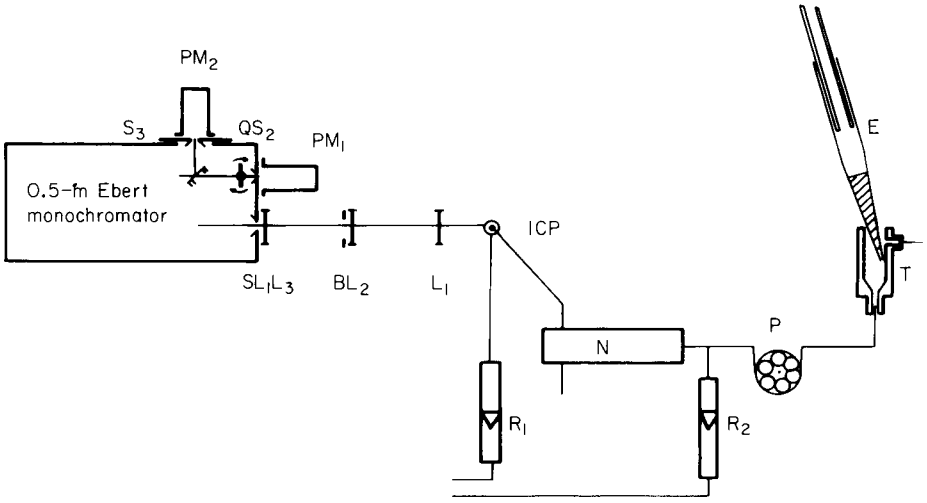

Fig. 1. The i.c.p.—injection set-up. Spherical quartz lenses (f = focal length, d = diameter): (L_1) f 104 mm, d 19 mm; (L_2) f 195 mm, d 35 mm; (L_3) f 177 mm, d 19 mm. (S_1) Entrance slit; (S_2) fixed exit slit; (S_3) movable exit slit (±2 mm); (Q) quartz refractor plate (1 mm thick) for alternative measurement of line and background intensity (background wavelength and analytical line wavelength are equal, ±0.04 to 0.15 nm). (PM_1) and (PM_2) Photomultipliers. (B) Diaphragm (30 mm × 30 mm) at intermediate image. (R_1) and (R_2) Rotameters in the gas supply lines; (N) spray chamber; (P) peristaltic pump; (T) Teflon sampling cup; (E) Eppendorff micropipette.

of the analysis line, to a movable slit in front of a second photomultiplier. This channel can be used to measure the spectral background intensity when the injection method is applied.

Sample aliquots ranging from 50 to 500 µl are fed to the pneumatic nebulizer from Eppendorff micropipettes [6]. The aliquots are placed in a Teflon cup (10 mm i.d., 20 mm high) which can be flushed with argon (Fig. 1). This prevents any sudden entrance of air into the i.c.p. between the uptake of samples, which can change the impedance matching of the i.c.p. to the generator. Especially with a low-power i.c.p., this may make the discharge unstable. In most cases, equal volumes of sample and water are injected alternatively. A peristaltic pump is placed between the sampling cup and the nebulizer to achieve regular sample feeding. When a peristaltic pump is used, argon flushing of the sampling cup can be omitted.

Calibration

Calibration graphs are prepared by plotting the peak heights of the direct signals, corrected for spectral background contributions, versus the concentrations in the standard solutions (Fig. 2). Standard solutions were obtained by dissolving metal nitrates (Merck p.a.) or sodium tetraborate in 0.1 M nitric acid (Merck Suprapur).

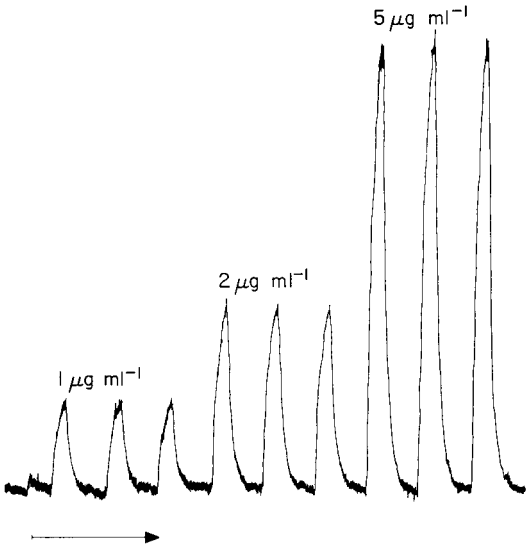

Fig. 2. Calibration of the i.c.p.—injection technique for iron at the Fe II 259.9-nm line. Aerosol gas flow, 0.43 l min^{-1}. Alternate 500-μl injections of sample solution and water.

RESULTS AND DISCUSSION

When the Meinhard nebulizer was combined with a low-power argon i.c.p., an argon flow of 0.5 l min^{-1} at a pressure of 3 bar was found to give the optimum sensitivity [12]. In the continuous method with a peristaltic pump for sample feeding, a 20-s integration time was used with sequential measurements of line and background intensities. When 0.1 M HCl was used for rinsing between two samples, so that memory effects were less than 2%, one measuring cycle required at least 4 min (Fig. 3). This time could be considerably lowered by using the injection method.

The influence of the volume of the injected sample on the line-to-background intensity ratio was determined in order to establish the optimum limits of detection for low sample consumption and short analysis times. It can be concluded from Fig. 4 that increasing the sample volume above 500 μl does not further improve the line-to-background intensity ratio. The sample volume can be decreased to as little as 10 μl, but the limits of detection inevitably suffer. As the aim of this work was not the analysis of small volumes of samples but trace analysis at short sampling times, an injection volume of 500 μl was used in all further measurements. The length of the measuring cycle, for injection volumes of 500 μl, was 1.5 min (Fig. 5). This time is determined by three factors. First, there is the time required to fill the nebulization chamber with the analyte aerosol or to rinse it. This time, which is 20 s here, depends greatly on the volume of the nebulization chamber (220 cm^3 here) as the chamber must be filled at a gas flow rate of about 1.5 l min^{-1}. The second

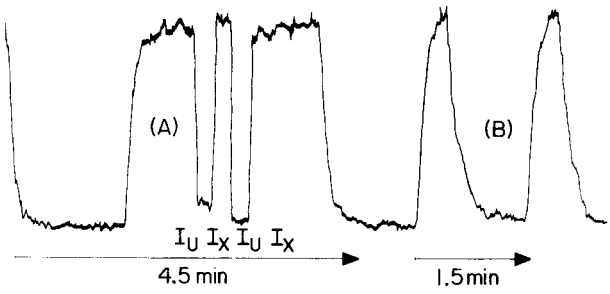

Fig. 3. Measurement cycles for the continuous method with sequential measurement of line and background intensities, and for the injection method. Fe II 259.9-nm line with 5 μg Fe ml^{-1} solution. Aerosol gas flow, 0.43 l min^{-1}. (A) Direct signals for line (I_X) and background (I_U) intensities with 20-s measurement times. (B) Alternative injections of 500 μl of sample solution and 500 μl of water.

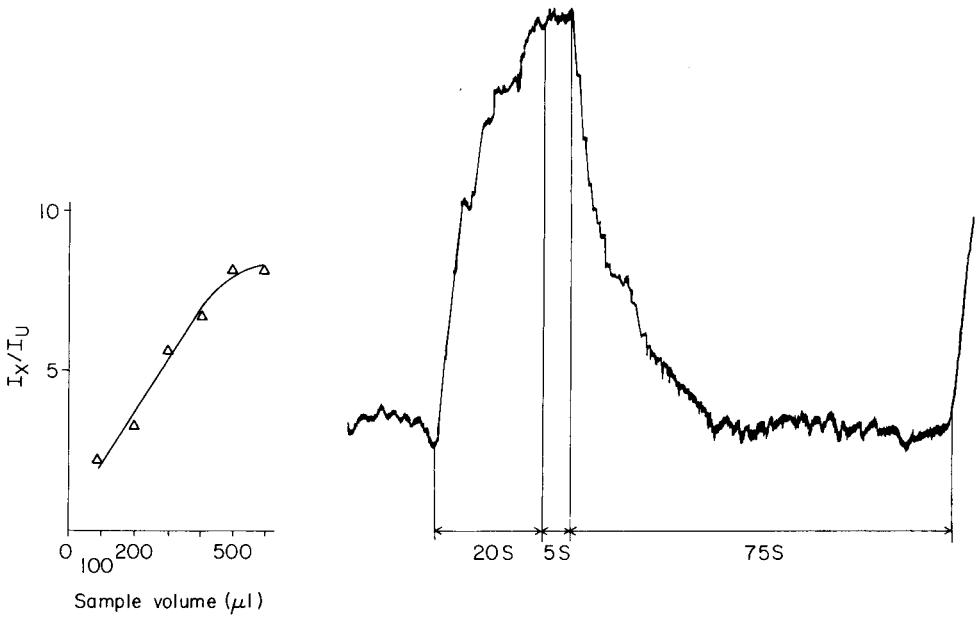

Fig. 4. Influence of the sample volume on the line-to-background intensity ratio at the Fe II 259.9-nm line for 1 μg Fe ml^{-1} solutions. I_X and I_U were measured simultaneously. Mean values were calculated from ten replicates. Aerosol gas flow; 0.43 l min^{-1}.

Fig. 5. Measurement cycle for the i.c.p.—injection method at the Fe II 259.9-nm line with 5 μg Fe ml^{-1} solution. Aerosol gas flow; 0.43 l min^{-1}. Alternate injections of 500 μl of sample solution and 500 μl of water.

factor involves both the sample uptake rate (1.5—2 ml min^{-1}) and the aerosol carrier-gas flow (0.5 l min^{-1} at 3 bar), which are governed by the requirement for optimal limits of detection. Finally, the time for the intensity measurement is about 5 s.

Sebastiani et al. [9] showed that injection techniques lead to shorter analysis times and avoid nebulizer blockages in flame atomic absorption spectrometry; the results obtained here show that this is also true for i.c.p.-a.e.s. The use of the i.c.p.—injection technique allows the analysis of solutions with salt concentrations up to 20 mg ml^{-1}, which cannot be nebulized reproducibly when samples are fed continuously into the Meinhard nebulizer operated at an argon flow of 0.5 l min^{-1} (3 bar). When a peristaltic pump is used, reproducible sample feeding is guaranteed, and the precision of the injection method in terms of the relative standard deviation of the intensity signal is about 2—6%, even at high salt concentrations.

Detection limits for boron and a series of metals

For each element the aerosol gas flow giving the highest line-to-background intensity ratio was established first. The optimized values lay between 0.4 and 0.6 l min^{-1} at an argon pressure of 3 bar. The detection limits obtained for 500-μl sample injections and for continuous sample feeding with signal integration are listed in Table 2. The detection limits for the injection method are 2—10 times higher than those for the continuous method.

These differences are due to the different relative standard deviations of the measured background intensities, $s_r(I_U)$, involved in the calculation of the detection limits [13]. Differences of $s_r(I_U)$ are caused by the different measure-

TABLE 2

Detection limits[a] for boron and several metals[b]

Element/line (nm)	Continuous sample feeding and integration for 20 s		Injection method (500-μl samples)	
	c_L (μg ml^{-1})	$s_r(I_U)$[a]	c_L (μg ml^{-1})	$s_r(I_U)$[a]
B I 249.68	0.045	0.05	0.15	0.15
Ba II 413.07[c]	0.09	0.05	0.2	0.10
Cd I 228.80	0.06	0.04	0.3	0.10
Cr I 359.35	0.025	0.05	0.05	0.10
Cu I 324.75	0.035	0.03	0.04	0.05
Fe II 259.94	0.015	0.03	0.09	0.05
Mn II 257.61	0.003	0.03	0.055	0.10
Mo I 379.82	0.04	0.05	0.09	0.10
Ni I 352.45	0.10	0.02	0.2	0.03
Zn I 313.86	0.09	0.03	0.15	0.05

[a]Detection limits are defined as the concentrations giving an analytical signal $x = \bar{I}_U + 3\sqrt{2}\, s_r(I_U)$, where $\bar{I}_U$ is the mean and $s_r(I_U)$ the relative standard deviation calculated from 10 background measurements [13].

[b]Aerosol gas flow, 0.4—0.6 l min^{-1} (3 bar), optimized for maximum line-to-background intensity ratio.

[c]Ba II 455.40 is not available.

ment times and by the methods of reading the measured values in the two cases; with the continuous method the signal is integrated for 20 s with negligible reading error, whereas with the injection method the measuring time is about 5 s and the fluctuations on the signal peak are visibly smoothed (Fig. 3). This agrees with the $s_r(I_U)$ values obtained from ten measurements in Table 2.

Special attention was given to the measurement of spectral background intensities. When the analysis lines are situated in a spectral region where OH bands occur, the spectral background with sample significantly differs from that obtained with argon alone. This could be due to phenomena in the plasma but also to stray light in the spectral equipment [14, 15]. For the B I 249.6-nm, Ba II 413.1-nm and Cr I 359.3-nm lines, spectral background intensities were measured from the peak heights in ten recordings for a blank solution. In the other cases, the background intensities without and with sample injection were the same. Then $s_r(I_U)$ was determined from ten values of the background intensity signal sampled at intervals of 1 min.

Matrix effects caused by increasing concentrations of sodium

As has already been stated by Greenfield et al. [16], many matrix effects in i.c.p.-a.e.s. are actually nebulization effects. However, in injection methods the nebulizer is exposed to the sample solution for only short periods, hence nebulizer effects arising from the deposition of salts at the nozzle and from ion-exchange phenomena on the glass wall, which are particularly noticeable when the alkaline concentration in the sample is high, are significantly reduced. It has been shown [12] that matrix effects in i.c.p.-a.e.s. can be minimized by adjusting the aerosol gas flow to the value giving maximum net intensity for the analysis line. The results in Fig. 6 show that in i.c.p.—injection methods, matrix effects can likewise be minimized by optimization of the carrier gas flow for the aerosol. Matrix effects caused by sodium nitrate at concentrations up to 20 mg ml^{-1} (Table 3) are less than 20%, if a peristaltic pump is used for sample feeding (Fig. 7) and the aerosol gas flow has been optimized for each element.

Matrix effects caused by very high sodium concentrations can be decreased by simultaneous measurements of the intensities of the analysis line (λ_L) and the spectral background at $\lambda_L \pm 0.1$ nm, which allows a more accurate background correction. Results for the B I 249.6-nm, Ba II 413.1-nm and Cu I 324.7-nm analytical lines are presented in Table 3. As no systematic relationship between the intensity of argon lines and the alkali metal concentration was found, the intensity of an argon line could not be used for the correction of matrix effects.

Application of the method to the analysis of waste-water samples

The i.c.p.—injection method was applied to the analysis of the samples listed in Table 4. Immediately after sampling, the pH of the waste water was adjusted to 1 with nitric acid; Suprapur nitric acid was used in all subsequent steps.

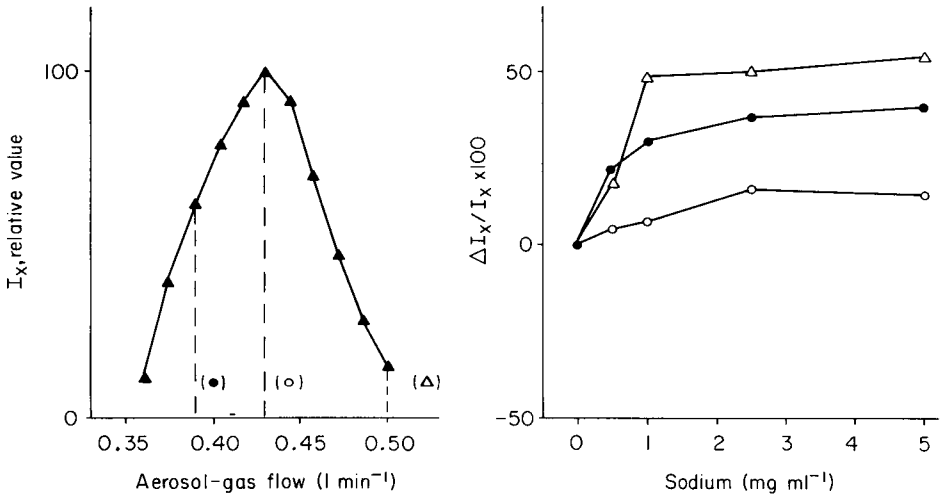

Fig. 6. Influence of the aerosol gas flow rate (at 3 bar) on the matrix effect caused by sodium salts ($NaNO_3$) in the i.c.p.—injection method. B I 249.6-nm line with 5 μg B ml^{-1} samples. Mean values were calculated from five measurements. For the figure on the right, the argon gas flows are: (•) 0.39 l min^{-1}; (○) 0.43 l min^{-1}; (△) 0.50 l min^{-1}.

TABLE 3

Matrix effects[a] measured at different concentrations of sodium ($NaNO_3$) in solution[b] for analyte concentrations of 5 μg ml^{-1}
[(A) Measurements with one channel; (B) simultaneous measurement of line (λ_L) and background ($\lambda_L \pm 0.1$ nm) intensities with two channels.]

Na (μg ml^{-1})	B I 249.6 nm		Ba II 413.0 nm		Cu I 324.7 nm	
	(A)	(B)	(A)	(B)	(A)	(B)
500	—	+4	—3	—	—8	—
1000	+3	+4	—	+3	—7	—
2500	—3	+4	—10	+6	—8	—
5000	—7	—	—20	+12	—4	+3

[a]Matrix effect is defined as $(I - I_0)/I_0 \times 100$, where I_0 and I are the line intensities measured respectively without and with sodium in solution; mean values were calculated from five measurements.
[b]Aerosol gas flow, 0.4—0.6 l min^{-1} (3 bar), optimized for maximum net line intensity.

The samples were stored at 4°C. The amount of total inorganic substances was determined by the standard method [17]. In order to guarantee representative sampling and to dissolve all suspended matter, the following procedure was used: 1 ml of perhydrol and 1 ml of concentrated nitric acid were added to 100 ml of sample solution. The solution was evaporated to dryness at 110°C and the residue was taken up in 50 ml of 0.1 M HNO_3. Sample volumes of 500 μl were used for the i.c.p.—injection method.

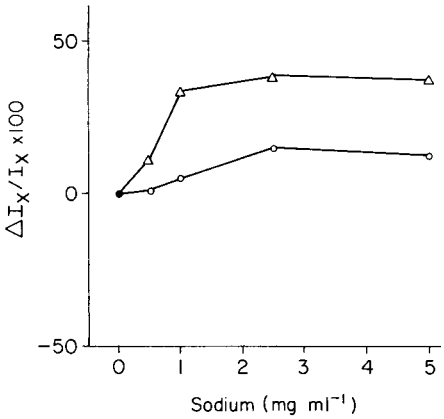

Fig. 7 Matrix effect caused by different concentrations of sodium salts in the i.c.p.—injection technique with (○) and without (△) a peristaltic pump. B I 249.6-nm line with 5 μg B ml^{-1} samples. Mean values were calculated from five measurements. Aerosol gas flow, 0.43 l min^{-1} at 3 bar.

TABLE 4

Waste-water samples analyzed

Sample	Total inorganic salt contents (mg ml^{-1})	Origin
1	1.02	Exit of a purification plant fed with waste water from a galvanic industry
2	1.28	Waste water from galvanic plant
3	120.23[a]	Waste water of steel-tempering works
4	10.50	Exit of the decontamination unit in a galvanic plant
5	2.26	Waste water of cellulose plant

[a]Diluted (1 + 9) with 0.1 M HNO_3 (Suprapur) prior to analysis.

The analytical results for sample no. 1 obtained by the injection method and by the continuous method (Table 5) are in good agreement with results obtained by atomic absorption spectrometry (a.a.s.) and colorimetry. The results for the other samples are given in Table 6. Samples 3 and 4 could be analysed only by the injection method because of their high concentrations of sodium salts. In order to minimize the matrix effects simultaneous measurements of line and background intensities were applied. The relative standard deviations for the analyses were of the order 4—7%.

From these results obtained in the problematic field of waste-water analysis, it can be concluded that the i.c.p.—injection method is a powerful tool for sequential multi-element analyses of routine samples. The short analytical times and the possibility of analyzing solutions with high salt concentrations recommend the method as a worthwhile alternative to other i.c.p. techniques.

TABLE 5

Analytical results (in μg ml^{-1}) for sample no. 1

	Injection method		Continuous method	Other methods
	Found	s_r[a]	Found	Found
Boron	1.3	0.03	1.25	1.5 (colorimetry)
Chromium	0.21	0.06	0.19	0.13 (a.a.s.)
Copper	0.19	0.06	0.21	0.20 ,,
Iron	0.42	0.04	0.39	0.28 ,,
Manganese	0.074	0.02	0.064	0.065 ,,
Nickel	0.73	0.04	0.68	0.65 ,,
Zinc	0.56	0.02	0.54	0.53 ,,

[a]Relative standard deviations calculated from ten measurements.

TABLE 6

Analytical results[a] for samples 2, 3, 4 and 5
[(A) Injection method; (B) continuous sample uptake.]

	Sample 2		Sample 3		Sample 4		Sample 5	
	A	B	A	B	A	B	A	B
Boron	2.9	2.2	—	—	5.1	—	0.15	—
Barium	0.25	0.22	14.5	—	—	—	—	—
Cadmium	0.35	0.35	—	—	0.06	—	—	—
Chromium	0.68	0.55	—	—	0.7	—	—	—
Copper	1.6	1.6	—	—	4.5	—	—	—
Iron	0.74	0.85	23	—	0.85	—	0.54	0.65
Manganese	—	—	—	—	0.6	—	0.13	0.1
Molybdenum	—	—	0.2	—	—	—	—	—
Nickel	5.2	5.1	—	—	—	—	—	—
Zinc	9.5	9.7	—	—	0.45	—	—	—

[a]Concentrations in μg ml^{-1}; mean values calculated from ten measurements.

The authors thank Mr. E. Spencer (Coventry, U.K.) for his contribution to the experimental work. This work was supported by the Ministerium für Wissenschaft und Forschung des Landes Nordrhein-Westfalen.

REFERENCES

1 V. A. Fassel and R. N. Kniseley, Anal. Chem., 46 (1974) 1155A.
2 G. F. Larson, V. A. Fassel, R. H. Scott and R. N. Kniseley, Anal. Chem., 47 (1975) 238.
3 P. W. J. M. Boumans, Fresenius Z. Anal. Chem., 279 (1976) 1.
4 S. Greenfield, H. McD. McGeachin and P. B. Smith, Talanta, 23 (1976) 1.
5 R. H. Scott, V. A. Fassel and R. N. Kniseley, Anal. Chem., 46 (1974) 75.
6 H. Berndt and E. Jackwerth, Spectrochim. Acta, Part B, 30 (1975) 169.
7 S. Greenfield and P. B. Smith, Anal. Chim. Acta, 59 (1972) 341.

8 R. N. Kniseley, V. A. Fassel and C. C. Butler, Clin. Chem., 19 (1973) 807.
9 E. Sebastiani, K. Ohls and G. Riemer, Fresenius Z. Anal. Chem., 264 (1973) 105.
10 J. A. C. Broekaert, F. Leis and K. Laqua, Spectrochim. Acta, Part B, in press.
11 N. Nordmeyer, Fresenius Z. Anal. Chem., 225 (1967) 247.
12 J. A. C. Broekaert, F. Leis and K. Laqua, Spectrochim. Acta, Part B, in press.
13 H. Kaiser and H. Specker, Fresenius Z. Anal. Chem., 149 (1956) 46.
14 G. F. Larson, V. A. Fassel, R. K. Winge and R. N. Kniseley, Appl. Spectrosc., 30 (1976) 384.
15 R. K. Winge, V. A. Fassel, R. N. Kniseley, E. DeKalb and W. J. Haase, Jr., Spectrochim. Acta, Part B, 23 (1977) 327.
16 S. Greenfield, H. McD. McGeachin and P. B. Smith, Anal. Chim. Acta, 84 (1976) 67.
17 Deutsche Einheitsverfahren zur Wasser-, Abwasser- und Schlammuntersuchung, Fachgruppe Wasserchemie in der Gesellschaft Deutscher Chemiker, Verlag Chemie GmbH, Weinheim, 1960, H 1.

Analytica Chimica Acta, 109 (1979) 85—95

MULTI-ELEMENT ANALYSIS OF GEOLOGICAL SAMPLES BY ENERGY-DISPERSIVE X-RAY FLUORESCENCE

P. VERBEKE** and F. ADAMS*

Department of Chemistry, University of Antwerpen (U.I.A.), B-2610 Wilrijk (Belgium)

(Received 12th March 1979)

SUMMARY

A rapid multi-element analysis of thick geochemical specimens by energy-dispersive x-ray fluorescence with a secondary target set-up is described. The simple sample preparation consists of pressing the powdered material into pellets. Calibration is based on the use of thin foils of the pure element. Matrix effects are corrected by a simplified fundamental parameter technique. The method has been applied to the analysis of a series of geochemical standard samples. A fair agreement is obtained between the results and the reported data with accuracies typically of 10%. The detection limit reached is about 1 ppm, provided that serious spectral interferences are absent. Samples of widely varying composition may be analyzed.

Energy-dispersive x-ray fluorescence spectrometry (x.r.f.) is an important tool in chemical analysis, for it is far more convenient than classical methods which require trained personnel. The method provides rapid, non-destructive, cheap multi-element analyses for a wide variety of samples. The detection limits are sufficient for most applications. When "thin samples" are measured, reduction of the spectral information is easily done, since matrix effects are negligible and a linear calibration graph may be used. In some cases where the specimen does not really obey the "thin sample" criterion, correction factors for self-absorption may readily be calculated.

The accurate analysis of infinitely thick samples, however, requires a closer investigation of the absorption-enhancement effects. Different approaches of varying complexity may be used to correct for them: (1) correction methods based on experimentally determined influence coefficients, which require a large number of calibration standards with a composition similar to that of the unknown, and (2) corrections calculated by using mathematical expressions that contain mainly physical parameters for the elements of interest. The latter procedure requires large computer facilities when polychromatic radiation excitation is applied but when monochromatic excitation conditions are employed, as in the case of a radio-isotope source or a secondary target set-up, the calculations are greatly simplified.

**Research associate of the Instituut ter Aanmoediging van het Wetenschappelijk Onderzoek in Nijverheid en Landbouw, Belgium.

Earlier, the combination of energy-dispersive x.r.f. and the fundamental parameter technique was investigated for the analysis of metallic specimens [1]. It was concluded that the spectral deconvolution method and the matrix correction scheme employed allowed accurate elemental determination in metallic samples of widely varying compositions. It was suggested that the method was not restricted to metallic specimens and might be applied to other materials as well.

In this paper a procedure is described for the analysis of geological materials available in powder form. The classical wet chemical analysis of such specimens is especially time-consuming because of the need for decomposition of the silicate matrix by hydrofluoric acid. Several geological reference materials were available as homogeneous finely divided powders for the evaluation of the procedure. The results obtained for over twenty elements in the samples generally agree within ca. 10% with reported values obtained by other analytical techniques.

EXPERIMENTAL

Instrumentation

The operating system used consists of a Kevex subsystem 0810, a Siemens Kristalloflex 2 generator and a Northern NS720 multichannel analyzer.

Samples are excited by the K_α—K_β radiation of a secondary target, irradiated by the x-ray tube. Six secondary targets are available, which allows the effective excitation of a wide range of fluorescence energies. For the simultaneous excitation and measurement of elements with $Z \geqslant 20$, a molybdenum target is optimum, while for the lower Z-elements the radiation generated from a titanium target is preferable. All samples are measured under vacuum conditions (10^{-2} torr). Both the excitation radiation and the detected radiation are at an angle of 45° to the sample surface. The pulses are processed through a 30-mm^2 Si(Li) detector with a resolution of 160 eV at 5.895 keV, a FET-preamplifier and a linear amplifier with a pulse pile-up rejector. The data collected subsequently in the multichannel analyzer can be transferred to a magnetic tape unit for further off-line calculations with a PDP 11/45 computer using the software described elsewhere [3, 4].

To account for instabilities in the excitation conditions, a thin wire is placed reproducibly in the radiation path; this gives a fluorescence signal in each spectrum that can be used as a reference [2]. It was checked that spectral distortions caused by count-rate effects did not influence the accuracy of spectral analysis.

Samples

The geological standard materials used for evaluation of the analytical procedure were: granite NIM-G and norite NIM-N of the National Institute for Metallurgy, South African Bureau of Standards; basalt JB 1 and granodiorite JG 1 of the Geological Survey of Japan; granite GA and basalt BR of the

Centre de Recherches Pétrographiques et Géochimiques (France); basalt BCR 1 of the U.S. Geological Survey.

Spectral deconvolution

The composite x-ray spectra are analyzed by a non-linear least-squares fitting program [3], which is based on a model consisting of a background continuum and Gaussian functions with numerical corrections. The functional form for the fitting of K_α—K_β doublets can be represented for every data point i as

$$Y(i) = H_{K_\alpha} G_{K_\alpha}(i) + H_{K_\beta} G_{K_\beta}(i) + C_{K_{\alpha\beta}}(i)$$

Here, $G_{K_\alpha}(i)$ and $G_{K_\beta}(i)$ are the Gaussian functions of the K_α and K_β peaks, and $C_{K_{\alpha\beta}}(i)$ is a numerical correction value that accounts for deviations from the Gaussian shape [4]. In order to minimize the required number of variable parameters, linear dependence of the peak position on energy and the square-root variation of peak resolution with energy are assumed in the calculations. The fit yields the peak parameters for the fluorescent lines: height, position, width, total intensity and the standard deviation on the counting statistics and the spectral deconvolution procedure.

The number of variables in the program may be further reduced and corrections for interferences may be optimized by also fixing the intensity ratio of the K_β—K_α or L_β—L_α fluorescence lines. These ratios may be determined experimentally from the measurement of pure element films, or calculated from physical data tables and detection efficiency values. As far as thin samples are concerned, there is a negligible overall absorption and the line intensity ratios remain constant. For thick samples, absorption phenomena have to be accounted for. Their effect is fairly predictable, however, because plots of mass absorption coefficients of different elements versus energy show that the relative absorptions of the elements are virtually constant at all energies [5]. This, of course, is true only in energy regions free from absorption edges. For example, the K_β—K_α absorption coefficient ratios for a number of elements were calculated from the known composition for two geological standards, and also for cellulose, a very different type of material, which is often used as a mixing product in the preparation of x-ray samples. Comparison of the values in Table 1 shows that the absorption effects significantly change the K_β—K_α intensity ratio but the absorption coefficient ratios are comparable for the three matrices involved. The pronounced difference in the absorption ratio for the cobalt lines is due to the occurrence of the absorption edge of iron, a major element in geological materials. The other values agree generally within 3—4%.

It may be concluded that, even for thick samples, the line intensity ratios can be considered as constant, although they must be calculated from the values obtained experimentally from thin element samples. Elements with K_α and K_β lines on either side of the absorption edge of a major constituent cannot be determined with high precision, but the precision may be improved if for each sample the relative absorption is calculated from the data of a preliminary analysis, after which the fitting procedure is done by iteration.

TABLE 1

Absorption coefficient ratios ($\mu_{K_\beta}/\mu_{K_\alpha}$) for K_β—K_α lines in different matrices

Element	Cellulose	Basalt BR	Norite NIM-N
K	0.786	0.806	0.802
Ca	0.777	0.797	0.793
Ti	0.759	0.783	0.777
V	0.751	0.828	0.774
Cr	0.747	0.771	0.768
Mn	0.746	0.764	0.760
Fe	0.739	0.768	0.762
Co	0.738	1.166	1.029
Ni	0.734	0.762	0.757
Cu	0.724	0.757	0.752
Zn	0.731	0.753	0.749
Ga	0.731	0.749	0.745

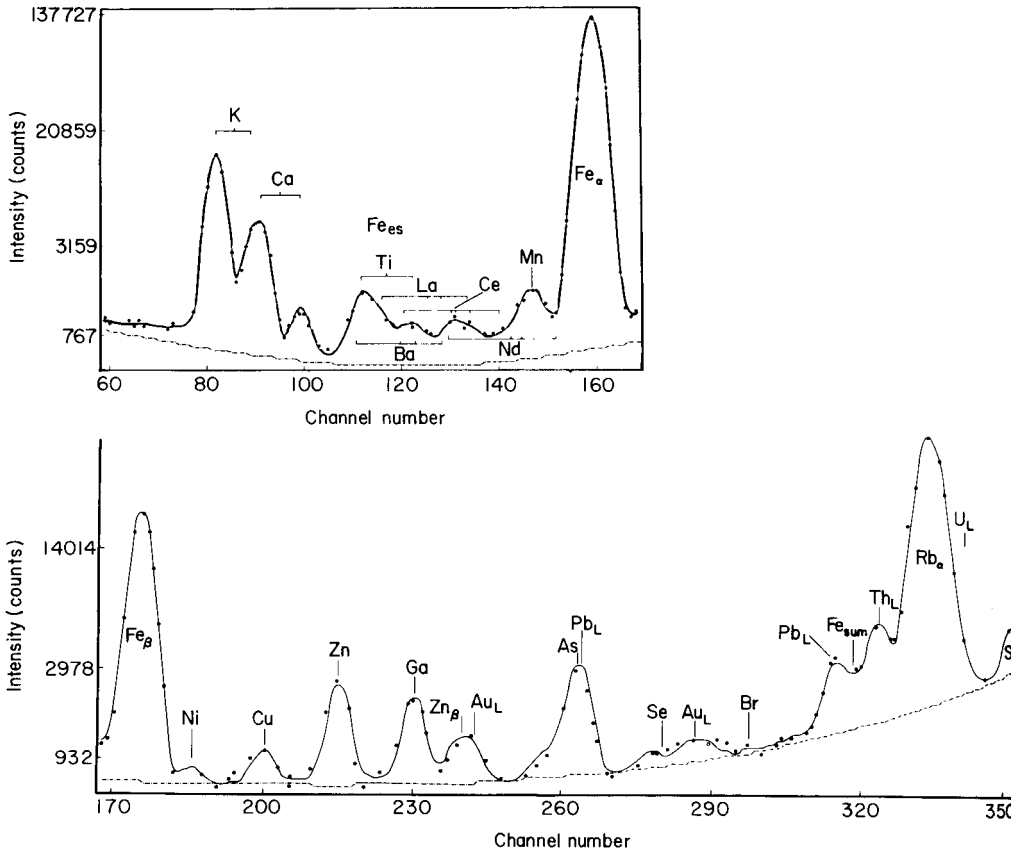

Fig. 1. Spectrum of the NIM-G sample with molybdenum excitation, showing the spectral regions from 2.5 to 6.7 keV (top) and from 6.7 to 14.4 keV (bottom). The full line indicates the fitted spectrum, and the dots the experimental points.

Figure 1 shows the spectrum obtained from a measurement with molybdenum *K*-lines excitation for the granite NIM-G sample. It is immediately apparent that the spectral region between titanium and manganese is complicated by the presence of *L*-lines from high *Z*-elements in the sample. This may affect the results for the determination of small concentrations of elements such as vanadium, chromium, cerium and neodymium.

The spectra obtained by titanium excitation, which cover the low-energy region, are also handled by the program, despite the strong deviation from the Gaussian peak shape. As most of the low *Z*-elements in the samples analyzed are present in the percentage concentration range, the interference of *L*-lines from high *Z*-elements is negligible.

Sample presentation

A major difficulty in the analysis of powdered materials is the occurrence of particle size effects which originate from local inhomogeneities in the thin layer of sample that is penetrated by the fluorescence radiation [6]. The effects may be corrected for by means of mathematical models [7] when the necessary information concerning the size and the composition of the particles is available. Alternatively the effects may be minimized by reducing the particle size and by increasing the compactness of the samples. Another possibility is to fuse the material with a suitable flux [8].

In this work the sample preparation consisted of pressing ca. 3 g of the material to a pellet at a pressure of 20 ton over the pellet surface of 8.0 cm^2. Aluminum cups (30-mm diameter, 5-ml effective volume) were used as a support, which ensures ready removal of the pellet from the press and better endurance. When necessary, the original particle size of ca. 100 μm was reduced to ca. 10 μm by grinding the sample in a McCrone micronizing mill. The pellets were measured in a 32-mm diameter Teflon support ring with a 4-μm thick mylar backing.

The reproducibility of the sample preparation and the measurement was verified by measuring 5 different pellets of the same material. The intensity data shown in Table 2 indicate that the reproducibility is fair.

If particle size effects occur, grinding of the original samples to a particle size of ca. 10 μm and the packing density of the material should have a noticeable effect on the measured intensities. However, the measured intensities for samples prepared with and without preliminary grinding (Table 3) show that grinding does not significantly affect the measured fluorescence intensities. The influence of the packing density was checked by measuring loose powders and pellets pressed at 2.5 ton per cm^2. The results summarized in Table 4 prove that again no important deviations were observed. However, it should be emphasized that these results relate to standard materials available in an homogeneous and finely-divided physical state; rock or soil samples usually contain different minerals and particles of extremely variable composition, hardness and diameter range, and careful grinding would then be essential.

TABLE 2

Precision of sample preparation and measurement for 5 different pellets (material NIM-G; particle size 100 μm)

Element	Measured intensities for 5 pellets					s_r (%)[a]	
	1	2	3	4	5	Expected	Found
K	42800	43700	41900	42200	42700	0.5	1.6
Ca	10300	10100	10200	10700	10500	1.2	2.4
Fe	470600	470300	471200	471500	464200	0.1	0.7
Rb	308400	306600	310200	306900	306000	0.1	0.6
Sr	13100	12700	11700	13200	12900	1.3	4.9

[a]Relative standard deviation on a single measurement. The percentages given are those expected statistically and found experimentally.

TABLE 3

Influence of the particle size (ca. 100 μm and 10 μm) of the material on the measured intensities for basalt JB 1 and granite NIM-G
(Al and Si were measured with titanium excitation, and the other elements with molybdenum excitation.)

Element	Intensity, JB 1				Intensity, NIM-G			
	100 μm	10 μm	s_r (%)	Diff. (%)	100 μm	10 μm	s_r (%)	Diff. (%)
Al	46200	43800	0.6	5	58500	55300	0.6	5
Si	356700	351600	0.2	1	840000	849000	0.1	1
K	15100	14400	1.1	5.1	42800	40200	2.1	6.1
Ca	132600	135800	0.3	2.4	10200	9560	1.0	6.4
Ti	41400	38400	0.9	7.2	2840	2940	3.3	3.9
Mn	22500	23300	0.2	3.6	3630	3570	4.8	1.5
Fe	1826000	1840000	0.5	0.7	470700	461000	0.1	2.1
Zn	8860	9150	0.9	3.3	7920	7940	1.4	0.3
Rb	26200	24900	1.9	4.7	308400	307700	0.6	0.2
Sr	362500	351000	0.1	3.2	12500	13900	6.1	11.2

Absorption correction procedure

The fundamental parameters technique used is based on the model proposed by Criss and Birks [9]. The general form of the working equation, which has been discussed earlier for the analysis of metallic samples [1], is:

$$C_i = [I_i/I_i^*]\ [\mu_{Me} + \mu_{Mi}]\ [1/(1 + \sum_j f[C_j\, \mu_{je}\, \mu_{ij}])] \qquad (1)$$

where C_i is the concentration of element i, I_i the measured fluorescence intensity, I_i^* the calibration factor, μ_{Me} the matrix mass absorption coefficient for the exciting radiation, μ_{Mi} the matrix mass absorption coefficient for the fluorescence radiation of element i, μ_{je} the mass absorption coefficient of

TABLE 4

Influence of the packing density of the materials on the measured intensities (powders of original particle size) for basalt JB 1 and norite NIM-N
(Measuring conditions as in Table 3.)

Element	Intensity, JB 1				Intensity, NIM-N			
	Pellet	Powder	s_r (%)	Diff. (%)	Pellet	Powder	s_r (%)	Diff. (%)
Al	63000	61200	0.5	3	69900	68700	0.5	2
Si	492000	483000	0.2	2	446700	442200	0.2	1
K	15100	14700	1.1	2.5	2800	2870	3.3	2.9
Ca	132600	130300	0.3	1.8	174800	171300	0.2	2.0
Ti	41400	41000	0.9	1.0	5640	5580	2.7	1.1
Mn	22500	22200	0.2	1.2	27000	26900	0.7	0.2
Fe	1826000	1796000	0.5	1.7	1848000	1823000	0.1	1.4
Zn	8860	8860	0.9	0.0	6330	6280	1.5	0.7
Rb	26200	25700	1.9	1.8	2580	2530	3.5	1.9
Sr	362500	362200	0.1	0.1	212400	211800	0.2	0.3

element j for the exciting radiation, and μ_{ij} the mass absorption coefficient of element i for the radiation from element j. The concentrations are calculated by iterative approximations. The equipment allows the determination of all major elements with $Z \geqslant 13$. Because the sum of the major constituents, when expressed as oxides, amounts to more than 99% of the geological material present, it was assumed that of the elements below $Z = 13$, only oxygen was present. A major element is defined as an element at a concentration exceeding 0.1%. Moreover, since the major elements comprise more than 99% of the matrix, absorption and enhancement effects from other elements can be neglected. This reduces the number of parameters to be dealt with significantly. For the geological materials considered, the matrix is supposed to consist only of the elements O, Mg, Al, Si, K, Ca, Ti, Mn and Fe. The error induced by this approximation in the calculation of the mass absorption coefficients is generally smaller than 1%, as can be readily calculated.

Absorption correction based on the scatter peak intensity

According to Reynolds [10], the mass absorption coefficient for infinitely thick samples is inversely proportional to the peak intensity of the Compton scattered radiation. Reynolds applied this to compensate for matrix absorption effects in the determination of the elements Ni ($Z = 28$) to Zn ($Z = 40$) in geological samples. For the determination of elements below nickel, it is essential to consider the iron absorption edge, which causes an abrupt discontinuity in the matrix absorption versus energy curve. Even so, the analysis is restricted to elements with atomic numbers above titanium, which is another major element in most geological samples. The approach is semi-empirical and in order to verify its applicability in the case of energy-dispersive equipment, the method was investigated for the determination of the absorption correction of an arbitrarily chosen element, namely zinc.

The Compton scatter peak intensities and the mass absorption coefficient for the zinc K_α line are listed for a number of pure elements or compounds in Table 5. Linear regression on the data yields the relation

$$(1/\mu)10^4 = 66 \,.\, Mo_{INC} + 17.11 \quad (r = 0.997) \qquad (2)$$

Similar data are also presented for five geological materials. The average difference between the calculated absorption coefficient for the zinc line and the value obtained from eqn. (2) is only ca. 1%. As the ratio of mass absorption coefficients for different energies is approximately constant, the absorption corrections for other fluorescence lines in the energy region above the iron edge may also be easily calculated.

This procedure enables the absorption contribution for a number of trace elements to be determined readily without knowledge of the complete matrix composition. The method may therefore be very useful for specific applications, where a total analysis of the sample is of no interest. Examples are the analysis of uranium ores through the *U—L* lines [11] and the determination of rubidium and strontium in radiometric dating measurements [12, 13]. For the present work on the multi-element analysis of geochemical samples, the method is not readily adaptable, nor is its use strictly necessary.

Calibration parameters and physical data for radiation absorption

The sensitivity factors for calibration were determined from the measurement of thin films of pure elements, with an accuracy certified within 5%. The accuracy was checked earlier for a number of medium *Z* elements and found to be about 4% for the elements considered [1]. For the low *Z* elements Cl, K and Ca, the calibration data were compared to values obtained from

TABLE 5

Incoherent scatter peak intensities (relative units) and absorption coefficients for pure compounds and geological materials

Sample	Intensity of incoherent scattering, Mo K_α	μ_{Zn} (g cm^{-2})	Fitted value from eqn. (2)
Ti	0.566	167	184
CaF_2	1.700	78.5	77.3
S	1.528	75.5	84.8
$CaSO_4 \cdot 2$ aq.	2.606	53.0	52.9
Al_2O_3	6.095	26.5	23.8
NaF	7.429	19.2	19.7
$NaHCO_3$	11.776	12.4	12.6
NIM-G	4.050	35.9	35.2
JG 1	3.903	36.6	36.4
JB 1	2.739	50.6	50.5
GA	3.846	37.8	36.9
BCR 1	2.364	56.8	57.8

the measurement of pure compounds pressed to a pellet. After correction for radiation absorption by eqn. (1), the calibration factors caused positive deviations of +11%, +6% and +7%, respectively. This bias could have been corrected for but this was considered inappropriate, because it could not be established with certainty whether the thin-film calibration or the absorption corrections used were erroneous.

The absorption coefficients were calculated from the fitting equations listed by McMasters et al. [14]. Fluorescence yields were taken from Bambynek et al. [15].

RESULTS

The accuracy of the method was demonstrated by analysis of the seven geochemical reference materials available. For three of the standards, the results are shown in Table 6. The recommended data were taken from the compilation of Flanagan [16]. For the undetected elements, three times the standard deviations of the calculated background fluctuation are reported as a detection limit. The average absolute deviations between the results obtained and those reported are 11%, 9.4% and 7.3% for the major constituents (>0.1%) in the granite, norite and basalt samples, respectively; the largest deviations occur for the lowest Z-elements. For the minor constituents the corresponding

TABLE 6

Comparison between the x.r.f. results and the values compiled by Flanagan [16] (Results are based on excitation with titanium excitation and molybdenum excitation. Each result is the mean of 3 separate determinations.)

Sample	Granite NIM-G		Norite NIM-N		Basalt JB 1	
	X.r.f.	Compiled	X.r.f.	Compiled	X.r.f.	Compiled
Mg	<0.35%	0.06%	5.8%	4.48%	4.67 ± 0.36%	4.64%
Al	7.22 ± 0.47%	6.39%	11.4 ± 1.1%	8.80%	9.61 ± 0.63%	7.69%
Si	31.6 ± 1.4%	35.3%	21.7 ± 1.2%	24.5%	22.2 ± 1.2%	24.3%
K	4.02 ± 0.07%	4.13%	0.213 ± 0.001%	0.216%	1.20 ± 0.6%	1.18%
Ca	0.68 ± 0.04%	0.57%	8.88 ± 0.04%	8.25%	6.87 ± 0.08%	6.58%
Ti	0.056 ± 0.002%	0.054%	0.123 ± 0.005%	0.114%	0.807 ± 0.033%	0.804%
V	<30 ppm	2 ppm	294 ± 20 ppm	(225 ppm)	324 ± 19 ppm	(300 ppm)
Cr	<20 ppm	12 ppm	47 ± 4 ppm	40 ppm	468 ± 47 ppm	417 ppm
Mn	0.0156 ± 0.0001%	0.016%	0.139 ± 0.002%	0.132%	0.112 ± 0.004%	0.124%
Fe	1.27 ± 0.03%	1.41%	6.14 ± 0.08%	6.30%	5.82 ± 0.12%	6.33%
Co	<45 ppm	(6 ppm)	(88 ppm)	(65 ppm)	<45 ppm	39 ppm
Ni	<30 ppm	11 ppm	(137 ppm)	(120 ppm)	(134 ppm)	139 ppm
Cu	23 ± 2 ppm	15 ppm	(19 ppm)	13 ppm	62 ± 3 ppm	52 ppm
Zn	48 ± 6 ppm	60 ppm	65 ± 4 ppm	80 ppm	84 ± 6 ppm	83 ppm
Ga	29 ± 2 ppm	32 ppm	20 ± 1 ppm	19 ppm	18 ± 2 ppm	(17 ppm)
Ge	3 ± 1 ppm	<6 ppm	2 ± 1 ppm	<6 ppm	2 ± 1 ppm	—
As	16 ± 2 ppm	—	3 ± 1 ppm	—	4 ± 1 ppm	—
Se	<1 ppm	—	<1 ppm	—	(1.4 ppm)	—
Br	<1 ppm	—	<1 ppm	0.15 ppm	<1 ppm	(0.6 ppm)
Rb	323 ± 2 ppm	274 ppm	5 ± 1 ppm	9 ppm	42 ± 2 ppm	41 ppm
Sr	11 ± 1 ppm	13 ppm	300 ± 7 ppm	254 ppm	477 ± 6 ppm	438 ppm
Pb	50 ± 2 ppm	38 ppm	<2 ppm	<10 ppm	(13 ppm)	14 ppm
Th	58 ± 2 ppm	(56 ppm)	<1 ppm	0.5 ppm	9 ± 1 ppm	9.4 ppm

deviations are 15%, 25% and 7.3%. These data, especially those for the norite samples, may be affected by inaccuracies in the reported concentrations.

The importance of the enhancement effects depends directly on the calculations; for one of the samples, this is shown in Table 7. The results for calcium and iron are not significantly enhanced as they are the major elements with the highest Z values in the two series of elements that are determined with the titanium and the molybdenum excitation radiation, respectively. The effects of enhancement on the concentrations of the other major elements are limited to a maximum of 8%, which is rather low compared to the previously reported enhancement factors in analyses of metals [1]. Moreover, in the case of elements such as aluminum and silicon, for which the accuracy is limited to ca. 20% by the low detection efficiency and the considerable radiation absorption effect, the enhancement factor can easily be omitted from the calculations without significantly affecting the accuracy of the results.

It appears that the method is suitable for application over the full compositional range. Practically, the limitations occur from counting statistics. The presence of L-lines from heavy elements like barium, neodymium, etc., was observed, but the results obtained from them were irreproducible because of strong spectral interference from the K-lines of the medium Z elements.

So far, the analyses have been restricted to standard geological samples, but the procedure may obviously be extended to other materials for which an effective strategy to insure small particle size and good homogeneity then becomes mandatory. At present work is in progress to test the method for the analysis of coal fly ash and air-particulate matter; the results of this study will be published in due course.

CONCLUSIONS

Energy-dispersive x-ray fluorescence is satisfactory as a rapid method for the analysis of geological samples. The computerized non-linear least-squares fitting procedure reported earlier allows precise deconvolution of the complex

TABLE 7

Concentration values (in %) for the major elements in NIM-N, calculated with and without the enhancement contributions

Element	Full absorption enhancement correction	Absorption correction only
Al	11.4	12.0
Si	21.7	22.4
K	0.213	0.220
Ca	8.88	8.88
Ti	0.123	0.133
Mn	0.139	0.139
Fe	6.14	6.14

spectra with a medium-size minicomputer. A simple sample preparation consisting of pressing the powder to a pellet is appropriate. No significant particle size effects were noticed for the standard samples considered. The fundamental parameter technique allows an accurate correction for radiation absorption. In most cases, enhancement effects are of marginal importance but they can easily be calculated. The correction method based on the Compton-scattered excitation radiation may be very useful for specific applications involving the determination of one or a few elements, such as the determination of rubidium and strontium for rock dating. Calibration factors were determined from pure thin element films. If there are no serious spectral interferences, the detection limit for a typical transition element is ca. 1 ppm. This is the case for elements like germanium, selenium and bromine. For elements adjacent to major elements, such as cobalt, the detection limit is ca. 50 ppm. Line overcrowding in the spectral region between 4.5 and 6.4 keV leads also to high detection limits for elements such as vanadium and chromium.

Energy-dispersive x-ray fluorescence is successful for the routine analysis of thick geological samples with an accuracy of approximately 10%. The accuracy is restricted mainly for the determination of minor elements with fluorescent lines in overcrowded spectral regions.

The assistance of H. Nullens with the data reduction procedures is gratefully acknowledged. This work was financially supported by IWONL and NFWO, Belgium.

REFERENCES

1 P. Verbeke, H. Nullens and F. Adams, Anal. Chim. Acta, 97 (1978) 283.
2 P. Van Espen and F. Adams, Anal. Chem., 48 (1976) 1823.
3 P. Van Espen, H. Nullens and F. Adams, Nucl. Instrum. Methods, 142 (1977) 243.
4 P. Van Espen, H. Nullens and F. Adams, Nucl. Instrum. Methods, 142 (1977) 579.
5 J. Hower, Am. Mineral., 44 (1959) 19.
6 R. Jenkins, An Introduction to X-ray Spectrometry, Heyden, London, 1976.
7 P. F. Berry, T. Furuta and J. R. Rhodes, Adv. X-ray Anal., 12 (1969) 612.
8 P. A. Pella, K. E. Lorber and K. F. J. Heinrich, Anal. Chem., 50 (1978) 1268.
9 J. Criss and L. Birks, Anal. Chem., 40 (1968) 1080.
10 R. C. Reynolds, Am. Mineral., 48 (1963) 1133.
11 J. W. Rowson and S. A. Hontzeas, Can. J. Spectrosc., 22 (1977) 24.
12 A. Turek, C. Riddle and T. E. Smith, Can. J. Spectrosc., 22 (1977) 20.
13 E. A. Th. Verdurmen, X-ray Spectrom., 6 (1977) 117.
14 W. H. McMaster, N. K. Del Grande, J. H. Mallett and J. H. Hubbell, Compilation of X-ray Cross Sections, UCRL-50174, Sec II, Rev 1 (1969).
15 W. Bambynek, B. Crasemann, R. W. Fink, H.-U. Freund, H. Mark, C. D. Swift, R. E. Price and P. V. Rao, Rev. Mod. Phys., 44 (1972) 716.
16 F. J. Flanagan, Geochem. Cosmochim. Acta, 37 (1973) 1189.

Analytica Chimica Acta, 109 (1979) 97—106

SIGNAL DEPRESSION IN ELECTROTHERMAL ATOMIC ABSORPTION SPECTROMETRY BY NITRATE AND SULFATE IONS

R. H. EKLUND and J. A. HOLCOMBE*

Department of Chemistry, University of Texas at Austin, Austin, Texas 78712 (U.S.A.)

(Received 28th February 1979)

SUMMARY

The effects of nitrates and sulfates, which decompose to generate oxidants on heating, on the gaseous atom concentration for Ag, Cu and Ga have been investigated with a graphite filament atomizer and an optical arrangement which allows spatial information above the atomizer surface to be gathered. For the potassium and sodium salts, the largest signal depression, caused by gaseous atom oxidation, was found with the largest relative decomposition at the particular temperature, which therefore gives the largest partial pressure of the oxidants formed above the oxidizer. For the calcium salts, Ca metal was vaporized from the atomizer and competed successfully with the analyte, for any oxidants generated, thereby preventing oxidation of the analyte, so that, in some cases, the analyte atom concentration was increased.

Over the past few years, atomic absorption spectrometry with electrothermal atomization has attained widespread use for trace metal analysis. While this technique has many advantages, it has been plagued by interference effects. Such effects are often reported merely as a percentage change in the analyte absorbance while factors such as the counteranion (or cation), atomization temperature and spatial zone being viewed are often omitted thereby making it difficult to correlate and interpret data from different laboratories.

While surface phenomena may play a role in causing such interference effects, gas phase reactions are believed to be a major cause. Thermodynamics sometimes gives a reasonable prediction of the extent of these gas phase reactions, but recent work has shown that kinetics may also be important in predicting the extent of reaction [1]. Relatively slow reactions or reactions between species at low concentrations may require kinetic considerations to determine the extent of the gas phase interference on the time scale of the observed absorbance signal. Conversely, facile reactions or reactions where a large excess of interferent is present may permit local gas phase equilibrium or thermodynamic data to be used in predicting and explaining interactions.

Recent work [1—5] has shown that analyte reactions with oxygen are important in decreasing the magnitude of the absorbance signal obtained by electrothermal atomization. Diffusion of air into the sheath gas [3] and

decomposition of nitrate salts [2] have both been suggested as possible sources of oxygen. Assuming the existence of gas phase analyte — oxygen reactions, Eklund and Holcombe [4] have shown that interferent metal atoms could compete favorably for the oxidant, thus providing an explanation for many signal enhancements previously reported.

As a consequence of this theory, the roles of ions such as nitrate and sulfate which decompose thermally to produce oxygen and other gaseous oxidants must also be important in determining the magnitude of analyte absorbance. Most nitrates decompose in the following manner:

$$2MNO_3(s) \rightarrow M_2O(s) + 2NO_2(g) + \tfrac{1}{2}O_2(g)$$

Nitrogen dioxide is also capable of oxidizing most metals to the metal oxide at elevated temperatures. Sulfates also decompose to generate an oxidizing species:

$$MSO_4(s) \rightarrow MO(s) + SO_3(g) \rightarrow MO(s) + SO_2(g) + \tfrac{1}{2}O_2(g)$$

At the elevated temperatures encountered in electrothermal atomizers, MO, SO_2 and O_2 will be the predominant species formed. Based on the relationship reported previously [4], it can be shown that sulfur dioxide will be capable of oxidizing only those metals whose metal oxide bond energy is 120 kcal mol^{-1} or larger, whereas most metals will react with the oxygen generated. The following studies explore the effect of metal nitrates and sulfates in depressing atomic signals in electrothermal atomic absorption spectrometry.

EXPERIMENTAL

The atomizer and optical arrangement used to carry out the steady state experiments have been described previously [4]. The absorbance—height—time profiles for the transient studies were measured by using the optical arrangement described by Salmon and Holcombe [6]. The final atomization temperature for the steady state experiments was adjusted to give an absorbance signal of 0.2—0.6 from the analyte. These temperatures were typically 1300 K for silver and 1400 K for copper and gallium. For the transient studies, the dry and ash temperatures were 373 K for 10 s and 5 s, respectively, and the final atomization temperature was 2000 K for 2 s. The masses of the analyte used were 2.0×10^{-10} g of silver, 1.0×10^{-9} g of copper, and 1.7×10^{-8} g of gallium. An argon sheath flowing at 10 cm s^{-1} was used in all experiments.

Reagent-grade chemicals and triply distilled water were employed. For stock solutions, copper sulfate and silver nitrate were dissolved in water, and gallium was dissolved as the pure metal in a minimal amount of nitric acid.

RESULTS AND DISCUSSION

Steady state studies

In the thermal decomposition of nitrate and sulfate, oxygen is evolved. To test the effectiveness of oxygen in decreasing the concentration of free analyte atoms, steady state experiments were conducted. Milligram amounts of the analyte were placed in the wells in the atomizer, and 0.56 torr of oxygen was introduced into the sheath gas. The atomizer temperature was adjusted to give a 0.6 absorbance signal from the analyte, and the signal was recorded for 15 s. The percentage change in the analyte absorbance caused by the presence of oxygen is presented for Ag, Cu and Ga in Table 1. While thermodynamics would predict that copper, which forms the most stable metal oxide (M—O bond energy 96 kcal mol^{-1}), would show the most severe depression followed by gallium (70 kcal mol^{-1}) and then silver (47 kcal mol^{-1}), gallium gives the largest depression, possibly for kinetic reasons [1].

Initially, a series of steady state experiments was undertaken to ascertain the extent of the gas phase reaction between the analyte and the oxidants resulting from the decomposition of some nitrates and sulfates. Table 2 lists the equilibrium constants for the decomposition of the interferent salts at 800 K. By placing mg amounts of the metal of interest in one well in the graphite filament and similar quantities of a nitrate or sulfate in the other well, condensed phase interactions between the two compounds could be minimized, and changes in the gaseous atom concentration arising from gas phase reactions isolated. The rod temperature was held constant and the signal recorded for 15 s. This procedure insured gas phase coincidence between the metal and the oxidizing species.

Nitrates. Table 3 lists the percentage changes of the absorbance signals for Ag, Cu and Ga in the presence of calcium, potassium and sodium nitrates relative to that for the pure metal at different spatial zones above the atomizer. The results reported are the average of 5 measurements made at each height for the same filament. Repeating the experiment with a new filament gave

TABLE 1

Steady state effect of oxygen on Ag, Cu and Ga signals

Height (mm)	Change in absorbance (%)		
	Ag	Cu	Ga
0	−2	−2	−87
1	0	−8	−98
2	−18	−21	−100
3	−5	−36	−100
4	−4	−52	—[a]
5	−8	−65	—[a]

[a]Signal in the absence of oxygen did not persist at this height.

TABLE 2

Equilibrium constants for the decomposition of some nitrates and sulfates at 800 K [7,8]

Compound	Reaction	Equilibrium constant
$Ca(NO_3)_2$	$Ca(NO_3)_2 \rightarrow CaO + 2NO_2 + \frac{1}{2}O_2$	4.01×10^{-3}
$NaNO_3$	$2NaNO_3 \rightarrow Na_2O + 2NO_2 + \frac{1}{2}O_2$	1.60×10^{-18}
KNO_3	$2KNO_3 \rightarrow K_2O + 2NO_2 + \frac{1}{2}O_2$	8.84×10^{-27}
$CaSO_4$	$CaSO_4 \rightarrow CaO + SO_2 + \frac{1}{2}O_2$	3.55×10^{-17}
K_2SO_4	$K_2SO_4 \rightarrow K_2O + SO_2 + \frac{1}{2}O_2$	—[a]
Na_2SO_4	$Na_2SO_4 \rightarrow Na_2O + SO_2 + \frac{1}{2}O_2$	1.49×10^{-29}

[a]Data are not available; at 1413 K the percentage decomposition is approximately twice that for Na_2SO_4 at the same temperature.

TABLE 3

Steady state effect of nitrate decomposition on Ag, Cu and Ga absorbance

Height (mm)	Change in absorbance (%)								
	Ag			Cu			Ga		
	$+Ca(NO_3)_2$	$+KNO_3$	$+NaNO_3$	$+Ca(NO_3)_2$	$+KNO_3$	$+NaNO_3$	$+Ca(NO_3)_2$	$+KNO_3$	$+NaNO_3$
0	+10	—7	—18	+78	—22	—53	+32	—22	—22
1	+7	—23	—57	+34	—37	—52	+53	—38	—15
2	+8	—36	—80	+26	—60	—70	+91	—12	—49
3	+15	—41	—91	+17	—81	—86	+125	—52	—69
4	+26	—36	—95	+18	—95	—100	—[a]	—[a]	—[a]
5	+20	—44	—95	+15	—100	—100	—[a]	—[a]	—[a]

[a]Signal of pure metal did not persist above 3 mm.

slightly different values, because of differences in contact between the salt and the atomizer, etc.; however, the trends observed for the magnitude of the signal change as a function of the salt used remained the same. Table 3 shows that, with the exception of gallium at 1-mm height, $NaNO_3$ caused greater depressions of the absorbance than KNO_3. The equilibrium constant for the decomposition of $NaNO_3$ at 800 K is approximately 10^{11} times larger than that for KNO_3 (Table 2). This will make the partial pressure of the oxidizing species above the atomizer greater for $NaNO_3$, thereby increasing reaction rates and the magnitude of the signal depression. Occlusion of the analyte does not appear to be the cause of the observed signal depressions because at the temperature range of these studies (1300—1600 K), potassium and sodium have a vapor pressure of 1 atm and therefore will leave the rod at the rate at which the salts decompose and not at their equilibrium vapor pressures. Thus, as the sheath gas cools at elevated heights above the atomizer, supersaturation and condensation are minimal.

The unpredicted behavior of gallium at 1 mm where $NaNO_3$ gave less depression than KNO_3 possibly is due to factors such as contact of the salt with the rod. If there is poor contact between the salt and the rod, radiative and

convective heating will be the main means of heat transfer, and the salt may be several hundred degrees cooler than the rod and metal being studied, thereby reducing the partial pressure of the oxidizing species. Additionally, if good contact with the rod is achieved, the graphite could react with a significant fraction of the NO_2 and O_2 generated, forming NO, CO, and CO_2, which are poor oxidants for most metals. This will result in less significant signal depression.

In all cases, calcium nitrate enhanced the analyte signal. Table 2 shows that the equilibrium constant for the decomposition of $Ca(NO_3)_2$ is relatively large, and it is likely that only CaO will remain on the filament after the initial heating period. While CaO boils at 3123 K and could not be appreciably vaporized from the rod at the temperature used in these experiments, graphite reduction of the CaO would result in metallic calcium which boils at 1757 K. Once in the gas phase, calcium could enhance the analyte signal by blocking its oxidation through preferential scrubbing of the sheath gas of any oxidizing agents. The non-uniform nature of these enhancements at different heights may reflect on the role of the graphite in reducing CaO, in which the time-varying contact between the rod and CaO becomes important in determining how much calcium is formed and subsequently vaporized. It is unlikely that potassium would preferentially scrub the sheath gas of oxidizing agents because K_2O, a product of the scrubbing reaction, decomposes at 623 K [9] and would not be formed at the elevated temperatures found in the atomizer. Sodium can react with these oxidants, but the signal depressions observed instead of enhancements indicate that these reactions are not favorable and/or as fast as the oxidative reactions involving the analyte.

Sulfates. To examine the role of sulfate decomposition in causing signal depressions, experiments were done with calcium, potassium, and sodium sulfates. The results, (Table 4) exhibit trends similar to those observed for the nitrates where the salt with the largest degree of decomposition (potassium sulfate) gave the largest signal depression. The magnitude of the depressions

TABLE 4

Steady state effect of sulfate decomposition on Ag, Cu and Ga absorbance

Height (mm)	Change in absorbance (%)									
	Ag			Cu				Ga		
	$+CaSO_4$	$+K_2SO_4$	$+Na_2SO_4$	$+CaSO_4$	$+CaSO_4$[a]	$+K_2SO_4$	$+Na_2SO_4$	$+CaSO_4$	$+K_2SO_4$	$+Na_2SO_4$
0	+14	−55	−11	−24	+17	−92	−61	−95	−97	−96
1	+7	−84	−27	−29	+37	−100	−94	−99	−100	−100
2	+6	−98	−62	−50	+58	−100	−96	−100	−100	−100
3	+5	−99	−81	−76	+88	−100	−100	−100	−100	−100
4	−9	−100	−89	−85	+121	−100	−100	—[b]	—[b]	—[b]
5	−15	−100	−92	−91	+104	−100	−100	—[b]	—[b]	—[b]

[a] After atomizers had been preheated to elevated temperatures to convert $CaSO_4$ to CaO.
[b] Signal of pure metal did not persist above 3 mm.

observed for silver may seem excessive in relation to the weak silver oxide bond, but when compared to the even greater effects of the sulfates on the absorbances of copper and gallium, the observed depressions are reasonable.

For calcium sulfate, the observed enhancements and depressions may be a consequence of two factors. Unlike calcium nitrate, calcium sulfate may not decompose totally upon heating and the magnitude of the effects will depend on the relative amounts of oxidizing species and calcium metal evolved.

For gallium, it appears that sufficient oxygen is generated along with a fast metal oxidation reaction to reduce the gallium atomic concentration to 5% of its original value. The slightly smaller depression produced by calcium sulfate is probably a result of calcium metal removing a portion of the oxidizing agents. However, the fact that the effect is small suggests that gallium oxidation is faster than calcium oxidation.

When the atomizer was heated to a temperature that gave an absorbance of 0.6 for copper, $CaSO_4$ was found to depress the copper absorbance by at least 24% at all heights, but the magnitude of the depression was less than that caused by K_2SO_4 or Na_2SO_4, and was less than would be predicted from the thermal decomposition data for the sulfates. Possibly there is competition between the copper and calcium atoms for the oxidizing agents generated. When the atomizer temperature was momentarily elevated to complete the conversion of $CaSO_4$ to CaO and the experiment repeated, the copper absorbance was enhanced (by the scrubbing action of the calcium metal) at all heights (Table 4).

The enhancement at the lower heights observed for silver is again likely to be due to fast calcium atom scrubbing of the sheath gas. The depressions at 4 and 5 mm possibly are due to the slower oxidation of silver atoms by species that calcium did not react with, perhaps because they were in excess relative to the calcium initially. Less calcium would be vaporized in the silver experiments because the rod was several hundred degrees cooler than for copper. These studies with calcium sulfate provide an excellent example of problems that may arise when a concomitant can generate two species whose reactions may have opposing effects on the gaseous analyte atom concentration.

Transient studies

Unlike the steady state situation, certain factors in conventional electrothermal atomic absorption spectrometry may make it difficult for the oxidant generated by thermal decomposition to react with the metal. For example, the oxidant may not reach the gas phase because the concomitant is present in a lesser amount than the analyte, and also more intimate contact between the graphite and the desolvated sample may result in increased reaction probability between the oxidant and the graphite. Additionally, large differences between the decomposition temperature of the salt and the appearance temperature of the metal will reduce the probability of gas phase coincidence. In order to examine how the decomposition of sulfates and nitrates affects the magnitude of the analyte absorbance signal, a series of transient experiments

was conducted with the same metals and nitrate and sulfate salts studied above. All measurements were checked at a non-resonance line to insure that scatter was minimal. Transient studies on the effect of excess of nitrate on the copper absorbance were not undertaken because $Cu(NO_3)_2$ sublimes at less than 500 K [7] and would only serve to complicate the results.

To verify that the decomposition products of the nitrate or sulfate salts would exhibit gas phase coincidence with the analyte, the absorbance of the metal counter ion (K^+ or Na^+) was monitored as a function of time. Upon decomposition of the salt, any K or Na formed by graphite reduction of the oxide will have a sufficient vapor pressure to be immediately vaporized. Thus, the Na or K absorbance signal should reflect the time-dependent release of any oxidants from sulfate or nitrate. This approach is not valid for the calcium salts because the vapor pressure of calcium is not sufficiently high to guarantee vaporization of the metal simultaneously with the salt decomposition at the atomizer temperatures used in these studies. Results indicate that there is complete overlap between the absorbance of K and Na from their sulfates and the analytes Cu and Ga. Silver vaporizes earlier than the sulfates decompose and only the tail of the Ag peak overlaps with that from the sulfate decomposition. As for the nitrates, direct overlap is recorded for the decomposition products and the Ag absorbance peak. The nitrates begin to decompose before gallium vaporizes but continue to decompose for long enough to give substantial overlap with the Ga peak.

Nitrates. In examining the effects of nitrate decomposition on the silver absorbance signal, 10-, 100- and 1000-fold amounts of $Ca(NO_3)_2$, KNO_3 and $NaNO_3$ were used. The 10- and 100-fold amounts showed little effect on the signal at any spatial region but the 1000-fold amounts of KNO_3 and $NaNO_3$, but not $Ca(NO_3)_2$, caused pronounced effects, as shown in Fig. 1

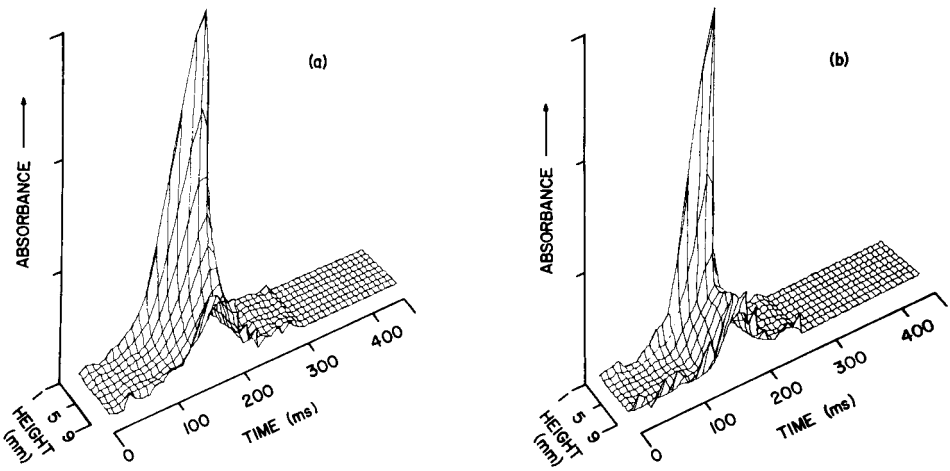

Fig. 1. Absorbance—height—time profile for (a) 2×10^{-10} g of Ag and (b) 2×10^{-10} g of Ag with a 1000-fold amount of $NaNO_3$. Peak absorbance in both cases is 0.50.

for $NaNO_3$. Figure 1 shows the more rapid decrease of the absorbance signal at the lower heights in the presence of the nitrates followed by a leveling of the signal at greater heights. A fast reaction in which one reactant is depleted or equilibrium is reached at several mm would account for the shape of this plot. Oxidation of the silver by NO_2 and not by O_2 is believed to be responsible for this decrease in the Ag signal since introduction of oxygen into the sheath gas (partial pressure 0.56 torr) had little effect on the silver atom concentration. Reduction of most of the NO_2 by the graphite may account for the fact that only the 1000-fold amounts of KNO_3 and $NaNO_3$ showed this depressive effect. Because of the large equilibrium constant for the decomposition of $Ca(NO_3)_2$ at low temperatures, gas phase coincidence between the analyte and any NO_2 generated is less likely. Since trace amounts of oxygen introduced into the sheath gas did not have any appreciable effect on the silver absorbance, preferential scrubbing by calcium of any oxygen present in the atomizer should not cause enhancement of the silver absorbance.

For gallium, only 10- and 100-fold amounts of the nitrates were used because the 1000-fold amount caused appreciable scatter signal. Both the 10- and 100-fold amounts of KNO_3 and $NaNO_3$ caused the absorbance signal to disappear approximately 3 mm nearer the atomizer surface. The KNO_3 decreased the magnitude of the absorbance signal twice as much as $NaNO_3$, which probably reflects the better gas phase coincidence between the reacting species caused by the higher decomposition temperature of KNO_3 relative to $NaNO_3$. With added $Ca(NO_3)_2$, both the 10- and 100-fold amounts enhanced the signal 30—200% in the first few mm above the atomizer surface but did not result in the signal being preserved further above the surface than in the sample containing gallium only.

In these studies, the nitrates caused visible deterioration of the atomizer surface, so that signals were less reproducible than in the absence of nitrates. This surface deterioration is probably due to the graphite reducing a portion of the oxidants generated by nitrate decomposition.

Sulfates. The role of sulfates was examined in a similar fashion with the exception of $CaSO_4$ which is not sufficiently soluble for these studies. For copper in the presence of 10- and 100-fold amounts of K_2SO_4 and Na_2SO_4, the absorbance signal became undetectable 7 to 8 mm above the atomizer surface, whereas a 1000-fold amount of these sulfates caused the signal to disappear at a height of 5—6 mm. This effect is shown in Fig. 2 for the 100-fold amount of K_2SO_4. The change in the magnitude of the absorbance signal is approximately the same for both salts, and there seems to be no correlation between the signal depression and the decomposition data for the sulfates.

Examination of the effect of sulfates on the silver absorbance signal shows that for 10-, 100- and 1000-fold amounts of K_2SO_4 or Na_2SO_4 the change of the absorbance is about 10% at all heights. Unlike the steady state mode, only partial overlap between the analyte and the decomposition products of the sulfates occurs. This, coupled with the fact that oxygen is the primary oxidant formed at the elevated temperatures in the atomizer, accounts for the lack of any significant depression of the silver absorbance.

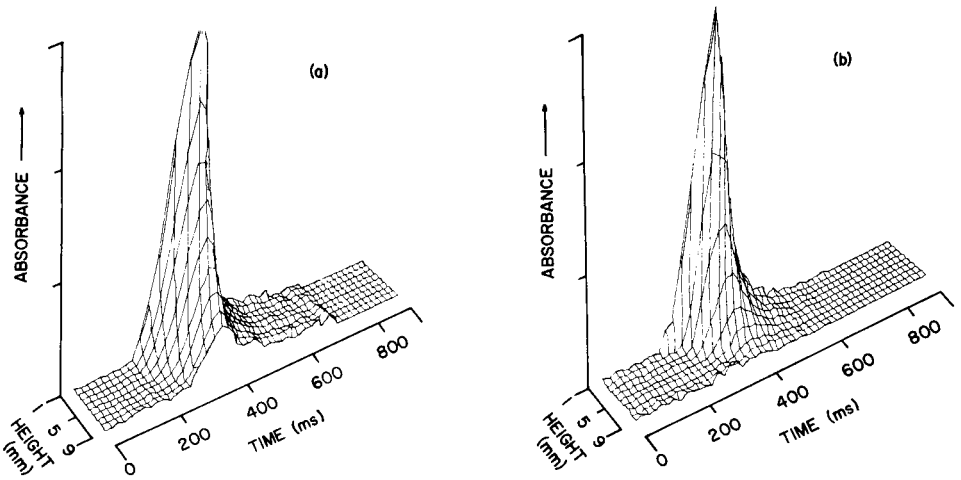

Fig. 2. Absorbance—height—time profile for (a) 1×10^{-9} g of Cu and (b) 1×10^{-9} g of Cu with a 100-fold amount of K_2SO_4. Peak absorbance in both cases is 0.65.

Examination of the effect of sulfates on the gallium absorbance signal revealed both a faster decay of the atomic signal with height above the atomizer and a decrease in the magnitude of the absorbance signal. A 10-fold amount of Na_2SO_4 decreased the signal by 40% and caused it to disappear within 3 mm instead of 4 mm as was the case for gallium without added interferents. A 10-fold amount of K_2SO_4 decreased the absorbance signal by 50% and also caused it to disappear 1 mm above the atomizer. No appreciable signal could be measured in the presence of a 100-fold amount of these sulfates. Rapid decomposition of both sulfates is expected at the temperature where the vapor pressure of gallium becomes appreciable. Consequently, the largest depression is expected for the metal sulfate which exhibits the greater partial pressure of oxygen, i.e. K_2SO_4.

Unlike the nitrates, the sulfates did not cause visible deterioration of the atomizer surface. Probably, the nitrates begin to decompose at an earlier part of the atomization cycle than the sulfates, thereby providing more time for attack of the atomizer surface. Similarly, the reproducibility when sulfates were present was better than in the nitrate studies.

Conclusions

Excess of nitrate and/or sulfate in a sample can cause erroneous results when compared to standards prepared in distilled water. In many cases, analytical errors can be accounted for in a predictable manner by gas phase oxidation reactions between the analyte and the thermal decomposition products of the nitrate and/or sulfate. The magnitude of the depression of the analyte signal is related to the extent of decomposition of the nitrate or sulfate studied with the largest depression being caused by the salt with the greatest decomposition

at that temperature. Many interference effects which have been previously reported in detail in the literature can be explained on this basis. For example, Belling and Jones [10] reported that $NaNO_3$ gave a larger depression of a manganese absorbance than KNO_3 even when the latter was present in greater concentration. Additionally, Ebdon et al. [11] have shown that KNO_3 depressed the manganese absorbance while added $Ca(NO_3)_2$ caused an enhancement. Frech and Cedergren [2] also demonstrated that ashing a sample at a temperature just below the vaporization temperature of the analyte was effective in eliminating nitrate interferences when analyzing for lead. It is likely that the nitrates are decomposed and the products swept out of the observation zone before analyte atomization occurs.

Even for a relatively simple sample matrix where nitric acid has been added, components of the sample such as Na or K may form the nitrate during the drying cycle. These salts can then undergo reactions similar to those demonstrated above, and significantly depress the analyte absorbance. Proper selection of the drying and ashing conditions for prevolatilization of these species should be effective in minimizing the resulting interferences. In the light of the results for $Ca(NO_3)_2$ and $CaSO_4$, care is needed in examining these interfering effects in electrothermal atomic absorption spectromety, to insure that the observed signal alteration is due to a single reaction and not to a combination of two or more opposing reactions.

The authors are grateful to the National Science Foundation for financial support of this project under Grant No. CHE78-15438.

REFERENCES

1 J. A. Holcombe, R. H. Eklund and J. E. Smith, Anal. Chem., in press.
2 W. Frech and A. Cedergren, Anal. Chim. Acta, 88 (1977) 57.
3 G. Guiochon, B. Hircq and C. Tailland, Anal. Chim. Acta, 99 (1978) 125.
4 R. H. Eklund and J. A. Holcombe, Anal. Chim. Acta, 108 (1979) 53.
5 R. D. Reeves, B. M. Patel, C. J. Molnar and J. D. Winefordner, Anal. Chem., 45 (1973) 246.
6 S. G. Salmon and J. A. Holcombe, Anal. Chem., 51 (1979) 648.
7 K. H. Stern, J. Phys. Chem. Ref. Data, 1 (1972) 747.
8 K. H. Stern and E. L. Weise, High Temperature Properties and Decomposition of Inorganic Salts, Part 1, Sulfates, National Bureau of Standards Bulletin 7, U.S. Government Printing Office, Washington, D.C., 1966.
9 R. C. Weast (Ed.), Handbook of Chemistry and Physics, 51st edn., Chemical Rubber Co., Cleveland, Ohio, 1970–71.
10 G. B. Belling and G. B. Jones, Anal. Chim. Acta, 80 (1975) 279.
11 L. Ebdon, G. F. Kirkbright and T. S. West, Anal. Chim. Acta, 58 (1972) 39.

Analytica Chimica Acta, 109 (1979) 107—113

SPECTROPHOTOMETRIC DETERMINATION OF TRACE AMOUNTS OF SILVER(I) BY FORMATION OF DICYANOARGENTATE(I) AND SOLVENT EXTRACTION WITH METHYLENE BLUE

TOMOZO KOH* and MASAHIDE KATOH

Department of Chemistry, Faculty of Science, Tokai University, Hiratsuka, Kanagawa 259-12 (Japan)

(Received 8th March 1979)

SUMMARY

The spectrophotometric method proposed for the determination of micro amounts of silver(I) is based on the formation of dicyanoargentate(I) and its extraction into 1,2-dichloroethane as an ion pair with methylene blue. The absorbance of the extract is stable for at least 3 days in a glass-stoppered tube. The apparent molar absorptivity for silver at 657 nm is 99500 l mol^{-1} cm^{-1} and the Sandell sensitivity is 0.0011 μg Ag cm^{-2} for 0.001 absorbance. Linear calibration graphs are obtained over the range 2.8×10^{-7}—1.0×10^{-5} M silver(I) (0.3—10.8 μg Ag in 10 ml); at the 6×10^{-6} M silver(I) level, the relative standard deviation is 0.3%. Very high selectivity is achieved with EDTA as masking agent.

Many methods for the spectrophotometric determination of silver(I) involve binary complex formation between silver(I) ions and chromogenic reagents [1—5], but these methods have drawbacks in sensitivity and selectivity. Another method [6] based on binary complex formation is very sensitive ($\epsilon_{530\,nm} = 9.38 \times 10^4$ l mol^{-1} cm^{-1}), but requires very precise pH control. In order to eliminate these drawbacks of binary complexes, Dagnall and West [7, 8] proposed a method based on ternary complex formation of silver(I) with 1,10-phenanthroline and bromopyrogallol red. A method [9] involving reaction of silver with eosine in the presence of 1,10-phenanthroline, though much less sensitive than Cheng's method [6], improved the selectivity, and the complex formed was stable.

Methylene blue forms ion pairs with anions which can be extracted into organic solvents. Thus, methylene blue has been much used for the spectrophotometric determination of anions such as perchlorate [10], thiocyanate [11], boron (as BF_4^-) [12, 13], etc. In addition to these non-metals, copper(II) [14] and mercury(II) [15] can be extracted into an organic solvent by forming the cyano-complexes. A detailed examination of the reaction of silver(I) with cyanide led to the development of a very sensitive and selective method for the determination of silver. In the present study, the formation of dicyanoargentate(I) and its extraction as an ion pair with methylene blue into dichloroethane are discussed with special reference to the determination of

silver(I). The present method is more sensitive than any previous method, and can be applied over a wide pH range with good selectivity for silver.

EXPERIMENTAL

Apparatus and reagents

A Hitachi Model 139 spectrophotometer was used with 10-mm glass cells. A Hitachi-Horiba Model M-5 pH meter and an Iwaki Model KM shaker were also employed.

All chemicals used were of analytical grade and were used without further purification.

Standard silver solution. Dissolve about 7.9 g of silver(I) sulfate (Ag_2SO_4) in redistilled water, and dilute it to 1 l. Standardize the solution by the Mohr method, and prepare working standards by suitable dilution.

Methylene blue solution. Dissolve 759 mg of methylene blue ($C_{16}H_{18}N_3ClS \cdot 3H_2O$, 98.5%) in redistilled water, and then dilute to 250 ml to obtain an 8×10^{-3} M solution. Dilute this solution as required.

Procedure

Pipette 10 ml of a sample solution containing silver up to 10.8 μg (10^{-5} M Ag) into a 50-ml separatory funnel, and add 2 ml of 7.5×10^{-3} sulfuric acid and 2 ml of 8×10^{-3} M potassium cyanide. Dicyanoargentate(I) is formed instantaneously. To this mixture, add 1 ml of 1×10^{-3} M methylene blue and 10 ml of 1,2-dichloroethane. Shake the funnel for 1 min to extract the ion pair formed between methylene blue and the dicyanoargentate(I). After standing for a given period of time, transfer the organic phase to a 15-ml glass-stoppered tube and add some anhydrous sodium sulfate. Shake the mixture vigorously by hand until transparent and measure the absorbance at 657 nm against dichloroethane. Measure the absorbance of a blank solution prepared similarly and make appropriate corrections.

RESULTS AND DISCUSSION

Absorption spectra

Figure 1 shows the absorption spectra of the ion pair [MB^+, $Ag(CN)_2^-$] extracted into 1,2-dichloroethane and of the reagent blank, obtained as described in the Procedure. The shape of the absorption spectrum for [MB^+, $Ag(CN)_2^-$] is very similar not only to the reagent blank but also to the absorption spectra for perchlorate [10], thiocyanate [11], dicyanocuprate(I) [14] and tricyanomercurate(II) [15]. The spectra in both the presence and absence of silver have their maximum absorptions at 657 nm; this wavelength was used in all subsequent measurements of absorbance, because the difference in absorbance between the ion pair and the reagent blank is greatest at 657 nm. The wavelength of maximum absorption did not shift with a change in kind of acid or salt in aqueous solutions.

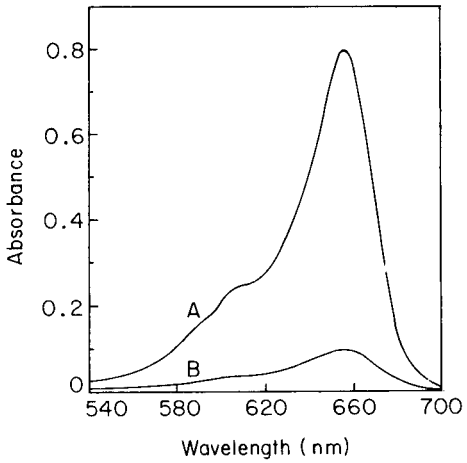

Fig. 1. Absorption spectra. (A) Methylene blue—dicyanoargentate(I) ion pair in 1,2-dichloroethane (reagent blank subtracted). [Ag(I)] = 8×10^{-6} M. (B) Reagent blank against 1,2-dichloroethane.

Effect of pH and amount of cyanide on the formation of dicyanoargentate(I)

The pH of the aqueous solution affected the formation of dicyanoargentate(I). In order to establish the optimum pH range, silver(I) was allowed to react with cyanide in aqueous solutions buffered to pH 1.3—8.0, and then the complex formed was extracted into dichloroethane as an ion pair with methylene blue. The pH of solutions below pH 5.8 was adjusted with sulfuric acid; the pH range 5.9—8.0 was adjusted with phosphate buffer solutions prepared by mixing 0.2 M sodium dihydrogenphosphate with 0.2 M sodium hydroxide in various ratios. Figure 2 shows that maximum constant absorbances were obtained over the wide pH range 2.5—6.7. The decrease in absorbance below pH 2.5 can be attributed to a decrease in the concentration of free cyanide by protonation. The decrease in absorbance above pH 6.7 is probably caused by the formation of unextractable tricyanoargentate(I), owing to an increase in the concentration of cyanide. In fact, as can be seen in Fig. 3, lower absorbances were obtained by increasing the amount of cyanide, though the pH of solutions was adjusted to the optimal range.

In measuring the effect of the amount of cyanide on the formation of dicyanoargentate(I), different amounts of potassium cyanide were employed and extractions were done as in the Procedure, where the solutions were buffered to the optimal pH range 2.5—6.7. When 2 ml of 3×10^{-3}, 8×10^{-3} or 2×10^{-2} M cyanide solution was used, the calibration graphs for silver (Fig. 3) were the most sensitive and coincided with one another when plotted after correction for the reagent blank. However, when 2 ml of $1—4 \times 10^{-4}$ M cyanide was used, formation of dicyanoargentate(I) was incomplete because of lack of cyanide, and so less sensitive graphs were obtained. In contrast, when 2 ml of 7×10^{-2} M cyanide was used, the absorbances were lower presumably

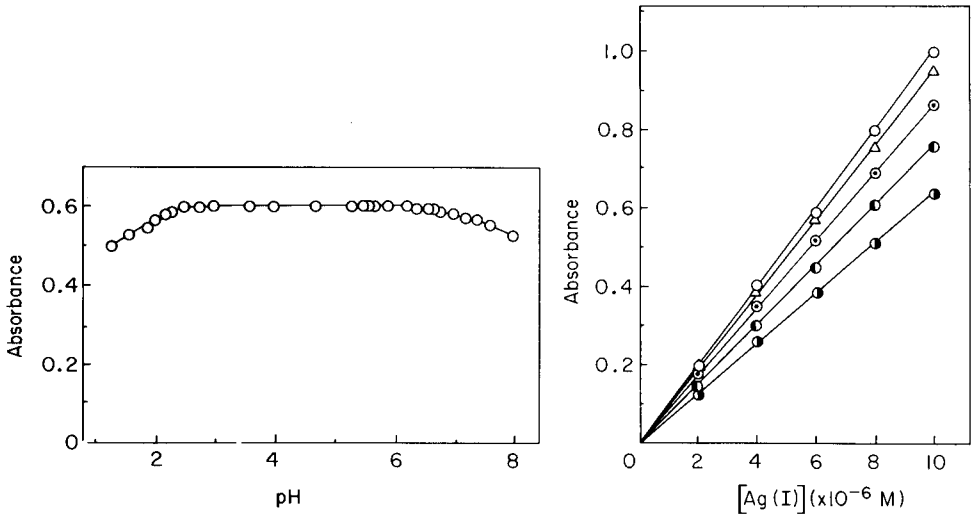

Fig. 2. Effect of pH on the formation of dicyanoargentate(I) (reagent blank subtracted). [Ag(I)] = 6×10^{-6} M.

Fig. 3. Effect of amount of cyanide on the formation of dicyanoargentate(I) (reagent blank subtracted). Concentration of KCN: (◑) 1×10^{-4} M; (◐) 2×10^{-4} M; (⊙) 4×10^{-4} M; (○) 3×10^{-3}, 8×10^{-3} or 2×10^{-2} M (recommended procedure); (△) 7×10^{-2} M.

because of the formation of the unextractable higher complex. Accordingly, 2 ml of 8×10^{-3} M potassium cyanide was employed in the recommended Procedure.

Effect of amount of methylene blue

The extraction of dicyanoargentate(I) as the ion pair with methylene blue can be affected by the concentration of methylene blue. To establish the optimal amount, 1 ml of 2.5×10^{-4}, 5×10^{-4}, 1×10^{-3} or 1.5×10^{-3} M methylene blue was used under the conditions given in the Procedure. The calibration graph with 1 ml of 2.5×10^{-4} M methylene blue gave the lowest reagent blank, but did not form a straight line. All the other graphs were linear, and were parallel with one another; the more methylene blue, the higher the reagent blank. Therefore, 1 ml of 1×10^{-3} M methylene blue was employed in further work.

Composition of extracted species

In order to identify the cyano-complex species concerned in the determination of silver, the reaction was investigated by the method of continuous variations. For application of this method, $10x$ (x = mole fraction of silver) ml of 4×10^{-4} M silver(I) solution and $10\ (1 - x)$ ml of 4×10^{-4} M cyanide solution were used with a varying mole ratio of silver to cyanide. In this case,

2 ml of 3.5×10^{-3} M sulfuric acid was added to adjust the pH to the optimal range, but the other conditions were as in the Procedure. The absorbances of a series of extracts were measured at three arbitrarily-selected wavelengths. Figure 4 shows the plots of absorbance vs. mole fraction of silver(I), in which the absorbance obtained either for the excess of cyanide in the region $x < 0.33$ or for the excess of silver(I) in the region $x > 0.33$ was subtracted. The two curves intersected at a point indicating a 0.33 mole fraction of silver at all three wavelengths. This signifies that silver and cyanide react in the conventional manner: $Ag^+ + 2CN^- \rightleftharpoons Ag(CN)_2^-$, in the recommended Procedure.

The continuous variation technique was also used to determine the composition of the extracted species. Methylene blue and silver(I) solutions of identical molarities were used to prepare a series of 10-ml solutions with varying methylene blue—silver ratios. The order of addition of the reagents and their amounts except for methylene blue were as in the recommended Procedure. The absorbances of the extracts were measured at three arbitrarily-selected wavelengths. The resulting curves, after correction for the absorbances obtained for the excess of methylene blue at $x > 0.5$, are shown in Fig. 5. The maxima at a 0.5-mole fraction of methylene blue at all three wavelengths indicate that a single ion-pair species with a MB:silver mole ratio of 1:1 is extracted. The absorption spectra obtained for Ag^+: CN^- mole ratios of 1:2, 1:4 and 4:1, and for MB—silver mole ratios of 1:1, 1:2 and 4:1, were of the same shape and did not intersect. From a consideration of these results, it was concluded that only the ion pair formed according to

$$MB^+ + Ag^+ + 2CN^- \rightarrow [MB^+, Ag(CN)_2^-]$$

can be extracted into 1,2-dichloroethane under the conditions recommended.

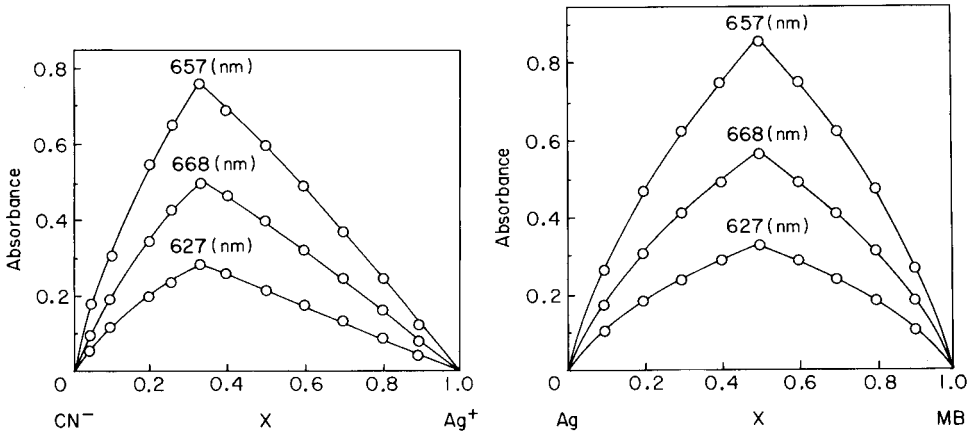

Fig. 4. Continuous variations plots for the silver—cyanide reaction. x = mole fraction of silver; $[Ag^+] + [CN^-] = 4 \times 10^{-4}$ M.

Fig. 5. Continuous variations plots for the MB^+—$Ag(CN)_2^-$ ion pair. x = mole fraction of methylene blue; $[MB^+] + [Ag^+] = 2.5 \times 10^{-5}$ M.

Percentage extraction

A 10-ml portion of 1×10^{-5} M silver solution and 10 ml of redistilled water were taken separately through the recommended procedure. The solutions were extracted with successive 10-ml portions of dichloroethane to determine the percentage extraction of silver, and the absorbance of the organic phase after each extraction was measured against dichloroethane at 657 nm. The results are given in Table 1. The absorbance of the third extract for silver was very similar to that of the third reagent blank, which indicates that extraction with two 10-ml portions of dichloroethane suffices for complete extraction of silver. However, two extractions are not desirable, because of procedural complication and the loss of sensitivity inherent in the increased volume of the organic phase. The reproducibility with a single extraction was so good that one 10-ml portion of dichloroethane was used in the recommended procedure. The percentage extraction with a single 10-ml portion of dichloroethane was about 92%.

Determination of silver

The calibration graph obtained by the recommended procedure (Fig. 3) was linear; there were no measurable changes in the absorbances of the extracts even after standing for 3 days in a glass-stoppered tube at room temperature. Shaking times ranging from 0.75 to 5 min did not produce any change in absorbance, and so a 1-min shaking time was selected. The apparent molar absorptivity for silver at 657 nm is 99500 l mol^{-1} cm^{-1} which shows even better sensitivity than Cheng's method [6]; the Sandell sensitivity is 0.0011 μg Ag cm^{-2} for an absorbance of 0.001. The precision was estimated from 11 results for 10-ml aliquots of 6×10^{-6} M silver solution; the mean absorbance value was 0.597 measured against a reagent blank, with a standard deviation of 0.002 absorbance unit, and a relative standard deviation of 0.3%.

Effect of diverse ions

An aliquot (10 ml) of solution containing various amounts of foreign ions and 6.47 μg of silver, was treated exactly as in the recommended procedure. The results are given in Table 2. Copper(II) interfered with the determination of silver when present in amounts of 10 μg, and Fe(II) and Hg(II) in amounts

TABLE 1

Extraction of the silver complex

No. of extns.	Absorbance		No. of extns.	Absorbance	
	1×10^{-5} M Ag(I)	Reagent blank		1×10^{-5} M Ag(I)	Reagent blank
1	1.100	0.099	4	0.081	0.075
2	0.172	0.082	5	0.075	0.072
3	0.085	0.078	6	0.070	0.069

TABLE 2

Effect of diverse ions on the determination of 6.47 μg of silver

Ion	Added as	Amount (μg)	Ag found (μg)	Ion	Added as	Amount (μg)	Ag found (μg)
Na^+	Na_2SO_4	10000	6.50			10000[a]	6.56
K^+	K_2SO_4	10000	6.50	Hg^{2+}	$HgSO_4$	100	4.02
NH_4^+	$(NH_4)_2SO_4$	10000	6.51			1000[a]	6.33
Mg^{2+}	$MgSO_4$	10000	6.47	Fe^{3+}	$Fe(NH_4)(SO_4)_2 \cdot 12H_2O$	10000	6.28
Zn^{2+}	$ZnSO_4 \cdot 7H_2O$	10000	6.42	Al^{3+}	$AlK(SO_4)_2 \cdot 12H_2O$	1000	6.47
Cd^{2+}	$CdSO_4 \cdot xH_2O$	10000	6.61	F^-	NaF	1000	6.50
Mn^{2+}	$MnSO_4 \cdot xH_2O$	10000	6.75	Cl^-	KCl	100	6.85
		10000[a]	6.45	Br^-	KBr	10	6.88
Cu^{2+}	$CuSO_4 \cdot 5H_2O$	10	7.50	I^-	KI	1	6.65
		10000[a]	6.54	NO_3^-	KNO_3	10	8.01
Fe^{2+}	$FeSO_4 \cdot 7H_2O$	100	5.64	NO_2^-	$NaNO_2$	10	7.72
		1000[a]	6.37	SO_4^{2-}	Na_2SO_4	10000	6.45
Co^{2+}	$CoSO_4 \cdot 7H_2O$	1000	2.98	$C_2O_4^{2-}$	$K_2C_2O_4 \cdot 2H_2O$	100	6.51
		1000[a]	6.69	Tartrate	$Na_2C_4H_4O_6 \cdot 2H_2O$	10000	6.56
Ni^{2+}	$Ni(NH_4)_2(SO_4)_2 \cdot 6H_2O$	1000	3.65	Citrate	$Na_3C_6H_5O_7 \cdot 2H_2O$	1000	6.85

[a]1.5 ml of 0.2 M EDTA solution was added, and the volume of sample solution was made up to 10 ml.

of 100 μg; Co(II) and Ni(II) could be tolerated up to 100 μg, and Mn(II) up to 1000 μg. The interferences of these transition metals could be eliminated by adding 1.5 ml of 0.2 M EDTA solution; Cu(II), Ni(II) and Mn(II) did not then interfere in amounts up to 10000 μg (about 1500-fold compared to silver), and Fe(II), Hg(II) and Co(II) up to 1000 μg (150-fold). Anions such as bromide, iodide, nitrate and nitrite interfered by being extracted into dichloroethane as their ion pairs with methylene blue. However, sulfate and tartrate did not interfere in amounts up to 10000 μg (1500-fold), or fluoride and oxalate up to 1000 μg (150-fold).

The proposed method has therefore the advantage of virtual freedom from interference of many transition metals, and should be of value in trace analysis for silver in practical samples.

REFERENCES

1 E. B. Sandell, Colorimetric Determination of Traces of Metals, 3rd edn., Interscience, New York, 1959.
2 R. M. Dagnall and T. S. West, Talanta, 8 (1961) 711.
3 O. K. Chung and C. E. Meloan, Anal. Chem., 39 (1967) 383.
4 M. C. Eshwar and B. Subrahmanyam, Fresenius Z. Anal. Chem., 272 (1974) 44.
5 R. R. Mulye and S. M. Khopkar, Anal. Chim. Acta, 76 (1975) 204.
6 K. L. Cheng Mikrochim. Acta, 5 (1967) 820.
7 R. M. Dagnall and T. S. West, Talanta, 11 (1964) 1533.
8 R. M. Dagnall and T. S. West, Talanta, 11 (1964) 1627.
9 M. T. El-Ghamry and R. W. Frei, Anal. Chem., 40 (1968) 1986.
10 I. Iwasaki, S. Utsumi and C. Kang, Bull. Chem. Soc. Jpn., 36 (1963) 325.
11 T. Koh and I. Iwasaki, Bull. Chem. Soc. Jpn., 40 (1967) 569.
12 L. Ducret, Anal. Chim. Acta, 17 (1957) 213.
13 L. Pasztor, J. D. Bode and Q. Fernando, Anal. Chem., 32 (1960) 277.
14 T. Koh, Y. Aoki and Y. Suzuki, Anal. Chem., 50 (1978) 881.
15 T. Koh and M. Katoh, J. Chem. Soc. Jpn., (1978) 695.

Analytica Chimica Acta, 109 (1979) 115—121

SPECTROPHOTOMETRIC DETERMINATION OF BORON IN NATURAL WATERS AND ROCKS AFTER SPECIFIC ADSORPTION ON SEPHADEX GEL

KAZUHISA YOSHIMURA*, RURI KARIYA and TOSHIKAZU TARUTANI

Department of Chemistry, Faculty of Science, Kyushu University 33, Hakozaki, Higashiku, Fukuoka 812 (Japan)

(Received 2 January 1979)

SUMMARY

Borate ions are adsorbed on Sephadex G-25 gel from alkaline media and desorbed reversibly into acidic media; the adsorption is ascribed to complex formation between borate and glucose units in the gel matrix. The coexistence of large amounts of salts, e.g. sodium chloride, ammonium chloride, sodium sulfate, and sodium perchlorate, has little effect on the adsorption. The effect of cations which form complexes with borate can be eliminated by the addition of EDTA. Boron present in natural waters and rocks at low levels can be selectively concentrated by means of a gel column and determined spectrophotometrically by the azomethine-H method.

Boron occurs widely in nature at low levels. Knowledge of the concentration of boron in natural waters and rocks is valuable for an understanding of its geochemical behavior; boron in sedimentary rocks has been noted as a paleosalinity index [1].

Traces of boron have been determined by spectrophotometry with curcumin or carmine, or by optical emission spectrometry. These methods, however, suffer from poor sensitivity, poor selectivity, interference by commonly-present solutes, and/or the need for very careful control of experimental conditions. Development of a simple separation and concentration method for boron was desirable.

Gel chromatographic separations of inorganic compounds have been achieved [2—4]. In addition to the well-known molecular-sieve effect, adsorption by Sephadex G-10 and G-15 gels has been applied [5—7]. Lindqvist pointed out that boric acid is bound to Sephadex gels and gives a relatively stable complex [8], but further studies have not been made.

Boric acid can be adsorbed specifically on Sephadex G-25 gel from alkaline solution and desorbed reversibly with acidic solution. After separation and concentration on a Sephadex gel column, the borate can be determined spectrophotometrically by the azomethine-H method [9] with minor modifications; this method can be applied in aqueous medium and is highly sensitive.

EXPERIMENTAL

Chemicals

All the reagents used were of analytical grade.

Buffer-masking solution. Dissolve 250 g of ammonium acetate and 15 g of EDTA (disodium salt) in 400 ml of deionized water and slowly add 125 ml of glacial acetic acid.

Azomethine-H reagent. Dissolve 0.90 g of azomethine-H (Dojin Pharmaceutical Laboratories) in 100 ml of 2% (w/v) L-ascorbic acid solution. Prepare the reagent freshly for each set of measurements.

Determination of boron

To a 4-ml sample containing 0.025—1.5 μmol of boron as borate, add 4 ml of buffer-masking solution and 2 ml of azomethine-H reagent, and stir. After standing at room temperature for 30 min, measure the absorbance at 415 nm with a Hitachi Model 101 spectrophotometer against a reagent blank that had also been allowed to stand for 30 min.

Sample preparation

For water samples, add 20 ml of 0.5 M EDTA solution (pH 10) and adjust the solution to pH 10 with sodium hydroxide.

For acid-soluble rocks, dissolve the sample (0.2—1 g) in a polyethylene beaker by adding 5 ml of concentrated hydrochloric acid. Prepare the sample solution as described above for waters.

For acid-insoluble rocks, fuse the sample (0.1—0.5 g) for 1 h with 2.5 g of sodium carbonate in a platinum crucible. After cooling, transfer the cake to a 300-ml polyethylene beaker, suspend it in 100 ml of water by mechanical stirring, and add 8 ml of concentrated hydrochloric acid. Prepare the sample solution as described above. If the resulting solution is nearly clear and contains large amounts of aluminium(III) and iron(III) that cannot be masked with EDTA, pass the solution through a column (15 mm i.d., 150 mm long) containing 30 ml of Dowex 50W-X12 (50—100 mesh) resin in the hydrogen form. Treat the effluent by the procedure described above.

Separation and concentration of boron on a Sephadex column

Use a column (16 mm i.d., 100 mm long) made of acrylic resin, containing 15 ml of Sephadex G-25 (medium) gel (Pharmacia, Uppsala, Sweden). Condition the column with ammonia solution (pH 10) and pass the sample solution through the column at a rate of 8 ml min^{-1}. Wash the column with 20 ml of ammonia solution (pH 10) and then desorb the boron with 0.02 M hydrochloric acid. Reject the first 10 ml of the effluent and collect the next 10 ml in a 10-ml volumetric flask. Determine the boron concentration by the azomethine-H method [9].

Distribution measurements

To investigate the adsorption of boron (as borate) on Sephadex G-25 gel,

the distribution coefficient K_d was measured by the batch technique. When m g of the gel is added to V ml of solution, $K_d = [(C_i - C_f)\ V/C_f m W_r] + 1$, where C_i and C_f are the initial concentration of boron and the concentration of boron in the equilibrated solution, respectively. The water W_r, of the Sephadex G-25 gel was 2.34 ml g^{-1} (separate test with Blue dextran 2000).

The effect of the pH of the equilibrated solution on the adsorption of borate was examined as follows. To 50 ml of 0.1 M sodium chloride solution containing 10 μmol of boric acid, with the pH adjusted by adding hydrochloric acid or sodium hydroxide, 1 g of the gel was added. The mixture was stirred mechanically for 2 h until equilibrium was reached. The gel was allowed to settle; the pH and the borate concentration of the supernatant solution were determined.

The extent of the adsorption of borate on the gel which was equilibrated with solutions containing various amounts of boric acid adjusted to pH 10, was determined by a similar procedure; a solution (50 ml) of 0.1 M ammonium chloride—ammonia (pH 10) and 5 g of the gel were used.

The effect of the concentration of background electrolytes, e.g. sodium chloride, ammonium chloride, sodium sulfate, sodium perchlorate and calcium chloride, was examined at pH 10 by a similar procedure; a solution (50 ml) of 0.1 M ammonium chloride containing 10 μmol of boric acid and 1 g of the gel were used. The electrolyte concentrations ranged from 0.2 to 1 M, and the solutions were adjusted to pH 10 by adding ammonia solution.

RESULTS AND DISCUSSION

Effects on the adsorption of boron

pH of the equilibrated solution. Figure 1 shows the effect of the pH of the equilibrated solution on the K_d value, i.e., the extent of the borate adsorption on Sephadex G-25 gel. More precise values of K_d in acidic solutions were determined in separate tests with a Sephadex G-25 column. The elution procedure was described previously [7]. The K_d values (1.04 at pH 2.0, 1.02 at pH 4.0 and 1.04 at pH 5.5) showed that boric acid is adsorbed very weakly; the value of K_d exceeds unity if solute—gel interactions are present [5—7]. The value of K_d increased to 50 in the range pH 9.5—11. Such a high value is not given by other solutes. This pH dependence of the K_d values agrees with the distribution of $B(OH)_4^-$ anion as a function of pH as calculated from the data of Ingri [10]; the main species participating in the adsorption is the borate anion, $B(OH)_4^-$. In the formation of complexes between the borate anion and polyhydroxy compounds, the borate anion is the active species rather than boric acid [11]; the complex formation probably involves polymerized glucose units in the gel matrix.

Concentration of borate. The amount of boron adsorbed as borate on the gel was determined as a function of the equilibrium concentration of borate in a solution at pH 10 (Fig. 2). In contrast to the behavior of the thiocyanate

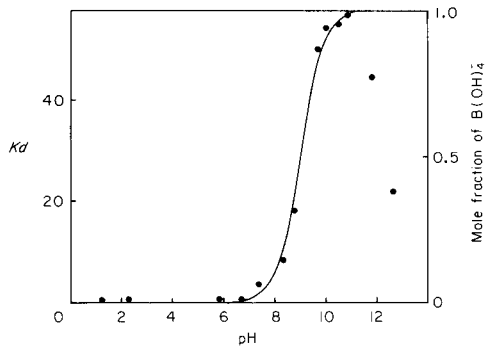

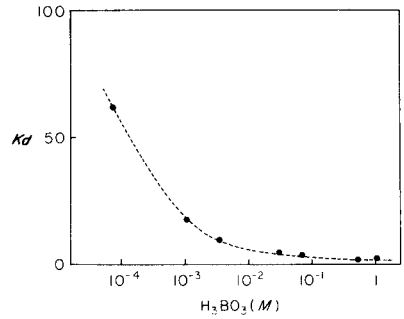

Fig. 1. pH-dependence of the adsorption of boric acid on 1 g of Sephadex G-25 gel. Solution: 50 ml of 0.1 M NaCl (HCl—NaOH) containing 2×10^{-4} M H_3BO_3. The solid line indicates the mole fraction curve for $B(OH)_4^-$.

Fig. 2. Variation of K_d with boric acid concentration on Sephadex G-25 gel (5 g). Solution: 50 ml of 0.1 M NH_4Cl—NH_3 (pH 10).

ion [7], a linear adsorption isotherm was not obtained; the value of K_d increased with decreasing concentrations of boron.

The concentration of coexisting background electrolyte. As shown in Fig. 3, the presence of sodium chloride, ammonium chloride, sodium sulfate and sodium perchlorate did not affect the adsorption of boron significantly. The concentration of these electrolytes was varied from 0.2 to 1 M. All the solutions contained 0.1 M ammonium chloride—ammonia buffer to maintain the pH at 10. The presence of calcium chloride decreased the K_d value, because of the complex formation between the calcium and borate; the stability con-

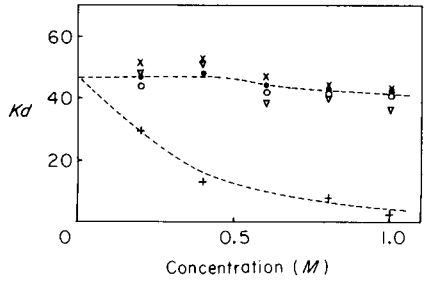

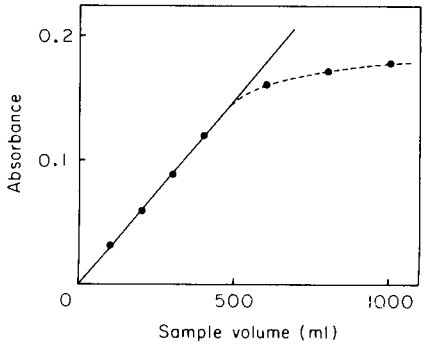

Fig. 3. Effect of neutral electrolytes on the adsorption of boric acid on 1 g of Sephadex G-25 gel. Solution: 50 ml of 0.1 M NH_4Cl—NH_3 (pH 10) containing 2×10^{-4} M H_3BO_3. Electrolytes: (•) NaCl; (▾) NH_4Cl; (×) Na_2SO_4; (○) $NaClO_4$; (+) $CaCl_2$.

Fig. 4. Determination of boron in water from Akiyoshi-dai (Yamaguchi Prefecture). Conditions as recommended in Experimental.

stant of this complex is $10^{1.8}$ [12]. This is much lower than that between calcium and EDTA [13] and the effect of calcium could be eliminated by adding EDTA. Amounts of EDTA up to 0.75 M did not alter the K_d value for 2×10^{-4} M boric acid.

All the results suggest that borate can be separated and concentrated from a bulk solution containing large amounts of salts by adsorption at pH 10 in the presence of EDTA and desorption at pH 2.

Selective concentration of borate with a Sephadex gel column

To minimize contamination with boron, glassware was avoided as much as possible; thus the solvent reservoir was made of polyethylene and the column of acrylic resin. The bed volume of the column, V_t, was 15.0 ml; the void volume, V_0, was 6.3 ml, as determined with Blue dextran 2000. Quantitative elution of borate was obtained with 0.02 M hydrochloric acid, the borate appearing in the 15 ± 2-ml portion of the effluent. Therefore, the first 10 ml of effluent was rejected and the fraction from 10 to 20 ml was collected in a 10-ml volumetric flask.

The effect of flow rate was checked for 100 ml of 0.1 M ammonium chloride solution containing 10 μmol of boric acid, the solution being adjusted to pH 10 with ammonia. The boron was completely recovered at flow rates up to 8 ml min^{-1}.

Figure 4 shows the absorbance plotted against the volume of solution taken. In solutions of up to 400 ml the boron could be completely concentrated into 10 ml of eluate at a flow rate of 8 ml min^{-1}. Further concentration may be accomplished at lower flow rates.

The batch experiment described above showed that large amounts of sodium chloride, ammonium chloride, sodium sulfate, sodium perchlorate and/or calcium chloride did not affect the concentration of borate in the presence of EDTA. The effects of interfering solutes on the azomethine-H method and of solutes which complex easily with borate were also studied (Table 1). Metals that interfere in the azomethine-H method, and fluoride in neutral and alkaline solutions, did not affect the adsorption of boron on the gel. The hydrolysis rate of BF_4^- at pH 10 may be very slow. Consequently, only borate-boron can be separated and concentrated by the present method. Glucose did not affect the recovery of boron when present at up to 100 times the concentration of boron.

Precision was measured with 100-ml samples containing boric acid concentrations of 5.0×10^{-6}, 1.0×10^{-5} and 2.0×10^{-5} M. The results are shown in Table 2.

Determination of boron in natural waters and rocks

The method was applied to the determination of boron in groundwater from a karst area (Akiyoshi-dai, Yamaguchi Prefecture). For 100—400-ml samples (see Fig. 4), the boron content was found to be $(9.7 \pm 0.3) \times 10^{-7}$ M, i.e., $0.010_5 \pm 0.0003$ ppm, by the calibration curve previously prepared. This value agreed with that (9.6×10^{-7} M) obtained by the standard addition

TABLE 1

Effects of foreign ions on the recovery of borate[a]

Species added	Molar ratio to B	Absorbance	B found ($\times 10^{-5}$ M)
Al(III)	100	0.320	0.99
	1000	0.330	1.02
Fe(III)	100	0.325	1.01
	1000	0.320	0.99
Cu(II)	100	0.323	1.00
	1000	0.326	1.01
NaF	5000[b]	0.325	1.01
	5000[c]	0.004	0.01
Glucose	10	0.323	1.00
	100	0.312	0.97
	1000	0.298	0.86

[a]Borate in 100-ml sample solutions was separated and concentrated to 10 ml on a Sephadex gel column. Sample solution: 100 ml of 1.00×10^{-5} M H_3BO_3 and 20 ml of 0.5 M EDTA (pH 10).
[b]The sample solution was stored for 1 day.
[c]The sample solution was stored for 1 day in 0.25 M sulfuric acid. Boron was therefore present as tetrafluoroborate.

TABLE 2

Reproducibility of measurements[a]

B ($\times 10^{-5}$ M)	Absorbance	Relative standard deviation (%)
0.50	0.161 ± 0.002[b]	0.98
1.0	0.324 ± 0.005	1.6
2.0	0.648 ± 0.005	0.76

[a]Boron in 100-ml sample solutions was concentrated to 10 ml on a Sephadex gel column. Sample solution: 100 ml + 20 ml of 0.5 M EDTA (pH 10).
[b]$n = 5$.

method with 200-ml samples. The slope of the graph was identical to that of the routine calibration graph, indicating that borate in the sample solution was concentrated quantitatively on the gel column.

The boron content of a limestone from Akiyoshi-dai (1-g samples) was found to be 2.6 ± 0.1 ppm (5 determinations). The absorbances were 0.082 ± 0.003. For acid-insoluble rocks, it was necessary to decompose the samples by carbonate fusion and in some cases to eliminate aluminium and iron by a cation-exchange resin column. These procedures gave a constant, small contamination with boron and a blank test is therefore necessary. For a shale sample from Yatsushiro (Kumamoto Prefecture), considered to be of marine origin, the boron content was 58.5 ± 0.3 ppm; the results obtained by the

TABLE 3

Boron content in JG-1 (Geological Survey of Japan reference sample of granodiorite)

B (ppm)	Method	Reference[a]
5.1	Optical emission spectrometry	Champ (1968)
7		Ikeda (1970)
12		Schmidt (1972)
8		Thompson (1972)
8.7	Absorption spectrophotometry	Isozaki et al. (1973)
8.3		This work

[a]Data cited in [14].

calibration curve and standard addition methods agreed well. Table 3 shows the analytical data for reference sample JG-1, granodiorite (Geological Survey of Japan); the result obtained by the standard addition method (0.5-g sample) agreed with other literature values [14].

REFERENCES

1 C. D. Curtis, Geochim. Cosmochim. Acta, 28 (1964) 1125.
2 S. Ohashi, N. Yoza and Y. Ueno, J. Chromatogr., 24 (1966) 300.
3 P. A. Neddermeyer and L. B. Rogers, Anal. Chem., 41 (1969) 94.
4 N. Yoza, J. Chromatogr., 86 (1975) 325.
5 M. Sinibaldi and M. Lederer, J. Chromatogr., 107 (1975) 210.
6 G. Bagliano, L. Ossicini and M. Lederer, J. Chromatogr., 21 (1966) 471.
7 G. Kura, A. Koyama and T. Tarutani, J. Chromatogr., 144 (1977) 245.
8 B. Lindqvist, Acta Chem. Scand., 16 (1962) 1794.
9 M. K. John, H. H. Chuah and J. H. Neufeld, Anal. Lett., 8(1975) 559.
10 N. Ingri, Acta Chem. Scand., 17 (1963) 573.
11 G. L. Roy, A. L. Laferriere and J. O. Edwards, J. Inorg. Nucl. Chem., 4 (1957) 106.
12 E. J. Reardon, Chem. Geol., 18 (1976) 309.
13 L. G. Sillén and A. E. Martell (Eds.), Stability Constants, Special Publication No. 25, Chemical Society, London, 1971.
14 A. Ando, H. Kurasawa, T. Ohmori and E. Takeda, Geochem. J., 8 (1974) 175.

Analytica Chimica Acta, 109 (1979) 123—127

EXTRACTIVE SEPARATION AND SPECTROPHOTOMETRIC DETERMINATION OF OSMIUM AND RUTHENIUM AS THIOCYANATE COMPLEXES

Z. MARCZENKO* and M. BALCERZAK

Department of Analytical Chemistry, Technical University, Warsaw (Poland)

(Received 8th March 1979)

SUMMARY

Conditions for the formation and extraction of the thiocyanate complexes of osmium and ruthenium are reported. The osmium complex formed in 0.1—0.3 M thiocyanate solution containing 0.4—1.5 M hydrochloric acid is extracted with peroxide-containing diethyl ether; the ruthenium complex is not extracted from 0.1—0.4 M HCl solutions with peroxide-containing ether but can be extracted from 1 M HCl solutions with methyl isobutyl ketone. The molar absorptivities are 1.71×10^4 l mol^{-1} cm^{-1} for the osmium complex at 620 nm and 5.5×10^3 l mol^{-1} cm^{-1} for the ruthenium complex at 570 nm. Application of the method to the usual distillates containing osmium and ruthenium provides specific determinations in mixtures containing 20—200 μg of each metal.

In the course of separation of the platinum metals, osmium and ruthenium are commonly separated by distillation as their volatile tetroxides. Since most oxidizing agents enable both metals to be converted to tetroxides, methods which make it possible to separate and determine osmium and ruthenium after their common distillation are of great importance.

The earlier literature indicates the possibilities of applying thiocyanate complexes to the spectrophotometric determination of osmium [1—3] and ruthenium [4—8]. In some of these papers, attempts were made to extract the thiocyanate complexes of osmium [2] or ruthenium [8]. In the work described here, the thiocyanate system was examined in detail. As a result, a method for the extractive separation of osmium and ruthenium and for their determination as thiocyanate complexes was developed.

EXPERIMENTAL

Reagents and apparatus

Osmium(VIII) standard solution: (1 mg Os ml^{-1}). Weigh a glass ampoule containing ca. 0.5 g OsO_4, score it with a file, and then crush it carefully in a beaker containing 100 ml of water acidified with 2 ml of 18 M H_2SO_4. Collect the glass fragments, wash them carefully, dry and weigh. The amount of OsO_4 used is found from the difference in the weights of the original

ampoule and the glass fragments. Dilute the solution with water to obtain a concentration of 1 mg Os ml^{-1}, and store in a bottle with a ground-glass stopper. Working solutions are obtained by diluting the stock solution with water.

Ruthenium standard solution (1 mg Ru ml^{-1}). Weigh exactly 100 mg of powdered ruthenium in a silver crucible and add 1 g of sodium peroxide. Fuse the contents of the crucible gradually, increasing the temperature to a dark red glow. Maintain this temperature for 10 min. Allow to cool, dissolve the melt in water (in a beaker covered with a watch glass), and acidify the solution with hydrochloric acid (1+3). Heat the mixture and filter off the coagulated AgCl, washing it with 0.1 M HCl. Transfer the filtrate to a 100-ml volumetric flask and dilute to the mark with hydrochloric acid in order to make the final solution 1 M in HCl. Working solutions are obtained by diluting the stock solution with 1 M HCl.

Diethyl ether. For peroxide-free ether, shake with a 2% solution of Mohr's salt in 2 M H_2SO_4 and then distil; use the freshly purified ether. For peroxide-containing ether, add one drop of 30% hydrogen peroxide per 15 ml of this purified ether.

A SFR-1 spectrophotometer (Poland) and a Specord u.v.-visible spectrophotometer were used with 1- and 5-cm cells.

Recommended procedures

Separation of osmium and ruthenium by distillation. Place the sample solution containing osmium and ruthenium in a distillation flask. Add 6 ml of 18 M H_2SO_4 and 2 ml of 72% perchloric acid. Attach the flask to a distillation apparatus equipped with two receivers in series. Place 5 ml of 0.2 M ammonium thiocyanate solution in 0.4 M hydrochloric acid in each of the two receivers, pass nitrogen continuously (2—3 bubbles per s) and heat the flask carefully until intense fumes of perchloric acid appear. Interrupt the heating, and continue to pass nitrogen until the distillation flask has cooled to room temperature.

Extractive separation and determination of osmium. Transfer the contents of the receivers quantitatively to a 100-ml conical flask and wash the receivers with a few millilitres of the absorbing solution. Heat the combined solutions for 5 min in a boiling water bath, allow to cool and transfer quantitatively to a separatory funnel. Extract the osmium complex with two 10-ml portions of peroxide-containing diethyl ether. Transfer the extracts to a 25-ml volumetric flask, dilute to the mark with the solvent and measure the absorbance at 620 nm.

Determination of ruthenium. Make the aqueous solution after separation of osmium, 0.3 M in ammonium thiocyanate and 1 M in hydrochloric acid. Extract the thiocyanatoruthenium complex with two 10-ml portions of methyl isobutyl ketone. Transfer the extracts to a 25-ml volumetric flask, dilute to the mark with the solvent and measure the absorbance of the solution at 570 nm.

RESULTS AND DISCUSSION

Formation and extraction of the osmium complex

When an aqueous solution of osmium (VIII or VI) containing thiocyanate ions and acidified with hydrochloric acid (to ca. 1 M) is heated (in a boiling water bath) a yellow-orange complex is formed. The complex can be extracted with isoamyl alcohol or tri-n-butyl phosphate without change in the colour. When the aqueous solution is shaken with methyl isobutyl ketone or peroxide-containing diethyl ether, quantitative extraction of the complex takes place and the solution turns blue. In contrast to the statements of Wiersma and Lott [2], the thiocyanato—osmium complex was not extracted by diethyl ether free of peroxides. The necessary peroxide concentration in the ether is obtained by adding 1—2 drops of 30% H_2O_2 to 25 ml of the purified ether. When the peroxide concentration is too low, extraction of the thiocyanato—osmium complex is less efficient, but excessive concentrations of peroxides in the ether also cause low recoveries.

The thiocyanate concentration range suitable for the formation of the osmium complex and its extraction with peroxide-containing ether is 0.1—0.3 M. At thiocyanate concentrations of 0.05 M, the percentage extraction is only about 75%; at concentrations above 0.3 M, recoveries decrease gradually, probably because the thiocyanic acid passes to the organic phase resulting in yellowing of the ether phase and formation of a precipitate at the phase boundary. For a thiocyanate concentration of 0.2 M the concentration of hydrochloric acid can vary in the range 0.4—1.5 M with no effect on the formation and extraction of the thiocyanate complex. At lower acidities, the percentage extraction decreases abruptly whereas at higher acidities it decreases more slowly, being about 70% from 4 M HCl. The effect of the heating time of the complex solution was examined. Heating for 5 min suffices to obtain the maximum colour intensity, but longer heating times (up to 40 min) have no deleterious effects.

An absorption spectrum of the thiocyanato—osmium complex is shown in Fig. 1. Solutions of the osmium complex in diethyl ether containing peroxides obey Beer's law within the concentration range 0—12 μg Os ml^{-1}. The molar absorptivity of the complex under these conditions is 1.71×10^4 l mol^{-1} cm^{-1} (specific absorptivity = 0.090) at 620 nm.

Formation and extraction of the ruthenium complex

When an acidic aqueous solution of ruthenium (ca. 1 M HCl) is heated (in a boiling water bath) with thiocyanate, a violet-blue complex is formed. The thiocyanato—ruthenium complex formed in the aqueous phase is easily extractable with methyl isobutyl ketone or tri-n-butyl phosphate (without change in colour). An absorption spectrum of the ruthenium complex in methyl isobutyl ketone is shown in Fig. 1.

The effect of the heating time on the formation of the thiocyanato—ruthenium complex is shown in Fig. 2. The optimum time is in the range 3—5 min; longer heating causes decomposition of the complex. Studies of the effects

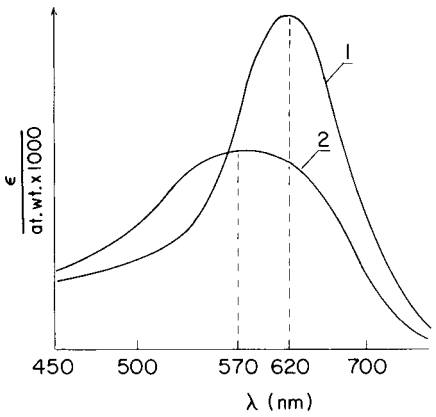

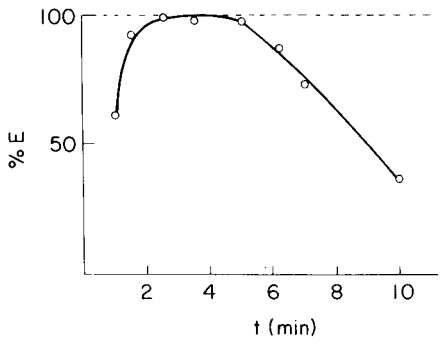

Fig. 1. Absorption spectra of the thiocyanato—osmium complex in diethyl ether containing peroxide (curve 1) and of the thiocyanato—ruthenium complex in methyl isobutyl ketone (curve 2).

Fig. 2. The effect of heating time on the formation of thiocyanato—ruthenium complex.

TABLE 1

Results of the extractive separation of osmium and ruthenium as thiocyanate complexes in mixed solutions and in common distillates

Added (μg)		Mixed solutions Found (μg)		Common distillates Found (μg)	
Os	Ru	Os	Ru	Os	Ru
100	100	100	105	—	—
		103	98	—	—
200	200	—	—	198	199
		—	—	203	200
100	200	97	198	100	198
		100	201	103	198
200	100	203	98	200	102
		200	105	198	102
20.0	200	20.4	196	19.6	198
		21.0	196	19.0	201
200	20.0	206	18.2	203	18.0
		198	22.8	198	18.0

of thiocyanate concentration and acidity showed that for the optimum hydrochloric acid concentration of 0.8—1.2 M, the thiocyanate concentration can vary in the range 0.25—0.35 M.

Solutions of the ruthenium complex in methyl isobutyl ketone obey Beer's law in the concentration range 0—20 μg Ru ml^{-1}. The molar absorptivity of the complex is 5.5×10^3 l mol^{-1} cm^{-1} (specific absorptivity = 0.054) at 570 nm.

Separation of osmium and ruthenium

Diethyl ether containing peroxides (a good extractant for the osmium—thiocyanate complex) does not extract the ruthenium—thiocyanate complex at low hydrochloric acid concentrations (0.1—0.4 M HCl). The extraction increases with increasing acidity (2% at 0.5 M HCl; 9% at 1 M HCl; 20% at 3 M HCl). The extractive separation of osmium and ruthenium with peroxide-containing diethyl ether is best achieved from a medium 0.4 M in HCl and 0.2 M in thiocyanate. Under these conditions, a double extraction transfers osmium quantitatively to the organic phase while ruthenium remains in the aqueous phase. Before extraction of ruthenium with methyl isobutyl ketone, the concentration of hydrochloric acid should be increased to 1 M and that of thiocyanate ions to ca. 0.3 M. Under these conditions, a double extraction with methyl isobutyl ketone is sufficient for quantitative transference of ruthenium from the aqueous phase.

The results of the extractive separation of osmium and ruthenium at various weight ratios of the metals in mixed solutions are shown in Table 1. Osmium and ruthenium were also separated and determined as their thiocyanate complexes after a preliminary oxidation and distillation of the metals (as tetroxides) from a medium of fuming perchloric acid [9]; these results are also given in Table 1. Considering the absolute quantities of the metals, the results of the determinations after the distillation and the extractive separation can be considered satisfactory.

REFERENCES

1 V. I. Shlenskaya and V. P. Khvostova, Zh. Anal. Khim., 23 (1968) 237.
2 J. H. Wiersma and P. F. Lott, Anal. Chem., 39 (1967) 674.
3 M. Qureshi and K. Mathur, Fresenius Z. Anal. Chem., 242 (1968) 159.
4 S. C. Ogburn, J. Am. Chem. Soc., 48 (1926) 2493.
5 W. L. Belew, G. R. Wilson and L. T. Corben, Anal. Chem., 33 (1961) 886.
6 V. I. Shlenskaya and E. M. Piskunov, Vestn. Mosk. Univ. Khim., 18 (1963) 35.
7 V. I. Shlenskaya, E. M. Piskunov and V. P. Khvostova, Vestn. Mosk. Univ. Khim., 19 (1964) 62.
8 J. H. Forsyte, R. J. Magee and C. L. Wilson, Talanta, 3 (1959) 324.
9 F. E. Beamish and J. C. Van Loon, Recent Advances in the Analytical Chemistry of the Noble Metals, Pergamon, Oxford, 1972.

Analytica Chimica Acta, 109 (1979) 129—138

DETERMINATION OF THE ACIDITY OF PETROLEUM BITUMENS BY CATALYTIC THERMOMETRIC TITRIMETRY

E. J. GREENHOW* and A. NADJAFI**

Department of Chemistry, Chelsea College, University of London, Manresa Road, London, SW3 6LX (Gt. Britain)

(Received 25th January 1979)

SUMMARY

The content of acids, including very weak acids, in straight-run and air-blown petroleum bitumens is determined by non-aqueous catalytic thermometric titrimetry. Titration values depend on the nature of the titrant and on the nature and amount of the sample solvent and thermometric indicator. Acrylonitrile is effective in low concentrations and is preferred to acetone as the indicator. With pyridine as the sample solvent, the measured acid contents are similar to those obtained by non-aqueous potentiometric titration. The thermometric method is more convenient.

Petroleum bitumens contain acidic substances, the nature of which depends on the origin of the crude oil, the methods of production and any subsequent treatment to modify their properties, such as air-blowing. Although the acids in bitumens are mainly carboxylic, very weak acids such as phenols are also present.

The acid content is important because it affects the adhesion, stability and ease of emulsification of the bitumen. Titrimetric methods — visual and potentiometric — are recommended by the Institute of Petroleum (IP) [1] and the American Society for the Testing of Materials (ASTM) [2] for the determination of acids in bitumens (asphalts). These methods do not determine all the acids present; only acids with pK_a values up to about 10 may be titrated [3].

In the titration of very weak acids, the nature of the titrant and of the solvents used is critical [4]. Nakajima and Tanobe [3] used pyridine and benzene—pyridine mixtures as solvents in potentiometric titration of bitumens with tetramethylammonium hydroxide in pyridine—propan-2-ol. They added benzoic acid and phenol to the bitumen sample, and obtained curves with two distinct inflections, corresponding to the weak carboxylic acids and the very weakly acidic phenols; even 2,6-di-t-butylphenol could be titrated. The technique of adding a known amount of a very weak acid to the sample to enhance

**Present address: Department of Chemistry, Arya-Mehr University of Technology, P.O. Box 3406, Tehran, Iran.

end-point inflection was applied earlier in potentiometric titrations of coal-tar pitch fractions [5].

Conventional thermometric titrimetry in propan-2-ol media with 0.2 M potassium hydroxide titrant, was used by Quilty [6] to determine acids in light and heavy petroleum oils, including lubricating oils; the acid numbers for 19 of the 21 lubricating oils examined were shown to be significantly higher by a potentiometric method than by the thermometric method. Satisfactory values were obtained for 5-mg amounts of phenol dissolved in 1 g of acid-free lubricating oil, which suggests that the acids in the oils not determined by the thermometric method are weaker than phenol (pK_a 9.9).

Catalytic thermometric titrimetry is a useful alternative to the conventional method for the determination of small amounts of acids in non-aqueous solution [7]. End-points are indicated, independent of sample size, by some exothermic reaction involving suitable reagents. Under favourable conditions, this reaction is catalysed by the first excess of titrant immediately after the acid has been neutralized [8]. The technique is suitable for the determination of very weak acids, including sterically-hindered phenols, and the acid numbers of mineral insulating oils can be measured [9].

In the present paper, the catalytic thermometric method is evaluated for the determination of acid contents of some straight run and air-blown bitumens, and is compared with the potentiometric method developed by Nakajima and Tanobe [3].

EXPERIMENTAL

Reagents and samples

Reagent-grade acetone, acrylonitrile (AN), toluene (C_7H_8), propan-2-ol (PrOH), pyridine (py) and dimethylformamide (DMF) were dried over molecular sieve before use. Phenol and benzoic acid were of analytical-reagent grade. Other solvents and phenols (reagent-grade) were used as received.

Tetra-n-butylammonium hydroxide (TBAH) reagent, 0.1 M in (3 + 1) toluene—methanol (reagent grade) was diluted with a (3 + 1) mixture of toluene and propan-2-ol to obtain the 0.03 M solution.

Tetramethylammonium hydroxide (TMAH) reagents, 0.1 and 0.03 M in pyridine—propan-2-ol (1 + 1), were prepared by evaporating an aqueous 25% solution of tetramethylammonium hydroxide (Cambrian Chemicals Ltd.) to a syrup under reduced pressure at temperatures below 27°C, adding pyridine, and continuing the evaporation until all the water was removed. The residue was then dissolved in propan-2-ol and diluted with an appropriate volume of pyridine.

Potassium hydroxide reagent, 0.1 M in propan-2-ol, was prepared by refluxing potassium hydroxide (analytical-reagent grade) in propan-2-ol. The propan-2-ol was purified previously by refluxing over potassium hydroxide for 4 h, then collecting the distillate boiling up to 84°C, and drying it over molecular sieve 4A. More dilute solutions were prepared by adding propan-2-ol or pyridine to the 0.1 M reagent.

All three titrants were standardized against 0.1 M benzoic acid solutions in dimethylformamide by the potentiometric and thermometric methods.

Bitumens with low and high acid contents were gifts from the Esso Research Centre, Abingdon. Straight-run and air-blown bitumens were gifts from Shell Composites Ltd., Chester.

Apparatus

The automatic thermometric apparatus, comprising a motor-driven micrometer syringe burette, a thermistor and a chart recorder, has been described [10]. Dewar beakers (15, 30 and 65 ml) were used as reaction vessels. An anchor-type stirrer was preferred to magnetic stirring for the rather sticky bitumen solutions.

A conventional manual potentiometric apparatus was used with a glass/calomel electrode system. The glass electrode was conditioned in the sample solvent for 10 min before use, and stored in distilled water after use.

Thermometric procedure

Toluene, propan-2-ol and dimethylformamide as solvents (method A). Bitumen (200—500 mg) was weighed into the 30 ml Dewar beaker and dissolved in toluene (3 or 7.5 ml), and propan-2-ol (2 or 2.5 ml), dimethylformamide (1 or 2 ml) and acrylonitrile (2—10 ml) were added. For replicate determinations 50-ml solutions of bitumens in toluene were prepared and aliquots were mixed with the above co-solvents. Titrant was added at a rate of 0.06 ml min^{-1}. The end-point was taken as the point on the temperature—volume curve where a tangent drawn to the main heat rise leaves the curve at its lower temperature end (see Fig. 1) [11].

Pyridine as solvent (method B). The procedure was similar to method A, but the bitumen (20—260 mg) was weighed into a 15, 30 or 65-ml Dewar beaker and dissolved in pyridine (2—30 ml), or solutions of bitumens in 50 ml of pyridine were prepared for replicate determinations and aliquots were taken. Acrylonitrile (0.5—4 ml) or acetone (2—4 ml) was then added to the bitumen solutions. For the tetramethylammonium hydroxide titrant, a further 0.2 ml of propan-2-ol was added to the sample. This procedure was used also when 1,1,3,3,-tetramethylurea or *N,N,N',N'*-tetramethylethylenediamine replaced pyridine as the sample solvent.

Potentiometric procedure

Bitumen, about 0.5 g, was weighed into a 100-ml titration flask, and dissolved in 50 ml of solvent by warming on a water bath. The electrodes were inserted, and titrant was added from a 10-ml burette while dry nitrogen was passed through the flask.

RESULTS AND DISCUSSION

The curves shown in Figs. 1—3 were obtained in the catalytic thermometric

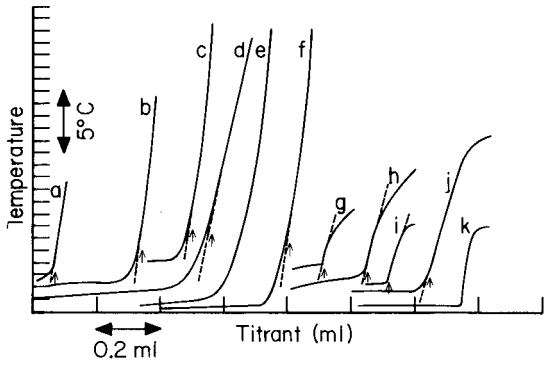

Fig. 1. Effect of solvents in the catalytic thermometric titration of high-acid and low-acid bitumens with potassium hydroxide reagents (acrylonitrile indicator). (a) Blank corresponding to conditions for curve b; (b) high-acid bitumen (268.4 mg), 0.1 M KOH titrant in PrOH, C_7H_8—PrOH—DMF—AN (3 + 2 + 1 + 10) solvent. (c) Blank corresponding to conditions for curve d; (d) high-acid bitumen (198.7 mg), 0.04 M KOH titrant in PrOH, solvent as curve b; (e) low-acid bitumen (201.0 mg), titrant and solvent as for curve d. (f) Benzoic acid (12.2 mg), 0.04 M KOH titrant in PrOH, solvent as curve b. (g) Blank corresponding to conditions for curve h; (h) low-acid bitumen (21.3 mg), 0.02 M KOH titrant in py—PrOH (1 + 1), py—AN (2 + 3) solvent. (i) Blank corresponding to conditions for curve j; (j) high-acid bitumen (100.6 mg), 0.08 M KOH titrant in py—PrOH (1 + 1), py—AN (5 + 10) solvent; (k) benzoic acid (24.4 mg), titrant and solvent as for curve j.

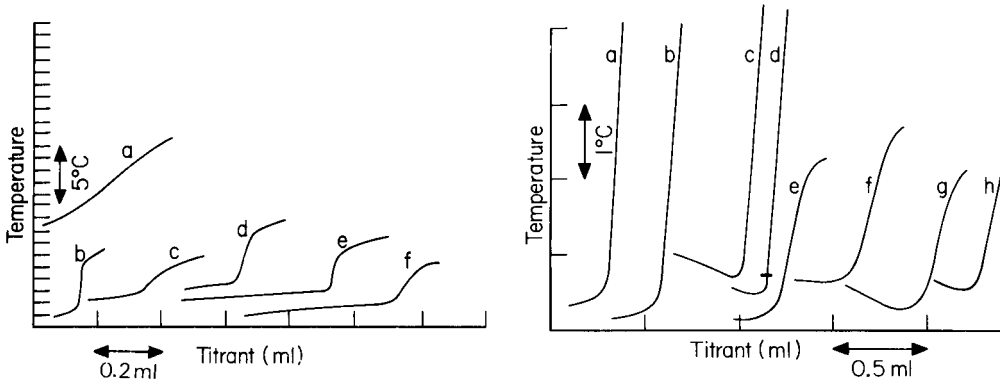

Fig. 2. Catalytic thermometric titration of high-acid bitumen with 0.02 M tetramethylammonium hydroxide in py—PrOH (1 + 1) (acrylonitrile indicator). (a) Blank corresponding to conditions for curve c; (b) blank corresponding to conditions for curve d; (c) high-acid bitumen (21.3 mg), py—AN (2 + 4) solvent; (d) high-acid bitumen (21.3 mg), py—PrOH—AN (2 + 0.25 + 4) solvent; (e) benzoic acid (12.2 mg), py—AN (2 + 4) solvent; (f) 2,6-di-t-butylphenol (20.6 mg), py—AN (2 + 4) solvent.

Fig. 3. Comparison of acrylonitrile and acetone as indicators in the titration of bitumens with 0.1 M KOH in propan-2-ol. The solvent was a mixture (5 + 3) of pyridine and acrylonitrile or acetone. Curves (a—d) relate to acrylonitrile and curves (e—f) to acetone. (a) Straight-run bitumen (160.4 mg); (b) roofing bitumen (150.7 mg); (c) high-acid bitumen (216.1 mg); (d) low-acid bitumen (172.9 mg); (e) straight-run bitumen (149.7 mg); (f) roofing bitumen (165.7 mg), (g) high-acid bitumen (216.1 mg); (h) low-acid bitumen (172.9 mg).

titration of the acidic constituents of commercial straight-run and air-blown (roofing) bitumens and two residual bitumens selected for their high and low acid contents. Curves for benzoic acid and 2,6-di-t-butylphenol are included in Fig. 2 for comparison. Potentiometric titration curves are shown in Fig. 4. The acid contents determined by the titrimetric methods, expressed as acid numbers (mg KOH g^{-1}) and milliequivalents of acid function per g are given in Table 1. Some values for the precision of results obtained by using the catalytic thermometric method are given in Table 2.

In catalytic thermometric titrimetry, the shape of the titration curve is influenced by the nature of the titrant, the sample solvent and the thermometric indicator. Acrylonitrile and acetone were evaluated as thermometric indicator reagents, potassium hydroxide and quaternary ammonium hydroxide solutions were compared as titrants, and pyridine, 1,1,3,3-tetramethylurea, *N,N,N',N'*-

TABLE 1

Catalytic thermometric and potentiometric titrations of low-acid bitumen (200 pen) and high-acid bitumen (200 pen)[a]

Sample	Weight (mg)	Titrant (M)	Indicator (ml)	Sample solvents (ml)[b]				Acid content	
				P	I	T	D	Acid No.	meq g^{-1}
Catalytic thermometric titrimetry with acrylonitrile indicator									
Low-acid	201.0	KOH, 0.04[c]	10		2	3	1	2.00	0.0358
	172.9	KOH, 0.1[d]	3	5				3.64	0.0650
	40.3	TMAH, 0.03[d]	4	2	0.2			3.32	0.0594
	495.0	KOH, 0.1[c]	2		2.5	7.5	2	5.13	0.0914
	259.3	KOH, 0.1[c]	0.5	30				9.03	0.1610
High-acid	259.5	KOH, 0.04[c]	10		2	3	1	5.04	0.0900
	256.3	KOH, 0.1[c]	3	5				7.67	0.1368
	130.0	KOH, 0.1[d]	3	5				9.23	0.1650
	21.3	TMAH, 0.03[d]	4	2	0.2			6.78	0.1210
	259.5	TBAH, 0.03[e]	10		2	3	1	4.44	0.0793
	242.4	KOH, 0.1[c]	2		2.5	7.5	2	8.50	0.1515
	217.6	KOH, 0.1[c]	0.5	25				12.53	0.2234
Catalytic thermometric titrimetry with acetone indicator									
High-acid	256.3	KOH, 0.1[c]	3	5				9.03	0.1610
	215.5	KOH, 0.1[c]	2	10				10.46	0.1865
	194.3	KOH, 0.1[d]	3	5				10.13	0.1810
Low-acid	259.3	KOH, 0.1[c]	4	20				8.19	0.146
Potentiometric titrimetry									
High-acid	479.0	KOH, 0.1[d]		50				11.93	0.2130
	474.5	TMAH, 0.1[d]		50				11.20	0.2000

[a]Each result is the mean of three determinations, with aliquots of solutions in toluene or pyridine. [b]P = pyridine; I = propan-2-ol; T = toluene; D = dimethylformamide. [c]In propan-2-ol. [d]In (1 + 1) pyridine—propan-2-ol. [e]In (8 + 1) toluene—methanol. [f]High-acid bitumen in 1,1,3,3,-tetramethylurea and *N,N,N',N'*-tetramethylethylenediamine (2 ml + 3 ml AN) gave acid values of 5.83 and 2.10, respectively (0.04 M KOH titrant in PrOH).

TABLE 2

Catalytic thermometric titration of bitumens with 0.1 M potassium hydroxide in propan-2-ol or 0.08 M potassium hydroxide in (1 + 1) pyridine—propan-2-ol. Mean results are given with the number of determinations (n), standard deviation (s) and relative standard deviation (s_r).

Bitumen[a] (mg)	Solvent[b] (ml)	Indicator (ml)	Titrant (M)	n	Mean titre (ml)	s	s_r	Mean acid no.
H, 198.7	I, 6	AN, 10	0.08	6	0.222	0.0069	3.1	4.20
H, 256.3	II, 5	AN, 3	0.1	4	0.341	0.0031	0.92	7.70
L, 172.9	II, 5	Ac, 3	0.1	4	0.241	0.0022	0.90	6.91
H, 217.6	II, 25	AN, 0.5	0.1	4	0.511	0.0227	4.45	12.56
L, 259.3	II, 20	Ac, 4	0.1	4	0.382	0.0084	2.2	8.19
S, 213.7	II, 20	AN, 0.5	0.1	5	0.549	0.0231	4.2	14.38
R, 178.4	II, 15	AN, 0.5	0.1	4	0.739	0.0214	2.9	22.10

[a] Aliquots of solutions in toluene or pyridine; H = high-acid bitumen; L = low-acid bitumen; S = straight-run bitumen (70 pen); R = roofing bitumen (15 pen).
[b] I = C_7H_8—PrOH—DMF (3 + 2 + 1); II = pyridine.

tetramethylethylenediamine, and a mixture of toluene, propan-2-ol and dimethylformamide were tested as solvents for the bitumens.

Effect of the sample solvent

The mixture of toluene and propan-2-ol recommended in the IP and ASTM methods [1] is unsatisfactory as a co-solvent with acrylonitrile when the catalytic thermometric method is used, because a sharp end-point inflection is not achieved. However, addition of dimethylformamide to this solvent mixture leads to acceptable titration curves (Fig. 1). When pyridine — the solvent recommended by Nakajima and Tanobe [3] — is used instead as the co-solvent with acrylonitrile, the titration curves obtained have a sharper end-point inflection, but the rise in temperature after this inflection is considerably reduced (Fig. 1).

The nature of the sample solvent influences the magnitude of the measured acid values in catalytic thermometric titrimetry, as it does in potentiometric titrimetry [3]. It can be seen in Table 1 that the acid values lie in the ranges 2.00—9.03, and 2.10—12.53, for the low-acid and high-acid bitumens, respectively. Titrations of the straight-run and air-blown (roofing) bitumens, in the same solvent systems, lead to acid values in the ranges 6.99—14.42 and 6.68—24.01, respectively.

Pyridine is the most effective solvent in terms of the magnitude of the acid value, while much lower values are obtained with the toluene—propan-2-ol—dimethylformamide system. Even lower values are observed when *N,N,N',N'*-tetramethylethylenediamine is used as the solvent. The acid values obtained with tetramethylurea as the co-solvent with acrylonitrile are similar to those

achieved with the toluene—propan-2-ol—dimethylformamide system. The low acid values may be considered to correspond to the content of the weak carboxylic acids and the high acid values to the content of these acids and the very weakly acidic phenols. The wide variation in the values would suggest that there is no sharp division between the weak and very weak acids in bitumens.

Effect of the titrant

Replacement of potassium hydroxide in propan-2-ol by tetramethylammonium hydroxide in pyridine—propan-2-ol (the titrant recommended earlier [3]) as the titrant leads to a reduction in the rise in temperature after the indicated end-point in the catalytic thermometric method with pyridine as the co-solvent (compare Figs. 1, curves g, h and k, and 2, curves b, c and d). The sharpness of the end-point in the titration of samples in mixtures of pyridine and acrylonitrile with tetramethylammonium hydroxide reagent can be improved significantly by including about 4% of propan-2-ol in the solvent (compare curves a and c with b and d in Fig. 2). This confirms an earlier observation [12] that the alcohol can play a part in the initiation of the acrylonitrile indicator reaction. Changing from the potassium hydroxide to the tetramethylammonium hydroxide titrant affects the acid value much less than changing the sample solvent (Table 1). The highest acid values are obtained by using pyridine as the sample solvent and potassium hydroxide in propan-2-ol, or a mixture of pyridine and propan-2-ol, as the titrant, and there is no advantage in using the more expensive, and less easily prepared, tetramethylammonium hydroxide.

Tetrabutylammonium hydroxide in methanol—toluene is significantly less efficient than the potassium hydroxide reagent, in terms of the acid value measured in the titration of the high-acid bitumen (Table 1).

Effect of the indicator reagent

The rise in temperature after the end-point, and the rate of this rise, are both less with acetone than with acrylonitrile as the indicator (see Fig. 3). The effect of the indicator on the measured acid value can be seen in Table 1. When pyridine is the sample solvent, higher acid values are obtained with acetone than with an equal volume of acrylonitrile as the indicator, and they increase as the indicator concentration is reduced. Both acetone and acrylonitrile are poor solvents for bitumens; when they are added to solutions of bitumen in pyridine, some of the acidic constituents are precipitated and, subsequently, are not titrated. Acetone is less effective than acrylonitrile as a precipitant, and this accounts for the higher acid values observed when it is used. However, acrylonitrile has the advantage over acetone in being effective as an end-point indicator at much lower concentration. Thus, 0.5 ml of acrylonitrile in up to 30 ml of pyridine will give rise to a measurable end-point, whereas about 5 ml of acetone is needed with this volume of pyridine. Consequently, the measured acid values obtained by using the minimum effective volume of indicator are higher with acrylonitrile. The sharpness of the end-

point inflection decreases as the concentration of acrylonitrile in pyridine is reduced. It is necessary to correct for the titration value of the solvent mixture alone because this varies with the solvent composition. Acetone is ineffective as an end-point indicator when used in conjunction with the toluene—propan-2-ol solvent, because the indicator reaction is inhibited by high concentrations of the alkanol.

Comparison of the catalytic thermometric and potentiometric methods

A comparison of the acid values determined by the potentiometric and catalytic thermometric methods (Table 1), reveals that the highest values obtained for the high-acid bitumen are in agreement, within experimental error.

The graphs shown in Fig. 5 relate acid values for high- and low-acid bitumens determined by catalytic thermometric titrimetry with the volume of pyridine solvent, when the acrylonitrile volume and bitumen content are maintained constant. The values reach a constant maximum value as the bitumen concentration is reduced. This suggests that variations in the acid value with solvent composition are due to the limited solubility of the bitumens in the solvent mixtures. Neither potentiometry nor catalytic thermometric titrimetry can be carried out successfully on samples dissolved solely in the non-polar hydrocarbon solvents in which bitumens are most readily soluble. Pyridine appears to be a satisfactory compromise in that it is a moderately effective solvent for bitumens, and gives solutions that respond to end-point detection systems at the sample concentrations required in titrimetric procedures.

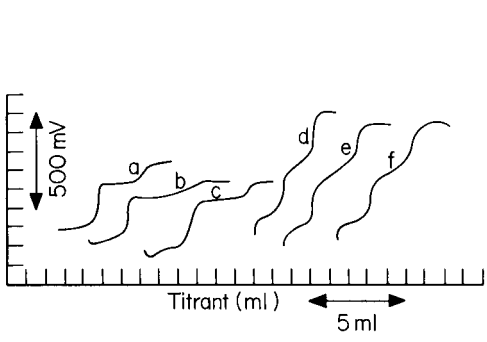

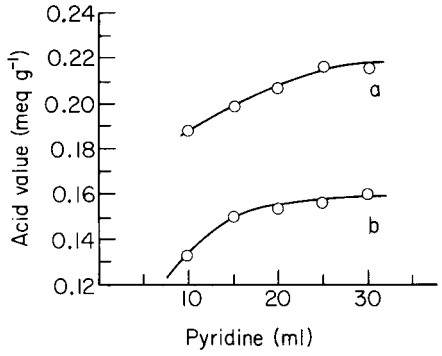

Fig. 4. Potentiometric titrations of high-acid bitumen and mixtures of benzoic acid and phenols in 50 ml of pyridine. Curves (a—c) relate to titrations with 0.1 M KOH in py—PrOH (1 + 1) and curves (d—f) to titrations with 0.14 M TMAH in py—PrOH (1 + 1). (a) Benzoic acid (24.4 mg) + phenol (18.8 mg); (b) as for (a) plus 2,6-di-t-butyl-4-methylphenol (20.0 mg); (c) as for (a) plus high-acid bitumen (479.0 mg). (d) As for (a); (e) as for (a) plus 2,6-di-t-butyl-4-methylphenol (20.0 mg); (f) as for (a) plus high-acid bitumen (474.5 mg).

Fig. 5. Effect of sample concentration on the measured acidity of (a) high-acid bitumen (217.6 mg) and (b) low-acid bitumen (259.3 mg). Solvent, 10—30 ml py + 0.5 ml AN; titrant, 0.1 M KOH in PrOH.

End-point inflections

The sharpness of the end-point inflections in the catalytic thermometric titration curves is probably influenced by the composition of the acidic constituents of the sample and particularly the ratio of the content of strong and weak acids to the very weak acids. It can be seen in Fig. 2 that the titration curve for benzoic acid (e) has a sharper inflection than that for 2,6-di-t-butylphenol (f), while that for the high-acid bitumen (d) is of intermediate sharpness. The more rounded end-point inflections are obtained with very weak acids, such as phenols [12], and an inflection of intermediate sharpness would indicate that the sample contains a mixture of very weak acids with stronger acids.

In the potentiometric titrations, with pyridine as solvent (Fig. 4), the titration curves show two inflections corresponding to the neutralization of weak acids (similar in strength to benzoic acid) and very weak acids (e.g., phenols). The nature of the titrant affects the shape of the curves; thus, the first inflections corresponding to the weak acids are slightly sharper when potassium hydroxide is used, but the second inflections corresponding to the very weak acids are significantly sharper when tetramethylammonium hydroxide is the titrant. Such marked differences for the final end-point inflection were not observed in the corresponding catalytic thermometric titrations with the two titrants.

In catalytic thermometric titrimetry, the addition of benzoic acid or phenol to the sample before titration has little effect on the sharpness of the end-point, because it does not influence the response of the end-point indicator.

Satisfactory results were obtained by catalytic thermometric titrimetry for smaller samples than are recommended for the potentiometric method; samples of about 200 and 30 mg proved suitable for titrations with 0.1 and 0.03 M solutions, respectively, compared to the 500-mg samples required for potentiometric determinations. When the solubility of the sample in the available solvents is a problem, as in these analyses, smaller samples are advantageous. The relative standard deviation of the catalytic thermometric method ranges from 1 to 5%, depending on the solvent system and the titrant used, and is of the same order as that claimed by Nakajima and Tanobe [3] for the potentiometric method (Table 2).

Catalytic thermometric titrimetry has the advantage over potentiometry of being simpler and quicker. The temperature probe is unaffected by the bitumen solutions, unlike the electrodes which can lose their sensitivity when coated with a precipitate.

The Esso Petroleum Co. Ltd. and Shell Composites Ltd. are thanked for gifts of bitumen samples.

REFERENCES

1 IP Standards for Petroleum and its Products, Part 1, Methods for Analysis and Testing, 36th edn., Vol. 1, IP 139/65, IP 177/64 and IP 213/76T, Heydon, London, 1977.
2 Annual Book of ASTM Standards, Part 23, D664-58 and D974-64, and Part 25, ANSI/ASTM D3339-74, American Society for Testing and Materials, Philadelphia, 1976.
3 T. Nakajima and C. Tanobe, J. Inst. Pet., 59 (1973) 32.
4 M. L. Moss, J. H. Elliott and T. R. Hall, Anal. Chem., 20 (1948) 784.
5 E. J. Greenhow and J. W. Smith, Analyst, 84 (1959) 457.
6 C. J. Quilty, Anal. Chem., 39 (1967) 666.
7 E. J. Greenhow and L. E. Spencer, Analyst, 98 (1973) 90.
8 E. J. Greenhow, Chem. Rev., 77 (1977) 835.
9 D. A. Castle and E. J. Greenhow, Inst. Petroleum Technical Publ. IP 75-015, Inst. of Petroleum, London, 1975.
10 E. J. Greenhow and L. E. Spencer, Analyst, 98 (1973) 98.
11 G. A. Vaughan and J. J. Swithenbank, Analyst, 95 (1970) 890.
12 E. J. Greenhow and A. A. Shafi, Analyst, 101 (1976) 421.

Analytica Chimica Acta, 109 (1979) 139—143

A SEARCH FOR LOSSES OF CHROMIUM AND OTHER TRACE ELEMENTS DURING LYOPHILIZATION OF HUMAN LIVER TISSUE

J. J. M. de GOEIJ*, K. J. VOLKERS and P. S. TJIOE

Interuniversity Reactor Institute, Mekelweg 15, 2629 JB Delft (The Netherlands)

(Received 22nd February 1979)

SUMMARY

Human liver tissues were investigated for possible trace-element losses during lyophilization by comparison of concentrations in lyophilized and untreated (wet) samples. When destructive neutron activation analysis (n.a.a.) was used, no significant losses were observed for As, Br, Cd, Co, Cr, Cu, Fe, Hg, Mo, Sb, Se, and Zn. The advantages of n.a.a. over radiotracer techniques for studies of trace-element volatility are discussed.

Losses of volatile trace elements from biological materials during various analytical operations are well known and have been investigated in some detail, but less attention has been given to trace elements, which are not normally considered volatile. In recent years, evidence has been gathered that chromium may be lost by volatilization in treatments such as oven-drying or dry ashing [1—3]. Even drying at room temperature and lyophilization (freeze-drying) have been suspected as a cause of losses of chromium from biological materials [4]. The volatility of chromium is sometimes linked with the occurrence of a special organic chromium-containing complex, usually called GTF (glucose tolerance factor). This complex, isolated from brewer's yeast, contains chromium(III) as well as nicotinic acid, glycine, glutamic acid and cysteine [5].

Several authors have attempted to confirm the alleged volatility of chromium upon drying or ashing by incorporating radioactive chromium-51 in various biological materials. When this technique was applied, significant losses were not observed for blood and tissues of the rat [6], oysters [7, 8], or even brewer's yeast [9, 10], which contains appreciable amounts of chromium with GTF activity [5].

However, the value of such tracer experiments is limited, as there is no guarantee that the radioactive element injected into the organism or added to its food or drinking water will behave identically to the various chemical species of non-radioactive element incorporated in the organism. This applies especially for higher organisms, which feed on a variety of foods and depend on other (lower) organisms for the synthesis of some metal-containing complexes. Therefore, the most reliable way of studying the possible volatility of

elements in many biological materials is to analyze samples with and without the particular drying or ashing pretreatment under suspicion. This requires a technique which is adequate for analyzing both wet and treated samples. Destructive neutron activation analysis (n.a.a.) meets this requirement. It is possible to irradiate wet, dry and ashed samples in sufficiently large integrated neutron fluxes, so that the results obtained after different pretreatments can be compared. In the case of chromium, recoil effects during irradiation convert the element to an inorganic form [11] which does not exhibit volatility. For chromium, the determination limit is about 2 ng per sample [12], which is sufficiently low for most biological materials.

Destructive n.a.a. was therefore used to study the occurrence of chromium losses from human liver tissue during lyophilization. Liver tissue — sampled via biopsy or autopsy — is one of the most frequently analyzed human organs for trace elements, e.g. in measurements of the exposure of humans to trace elements from the environment. Lyophilization of human tissue samples is often used, since it facilitates homogenization, storage, and shipment. Moreover, when n.a.a. is used, lyophilization allows the use of longer irradiation times and high neutron fluxes, so that for many trace elements the determination limit may be improved.

EXPERIMENTAL

Three fresh human livers from autopsies were each homogenized to a smooth slurry with a Potter blender. The Potter blender was a commercially available type, in which the stainless steel parts were replaced by titanium parts, in order to prevent contamination with trace elements of interest in this study. From each slurry, twenty-four 1-g aliquots were weighed into quartz vials. From each set of 24 aliquots, twelve aliquots were taken randomly for lyophilization at 10^{-5} atm. for 48 h. After sealing of the vials, sample pairs along with standards and empty vials as blanks were irradiated in a neutron flux of 1×10^{13} n cm^{-2} s^{-1} (Interuniversity Reactor Institute) for 9 h. Each sample pair consisted of one lyophilized and one wet aliquot of the same liver slurry. After irradiation, the vials were processed in the automated chemical separation scheme developed at the Interuniversity Reactor Institute [13]. This scheme allows the determination not only of chromium, but also of arsenic, antimony, bromine, cadmium, cobalt, copper, iron, mercury, molybdenum, selenium, and zinc. The final measurements were done with a NaI(Tl) scintillation detector [13]. All results were corrected for the blank, i.e. the trace-element contribution from the quartz irradiation vial. The chromium value was also adjusted for the ^{51}Cr contribution from the $^{54}Fe(n,\alpha)$ reaction, which amounts to 14 μg of (apparent) chromium per gram of iron.

RESULTS AND DISCUSSION

The trace-element levels found in the wet samples are presented in Table 1.

TABLE 1

Trace-element levels in human livers expressed in $\mu g\ g^{-1}$ of wet tissue

Element	This study			Range of averages and standard deviations [14—19]
	Liver I	Liver II	Liver III	
As	6.0×10^{-3}	4.8×10^{-3}	5.0×10^{-3}	$(6.5 \pm 3.9) \times 10^{-3}$—$(8.7 \pm 5.1) \times 10^{-3}$
Br	3.1	2.5	1.9	(1.7 ± 0.7)—(3.1 ± 1.0)
Cd	2.5	0.78	2.0	(0.7 ± 0.2)—(2.6 ± 2.7)
Co	3.7×10^{-2}	4.6×10^{-2}	3.7×10^{-2}	$(1.6 \pm 0.9) \times 10^{-2}$—$(3.4 \pm 0.7) \times 10^{-2}$
Cr	3.0×10^{-2}	1.0×10^{-2}	4.2×10^{-2}	$(0.5 \pm 0.3) \times 10^{-2}$—$(4.1 \pm 5.1) \times 10^{-2}$
Cu	7.4	5.2	9.7	(4.6 ± 3.1)—(8.4 ± 8.6)
Fe	$2.4 \times 10^{+2}$	$2.0 \times 10^{+2}$	$1.7 \times 10^{+2}$	$(0.4 \pm 0.2) \times 10^{+2}$—$(2.2 \pm 1.6) \times 10^{+2}$
Hg	3.3×10^{-2}	9.3×10^{-2}	4.3×10^{-2}	$(2.5 \pm 0.8) \times 10^{-2}$—$(7.7 \pm 2.0) \times 10^{-2}$
Mo	1.1	1.0	1.3	$(3.5 \pm 1.3) \times 10^{-1}$—$(7.1 \pm 2.9) \times 10^{-1}$
Sb	1.8×10^{-2}	0.4×10^{-2}	0.9×10^{-2}	$(1.1 \pm 0.8) \times 10^{-2}$—$(1.7 \pm 1.5) \times 10^{-2}$
Se	2.2×10^{-1}	4.0×10^{-1}	3.9×10^{-1}	$(2.0 \pm 0.8) \times 10^{-1}$—$(2.7 \pm 0.9) \times 10^{-1}$
Zn	$14.2 \times 10^{+1}$	$17.3 \times 10^{+1}$	$5.8 \times 10^{+1}$	$(4.0 \pm 1.5) \times 10^{+1}$—$(6.1 \pm 2.4) \times 10^{+1}$

The data were compared with trace-element data for liver material collected in Europe, viz. The Netherlands [14], Belgium [15], Germany [16], Sweden [17, 18], and Norway [19]. For comparison, literature data on a dry weight basis were converted to data on wet weight basis by multiplying by 0.28; this factor was established experimentally. The comparison did not reveal any anomalously low or high values, except that the zinc levels of liver I and II seem to be rather high.

The results of the lyophilization experiments are presented in Fig. 1 by the ratio parameter R: $R_i = (1/N)\ \Sigma_{j=1}^{j=N}\ (x_{i,j}/y_{i,j})$, where $x_{i,j}$ and $y_{i,j}$ denote the concentration of element i in a lyophilized aliquot and a wet aliquot, respect-

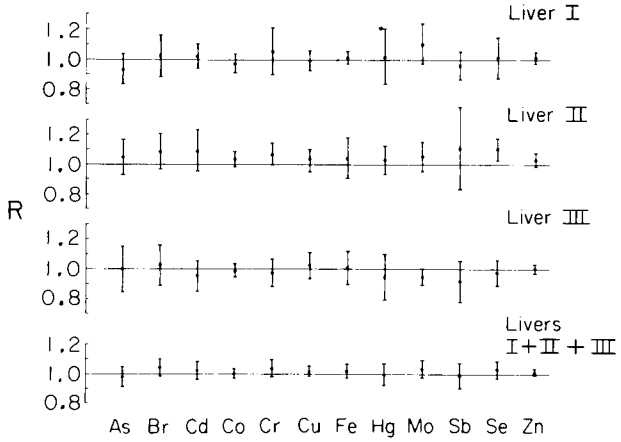

Fig. 1. Ratios R and 99-% confidence intervals for 12 trace elements in human liver material.

ively; N denotes the number of replicate measurements, i.e. the sum of pairs j of lyophilized and wet aliquots analyzed. The error limits indicated are the 99-% confidence intervals, which were calculated from 99-% confidence interval = $t\ \sigma_{x/y} N^{-\frac{1}{2}}$, where $\sigma_{x/y}$ denotes the standard deviation in the replicate measurements of R, and t denotes the Student's t-factor for $(N - 1)$ degrees of freedom at the 99-% confidence level.

As may be seen from Fig. 1, only the result for selenium in liver II deviates significantly from unity. However, this deviation — which was not confirmed by the results for the same element in liver I and III -- indicates an increase on lyophilization rather than a decrease. The origin of this increase is not clear.

Since all aliquots were taken from homogenized liver slurries, the error limits in the resulting values of R should be attributed almost entirely to analytical variations. Thus, by pooling all results per element, smaller error limits may be obtained. However, this approach is justified only if each trace element does not differ significantly in behaviour in the three livers on lyophilization. Since the results for the separate livers do not clearly show differences, all the results were pooled. With the above formulae, an overall value for R as well as a 99-% confidence interval were calculated as plotted in Fig. 1.

The overall R-values indicate that there are no significant losses during lyophilization, for chromium or for any of the other eleven elements. Even notoriously volatile trace elements — such as arsenic, bromine and mercury, which sometimes show substantial losses during sample pretreatment — are retained entirely or almost entirely in the sample. The mechanism of retention is not fully understood yet, but protein sulfhydryl groups probably play an important part in the binding of some volatile elements, e.g. mercury [20, 21].

The extrapolation of the validity of the results for human liver material to other biological tissues, especially to non-human materials, should be done with extreme reserve. Various factors may determine trace-element losses during lyophilization. These factors include matrix composition (e.g. acidity, presence of complexing groups), physical and chemical state of the trace elements, pre-analysis conditions (e.g. decomposition by microbiological action or radiation exposure), and mutual interaction between trace elements during lyophilization [20—24].

REFERENCES

1 D. Behne, R. Brätter, H. Gessner, G. Hube, W. Mertz and U. Rösick, Fresenius Z. Anal. Chem., 278 (1976) 269.
2 W. R. Wolf and F. E. Green, in Accuracy in Trace Analysis: Sampling, Sample Handling, and Analysis, NBS Spec. Publ. 422, National Bureau of Standards, Washington, D.C. (1976), 605
3 W. Mertz, E. W. Toepfer, E. E. Roginski and M. M. Polanski, Fed. Proc. Fed. Am. Soc. Exp. Biol., 33 (1974) 2275.
4 R. M. Parr, J. Radioanal. Chem., 39 (1977) 421.

5 E. W. Toepfer, W. Mertz, M. M. Polanski, E. E. Roginski and W. R. Wolf, J. Agric. Food Chem., 25 (1977) 162.
6 S. R. Koirtyohan and C. A. Hopkins, Analyst, 101 (1976) 870.
7 H. O. Fourie and M. Peisach, Radiochem. Radioanal. Lett., 26 (1976) 277.
8 H. O. Fourie and M. Peisach, Analyst, 102 (1977) 193.
9 J. Kumpulainen, Anal. Chim. Acta, 91 (1977) 403.
10 G. B. Jones, R. A. Buckley and C. S. Chandler, Anal. Chim. Acta, 80 (1975) 389.
11 D. Brune, Report AE-172, Aktiebolaget Atomenergi, Stockholm, 1965.
12 P. S. Tjioe, J. J. M. de Goeij and K. J. Volkers, Paper presented at the 5th Symposium on Recent Developments in Activation Analysis, Oxford, England, July 1978, IRI-report 133-79-02.
13 P. S. Tjioe, J. J. M. de Goeij and J. P. W. Houtman, J. Radioanal. Chem., 37 (1977) 511.
14 W. Edel, J. J. L. Pieters and L. J. Schuddeboom, Report 1978/13, State Supervisory Public Health Service, Ministry of Public Health and Environmental Protection, Leidschendam, The Netherlands (1978), table 3.
15 P. Lievens, J. Versieck, R. Cornelis and J. Hoste, J. Radioanal. Chem., 37 (1977) 483.
16 W. Leonhardt, S. Niese, W. Jarosz, M. Hanefeld, K. U. Schentke and D. Meiszner, Isotopenpraxis, 11 (1975) 130.
17 K. Samsahl and D. Brune, Int. J. Appl. Radiat. Isot., 16 (1965) 273.
18 L. O. Plantin, Paper presented at the International Symposium on Nuclear Activation Techniques in the Life Sciences, May 1978, Vienna, Austria.
19 C. Halvorsen and E. Steinnes, Fresenius Z. Anal. Chem., 274 (1975) 199.
20 A. Foldzinska and W. Zmijewska, Radiochem. Radioanal. Lett., 27 (1976) 225.
21 P. D. LaFleur, Anal. Chem., 45 (1973) 1534.
22 K. K. S. Pillay, C. C. Thomas, J. A. Sondel and C. M. Hyche, Anal. Chem., 43 (1971) 1419.
23 S. H. Harrison, P. D. LaFleur and W. H. Zoller, Anal. Chem., 47 (1975) 1685.
24 M. Carlson and R. Litman, Radiochem. Radioanal. Lett., 35 (1978) 161.

Analytica Chimica Acta, 109 (1979) 145—148

Short Communication

THE ION-SENSITIVE FIELD EFFECT TRANSISTOR IN RAPID ACID—BASE TITRATIONS

M. BOS*, P. BERGVELD and A. M. W. VAN VEEN-BLAAUW

Department of Chemical Technology, Twente University of Technology, Enschede (The Netherlands)

(Received 12th March 1979)

Summary. Ion-sensitive field effect transistors (ISFETs) are used as the pH sensor in rapid acid—base titrations. Titration speeds at least five times greater than those with glass electrodes are possible for accuracies better than ±1%.

The speed of automated acid—base titrations is normally limited by the slow response of the glass electrode [1]. Computer control of the titrant delivery in titrations to preset end-points [2], as well as in equilibrium titrations [3], improves the situation but results better than ±1% still require titration times of the order of 4 min [4].

Field effect transistors can be used as pH sensors by replacing the gate metal with silicon nitride or polymeric pH-selective membranes [5]. The silicon dioxide of the transistor structure itself, that normally insulates the gate metal, also exhibits pH sensitivity [6]. In contrast to the glass electrode, ISFETs do not need high-impedance metering circuits, hence the long time constants caused by cable capacity and high internal resistance of glass electrodes are absent [7]. Accordingly, the use of ISFETs to monitor acid—base titrations should allow considerably higher speeds in these titrations. Moreover, the size of the ISFET, mounted as a probe, is only a few mm^2 so that if a small enough reference electrode were available, it would be possible to monitor titrations on the microliter scale.

This work was undertaken to study the possibility of rapid acid—base titrations with the aid of an ISFET with the silicon dioxide of its gate area used as the pH-sensitive layer. This use of the dioxide of the transistor itself was preferred, as a shorter response time was expected with this device than with the membrane-covered types of pH-sensitive ISFETs.

Experimental

Chemicals. Potassium chloride (Merck, reagent grade) and tris(hydroxymethyl)aminomethane (Tris, Fluka, puriss) were used as received. Standard solutions of hydrochloric acid, sodium hydroxide and acetic acid (all in 1 M KCl) were prepared from Merck Titrisol ampoules by adding the calculated amount of potassium chloride to a 1-l volumetric flask together with the

content of the ampoules and filling to the mark with twice-distilled CO_2-free water.

The ISFET and its amplification system. The ISFET configuration was similar to that described by Matsuo and Wise [7] and was mounted on a ceramic support (1.6 mm by 50 mm). Source, drain and bulk connections were wire-bonded with fine gold wires to three conducting silver palladium pads, which were deposited on the ceramic support by means of thick-film technology and soldered at the distal end to a small connector. The whole probe was insulated, except for the gate area, with three layers of diluted silicone rubber. The 500Å thermal dioxide of the gate was protected during mounting and storage by evaporated aluminium, which was removed (see below) just before the measurement.

The ISFET was connected to a specially developed ISFET amplifier [8], which supplies a constant drain-to-source voltage of 100 mV, while the source and drain potential, having a mean value of 1 V with respect to earth, follows the gate potential because of feedback (bootstrapping). The bulk was connected to earth as well as to the reference electrode in the liquid. This system is capable of transferring very high frequencies, because the capacitances between the liquid and the source and drain, as well as between the source and drain potential, having a mean value of 1 V with respect to earth, connected to low impedances, preventing interference from ambient electrical fields. The output voltage of the ISFET amplifier can be simply calibrated in pH units, independent of ISFET characteristics, because of the feedback principle.

Titration equipment. A schematic diagram of the titration equipment is shown in Fig. 1. A recorder (Kipp, type BD8) connected to the ISFET amplifier registers pH versus time. The motor burette (Mettler, type DV11) is operated at constant speed, so that the time-axis of the chart can be calibrated in volume units. This is done by generating markers on the recorder paper with the switch that also starts and stops the burette. The ref-

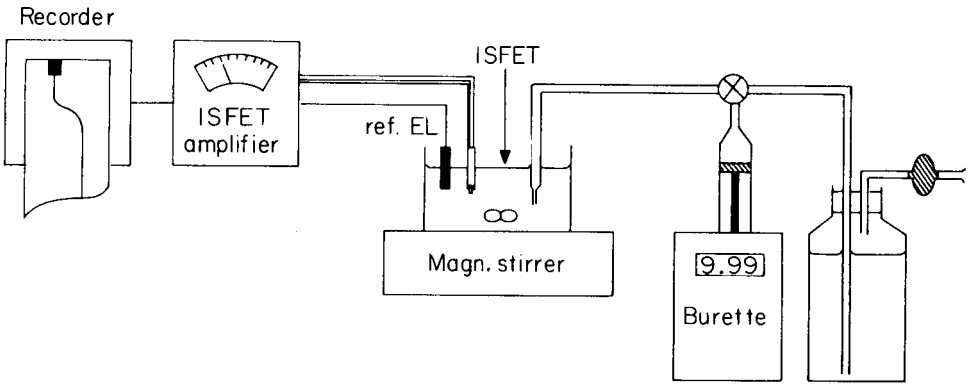

Fig. 1. Schematic diagram of titration equipment with ISFET.

erence electrode used in conjunction with the ISFET is a silver/silver chloride electrode (Ingold, type 363-NS-M5). The magnetic stirrer runs at about 450 rpm with a 21 × 5-mm Teflon bar in a titration beaker (3.4-cm inner diameter).

Procedures. Before the ISFET is used, its aluminium gate metal is removed from the underlying silicon dioxide by etching the ISFET for about 10 min at 50°C with a drop of a solution of 75% phosphoric acid, 10% acetic acid, 5% nitric acid and 15% water. During this treatment the silicon dioxide becomes hydrated and pH-sensitive. When not in use the ISFET is stored dry after rinsing with distilled water.

Titrations of bases were carried out under a nitrogen blanket. For comparison purposes, all titrations were also performed with the use of a combined glass electrode, the 1% errors obtained only for titrant addition rates of 0.9 ml min^{-1} or less. That the titration speed is not limited by the ISFET were done in 1 M potassium chloride solutions so that activity coefficients, theoretical titration curves and the pH values of equivalence points could be calculated easily. In all cases the starting volume in the titration vessel was 20.0 ml.

Results

Figure 2A shows a comparison between the performance of the glass electrode and the ISFET in the titration of samples of 0.500 mmol Tris with 0.1000 M hydrochloric acid at various speeds. The rate of addition of titrant varied between 5.0 and 0.17 ml min^{-1}. The results given are mean values and the standard deviations for the results obtained at one titration speed were below ± 0.2%. It can be seen that, even at the highest titration speed of 5.0 ml min^{-1}, the ISFET produces titration errors smaller than 1%. For the glass electrode, the 1% errors obtained only for titrant addition rates of 0.9 ml min^{-1} or less. That the titration speed is not limited by the ISFET response can be seen from Fig. 2A, where the lowest trace corresponds to the results for some titrations in a smaller vessel in which mixing was promoted by two glass strips on the wall causing better turbulence.

In the reverse titration, i.e. titrations of 0.500 mmol of hydrochloric acid with 0.1000 M Tris, the difference in performance between the glass electrode and the ISFET is less pronounced, but the results for the titrations with the ISFET are considerably better for all titration speeds (Fig. 2B). These error curves also show that both the ISFET and the glass electrode respond more slowly to changes from acid to alkaline pH values than to the reverse changes.

The response of the ISFET to pH changes is not Nernstian over the entire pH range [6], so that it depends on the pH values of the respective equivalence points whether or not differential titrations of mixtures can be successful. The differential titration of a mixture of 0.450 meq of hydrochloric acid and 0.450 meq of acetic acid is possible with the use of a glass electrode (Table 1), but the accuracy is better than 1% only at titration speeds below 0.50 ml min^{-1}. If an ISFET is used as pH sensor, only one inflection point is observed in the titration curve; this end-point corresponds to the

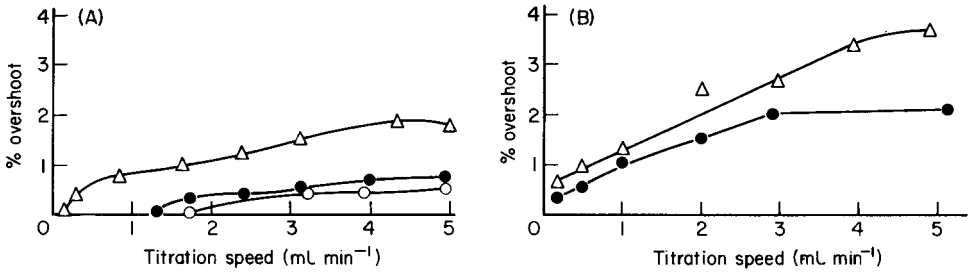

Fig. 2. Overshoot in the titration of (A) 0.5 mmol Tris with 0.1000 M hydrochloric acid, and (B) 0.5 mmol hydrochloric acid with 0.1000 M Tris. (△) Glass electrode; (•) ISFET; (○) ISFET with improved stirring.

TABLE 1

Overshoot in the titration of mixtures of 0.45 meq of hydrochloric acid and 0.45 meq of acetic acid by titration with 0.1000 M sodium hydroxide

	Glass electrode		ISFET
Titration speed (ml min^{-1})	Overshoot for HCl end-point (%)	Overshoot for final end-point (%)	Overshoot for end-point[a] (%)
5.07	2.95	2.04	0.6
2.94	2.45	1.62	
0.98	1.40	0.81	
0.50	1.19	0.18	
0.20	0.53	−0.71	

[a]HCl end-point undetectable.

total amount of hydrochloric and acetic acid, and at the full speed of the burette (5.0 ml min^{-1}) the accuracy is 0.6%.

The authors thank Mr. A. J. Verloop for accurate construction of the ISFET probes, Ms. M. Muring for preparing the manuscript, and Prof. E. A. M. F. Dahmen for his interest in this work.

REFERENCES

1 G. H. B. Eelderink, H. B. Verbruggen, F. A. Jutte, W. J. van. Oort and B. Griepink, Fresenius Z. Anal. Chem., 280 (1976) 273.
2 W. E. Earle and K. S. Fletcher, Chem. Instrum., 7 (1976) 101.
3 D. J. Leggett, Anal. Chem., 50 (1978) 718.
4 T. W. Hunter, J. T. Sinnamon and G. M. Hieftje, Anal. Chem., 47 (1975) 497.
5 P. T. McBride, J. Janata, P. A. Comte, S. D. Moss and C. C. Johnson, Anal. Chim. Acta, 101 (1978) 239.
6 N. F. de Rooy, The ISFET in Electrochemistry, Thesis, Technical University Twente, 1978, p. 32.
7 T. Matsuo and K. P. Wise, IEEE Trans. Biomed. Eng. Vol. BME-21 No. 6 (1974) 485.
8 P. Bergveld, Med. Biol. Eng. & Comp., in press.

Analytica Chimica Acta, 109 (1979) 149—155

Short Communication

POTENTIOMETRIC BEHAVIOUR AND SURFACE COMPOSITION OF A PROTOTYPE MONOHYDROGENPHOSPHATE-SELECTIVE ELECTRODE

ALAN C. WILSON ** and KARL H. POOL*

Department of Chemistry, Washington State University, Pullman, WA 99164 (U.S.A.)

(Received 27th February 1979)

Summary. The solid-state electrode is based on tris(thiourea)copper(I) monohydrogenphosphate and silver(I) sulfide. Potentiometric characteristics are initially excellent but change with continued use. The model proposed to explain the potentiometric behaviour was verified by e.s.c.a. studies.

Since the introduction of ion-selective electrodes for many common ions during the last 15 years, many attempts to construct a potentiometric sensor for some form of orthophosphate have been reported [1—8], but no satisfactory general-purpose phosphate-selective electrode has resulted. Yet another attempt is described below. In order to explain the non-reproducible behaviour, several experiments were done to characterize the surface composition of the solid-state membrane as a function of its previous history. The model postulated explains the potentiometric behaviour observed and also helps to explain response degradations reported for other Ag_2S-based electrodes.

Experimental

Instrumentation. An Orion Digital Ionalyzer Model 801 was used with a Beckman 10-in. strip-chart recorder. Recorder sensitivity was maintained at 1 mV/in. by means of a Rubicon Type B potentiometer in series with the recorder. A Corning SCE was used as external reference electrode. Tests were performed in a jacketed beaker maintained at 25°C by circulating water; solutions were stirred by a Teflon-coated bar driven by air, all contained in a Faraday cage. The pH was monitored simultaneously with a Corning combination electrode connected to a Beckman Research pH meter.

E.s.c.a. spectra were obtained with a DuPont Model 650B spectrometer (Kenan Laboratories of Chemistry, University of North Carolina, Chapel Hill, NC). Neutron activation and γ-activity measurements were performed at the Nuclear Radiation Center at Washington State University.

Chemicals. Tris(thiourea)copper(I) monohydrogenphosphate was prepared as follows: 1.7 g of copper(I) chloride and 12 g of thiourea were dissolved in

**Present address: Analytical and Physical Laboratories, Hercules Inc., Bacchus Works, Magna, UT 84044, U.S.A.

250 ml of water. This solution was filtered through a fine glass filter into 250 ml of a solution containing 1.7 g of disodium hydrogenphosphate, 0.1 g of sodium dihydrogenphosphate, and 8 g of thiourea. The white precipitate that slowly formed at ice temperature was collected, washed three times with a thiourea solution and three times with acetone, and dried under vacuum over phosphorus pentoxide. Infrared spectra of the solid showed bands characteristic of both phosphate and ligand. Elemental analysis: found; 10.6% C, 3.9% H, 24.5% N, 18.5% Cu: calculated ($C_6H_{25}N_{12}Cu_2O_4PS_6$); 10.6% C, 3.7% H, 24.7% N, 18.7% Cu. The solubility of the compound was estimated by atomic absorption spectrometry to be 10^{-5} M in distilled water (pH $\approx$ 5.5).

All other chemicals were reagent grade and were dried at 110°C whenever possible.

Electrode fabrication. Silver sulfide and $[Cutu_3]_2HPO_4$ in 10:1 weight ratio were mixed and ground very thoroughly with a mortar and pestle. The solid mixture was placed in an evacuated KBr pellet die (13-mm diameter) and pressure was gradually applied by a Carver press until a 10-ton load was reached; maximum pressure was sustained for about 4 h and then gradually released. The 2—3 mm thick pellet was glued to the end of Plexiglas tubing with epoxy cement. The electrode surface was polished to remove excess of cement, and then finally polished with an Orion polishing strip. The internal filling solution was a pH 7 phosphate buffer (0.01 M) in contact with a conventional glass pH electrode. Use of a silver wire immersed in phosphate buffer as internal reference electrode shifted the E^0 value but did not affect the dynamic response characteristics.

Potentiometric response of the $[Cutu_3]_2HPO_4$ electrode

Figure 1 illustrates the response of a fresh electrode which had never been exposed to any solution. Data points were obtained by adding successive

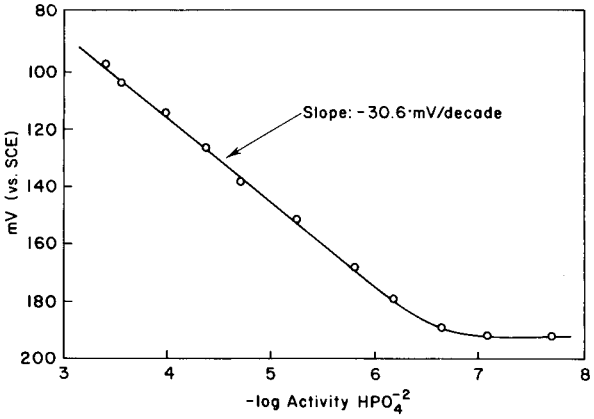

Fig. 1. Calibration curve for a freshly prepared electrode.

aliquots of Na_2HPO_4 solution to deionized water initially adjusted to pH 8 with sodium hydroxide. Dynamic response was rapid; steady potentials were obtained within ca. 20s. However, attempts to reproduce this response with the same electrode were unsuccessful. Initial equilibration times became long (>1 h) and dynamic response to increased HPO_4^{2-} concentrations slow (⩾5 min). Polishing the electrode surface only partially regenerated the desirable response characteristics of new electrodes.

Another disturbing characteristic was that longer times were needed to attain steady potentials at the higher monohydrogenphosphate concentrations; this trend is exactly opposite to what is now conventionally expected from successful electrodes. Potential drift in solutions of lower HPO_4^{2-} concentrations (ca. 10^{-4} M) could be partially eliminated by rigorously excluding oxygen by purging with nitrogen. Other observations such as irreproducible E^0 values and variable slopes of the calibration curves also indicated that the composition of the electrode surface was not stable. The surface changes could be a result of oxidation of a membrane component (Ag_2S or $(Cutu_3)_2HPO_4$), or a combination of oxidation and reaction among species on the membrane surface.

Plots of potential vs. dihydrogenphosphate concentration added were obtained at various constant pH values. At pH 5—6.5, the slopes of the rather narrow linear portions (1.5—2 decades concentration) of the plots varied between —45 and —60 mV/decade. At higher pH values (8—8.5) slopes nearer the theoretical divalent values were obtained, usually in the range of —30 to —35 mV/decade.

If the electrode had previously been exposed to high phosphate concentrations (ca. 10^{-2} M), the observed slope fell to ca. —20 mV/decade when response was tested in the 10^{-5}—10^{-3} M range. The time needed to reach a steady potential in these experiments was very long, often exceeding 1 h.

Surface studies

To obtain a better understanding of the observed ageing effects, e.s.c.a. was employed to examine the surface composition of electrode pellets which had differing previous histories. All three pellets examined were composed of 10:1 Ag_2S:$(Cutu_3)_2HPO_4$ by weight, and were prepared identically. Pellet 1 was never exposed to any solution. Pellet 2 was exposed to aerated distilled water for 4 days. Pellet 3 had been used extensively in analysis and therefore had been exposed to solution of high phosphate concentration. Pellet 1 was assumed to have the same surface and bulk composition. Sensitivity factors for the elements examined were calculated from the observed peak areas obtained for pellet 1. These sensitivity factors were then used to calculate the surface compositions of pellets 2 and 3. Results are shown in Table 1. Figure 2A shows the copper $2P_{3/2}$ region of the e.s.c.a. spectrum of pellet 2. On the basis of e.s.c.a. results reported for copper(I) and copper(II) complexes by Frost et al. [9], Fig. 2A indicates that the copper in the surface layer of pellet 2 is in the +1 state.

TABLE 1

Atom to copper ratios for tris(thiourea)copper(II) monohydrogenphosphate—silver sulfide pellets exposed to various conditions calculated from e.s.c.a. results

Element	Pellet number		
	1[a]	2[b]	3[c]
Cu	1	1	1
N	6	5.81	5.92
O	2	2.30	3.15
P	0.5	0.34	0.65
Ag	27.3	24.5	7.34
S	16.7	16.2	7.31

[a]Virgin pellet. [b]Pellet exposed to only aqueous oxygen solution. [c]Pellet used for analysis; exposed to oxygen and high concentrations of phosphate.

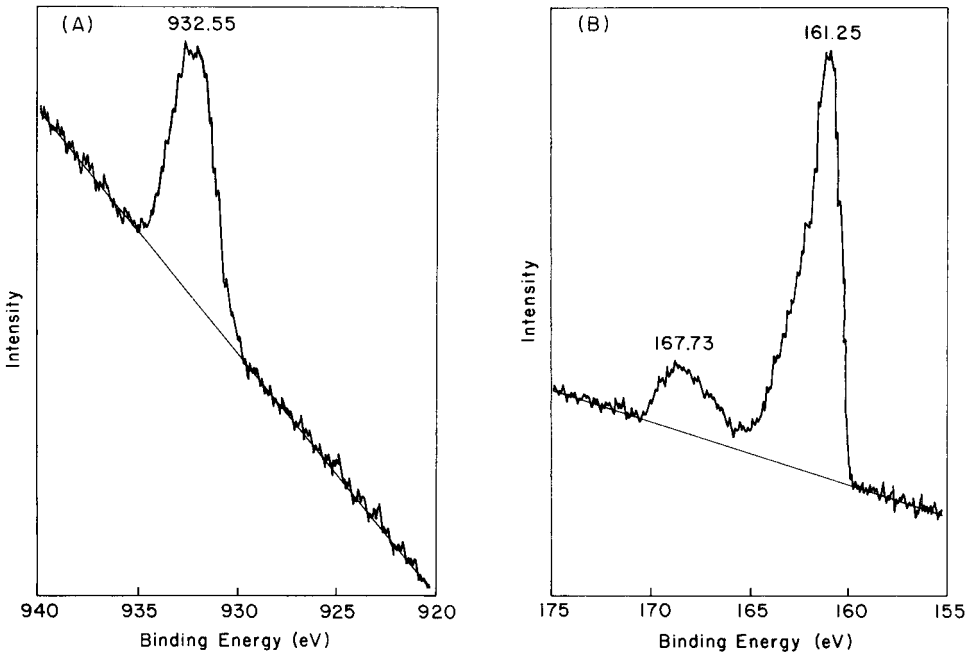

Fig. 2. E.s.c.a. spectra of electrode surface exposed to oxygenated water only: (A) copper $2P_{3/2}$ portion; (B) sulfur $2P$ portion.

The sulfur $2P$ region (Fig. 2B) suggests that some of the original sulfide or thiourea sulfur has been oxidized to sulfate by exposure to oxygenated water. This evidence, along with the constancy of the N/Cu ratio, suggests that the $[Cutu_3]^+$ moiety remains intact and that it is the silver sulfide which is oxidized.

To verify this hypothesis, the solubility of Ag_2S in oxygenated and deoxy-

genated water was measured. Pellets of pure Ag_2S containing ^{110m}Ag were exposed either to oxygenated water or to deaerated water (after nitrogen bubbling). After 1 week, the water was analyzed for radioactive ^{110m}Ag. The pellet exposed only to deaerated water yielded an approximate apparent solubility of 6×10^{-6} M silver(I) whereas the pellet exposed to oxygen showed an apparent solubility of 8×10^{-5} M. This increase in solubility in the oxygenated solution is most readily attributable to oxidation of Ag_2S to Ag_2SO_4 and subsequent dissolution of the latter compound.

Oxidation phenomena involving Ag_2S-based electrodes have been described previously. Mascini and Liberti [10] postulated a slow oxidation process of the membrane surface for a Ag_2S—PbS electrode. The phenomena associated with the postulated membrane surface oxidation, i.e., drifting potentials, higher resistance, poor reproducibility, and sluggish dynamic response, are essentially the same as observed in this work. Similar observations were reported by Kivalo el al. [11] in a comparison of commercial lead-selective electrodes, although correct response could then be restored by periodic polishing of the surface, in contrast to the present case. Midgley [12] and Heijne et al. [13] reported surface oxidation phenomena for copper-selective electrodes based on Ag_2S—CuS pellets. These authors postulated the direct oxidation of CuS as the most reasonable mechanism for formation of oxidized sulfur species.

Proposed model and discussion

The model proposed to explain potentiometric behaviour as well as chemical transformations responsible for the variation in membrane surface composition is represented in Fig. 3. The original (1:10) pellet composition

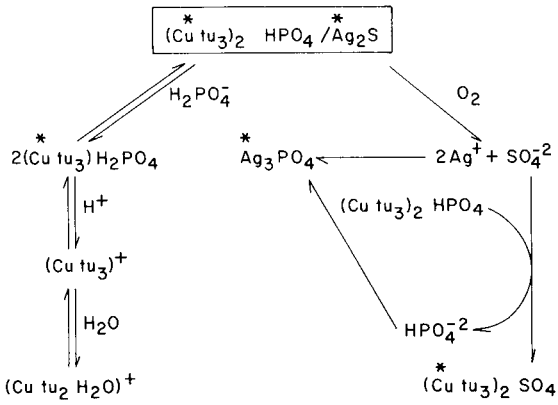

Fig. 3. Probable reactions and equilibria within the surface layer of the membrane and at the membrane—electrolyte interface. The substances asterisked are solids under normal circumstances.

is shown with the reactions and equilibria postulated. The solids can be formed in the membrane surface layer and hence behave as ionic exchangers. The oxidation of Ag_2S and subsequent exchange reaction of SO_4^{2-} with $(Cutu_3)_2HPO_4$ would liberate HPO_4^{2-} which may or may not precipitate as Ag_3PO_4 depending on the ambient silver ion activity. Since the solubilities of both the sulfate and monohydrogenphosphate salts of $Cutu_3^+$ are approximately the same [14], and the standard free energy for the reaction $Ag_2S(s) + 2O_2(g) \rightarrow 2Ag^+(aq) + SO_4^{2-}(aq)$ is favourable (−548 kJ mol^{-1}), all reactions depicted on the right-hand branch of Fig. 3 are known and reasonable.

The equilibria depicted in the left-hand branch of Fig. 3 account for the observed pH dependence. As pH decreases, the monohydrogenphosphate—dihydrogenphosphate equilibrium lies to the right, and $(Cutu_3)_2HPO_4$ is expected to increase in solubility. Similarly, the dihydrogenphosphate salt of $Cutu_3^+$ would decrease in solubility as pH decreases. At still lower pH, any phosphate salt will tend to dissolve unless the total phosphate ion concentration is relatively high. The $Cutu_3H_2PO_4$ was not isolated, but the analogous hydrogensulfate salt, $Cutu_3HSO_4$ is known [14].

The overall non-theoretical response of the prototype phosphate sensitive electrode reported here can be rationalized in terms of the proposed model. Depending on conditions and previous history, monovalent ($Cutu_3H_2PO_4$), divalent ($[Cutu_3]_2HPO_4$ and $[Cutu_3]_2SO_4$), and trivalent (Ag_3PO_4) ionic exchangers are all possible components of the electrode surface layer.

Conclusion

The irreproducibility of the potentiometric response characteristics, such as variable slopes of calibration curves, and variable and slow equilibration times can be related to the variable composition of the membrane surface. In all cases, except those involving a fresh electrode, the mixed response observed depended on the previous history of the electrode. During measurements, the membrane surface strives to attain not only dynamic equilibrium with solution components, but also thermodynamic equilibrium among the possible insoluble compounds (possible exchangers) in the surface itself. The relatively slow approach to equilibrium at the membrane—solution interface, especially among the solids in the membrane surface, accounts for the above defective characteristics.

REFERENCES

1 E. Pungor, K. Tóth and J. Havas, Mikrochim. Acta, (1966) 689.
2 G. Guilbault and P. Brignac, Jr., Anal. Chem., 41 (1969) 1136; Anal. Chim. Acta, 56 (1971) 139.
3 G. A. Rechnitz, Z. F. Lin and S. B. Zamochnick, Anal. Lett., 1 (1967) 29.
4 I. Novozamsky and W. H. van Riemsdijk, Anal. Chim. Acta, 85 (1976) 41.
5 F. R. Shu and G. Guilbault, Anal. Lett., 5 (1972) 559.

6 I. Nagelberg, L. I. Braddock and G. Barbero, Science, 166 (1969) 1403.
7 M. Nanjo, T. J. Rohm and G. Guilbault, Anal. Chim. Acta, 77 (1975) 19.
8 G. Guilbault and M. Nanjo, Anal. Chim. Acta, 78 (1975) 69.
9 D. C. Frost, A. Ishitani and C. A. McDowell, Mol. Phys., 24 (1972) 861.
10 M. Mascini and A. Liberti, Anal. Chim. Acta, 60 (1972) 405.
11 P. Kivalo, R. Virtanen, K. Wickstrom, M. Wilson, E. Pungor, G. Horvai and K. Tóth, Anal. Chim. Acta, 87 (1976) 401.
12 D. Midgley, Anal. Chim. Acta, 87 (1976) 7.
13 G. J. M. Heijne, W. E. van der Linden and G. den Boef, Anal. Chim. Acta, 89 (1977) 287.
14 V. Kohlschutter and C. Brittlebank, Justus Liebigs Ann. Chem., 349 (1906) 232.

Analytica Chimica Acta, 109 (1979) 157—160

Short Communication

DETERMINATION OF COBALT BY ANODIC STRIPPING VOLTAMMETRY AT A MERCURY FILM ELECTRODE

HARRY BLOOM*, BARRY N. NOLLER** and DESMOND E. RICHARDSON***

Department of Chemistry, The University of Tasmania, G.P.O. Box 252C, Hobart 7001 (Australia)

(Received 27th February 1979)

Summary. Cobalt can be determined at the 10^{-6} M level in 0.1 M NaH_2PO_4—0.05 M pyridine by its peak at —0.27 V vs. SCE. To avoid peak overlap, copper concentrations must not exceed 10^{-6} M. Formation of a cobalt/zinc intermetallic compound prevents application of the method to on-line monitoring of zinc plant electrolyte.

Several authors [1—3] have reported methods for cobalt determination at a variety of electrode surfaces by anodic stripping voltammetry (a.s.v.). Hovsepian and Shain [1] determined cobalt(II) in a phosphate buffer containing pyridine at the hanging mercury drop electrode. Previous studies reported by these authors showed that the cobalt(II) reduction appeared to be reversible in systems involving pyridine (pyridinium chloride) or pyridine in phosphate buffer at pH 6 whereas cobalt(II) alone showed irreversible behaviour. They also confirmed that addition of pyridine to solutions containing Co^{2+} gave an anodic half-wave potential shift of 200 mV. However, a compromise between the effects of irreversibility observed for solutions with low pyridine concentrations and streaming phenomena obtained at high pyridine concentrations necessitated the choice of 0.05 M pyridine in 0.1 M phosphate buffer (pH 6) and a deposition potential of —1.20 V vs SCE [1]. A single anodic peak was found at —0.14 V vs. SCE, giving a relative standard deviation of <4% (6 determinations). Smith and Redmond [2] examined the behaviour of Co^{2+} added to sea water and found a single peak at —0.22 V vs. SCE for the hanging mercury drop electrode, finding a sensitivity of 7.2 nA l μg^{-1}.

Methods for the determination of Cu, Pb, Cd, Zn, Bi, In, Tl and Sn at the mercury film electrode (MFE) by a.s.v. have been established [3] but little work has been done on cobalt determination with this electrode. Luong and Vydra [4] reported that cobalt(II) ions gave a single peak at —0.23 V vs. SCE at a MFE, but no other details were given.

This report describes an investigation of the determination of cobalt in the pyridine-buffered electrolyte described by Hovsepian and Shain [1] by a.s.v.

**Present address: Research School of Chemistry, Australian National University, Canberra, A.C.T.

***Present address: Australian Newsprint Mills, Boyer, Tasmania.

at the MFE with particular attention to deposition potential, zinc and copper interferences and intermetallic compound formation. The possible determination of cobalt in zinc sulphate feed solutions for electrolytic zinc production was also examined.

Experimental

Instrumentation. The instrument was designed and built at the Chemistry Department, University of Tasmania, and has been described previously [5]. The Perspex cell was equipped with a rotating glassy-carbon electrode (Grade GC-20, Tokai Electrode Manufacturing Co., Tokyo), a platinum wire auxiliary electrode, a saturated calomel reference electrode and a purge tube to allow deaeration with high-purity nitrogen [5].

Reagents. A 0.2 M NaH_2PO_4—0.1 M pyridine supporting electrolyte solution was prepared from analytical-grade materials and double-distilled water. Cobalt, copper and mercury stock solutions were prepared by dissolving the respective metal in double-distilled nitric acid and diluting with double-distilled water. Cobalt standards in the range $0—2 \times 10^{-5}$ M and a 1.5×10^{-4} M mercury solution were prepared daily. Zinc sulphate solutions were prepared from the analytical-grade reagent.

Procedure. Typically, a 2.0-ml portion of 0.2 M NaH_2PO_4—0.1 M pyridine electrolyte, 1.0 ml of cobalt standard, and 1.0 ml of 1.5×10^{-4} M mercury(II) solution were added to the cell and deaerated for 10 min. A deposition potential of —1.30 V vs. SCE was applied for 2 min prior to a preliminary scan over a 1.4-V range at 1 V min^{-1}. A second scan using similar parameters was done after a further 2.0-min deaeration. Measurements were taken from three or four successive scans for each solution. All voltages quoted are referred to the SCE.

Results and discussion

Figure 1 shows the response from 2.1×10^{-6} M cobalt in the phosphate—pyridine buffer. The height of the peak at —0.27 V was dependent on deposition potential with no peak being recorded for a deposition potential more positive than —1.15 V. The peak at 0.0 V in Fig. 1 did not increase with added cobalt, but did not occur in its absence.

A calibration curve based on the area of the cobalt peak at —0.27 V was non-linear but reproducible and could be used for the determination of 0.25—1.0 μg of cobalt (equivalent to overall concentrations of $1.1—4.2 \times 10^{-6}$ M) with relative standard deviations of 9.4—13.0%, respectively. The non-linearity of the calibration curve suggested that the limit of solubility of cobalt in the mercury film may have been approached as the cobalt concentration was increased. Florence [6] reported that attempts to measure metals at concentrations above 10^{-6} M by a.s.v. at the MFE resulted in loss of sensitivity.

As the peak potential of cobalt was in the same potential region as the stripping peak for copper, it was decided to investigate the interference of copper on the cobalt peak. It was found that the determination of 2×10^{-6} M

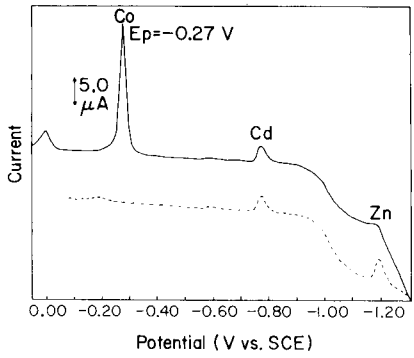

Fig. 1. Response from 2.1×10^{-6} M Co in 0.1 M NaH_2PO_4—0.05 M pyridine. (---) Blank; (—) 2.1×10^{-6} M cobalt. Deposition potential, —1.30 V vs. SCE.

cobalt was not affected by the presence of less than 4×10^{-7} M copper. Copper concentrations exceeding 10^{-6} M resulted in overlap of the cobalt and copper peaks.

The effect of zinc on the determination of cobalt was very significant. A 50% reduction in cobalt peak area occurred in the presence of 10^{-6} M zinc sulphate after deposition at —1.30 V. Changing the deposition potential to —1.20 V resulted in 1.5×10^{-5} M zinc sulphate being required to decrease the cobalt peak area by 50%. Increasing the zinc concentration further resulted in the elimination of the cobalt peak at —0.27 V and the formation of a new peak at —1.12 V (Fig. 2). This peak increased linearly with increased cobalt

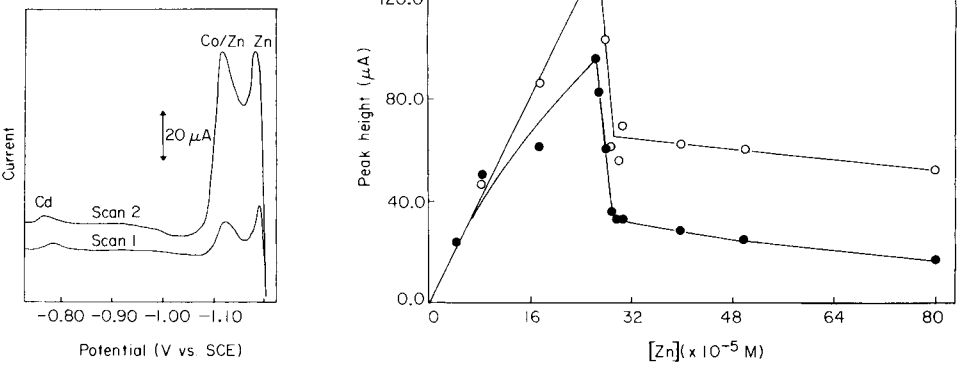

Fig. 2. Current—potential curves showing the formation of a cobalt/zinc intermetallic compound. Deposition potential, —1.20 V. [Zn] = 1.76×10^{-4} M. [Co] = 2.1×10^{-6} M. E_p = —1.12 V for the Co/Zn peak; E_p = —1.18 V for the Zn peak.

Fig. 3. Effect of zinc concentration on the Zn (○) and Co/Zn (●) peak heights for 2.1×10^{-6} M cobalt in 0.1 M NaH_2PO_4—0.05 M pyridine. Deposition potential, —1.20 V.

concentration at a fixed zinc concentration. The evidence suggests that an intermetallic compound of cobalt and zinc was being formed. Intermetallic compound formation is a common interference in a.s.v. and a number of metals, including Cu [7, 8], Ni [9], Au [9] and Co [10], have been shown to form intermetallic compounds with zinc; the intermetallic compound reported by Hovsepian and Shain [10] had the formula CoZn. The behaviour of the intermetallic compound formed at the MFE had similar characteristics to those described earlier [10]; the concentration of zinc required to depress entirely the cobalt peak at —0.27 V was approximately equal to the cobalt concentration in the solution, suggesting that a 1:1 compound was formed.

The Co/Zn peak illustrated in Fig. 2 responded to changes in zinc concentration in the manner shown in Fig. 3. The discontinuity at 2.6×10^{-4} M zinc sulphate was due to formation of a precipitate which coprecipitated zinc ions. The maximum zinc sulphate concentration at which the Co/Zn peak could be resolved was about 10^{-3} M. As the zinc sulphate concentration in a cell feed for electrolytic zinc production is normally 1.8 M, the dilution required to reduce the zinc sulphate concentration to 10^{-3} M would result in reduction of the cobalt concentration below the level at which it could be measured. The usual limits of these elements in cell feed solution are 50—100 μg Cu l^{-1} and 8—10 mg Co l^{-1}. Accordingly, the a.s.v. method could not be used for on-line monitoring of zinc plant electrolytes.

Financial support, the supply of electrolyte solutions and technical advice from the Electrolytic Zinc Company of Australasia are gratefully acknowledged. The University of Tasmania also provided financial support.

REFERENCES

1 B. K. Hovsepian and I. Shain, J. Electroanal. Chem., 12 (1966) 397.
2 J. D. Smith and J. D. Redmond, J. Electroanal. Chem., 33 (1971) 169.
3 G. E. Batley and T. M. Florence, J. Electroanal. Chem., 55 (1974) 23.
4 L. Luong and F. Vydra, J. Electroanal. Chem., 50 (1974) 379.
5 H. Bloom and B. N. Noller, Application of Anodic Stripping Voltammetry to Trace Metal Analysis, chapter in J. O'M. Bockris, D. A. J. Rand and B. J. Welch (Eds.), Trends in Electrochemistry, 1977, Plenum, New York, pp. 241—252.
6 T. M. Florence, J. Electroanal. Chem., 27 (1970) 273.
7 T. R. Copeland, R. A. Osteryoung and R. K. Skogerboe, Anal. Chem., 46 (1974) 2093.
8 M. S. Shuman and G. P. Woodward, Anal. Chem., 48 (1976) 1979.
9 R. S. Rodgers and L. Meites, J. Electroanal. Chem., 38 (1972) 359.
10 B. K. Hovsepian and I. Shain, J. Electroanal. Chem., 14 (1967) 1.

Analytica Chimica Acta, 109 (1979) 161—164

Short Communication

NAPHTHYLDIAZOMETHANE AS A DERIVATIZING AGENT FOR THE HIGH-PERFORMANCE LIQUID CHROMATOGRAPHY DETECTION OF BILE ACIDS†

DUANE P. MATTHEES

Organic Analytical Research Division, National Bureau of Standards, Washington, D.C. 20234 (U.S.A.)

WILLIAM C. PURDY*

Department of Chemistry, McGill University, Montreal, Quebec, H3A 2K6 (Canada)

(Received 6th February 1979)

Summary. Bile acids are derivatized with 1-naphthyldiazomethane and separated by h.p.l.c. on silica gel columns with a hexane—tetrahydrofuran—methanol solvent. Reactions proceed quickly at room temperature under mild conditions, to give strongly absorbing species for u.v. detection. Deoxycholic acid can be detected in cat feces.

The bile acids play a vital role in digestion and cholesterol metabolism, and recent interest has centered on their correlation with cancer of the colon [1, 2]. In addition, the identification and quantification of the various bile acids may be of value in the diagnosis of liver disease [3].

While there has been considerable effort to develop thin-layer and gas chromatographic methods of measurement, high-performance liquid chromatography (h.p.l.c.) appears to be particularly well suited for the measurement of bile acids, because it combines the advantages of mild separation conditions with fairly easy quantification, provided that a suitable detector is available. Underivatized bile acids have been detected by monitoring the column effluent in the far ultraviolet [4, 5], but derivatization of the bile acids with chromophores, such as the aromatic esters, has advantages. Derivatization of the carboxyl group allows some degree of selectivity, especially in the analysis of biological materials where potential interferences (e.g., neutral sterols) are likely to be present. Furthermore, if the derivative absorbs strongly in the 250—280-nm region, highly sensitive fixed-wavelength detectors can be employed, and the choice of solvents is greater than when the effluent is monitored at 205—220 nm.

Diazomethane has long been a favorite reagent for the formation of methyl esters of carboxylic acids because of its high reactivity under mild conditions [6]. Similarly, the aryldiazoalkanes should readily form esters with strong

†Taken in part from the Ph.D. Dissertation of D. P. Matthees, University of Maryland, 1978.

chromophores for u.v. detection in h.p.l.c. For this study, 1-naphthyldiazomethane was chosen as a derivatizing agent since it can be easily made from inexpensive, readily obtainable reagents, and the naphthyl group is an excellent chromophore [7]. Moreover, a general advantage of the aryldiazoalkanes is their intense color, which fades as the reaction progresses. This color change makes it easier to determine whether enough reagent has been added, particularly when the exact amount of bile acid is unknown.

Experimental

Apparatus. The chromatograph equipment used was the same as described earlier with fixed-wavelength (254 nm) and variable-wavelength detectors [7]. The column contained μPorasil, 30 cm long; Waters Associates.

Reagents. 1-Naphthaldehyde, hydrazine, mercury(II) oxide, and cholic and deoxycholic acids were obtained from common commercial sources. Other bile acids were prepared from cholic or deoxycholic acids. Solvents were of the usual reagent-grade redistilled from all-glass apparatus (rejecting the first and last 10%) and filtered before use. Bulk hexane was purified by refluxing with concentrated sulfuric acid, followed by water washing and drying over sodium hydroxide before redistillation.

Preparation of reagent. 1-Naphthyldiazomethane was prepared by oxidation of 1-naphthaldehyde hydrazone with mercury(II) oxide essentially as described by Nakaya et al. [8]; magnetic stirring in a loosely stoppered flask was found to be more convenient than shaking in a pressure bottle. While 1-naphthyldiazomethane is soluble in many organic solvents, diethyl ether is most satisfactory for application to the bile acid derivatization. Solutions were prepared as described earlier [7].

Derivatization. Dry, crystalline bile acid standards were dissolved in chloroform, with enough methanol added to bring them into solution; typically 1—5 mg of each bile acid was dissolved in 0.5 ml of solvent. When a hydrolysate of bile salts was analyzed, it was acidified and extracted with ethyl acetate or butanol and a known aliquot taken. Several drops of the 1-naphthyldiazoalkane solution were then mixed, in a 1-ml graduated tube, with the bile acid solution to give a reddish-orange color. More reagent was added if the color disappeared within an hour as described for derivatization of fatty acids [7]. After reaction, the excess of derivatizing agent could be decomposed by a drop of acetic acid, if desired. The mixture was then diluted to volume and an aliquot of 5 μl or so was taken for chromatography.

Chromatographic conditions. There is a considerable volume of data on the separation of bile acids and their esters by thin-layer chromatography [9], and many of the solvent systems may be adapted to h.p.l.c. on silica gel columns. A 300:120:8 mixture of hexane—tetrahydrofuran—methanol proved to be an excellent isocratic solvent for the separation of the 1-naphthylmethyl esters of the bile acids; flow rates of 1.0—1.5 ml min^{-1} were satisfactory. The amount of methanol in the system sharply affects the retention volumes of the bile acid derivatives, especially the polar acids, so that the solvent com-

position may be optimized for the polar or nonpolar acids. A 200:85:5 hexane—tetrahydrofuran—acetic acid solvent system gave similar behavior. A number of different solvent systems were tested, with one of the most important criteria being the ability to resolve positional isomers.

Results and discussion

Figures 1A and 2 show separations of bile acid derivatives in solvent systems of hexane—tetrahydrofuran with a polar modifier of methanol or acetic acid. The dihydroxy acid derivatives, deoxycholic and chenodeoxycholic, were well resolved, in addition to acids with different numbers of hydroxyl groups.

Figure 1B shows the separation of deoxycholic acid from other constituents of cat feces. A Soxhlet extract of cat feces with 1:1 chloroform—methanol was concentrated and a portion reacted with 1-naphthyldiazomethane. The

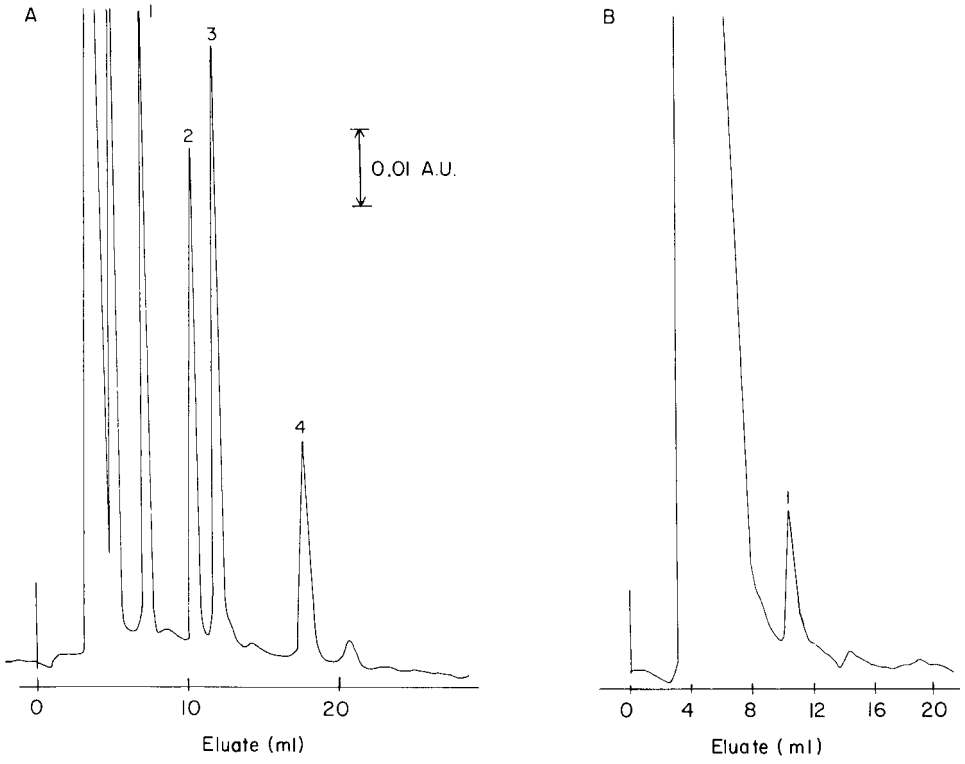

Fig. 1. (A) Naphthyldiazomethane derivatives of some less polar bile acids. Mobile phase, 300:120:8 hexane—tetrahydrofuran—methanol, flow rate, 1.0 ml min^{-1}; 2-μl injections containing about 15 μg of each bile acid; detection at 280 nm (Schoeffel). Peak identity: (1) lithocholic, (2) deoxycholic, (3) chenodeoxycholic, (4) 3,7-dihydroxy-12-ketocholanic acid. (B) Deoxycholic acid from cat feces. Conditions as for Fig. 1A; 5-μl injection corresponding to the derivatized extract of 2 mg of feces (wet weight). Peak (1) is the deoxycholic acid derivative.

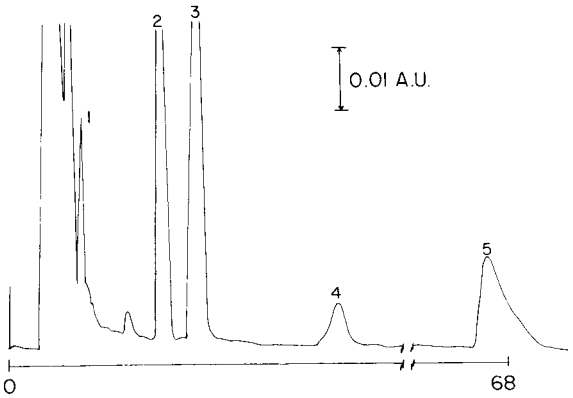

Fig. 2. Naphthyldiazomethane derivatives of bile acids (about 20 μg of cholic, deoxycholic, and chenodeoxycholic acids and 5 μg of lithocholic and 3,7-dihydroxy-12-ketocholanic acids). Mobile phase, 200:85:5 hexane—tetrahydrofuran—acetic acid; flow rate, 1.0 ml min^{-1}; detection at 254 nm (Waters). Peak identity: (1) lithocholic, (2) deoxycholic, (3) chenodeoxycholic, (4) 3,7-dihydroxy-12-ketocholanic acid, (5) cholic acid.

reaction mixture was injected directly onto the column and eluted. This sample contained sufficient bile acid to permit detection without additional cleanup or preconcentration. The other fecal constituents were eluted from the silica gel column before the deoxycholate derivative.

The aryldiazoalkanes react completely with carboxylic acids, so that the corresponding esters of the free bile acids and their glycine conjugates can be prepared. However, the taurine conjugates, which are sulfonic acids, do not esterify. The detection limits for these derivatives depend on peak sharpness, retention volume, and other factors, but with the fixed-wavelength detector (254 nm), 20—30 ng of the bile acid should be detectable. Since all the derivatives have the same chromophore, the detector response is proportional to the number of moles of acid derivatized.

REFERENCES

1 M. Winick, Nutrition and Aging, J. Wiley, New York, 1976, p. 161.
2 D. S. Reddy, A. Mastromarino and E. L. Wynder, Cancer Res., 35 (1975) 3403.
3 J. B. Carey, Jr., in P. P. Nair and D. Kritchevsky (Eds.), The Bile Acids, Vol. 2, Plenum Press, New York, 1973, p. 68.
4 S. Okuyama, D. Uemura and Y. Hirata, Chem. Lett., (1977) 679.
5 N. A. Parris, J. Chromatogr., 133 (1977) 273.
6 K. Blau and G. S. King (Eds.), Handbook of Derivatives for Chromatography, Heyden, London, 1978, p. 49.
7 D. P. Matthees and W. C. Purdy, Anal. Chim. Acta, 109 (1979) 61.
8 T. Nakaya, T. Tomomoto and M. Imoto, Bull. Chem. Soc. Jpn., 40 (1967) 691.
9 P. Eneroth, in G. V. Marinetti (Ed.), Lipid Chromatographic Analysis, Vol. 2, M. Dekker, New York, 1969, p. 149.

Analytica Chimica Acta, 109 (1979) 165—169

Short Communication

GENERAL DISSOLUTION PROCEDURE FOR THE ANALYSIS OF ALUMINIUM ALLOYS BY ATOMIC ABSORPTION SPECTROMETRY

B. A. MILNER, P. J. WHITESIDE and W. J. PRICE*

Pye Unicam Ltd., York Street, Cambridge (Gt. Britain)

(Received 9th March 1979)

Summary. Alloys are dissolved in nitric acid followed by hydrofluoric acid. Borax is added to complex the excess of fluoride and to act as spectroscopic buffer. Results obtained for up to 12 elements in 7 standard alloys are accurate.

Some of the earliest atomic absorption methods for aluminium alloys were concerned with the measurement of individual elements but it soon became clear that most dissolution methods would be common to the determination of a number of elements in the same alloy. Both caustic soda [1] and acid dissolutions [2, 3] were evolved and it was also shown [1] how interelement interference effects decrease with increasing flame temperature. Caustic dissolution methods are generally less suitable for atomic absorption because of the comparatively high total dissolved solids content of the resulting working solutions. This causes higher light emission from the flame and also severe molecular absorption and scatter background in the air—acetylene flame, though in modern instruments with well designed burners and background correction, it may not be a particular disadvantage.

Simple acid dissolutions, though quicker and easier to handle, may not completely dissolve all aluminium alloys. Hydrogen peroxide assists in solubilizing low silicon concentrations. An earlier general method originating in this laboratory [4] used hydrochloric acid/hydrogen peroxide, though at that time silicon was not determined, and a severe depressive interference of aluminium on magnesium absorption in the absence of a suitable releasing agent (strontium chloride was recommended) was observed unless a dinitrogen oxide—acetylene flame was used.

To dissolve larger silicon contents, the sample was heated with the same solvents in a polythene beaker and hydrofluoric acid was added to the cooled solution [5]. It was confirmed that in cool solutions silicon was not lost as silicon tetrafluoride. Magnesium, however, above certain concentrations may precipitate as magnesium fluoride. The use of hydrofluoric acid thus seemed to preclude the accurate determination of significant amounts of magnesium.

Recent work [6] has shown that insoluble fluorides can be converted to soluble fluoroborates with boric acid, prior to atomic absorption analysis of siliceous materials and a silicon—aluminium alloy. Preliminary experiments

with high magnesium—aluminium alloys confirmed that the addition of boric acid, after the dissolution of the sample in nitric and hydrofluoric acids, is also effective in completely redissolving magnesium fluoride. Solid boric acid can be added, but this is time-consuming as it necessitates the weighing of individual amounts of the solid reagent into each sample solution. The relatively low solubility of boric acid precludes the use of a solution for this purpose, so disodium tetraborate (borax) solution was investigated as an alternative. Fluoroborate acts as a spectroscopic releasing agent [6] so that, with the use of a dinitrogen oxide—acetylene flame, no other releasing agent need be added. Borax solution also provides a convenient source of sodium ions to act as an ionization buffer, thus obviating the need to add a further reagent for this purpose. The performance of borax solution as a replacement for boric acid, after nitric—hydrofluoric acid dissolution, was evaluated for the analysis of seven British Chemical Standard aluminium alloys.

Experimental

Instrumentation and reagents. The atomic absorption spectrometers used were the SP9-800 with SP9 computer and the SP2900 with background corrector and Data Centre on-line programmable calculator, all from Pye Unicam. Principal settings and conditions are summarized in Table 1.

Nitric acid (sp. gr. 1.42) and hydrofluoric acid (42% w/v) were both analytical grade.

Disodium tetraborate solution (20% w/v). Dissolve 100 g of $Na_2B_4O_7 \cdot 10H_2O$, (analytical grade) in 400 ml of deionized water and warm with gentle

TABLE 1

Instrumental conditions

(A 5-cm slot N_2O—C_2H_2 burner is recommended unless otherwise stated. The burner height is 10 mm, and the slot is in line with the optical axis, except for high concentrations of Cu, Mg and Zn when it is placed at 90° to the axis. Where trace levels of elements are sought, the use of a 10-cm slot air—C_2H_2 burner is recommended for those determinations involving the use of the air—C_2H_2 flame. This burner should give up to a 40% increase in sensitivity. The bandpass for all elements is 0.4 or 0.5 nm. Background correction is used as required for low wavelengths to minimize the "blank" reading.)

Element	Sb	Cr	Cu	Fe	Pb	Mg
Wavelength (nm)	217.6	357.9	324.8	248.3	217.0	285.2
Lamp current (mA)	12	8	5	12	6	4
C_2H_2 flow (l min^{-1})	1.1—1.3[a]	4.0—4.5[b]	1.0—1.2[a]	1.1—1.3[a]	1.0—1.2[a]	4.0

Element	Mn	Ni	Si	Sn	Ti	Zn
Wavelength (nm)	279.5	341.5	251.6	224.6	364.3	213.9
Lamp current (mA)	10	12	12	6	12	10
C_2H_2 flow (l min^{-1})	1.1—1.3[a]	1.1—1.3[a]	4.2—4.6[b]	4.0—4.4[b]	4.4—5.0[b]	1.0

[a]Air flow rate: 4.5—5.5 l min^{-1}. [b]N_2O flow rate: 4.5—5.5 l min^{-1}.

agitation until dissolved. Dilute to 500 ml. If recrystallization occurs on cooling, gentle warming to redissolve the crystals may be necessary before use.

Aluminium stock solution (0.5% w/v). Transfer 2.50 g of high-purity aluminium (British Chemical Standard 198e) to a 250-ml polypropylene beaker and add 125 ml of 40% (w/v) nitric acid followed by the cautious slow addition of 25 ml of the 42% (w/v) hydrofluoric acid. The dissolution is very vigorous and it may be necessary to slow the reaction by addition of water. When dissolution is complete, transfer the solution to a 500-ml polypropylene volumetric flask, add 100 ml of the disodium tetraborate solution, and dilute to the mark with deionized water.

Standard element stock solutions (1000 mg l^{-1}). For the silicon stock solution, dissolve about 7.6 g of sodium metasilicate (standardized previously by the gravimetric method to establish the exact weight required) in water and dilute to 1 l in a volumetric flask. For the metals, weigh out exactly 1.000 g of the high-purity element, dissolve appropriately with heating if necessary, cool and dilute to 1 l with deionized water in a volumetric flask. Store each separate solution in plastic bottles. Appropriate solvents for the metals are as follows: for chromium, manganese and titanium, use 50 ml of concentrated hydrochloric acid; for copper, lead and nickel, use 50 ml of 5 M nitric acid; for magnesium and zinc, use 50 ml of 5 M hydrochloric acid; for antimony, use 10 ml of concentrated hydrochloric acid, 1 ml of concentrated nitric acid and 10 g of tartaric acid; for iron, use 20 ml of 5 M hydrochloric acid and 5 ml of concentrated nitric acid; for tin, use 200 ml of concentrated hydrochloric acid and 5 ml of concentrated nitric acid.

Mixed standard element stock solution. Pipette 50-ml aliquots of the Cr, Cu, Fe, Mg, Mn, Ni, Si and Zn stock solutions, and 20-ml aliquots of the Pb, Sb, Sn and Ti stock solutions into a 500-ml volumetric flask, dilute to the mark with deionized water and transfer to a plastic container. The concentrations of the two groups of elements are 100 and 40 mg l^{-1}.

Preparation of sample solution. Weigh 0.500 g of the sample into a 100-ml plastic beaker and add 25 ml of nitric acid (40% w/v). Warm the beaker on a hot water bath until there is no further reaction. Remove from the water bath and cool to below 50°C. Add, carefully, 5 ml of the hydrofluoric acid and allow to stand for 10 min. Add 20 ml of the disodium tetraborate solution. Allow to stand for 5 min and dilute to 100 ml in a polypropylene volumetric flask with deionized water. This solution (A) is used for the determination of all elements in the range 0—1%. For elements with an expected concentration between 1 and 10%, dilute a 10-ml aliquot of solution A to 100 ml in a volumetric flask with deionized water. For elements with an expected concentration greater than 10%, pipette a 5-ml aliquot of solution A into a 100-ml volumetric flask, together with 5 ml of the aluminium stock solution, and dilute to the mark with deionized water.

Preparation of calibration solutions. Weigh 0.50 g of high-purity aluminium (British Chemical Standard 198e) into each of five 100-ml plastic beakers. To each add 25 ml of nitric acid (40% w/v) followed by cautious addition of

5 ml of hydrofluoric acid (42% w/v). When dissolution is complete, add to each 20 ml of the disodium tetraborate solution and transfer to five 100-ml polypropylene volumetric flasks. Add appropriate aliquots of the mixed standard stock solution as given in Table 2, to four of the flasks and dilute to the mark with deionized water. Dilute the fifth solution (the blank) to the mark with deionized water.

For element concentrations exceeding 1% pipette 10-ml aliquots of the stock aluminium solution (0.50% w/v) into each of five 100-ml volumetric flasks. Add appropriate aliquots of the mixed standard stock solutions as in Table 2.

Results and discussion

The results obtained for twelve elements in seven standard alloys are presented in Table 3. They are in close agreement with the certified values. The dissolution procedure is relatively simple and rapid and requires no expensive

TABLE 2

Preparation of calibration solutions

Pipetted aliquot of mixed element stock solution (ml)	Equivalent concentration in sample solution (%)			
	Cr, Cu, Fe, Mg, Mn, Ni, Si, Zn		Sb, Pb, Sn, Ti	
	0.5% w/v sample soln.	0.05% w/v sample soln.	0.5% sample soln.	0.05% sample soln.
50	1.00	10.0	0.40	4.00
25	0.50	5.0	0.20	2.00
12.5	0.25	2.5	0.10	1.00
5	0.10	1.0	0.04	0.40

TABLE 3

Results obtained for B.C.S. aluminium alloys

B.C.S. No.		Cr	Cu	Fe	Pb[a]	Mg	Mn	Ni	Si[a]	Sn[a]	Ti
181/2	Cert.	0.008	3.96	0.42	0.04	1.56	0.20	1.90	0.27	0.03	0.019
4% Cu/Al	Found	0.007	3.92	0.42	0.041	1.53	0.20	1.90	0.26	0.025	0.02
182/2	Cert.	—	0.045	0.47	0.05	0.07	0.21	0.05	11.02	0.02	0.11
11% Si/Al	Found		0.045	0.46	0.046	0.075	0.20	0.052	11.00	0.02	0.10
216/1	Cert.	—	4.42	0.40	0.05	0.74	0.73	0.06	0.74	0.05	0.10
Duralumin[b]	Found		4.35	0.39	0.056	0.76	0.72	0.051	0.73	0.05	0.095
262	Cert.	0.06	0.03	0.19	—	10.57	0.06	—	0.10	—	0.10
10% Mg/Al	Found	0.06	0.025	0.18		10.65	0.068		0.08		0.095
263/1	Cert.	0.24	0.09	0.35	—	4.92	0.36	—	0.12	—	0.04
5% Mg/Al	Found	0.255	0.088	0.36		5.03	0.38		0.10		0.04
268	Cert.	—	1.34	0.39	0.035	0.56	0.22	0.12	4.85	0.03	<0.02
5% Si/Al	Found		1.32	0.38	0.034	0.59	0.205	0.117	4.80	0.03	0.015
300	Cert.	0.15	1.28	0.30	—	2.76	0.41	—	0.16	—	0.15
6% Zn/Al	Found	0.16	1.26	0.29		2.72	0.42		0.14		0.14

[a]Simultaneous background correction used.
[b]Sb: found 0.044%; cert. 0.05%.

reagents. It should be possible to extend the method without difficulty to cover determinations of arsenic, beryllium, cadmium, calcium, cobalt, lithium, silver and strontium. The procedure would therefore appear to be generally applicable to the analysis of aluminium alloys by atomic absorption spectrometry.

REFERENCES

1 L. Wilson, Anal. Chim. Acta, 30 (1964) 377; 40 (1968) 503.
2 G. F. Bell, At. Absorpt. Newsl., 5 (1966) 73.
3 R. E. Mansell, H. W. Emmel and E. L. McLaughlin, Appl. Spectrosc., 20 (1966) 231.
4 W. J. Price, Analytical Atomic Absorption Spectrometry, Heyden, London, 1972, p. 118; see also W. J. Price, Spectrochemical Analysis by Atomic Absorption, Heyden, London, 1979.
5 W. J. Price and J. T. H. Roos, Analyst, 93 (1968) 709.
6 W. J. Price and P. J. Whiteside, Analusis, 5 (1977) 275; Analyst, 102 (1977) 664.

Analytica Chimica Acta, 109 (1979) 171—175

Short Communication

THE DETERMINATION OF SILVER IN SILICATE ROCKS BY ELECTROTHERMAL ATOMIC ABSORPTION SPECTROMETRY

P. J. ARUSCAVAGE* and E. Y. CAMPBELL

U. S. Geological Survey, Reston, Virginia 22092 (U.S.A.)

(Received 26th February 1979)

Summary. Silver is extracted from a 20% tartaric acid solution by using butyl acetate and diphenylthiourea, and the organic layer is analyzed directly by the graphite-furnace technique. The precisions is ca. 8% as estimated from multiple analysis of 13 standard rocks; there are no systematic errors. The detection limit is 2.4 ppb for 250-mg samples.

Silver in rocks is usually determined by using neutron-activation analysis or isotope-dilution techniques [1—7] because of the high sensitivity normally required. Since the introduction of graphite-tube furnaces, however, very high sensitivity for silver can be attained by atomic absorption. Because of the extremely small amounts of silver to be determined in a complex matrix such as rocks, separations are usually required for the highest accuracy and best precision.

The extraction of silver with diphenylthiourea and its subsequent determination in rocks have been investigated extensively [8—12]. Silver was quantitatively extracted into chloroform, butyl acetate, MIBK, and mixtures of butanol and chloroform from hydrochloric acid, sulfuric acid, and nitric acid solutions. Hg, Au, Cu, Pt, Pd, Rh, Ru, Ir, Fe, Mn, and Sb were reported to extract or to interfere with the extraction of silver, depending on the conditions.

In this communication, a procedure is reported for the determination of silver in a wide variety of silicate rocks at low ppb levels.

Experimental

Reagents. All chemicals were of reagent-grade quality; however, the nitric acid, hydrofluoric acid, and distilled water should be checked by the graphite-furnace method to ensure low blanks. Some lots of hydrofluoric acid were found to contain silver.

Standard silver solution (1.000 mg Ag ml^{-1}). Dissolve 157.5 mg of silver nitrate in 100 ml of 0.5 M nitric acid and store in the dark. Prepare a 100-ppb silver solution by dilution of this stock standard with 0.5 M nitric acid. This solution is stable for several days.

Diphenylthiourea (1% w/v). Dissolve 0.5 g of diphenylthiourea (thiocarbanilide) in 50 ml of acetone. Prepare fresh daily.

Apparatus. A Perkin-Elmer model 503 atomic absorption spectrometer was used with a model HGA 2100 graphite furnace; a model 56 recorder was used for all peak height measurements. Deuterium background correction was used for all measurements.

The settings were as follows: wavelength, 328.1 nm; slit, 0.7 nm; argon gas with "interrupt" flow; dry, 110°C—20 s; char, 550°C—20 s; atomization, 2700°C — 7 s.

Procedure. Weigh 250 mg of sample into a Teflon beaker. Pipet several standards over the range of 5—20 ng Ag into separate beakers and process in the same manner as the rock samples. To all beakers, add 1 ml of 72% perchloric acid, 5 ml of concentrated nitric acid and 15 ml of 40% hydrofluoric acid. Evaporate overnight on a hotplate at about 140°C.

Dissolve the residues in 15 ml of 20% tartaric acid by gentle heating for 15 min. Transfer to separatory funnels and cool. Add 0.5 ml of 1% diphenylthiourea, mix, and allow to stand for 2 min. Extract with 5.0 ml of butyl acetate for 3 min, and allow 1 hour for layers to separate. Pipet 10 μl of the organic layer for analysis by graphite-furnace atomic absorption spectrometry. Determine the concentration of silver in the samples by comparison of the peak heights with those of the standard silver solutions.

Results and discussion

Vall et al. [8] reported that silver can be extracted quantitatively from solutions as concentrated as 10 M HCl and 0.1—2.5 M HNO_3 into chloroform; Au, Hg, and Cu are the only other elements extracted. However, they observed that poor reproducibility resulted when the chloroform solutions were analyzed by the graphite-furnace technique, and that copper affected the results significantly, giving both positive and negative interferences depending on its concentration. Bazhov and Sokolova [12] extracted silver quantitatively from 1—3 M HCl solutions into butyl acetate and determined silver by flame atomic absorption. They reported no interferences from K, Na, Ca, Mg, Pb, Zn, Sn, Fe, Mn, Ni, Co, Al, Ti, or As at the 5 mg ml^{-1} level, but Cu (500 μg ml^{-1}) suppressed the extraction. However, when this method was tested on rocks with the graphite-furnace technique, low and erratic results were obtained in this laboratory. When these rocks were spiked with silver and analyzed by the method of standard additions after this same extraction procedure, suppression of the silver absorption signal was confirmed by the differences in the slopes of the pure standard solutions and the spiked rocks. The extraction yields, where silver-110 tracer was used, exceeded 95% for standard and rocks solutions, indicating that the low results were caused by matrix suppression of the silver absorption and not by incomplete extraction of silver from the rock solutions. Additions of 10 μg Fe, 100 μg Cu, or 10 μg Au individually had no effect on the slope of the curve, which possibly indicates multiple effects from the complex matrix of rocks. Washing the organic layer with water, 1 M HCl, or 0.1 M EDTA

reduced the interference slightly, and the results were less erratic, but still low. Similar low results were obtained where extractions were made from 0.5 M sulfuric acid, 1 M perchloric acid or 0.2 M EDTA solutions into MIBK, amyl acetate, or butyl acetate. When 20% tartaric acid solutions of the rocks were extracted with butyl acetate or amyl acetate, however, there was no suppression; washed and unwashed organic layers gave the same values.

The graphite-furnace conditions were similar to those recommended in the Perkin-Elmer literature. The graphite tubes used were the regular uncoated tubes. The hole size was enlarged so that the pipet tip would touch the bottom of the tube; this provided more reproducible pipetting of the organic solutions because the final droplet was removed by capillary action. Pyrolitically coated graphite tubes were tried, and the sensitivity was found to increase by a factor of 2. However, experience with other elements had shown poor reproducibility when these tubes were used; therefore, they were not tested further.

When this procedure was used, the sensitivity for silver was 0.005 absorbance per 2 pg of silver, which agrees with the Perkin-Elmer literature where the sensitivity is stated as 3 pg for 0.0044 absorbance. The procedural blank was 2.8 ± 0.2 ng of silver, thus giving a detection limit of 2.4 ppb in the rock (for a 250-mg sample) based on three times the standard deviation of the blank.

An estimate of the precision and the degree of homogeneity among bottles of 13 USGS standard rocks is given in Table 1, and a one-way analysis of variance was made on the data. Random sampling (three determinations from each bottle) was performed on three bottles of each standard rock. The determinations were made in batches of 13 samples, 4 standards, and 1 blank over a period of 2 weeks in order to test the reliability with time. The precision is quite good, the relative standard deviation of the method being less than 8% except for the two ultramafic rocks DTS-1 and PCC-1. The silver content in both of these samples approaches the detection limit for this procedure; therefore, poorer precision is expected. Additionally, both were incompletely dissolved, leaving a black residue (probably chromite), which may have retained silver. The analysis of variance shows that at F (0.95) (d.f. = 2,6) there is no significant heterogeneity among bottles of any particular standard rock for silver. Thus, all bottles may be said to be homogeneous for silver within the precision of this method. A comparison of the mean silver contents of the various standard rocks determined by this method with literature values is given in Table 1. The agreement is good and no bias is apparent, indicating that the method is accurate and suitable for geochemical studies.

TABLE 1

Silver (ng g^{-1}) in 13 U.S. Geological Survey Standard Rocks (ns = not significant; s.d. = standard deviation)

Rock	Bottle No.	Individual results	F (0.95)	Mean ± s.d.	Literature values
AGV-1	10/24	86,80,80	0.134 ns	81.6 ± 2.4	80 [7], 94 [1], 110 [2], 99 [4]
	38/1	80,84,81			
	56/14	82,81,80			
BCR-1	5/32	34,31,30	1.647 ns	30.8 ± 1.4	35 [7], 36 [1], 36 [2], 28 [4], 27.1 [5]
	75/6	29,30,30			
	47/1	30,31,32			
BHVO-1	62/20	57,57,56	1.717 ns	57.9 ± 2.1	56 [7], 63 [3], 43 [4]
	10/7	61,62,56			
	31/13	56,57,59			
DTS-1	6/17	10, 7, 6	0.452 ns	7.6 ± 2.1	8 [7], 10.4 [1], 8 [2], 16 [4]
	3/9	10, 5,10			
	55/23	6, 8, 6			
MAG-1	38/19	68,66,69	0.446 ns	67.3 ± 2.3	74 [3]
	64/11	69,67,63			
	62/9	66,68,70			
G-2	3/30	36,36,33	1.235 ns	34.3 ± 1.4	43 [7], 40 [1], 49 [2], 52 [4]
	68/4	36,34,34			
	116/30	32,34,34			
GSP-1	80/16	76,86,78	3.062 ns	76.1 ± 3.5	75 [7], 84 [1], 100 [2], 86 [4]
	38/32	74,77,75			
	44/24	72,71,76			
PCC-1	43/4	9, 8, 7	3.700 ns	7.9 ± 1.1	10 [7], 9.1 [1], 5 [2], <10 [4]
	25/2	8,10, 9			
	19/32	6, 8, 6			
QLO-1	51/7	65,62,62	3.174 ns	65.1 ± 2.1	59 [3], (78,63,65) [7]
	36/30	64,70,68			
	31	65,66,64			
RGM-1	47/25	99,114,116	0.666 ns	105 ± 8	99 [7], 112 [3], 116 [4]
	63/19	104,101,104			
	19/18	114,94,102			
SCO-1	39/4	145,134,139	0.048 ns	140 ± 5	126 [3]
	46/23	137,141,143			
	53/29	142,135,144			
SDC-1	115/10	44,40,46	0.966 ns	42.3 ± 2.6	47 [7], 32 [3], 44 [4]
	76/13	40,40,42			
	120/28	46,40,43			
STM-1	57/14	77,80,80	2.567 ns	77.9 ± 2.7	78 [7], 80 [3], 91 [4]
	21/1	77,82,80			
	33/20	79,72,74			

REFERENCES

1 A. O. Brunfelt and E. Steinnes, Radiochem. Radioanal. Lett., 1 (1969) 219.
2 L. P. Greenland and R. Fones, N. Jb. Miner. Mh., 9 (1971) 393.
3 E. Steinnes, Geostandards Newsletter, 2 (1978) 13.
4 K. Govindaraju, J. Morel and N. L'homel, Geostandards Newsl., 1 (1977) 137.
5 R. R. Keays, R. Ganapathy, J. C. Laul, U. Krahenbuhl and J. Morgan, Anal. Chim. Acta, 72 (1974) 1.
6 V. Carmella-Crespi, U. Pisani, M. T. Ganzerli-Valentini, S. Meloni and V. Maxia, J. Radioanal. Chem., 4 (1970) 241.
7 E. G. Lillie, Anal. Chim. Acta, 71 (1975) 21.
8 G. A. Vall, M. V. Usol'tseva, I. G. Yudelevich, I. V. Seryakova and Yu. A. Zolotov, Zh. Anal. Khim., 31 (1976) 27.
9 I. V. Seryakova, G. A. Vorob'eva and Yu. A. Zolotov, Zh. Anal. Khim., 27 (1972) 1840.
10 G. A. Vorob'eva, Yu. A. Zolotov, L. A. Isosenkova, A. V. Karyakin, L. I. Pavlenko and O. M. Petrokhin, Zh. Anal. Khim., 29 (1974) 497.
11 N. V. Dvoryak and V. A. Pronin, Zh. Anal. Khim., 31 (1976) 179.
12 A. S. Bazhov and E. A. Sokolova, Zh. Anal. Khim., 32 (1977) 65.

Analytica Chimica Acta, 109 (1979) 177—179

Short Communication

SIMPLE BACKGROUND MONITORING DEVICE FOR ATOMIC ABSORPTION SPECTROMETRY

ROBERT F. M. HERBER* and JAN L. M. DE BOER**

Coronel Laboratory for Occupational and Environmental Hygiene, Faculty of Medicine, 1st Const. Huygensstraat 20, Amsterdam (The Netherlands)

(Received 2nd January 1979)

Summary. A cheap device which can be used to follow transient signals with a chart recorder is described.

Deuterium or hydrogen background correction is commonly used during the atomic absorption spectrometry of complex materials by electrothermal atomization. In most commercial apparatus, however, only one type of output can be obtained, the corrected signal or the background signal or the total signal. Maessen and Posma [1] showed that fast transient signals, such as those coming from volatile elements, cannot be followed by commercially available apparatus. They therefore used a lock-in-amplifier and waveform recorder instead of the commercial amplifier. Further, del Castilho and Herber [2] showed this combination to be a valuable tool for following the signals from corrected, background or analyte absorption. It was possible to obtain simultaneously digital or analog signals with medium time response (ca. 50 ms) and the corrected fast signal. The lock-in-amplifier and waveform recorder combination however, is rather expensive. This report describes an alternative, much cheaper, background monitoring device which can be used in conjunction with a chart recorder.

In Fig. 1, connections to the Varian AA6 CSB (BC6 correction) system for background monitoring are illustrated. The background signal can be taken from TP 52 and the corrected signal from TP 62. This allows the existing Varian system to present a total, background or corrected signal in digital (time constant $\approx$ 50 ms) or analog (time constant $\geqslant$ 300 ms) form, and permits the system described in this report (time constant 40 ms) to provide background or corrected information. These possibilities only apply to the Varian IM6D-BC6 system. For other background-corrected apparatus, the appropriate connections should be made. For apparatus without background correction, the monitor can be used to follow the analyte signal in a fast mode; connection should then be made directly after the photomultiplier—preamplifier output. Connection should always be made before any damping amplifier.

**Present address: Laboratory for Analytical Chemistry, Nieuwe Achtergracht 166, Amsterdam, The Netherlands.

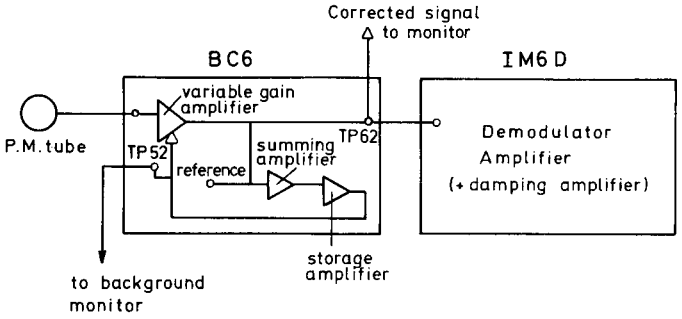

Fig. 1. Connection points for background or corrected signal monitor on existing Varian BC-6 system.

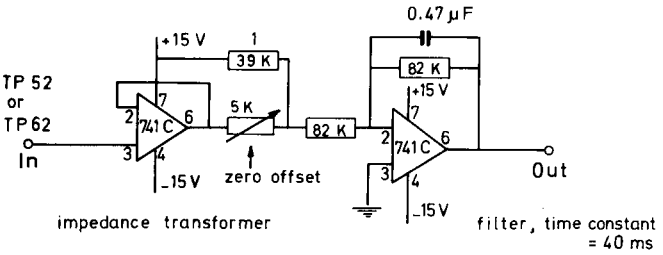

Fig. 2. Electronic circuit for background or corrected signal monitor.

Figure 2 shows the electronic circuit of the monitor. The impedance transformer lowers the high impedance of the photomultiplier and has an amplification of unity. The zero offset compensates any d.c. level. The low-pass filter has a time constant of 40 ms; the amplification is also unity. The time constant can be changed by varying the 0.47-µF capacitor and/or the 82-kΩ resistor. The monitoring system follows the background (or corrected) signal simultaneously with the digital (or analog) IM6D read-out, and so the signal can be reproduced on a fast chart recorder. This makes it possible to follow the separation between peaks, the ashing procedure and any manually controlled ashing/atomization steps on the chart paper. The system can be used to follow fast transient signals from volatile elements such as lead and cadmium, and enables them to be monitored in the corrected mode, and to follow the ashing/atomization steps in the background mode, while the commercial instrument is in the corrected mode.

Figure 3(a) shows a recorder trace obtained with the monitor in background mode for cadmium in whole blood [2]. The blood was diluted 5-fold with water and 5 µl of the diluted blood was injected into the furnace (Varian CRA 63). The atomization cycle used was 6.8 V for 4.2 s. Peak A is probably the organic matrix, while peak B is probably caused by inorganic salts. The cadmium peak appears between peaks A and B [2]. Changing the temperature setting causes a much greater change in the height of peak A than in peak B.

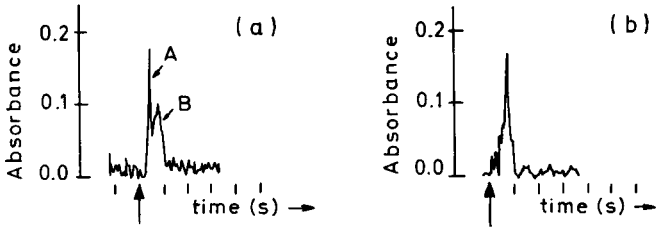

Fig. 3. Chart recorder tracings of (a) background monitor signal from cadmium in blood (for meaning of A and B, see text) and (b) corrected monitor signal from cadmium in blood. The arrows indicate the start of the atomization cycle.

TABLE 1

Effect of ashing voltage on determination of cadmium in blood

Voltage	Peak A A.U. ± s.d.[a]	Peak B A.U. ± s.d.[a]	Corrected Cd absorbance	C.V. (%)
0.58	180 ± 17	24 ± 1	0.072	6
0.62	53 ± 20	27 ± 3	0.079	10
0.67	6 ± 4	28 ± 4	0.089	9
0.70	1	7 ± 1	0.091	7
0.75	<1	10 ± 1	0.070	10

[a]Each result is the mean of 6 peak height measurements in arbitrary units (A.U.).

The monitoring device was used to find conditions for a good separation of analyte and matrix peaks and to find conditions for good precision with reasonable peak separation. The results obtained by using various ashing voltages are shown in Table 1. It shows that 0.70 V gives the highest corrected cadmium absorbance, with a 7% coefficient of variation. However, at higher voltage, there is a sharp decrease in the analyte signal, possibly because of loss of analyte [3]; thus the 0.70 V is a critical value, and it might be more reliable to use 0.67 V, with a 9% coefficient of variation and a peak A/peak B ratio of 0.2. In practice, this ratio is usually 0.5—2; too low an ashing voltage leads to a high peak A/peak B ratio which can lead to incorrect background correction [4]. Figure 3(b) shows a recorder trace of a cadmium signal from a blood sample (concentration 0.5 μg Cd l^{-1}, 5-fold diluted) monitored in the corrected mode, under the recommended conditions.

The authors are greatly indebted to H. J. Pieters for his technical assistance.

REFERENCES

1 F. J. M. J. Maessen and F. D. Posma, Anal. Chem., 46 (1974) 1439.
2 P. del Castilho and R. F. M. Herber, Anal. Chim. Acta, 94 (1977) 269.
3 C. W. Fuller, Anal. Chim. Acta, 62 (1972) 442.
4 P. Bailey and T. A. Kilroe-Smith, Anal. Chim. Acta, 77 (1975) 29.

Analytica Chimica Acta, 109 (1979) 181—185

Short Communication

CHEMICAL ANALYSIS OF MANGANESE NODULES
Part 5. Determination of Gallium after Anion-Exchange Separation

J. KORKISCH*, I. STEFFAN and JUNICHI NONAKA

Institute for Analytical Chemistry, University of Vienna, Währingerstrasse 38, A-1090 Vienna (Austria)

G. ARRHENIUS

University of California, Scripps Institution of Oceanography, Geological Research Division, La Jolla, California 92037 (U.S.A.)

(Received 9th March 1979)

Summary. A highly selective method is described for the determination of gallium at the ppm-level in manganese nodules and geological reference samples. After dissolution of the sample, gallium is adsorbed on Dowex 1 (chloride form) from hydrochloric acid solution containing titanium trichloride, which reduces iron(III) so that it is not adsorbed. After elution with dilute nitric acid and evaporation, gallium is determined by atomic-absorption spectrometry with an air—acetylene flame.

For the determination of gallium in geological samples such as ores [1] and limonite [2] by means of atomic-absorption spectrometry (a.a.s.), the gallium was first concentrated by solvent extraction from hydrochloric acid solutions in the presence of titanium trichloride to prevent the co-extraction of iron [3]. For measurement, the organic extracts, e.g. isopropyl ether [1] or methyl isobutyl ketone [2], were then aspirated into an air—acetylene flame.

Because gallium and iron(III) behave similarly towards anion- and cation-exchange resins in acidic media [3], techniques based on concentrating gallium by ion exchange have not been used in connection with the a.a.s. determination of gallium in geological samples. Such a method is described below.

Experimental

Solutions and reagents. A portion (2 g) of the strongly basic anion exchanger Dowex 1-X8 (Bio-Rad AG1-X8; 100—200 mesh; chloride form) was slurried with a few ml of 1 M hydrochloric acid; after ca. 30 min, the slurry was poured into an anion-exchange column of the usual dimensions [4] filled with the same acid.

Working standard solutions were prepared from aliquots of a stock solution (185.8 μg Ga ml^{-1}) by suitable dilution with 6 M hydrochloric acid. For the titanium trichloride solution a 15% solution of $TiCl_3$ in 10% hydrochloric acid (Merck Reagent) was diluted with an equal volume of 6 M hydrochloric acid.

Equipment. A Perkin-Elmer atomic-absorption spectrometer 303 was used

with a Hitachi Perkin-Elmer recorder and read-out accessory. The instrumental settings were as follows: 287.6 nm; slit 4 (1 mm; 0.7-nm bandpass); gallium hollow-cathode lamp at 20 mA; scale expansion up to 10; standard burner head; acetylene pressure 8 psi; air pressure 30 psi; noise suppression up to 4.

For 6 M hydrochloric acid solutions, the sensitivity is 3.05 ppm of gallium for 1% absorption.

Procedures. Dry the sample at 110°C for two days. Dissolve 1 g in a Teflon pressure vessel as described previously [5]. Dilute the final filtrate with 6 M hydrochloric acid to 50 ml (sample solution). To 20 ml of this sample solution (i.e., 0.4 g of the original sample) add sufficient titanium trichloride solution until the mixture becomes faintly violet, and then add a 10-ml excess of the reductant. Immediately afterwards pass the solution through the anion exchanger which has been pretreated successively with 50 ml of 6 M HCl, 10 ml of 4 M HCl and 10 ml of $TiCl_3$ solution) at a flow rate corresponding to the back-pressure (about 0.5 ml min^{-1}). Wash the resin with 25 ml of the titanium trichloride solution and 20 ml of 6 M hydrochloric acid. Finally elute the gallium with 50 ml of 2 M nitric acid.

Evaporate the gallium eluate on a steam bath, dissolve the residue in 10 ml of 6 M hydrochloric acid and evaporate to dryness again. Take up the residue in 10 ml of 6 M hydrochloric acid and aspirate the solution into the air—acetylene flame. Construct calibration curves by aspirating suitable standard solutions of gallium which have been taken through the entire procedure, before and after each batch of samples.

Results and discussion

Under the conditions employed above for the separation of gallium, a distribution coefficient of 200 was measured by the batch method [3]. As the hydrochloric acid concentration of the sorption solution always lies between 4.0 M and 6 M, very few elements will be co-adsorbed with gallium on the anion exchanger [3]. Examples are zinc and cadmium which are not only adsorbed along with gallium but are also eluted with 2 M nitric acid. However, these elements did not interfere with the a.a.s. determination of gallium.

Through the addition of an excess of titanium trichloride to the sample solution, iron(III) is reduced quantitatively to iron(II) which is not retained by the anion exchanger ($K_d < 1$) and passes into the effluent together with all other major and minor constituents of manganese nodules and other geological samples, e.g. Mn, Cu, Ni, Co, V, Al, Mg, Ca, Sr, Ba, Pb, Cr and the alkali metals. Consequently, this ion-exchange technique can be employed most effectively in place of the commonly used separation based on liquid—liquid extraction of gallium chloride with an ether or ketone and titanium trichloride as the reductant for iron(III) [3].

After adsorption of gallium as its anionic chloride complex, the resin bed is washed with titanium trichloride solution (see Procedure) to remove the last traces of iron; subsequent treatment of the exchanger with 6 M hydrochloric acid eliminates titanium from the resin bed before gallium is eluted with 2 M

nitric acid. The iron(III) reduction is essentially complete at hydrochloric acid concentrations in the range 4—6 M. At lower acidities, titanium(III) forms hydrolytic precipitates which interfere with the ion-exchange separation. At acidities higher than 6—7 M, the distribution coefficient of iron(II) increases to values for which quantitative separation of iron(II) from gallium on the anion exchanger is less readily achieved.

Table 1 gives the results obtained when the procedure was applied to the analysis of 10 samples of manganese nodules. Comparison of the results for gallium in columns A and B shows that direct a.a.s. gives results which are usually higher by more than an order of magnitude than those measured after anion-exchange separation. This was due to interferences in the a.a.s. measurements from iron and manganese as well as from minor constituents of the nodule samples such as copper, cobalt and nickel. All these elements enhanced the gallium absorption considerably so that reliable analyses of manganese nodule samples for gallium were impossible. After the anion-exchange separation of gallium, these interfering elements were virtually absent from the final eluate. Determinations of iron by a.a.s. in the gallium eluates give iron values which were never more than four times the gallium values; thus, essentially complete removal of iron was achieved by ion exchange. For example, when gallium was isolated from the Shafer 1 sample which contains 14% of iron (14×10^4 μg Fe g^{-1}) only 25 μg of iron was found in the entire 50-ml gallium eluate. Results very similar to those for iron were obtained when the gallium eluates were tested for other matrix elements. Known added amounts of gallium were recovered quantitatively in all cases (column B of Table 1).

The average gallium content of 16.3 ppm obtained in the 10 nodule samples tested (Table 1) is similar to the value of 0.001% found by other investigators [6] and is close to the crustal abundance of gallium (0.0015%). The

TABLE 1

Results for gallium in manganese nodules from the Pacific Ocean
[(A) Results obtained by direct a.a.s. of gallium in the 6 M HCl sample solutions. (B) Results obtained by the recommended procedure]

Sample	Gallium (ppm)		Sample	Gallium (ppm)	
	A	B[a]		A	B[a]
MR-33	169	17.7	V-18-270	207	13.7
MR-58	111	9.37 (9.02)	TRIPOD 3D	129	9.92 (9.51)
MR-61	108	6.25 (6.57)	TRIPOD 9D	123	22.0
MR-8	108	6.75 (6.62)	Shafer 1 (112 DK 20)[b]	123	7.40 (7.94)
MR-10	167	16.5	GRLD-108[c]	126	20.5

[a]The values in parentheses were obtained in parallel experiments after deduction of 9 μg of gallium which was added to the sorption solution as a spike before application of the recommended procedure.

[b]Metallgesellschaft AG, Frankfurt, West Germany.

[c]Kennecott Exploration, Inc., San Diego, California.

average gallium content for terrestrial rock standards (column B, Table 2) was 24.2 ppm, which is about 50% higher than that found for the nodule samples listed in Table 1. Consequently, in contrast to elements such as thallium, molybdenum and vanadium [7], manganese nodules apparently do not enrich gallium.

The results shown in Table 2 again indicate that direct a.a.s. determinations of gallium in the 6 M hydrochloric acid sample solutions give much higher gallium values than those obtained after application of the recommended procedure. Comparison of the results listed in columns B and C (Table 2) shows that in most cases there is reasonably good agreement between the present results and those obtained in other laboratories [8—10].

TABLE 2

Results of determinations of gallium in geochemical reference samples
[(A) Results obtained by direct a.a.s. of gallium in 6 M hydrochloric acid sample solutions. (B) Results obtained by application of the procedure. (C) Results obtained in other laboratories [8—10].]

Sample	Gallium (ppm)		
	A	B[a]	C[b]
Granite GA	87.9	15.4	8—35 (16)
Granite GH	85.9	19.9	13.5—50 (22)
Basalte BR	214	15.2	10—96 (20)
Biotite Mica-Fe	268	78.9	23—127 (95)
Phlogopite Mica-Mg	168	21.3	30 (30)
Diorite DR-N	142	21.4	18—35 (25)
Serpentine UB-N	123	6.7	<1; 3—18
Bauxite BX-N	226	53.9	68; 72; 115
Disthene DN-T	91.6	19.0	29; 30; 30
Granite GS-N	111	19.7	13—38
Feldspar FK-N	84.6	21.3	4—26
Glauconite GL-O	136	11.7	13—17
NIM-G (Granite)	74.9	24.4	27—36
NIM-S (Syenite)	87.7	18.3	10—12
NIM-L (Lujavrite)	153	49.5	51—60
NIM-N (Norite)	148	20.2	14—22
NIM-P (Pyroxenite)	129	8.3	7; <10; 11; 22
NIM-D (Dunite)	153	5.0	<2; <3; <10; 3
MRG-1	222	17.4	17—24 (18)
Syenite SY-2	167	34.2	24.6—40 (26)
Syenite SY-3	160	26.9	25.6—36 (28)

[a]Mean values from three separate experiments.
[b]The recommended average contents are given in parentheses.

This research was sponsored by the Fonds zur Förderung der wissenschaftlichen Forschung, Vienna, Austria. Samples were supplied by Lamont-Doherty Geological Observatory and M. B. Fisk at the Scripps Institution of Oceanography. Generous support from these sources is gratefully acknowledged.

REFERENCES

1 G. N. Lypka and A. Chow, Anal. Chim. Acta, 60 (1972) 65.
2 E. N. Pollock, At. Absorpt. Newsl., 10 (1971) 77.
3 J. Korkisch, Modern Methods for the Separation of Rarer Metal Ions, Pergamon Press, Oxford, 1969.
4 W. Koch and J. Korkisch, Mikrochim. Acta, (1972) 687.
5 J. Korkisch, I. Steffan, G. Arrhenius, M. Fisk and J. Frazer, Anal. Chim. Acta, 90 (1977) 151 (Part 2).
6 D. S. Cronan, in J. P. Riley and R. Chester (Eds.), Chemical Oceanography 2nd edn., Vol. 5, Academic Press, New York, 1976, p. 240.
7 J. Korkisch, I. Steffan and G. Arrhenius, Anal. Chim. Acta, 94 (1977) 237 (Part 3).
8 H. De La Roche and K. Govindaraju, Rev. GAMS, 4 (1971) 314.
9 B. G. Russell, R. G. Goudvis, G. Domel and J. Levin, NIM-Report No. 1351, 30th May 1972.
10 S. Abbey, Canada Centre for Mineral and Energy Technology, Report 76-36, November 1976.

Analytica Chimica Acta, 109 (1979) 187—190

Short Communication

AN ACCURATE SPECTROPHOTOMETRIC METHOD FOR DETERMINATION OF SMALL AMOUNTS OF WATER IN ACIDIC METHANOL

JEAN TOULLEC* and MOHIEDINE EL-ALAOUI (ex ALAYA)

Institut de Topologie et de Dynamique des Systèmes de l'Université Paris VII, Associé au C.N.R.S., 1, rue Guy de la Brosse, 75005 Paris (France)

(Received 14th March 1979)

Summary. The method is based on u.v. measurement of the keto—ketal equilibrium of substituted acetophenones; 4-methoxyacetophenone proved most satisfactory, the standard deviation for 67 ppm of water in hydrobromic acid-containing methanol being 3 ppm.

Many measurements (e.g., acidity constants, acidity functions, proton transfer rates, electrochemical measurements) in physical chemistry require accurate determinations of small amounts of water (usually in the 0—100 ppm range) in acidic methanol. Unfortunately, the classical Karl Fischer method is difficult to apply, mainly because of the very hygroscopic character of dry, acidic methanolic solutions which makes it difficult to avoid moisture contamination during the procedure. Other methods previously suggested for titration of water in organic solvents are either unsuitable or insufficiently accurate. For example, the Luke spectrophotometric method [1] is not valid for methanol, and the near-i.r. absorption method of Goulden and Manning [2] has a detection limit of only 10 mg l^{-1}.

The method proposed here is based on u.v. spectrometric measurement of the ketone/ketal ratio when a substituted acetophenone is added to acidic methanol:

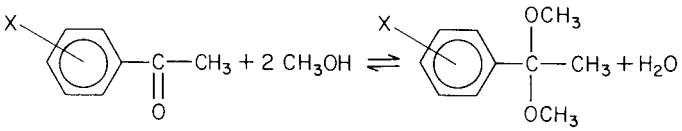

(1)

This keto—ketal equilibrium usually shifts towards the keto form so that only small water concentrations are needed to obtain a large proportion of ketal formation. The large molar absorptivities of ring-substituted acetophenones make it possible to carry out accurate spectrophotometric measurements in the u.v. range, even when small concentrations are used (ca. 10^{-5}—10^{-4} mol l^{-1}).

Ketone—ketal equilibrium constants (K) at 25°C were recently reported [3] for a series of substituted acetophenones; the constants were obtained by using a concentration jump method based on the amplitude measurement of the u.v. absorbance relaxation resulting from rapid addition of a small known

amount of water. Equilibrium constants were then deduced without direct titration of water. Some of these results, as well as the HBr concentrations needed to achieve full equilibrium after 5 min, are listed in Table 1.

Table 1 also lists the theoretical detection limits (calculated by assuming that a ratio [ketone]/[ketal] = 0.01 can be detected) which depend on the indicator. This shows that the most suitable substituted acetophenone to be used depends on the range of water concentrations to be titrated and on the acidity. Measurements of very low water concentrations are best done with 4-methoxyacetophenone.

Experimental

Apparatus. A Cary 16 spectrophotometer was used at the wavelength corresponding to the maximum absorption of the keto form (Table 1). One of the cells was thermostatted and closed by a soft well-fitting stopper made from silicone elastomer. The contents of this cell (2.5 ml) were stirred by a small Teflon-coated magnet rotated by a motor located beneath the cell-holder.

Reagents. Methanol (Baker Analyzed Reagent) was distilled in the presence of magnesium under nitrogen before use. Methanolic solutions of hydrobromic acid were prepared by bubbling hydrogen bromide (Baker Chemicals) and subsequent dilution. Commercial acetophenones were purified by gas chromatography, except for 4-methoxyacetophenone (m.p., 38—39°C) which was recrystallized in methanol. Bulk solutions of acetophenones in methanol were prepared by weighing and protected against moisture.

Procedure. The two cells were filled with sample solution containing hydrobromic acid in a dry-box and transferred to the spectrophotometer. After equilibration of the beams, and after a time lapse of 5 min to allow the temperature to stabilize, about 20 μl (carefully measured) of a methanolic solution (ca. 10^{-2} mol l^{-1}) of substituted acetophenone was injected into the thermostatted cell, through the stopper, from a microsyringe (Hamilton). Measurement of the absorbance when the system had equilibrated, usually gave the

TABLE 1

Spectrophotometric and equilibrium data relative to keto—ketal equilibrium for some substituted acetophenones ($XC_6H_4COCH_3$) used as water "indicators"

X	λ^a_{max} (nm)	ϵ (keto)[b] (l mol^{-1} cm^{-1})	ϵ (ketal)[b] (l mol^{-1} cm^{-1})	K^c ($\times 10^{-5}$ l mol^{-1})	$[H^+]_a$ ($\times 10^{-3}$ mol l^{-1})	TDL[e] (mg l^{-1})
4-OCH_3	271	16220	1480	0.361 ± 0.017	3	0.4
4-CH_3	252	14620	190	0.98 ± 0.06	5	1
H	241	12300	140	2.60 ± 0.12	8	3
3-Cl	240	10020	0	11.5 ± 0.2	40	12

[a] λ_{max} of $XC_6H_4COCH_3$. [b] Molar absorptivities of the keto and ketal forms at λ_{max}. [c] $K = [ketal]_{eq}[H_2O]/[CH_3OH]^2[ketone]_{eq}$; errors are standard deviations. [d] [HBr] concentrations needed to achieve full (99%) equilibrium after 5 min. [e] Theoretical detection limit for water calculated by assuming that a ratio [ketone]/[ketal] = 0.01 can be detected.

absorbance at equilibrium (A). However, a slow increase was sometimes observed (about 0.001 absorbance units per min), because of slight moisture contamination in the cell. Absorbance at equilibrium was then corrected by extrapolation to time zero, i.e. when the cells were taken out of the dry-box.

Results and discussion

A typical set of results obtained for a "dry" sample of methanol and a relatively small acid concentration is given in Table 2. The water concentration was deduced from the absorbance at equilibrium, A, by means of the equation

$$[H_2O] = K[CH_3OH]^2 (A - \epsilon_K [C]_0)/(\epsilon_C [C]_0 - A) \quad (2)$$

where ϵ_C and ϵ_K are the molar absorptivities of the ketone and ketal forms, respectively.

Since the equilibrium is

$$CH_3OH_2^+ + H_2O \underset{}{\overset{K_r}{\rightleftharpoons}} CH_3OH + H_3O^+ \quad (3)$$

it must be noted that the results usually correspond to the free water concentration and not to the overall water concentration (including $[H_3O^+]$ which is easily deduced from eqn. 4) which is obtained by the Karl Fischer method.

$$[H_3O^+] = [H^+]_a K_r [H_2O]/(K_r [H_2O] + [CH_3OH]) \quad (4)$$

Here, K_r (= 121) [4] is the equilibrium constant relative to eqn. 3, and $[H^+]_a$ is the overall acid concentration corresponding to complete dissociation. However, this correction is negligible for low acidities, e.g. for the results in Table 2.

The results in Table 2 indicate that the standard deviation is about 3 mg l^{-1} (which is similar to, or better than, that obtained by the Karl Fischer method for methanol) although the theoretical detection limit is lower. Similar results were obtained for more acidic and less dry solutions, and by using other indicators. Indeed, the standard deviations were always in the 2—10 mg l^{-1} range.

TABLE 2

Typical set of results obtained for spectrophotometric determination of water in a sample of "dry" methanol with 4-methoxyacetophenone in the presence of 2×10^{-3} mol l^{-1} HBr

$[C]_0$[a] ($\times 10^{-4}$ mol l^{-1})	A[b]	$[H_2O]$[c] (mg l^{-1})
0.854	0.9050	63.2
0.834	0.8882	64.1
0.930	1.0177	69.7
0.895	0.9797	69.8
0.945	1.0254	68.0
		Av. 67 ± 3[d]

[a]Overall ketone concentration. [b]Corrected absorbance at equilibrium (cf. experimental section). [c]Free water concentration, not including H_3O^+ concentration. [d]Standard deviation.

It should be emphasized that the scope of this method is not confined to acidic methanol but can easily be extended to neutral methanol. Preliminary results were obtained by following a slightly different experimental procedure (some μl of a concentrated hydrobromic acid solution were introduced into both cells after ketone injection). Standard deviations were in the 2—3 mg l^{-1} range for "dry" methanol containing 50 mg l^{-1} water.

When compared to the Karl Fischer method, the proposed method has some important advantages. First, it is easier to perform measurements under strictly dry conditions; secondly, the experimental procedure is simple and quick; finally, unstable reagents and prior calibration with a standard solution are unnecessary.

An interesting aspect of this method also lies in the possibility of measuring the water concentration in situ right after (or during) some other spectrophotometric measurement (e.g., rates of acid-catalyzed reactions, acid—base equilibria), if the reactants or products of the studied reaction do not interfere too much with one of the acetophenones in the u.v. spectrum. The method has recently been used extensively in this laboratory and has been very helpful in studying the kinetic behavior of acid-catalyzed processes in methanol. Provided that the equilibrium constants have been previously measured, this method could be extended to other alcohols.

REFERENCES

1 C. L. Luke, Anal. Chim. Acta, 54 (1971) 447.
2 J. D. S. Goulden and D. J. Manning, Analyst, 95 (1970) 308.
3 J. Toullec and M. Alaya, Tetrahedron Lett., (1978) 5207.
4 R. De Lisi, M. Goffredi and V. Turco Liveri, J. Chem. Soc. Faraday Trans. 1, (1978) 1096.

Analytica Chimica Acta, 109 (1979) 191—193

Short Communication

EXTRACTION SPECTROPHOTOMETRIC DETERMINATION OF ORGANIC BASES WITH SOME METALLOCHROMIC INDICATORS

MIROSLAV MALAT

Department of Analytical Chemistry, Charles University, 128 40 Prague 2 (Czechoslovakia)

(Received 1st March 1979)

Summary. Some metallochromic indicators are examined for ion-pair formation with alkaloids, cationic surfactants and some pharmaceutical products. Eriochrome red B is recommended for the determination of quinine at pH 3.6 with extraction into chloroform and measurement at 475 nm.

Many indicators have been applied in extraction spectrophotometric determinations of organic bases, but of the metallochromic indicators only eriochrome black T, plasmocorinth B [1] and solochrome green V150 [2] seem to have been examined. The present communication deals with other dye anions which form ion pairs extractable into organic solvents with organic base cations, and which offer new possibilities for extraction photometric determinations of organic bases. The dyes tested were acid alizarin black SN, SNADNS, SNAZOXS, zincon, PAR, murexide, thorin, calconalide I and II, pyrocatechol violet, pyrogallol and bromopyrogallol red. Some azo dyes and, in the group of triphenylmethane dyes, chromeazurol S are also suitable for the purpose. The recommended substances are listed in Table 1, where the wavelengths of maximum absorption are also given. Quininium chloride was used as the test substance.

All the indicators were checked to establish whether their anions form ion pairs with the quininium cation at a suitable pH and whether these ion pairs are extractable into chloroform, which was found to be the most suitable solvent; other solvents such as chlorobenzene, cyclohexanone, n-hexane, MIBK or iso-propyl ether are not suitable. The procedure always involved preparation of a solution containing 118 μg of quininium chloride, adjustment of its pH to 3.6 (1.4 or 6.8), addition of 2 ml of a 10^{-3} M indicator solution, dilution to 15—20 ml, and extraction with 10 ml of chloroform; the absorption spectrum of the extract was then measured from 400 to 700 nm.

The extractions were also tested at pH 1.4 (HCl—KCl) and 6.8 (sodium hydrogenmaleate—NaOH); at pH 1.4 there was no extraction with chromeazurol S, whereas at pH 6.8 the ion pair with eriochrome red B was not extracted. Extraction was impossible at pH 8.6 or in 1 M Na_2CO_3.

The absorbance values at the λ_{max} for solutions at pH 3.6 are also given in Table 1. The absorbances are higher at pH 1.4 (e.g., $A = 1.14$ for eriochrome red B), except for eriochrome black A, but are substantially lower at pH 6.8.

TABLE 1

Metallochromic indicators for the determination of organic bases at pH 3.6 with extraction into chloroform[a]

Indicator	Colour Index	λ_{max} (nm)			$A(\lambda_{max})^c$
		$[B^+]$ $[A^-]$	$[A^-]$	$[A^-]$ in H_2O	
Calcon	15 705	531 (506)[b]	—	510	1.09
Calmagite	—	488	—	530	0.52
Chromeazurol S	43 825	510	440	500	0.40
Eriochrome black A	15 710	527 (503)	—	510	1.08
Eriochrome blue black B	14 640	528 (510)	—	522	0.84
Eriochrome red B	18 760	475	—	455	0.85

[a] $[B^+]$ = base cation; $[A^-]$ = indicator anion; $[B^+]$ $[A^-]$ = ion pair. [b] The λ_{max} values in parentheses refer to a subsidiary maximum. [c] Absorbance of an extract containing 118 μg of quinine in 10 ml of chloroform.

The azo dye indicators alone are not extracted into chloroform, whereas chromeazurol S yields a lemon yellow extract at pH 3.6.

Other organic bases are also extracted as ion pairs with the six indicators: thus alkaloids such as papaverine and strychnine, cationic surfactants such as cetylpyridinium bromide and carbethoxypentadecyltrimethylammonium bromide (Septonex), and some pharmaceuticals such as tetracycline and 2-(1-naphthylmethyl)imidazolinium nitrate (Sanorin) can be extracted.

Eriochrome red B, which was further examined for the determination of quinine, reacts also with alkaloids, e.g. scopolamine, atropine, hyoscyamine, thebaine, brucine, morphine, cocaine, ephedrine, emetine, yohimbine and tubocurarine, with other cationic surfactants, e.g. zephiramine, cetyltrimethylammonium bromide, benzyldimethylhexadecylammonium chloride and dimethyllaurylbenzylammonium bromide, and with other pharmaceuticals e.g. Guanethidine Spofa, Benactyzine Spofa and Bromadryl F.

Determination of quininium chloride with eriochrome red B

The optimum pH for the ion-pair extraction was checked primarily for the determination of quininium chloride with eriochrome red B. The extraction was carried out in a hydrochloric acid (1.0, 0.5, 0.2 and 0.1 M), in a KCl—HCl mixture (pH 1.0—2.2) and in acetate (pH 3.6—5.6) and veronal buffers. The best results were obtained in an acetate buffer of pH 3.6. The amount of indicator was also varied; optimum results were obtained with 2 ml of a 10^{-3} M solution. It is best to carry out the extraction 5—10 min after mixing of the components and to measure the absorbance about 30 min after the extraction. The Lambert—Beer law is obeyed up to 1.18 μg of quininium chloride in 1.0 ml of chloroform, with a relative error not exceeding 4%.

Experimental

Apparatus and reagents. A Pye-Unicam SP 8-100 recording instrument and a Radiometer PHM 64 pH meter were used.

Prepare a 1×10^{-3} M solution of quininium chloride by dissolving 0.3969 g of the pharmaceutical-grade material in 1 l of redistilled water. Prepare a 1×10^{-3} M solution of eriochrome red B by dissolving 0.0424 g of the dye in 100 ml of redistilled water; 10^{-3} M solutions of the other indicators are prepared similarly.

An acetate buffer of pH 3.6 is used. Traces of oxidation products in the chloroform employed (p.a. purity) must be reduced by addition of about 5 g of hydroxylammonium sulphate in the presence of about 10 g of anhydrous sodium carbonate.

Procedure. To a solution in a separatory funnel containing up to 118 μg of quininium chloride, add 5 ml of the acetate buffer (pH 3.6) and 2 ml of 10^{-3} M eriochrome red B solution. Dilute with redistilled water to 20—25 ml and allow to stand for about 10 min. Extract for 1—2 min with 10 ml (accurately measured) of chloroform, and separate the organic layer. After 30 min, measure the absorbance at 475 nm against water or pure chloroform.

The procedure was applied to the determination of quinine in Chinascorbin Spofa pharmaceutical. Caffeine and ascorbic acid which were present in this preparation did not interfere.

Conclusions

The proposed metallochromic indicators meet the basic requirements for the extraction spectrophotometric determination of organic bases. The indicators themselves are mostly not extracted into chloroform, being protonated, and their anionic forms provide suitable extractable ion pairs with organic base cations.

The determination of quininium chloride with eriochrome red B was selected as an example; the application of the other indicators for the determination of other organic bases has also been studied, e.g. the determination of alkaloids with chromeazurol S [3], the determination of carbethoxypentadecyltrimethylammonium bromide (Septonex) and dimethyllaurylbenzylammonium bromide (Ajatin) [4], and the determination of some pharmaceutical products [5].

The author is grateful to Ms. Irén Šárová for technical assistance.

REFERENCES

1 B. Kakáč and Z. J. Vejdělek, Handbuch der photometrischen Analyse organischer Verbindungen, Verlag Chemie, Weinheim, 1974.
2 V. V. Rama Rao and S. N. Tandon; Fresenius Z. Anal. Chem., 286 (1977) 256; Chem. Anal. (Warsaw) 22 (1977) 965.
3 M. Ottis and M. Malát, unpublished results.
4 J. Jurkevičiúte and M. Malát, Cs. Farm., in press.
5 V. Berková, V. Suk and M. Malát, unpublished results.

Analytica Chimica Acta, 109 (1979) 195—197

Short Communication

INEXPENSIVE WET ASHING UNIT FOR ROUTINE TRACE ANALYSIS

M. OEHME

Department of Chemistry, University of Oslo, Box 1033, Blindern, Oslo 3 (Norway)

(Received 28th February 1979)

Summary. The unit consists of a specially designed aluminium block placed on a hot plate with a gas manifold and cover to prevent atmospheric contamination.

Sample pretreatment is usually necessary for the determination of trace elements such as heavy metals in different matrices. Digestion in Teflon-lined steel bombs, low-temperature ashing, and wet ashing with oxidizing acids are now the conventional techniques [1, 2]. The main advantage of wet ashing is its cheapness; only a simple heating block and a hot plate are needed. However, there are also some disadvantages. Large amounts of acids and chemicals are normally added to the sample, resulting in increased blank values. Furthermore, time-consuming operations involving long digestion times with repeated addition of reagants followed by heating to dryness are usually inevitable. When these operations are carried out in the laboratory atmosphere, there is an increased risk of contamination.

Many acids and chemicals are now available in ultrapure quality. The impurities are often considerably lower than the guaranteed maximum values, so that contamination of the sample by added chemicals may become unimportant compared to the contamination introduced through the handling of the sample. To reduce the latter type of contamination and to reach tolerable blank values even in routine wet ashing procedures, a simple and inexpensive wet digestion unit was constructed. The unit allows digestion of the sample under reflux, protects the sample against fall-out from the laboratory atmosphere, and facilitates accelerated heating to dryness by blowing an inert gas through the sample vessels. The unit has been used successfully for routine digestion of biological materials such as blood samples.

Experimental

Apparatus. The apparatus consists of an aluminium heating block, which is divided in two parts (see Fig. 1). It is provided with 4 or more holes for the sample containers and for the thermometer and is placed on a temperature-controlled hot plate. Observation slits in the side walls of the block facilitate control of the sample heating. The Pyrex sample vessels have a diameter of 15 mm, a height of 50 mm and a volume of 5 ml. To protect the samples from dust from the laboratory atmosphere, a manifold for passing nitrogen is placed

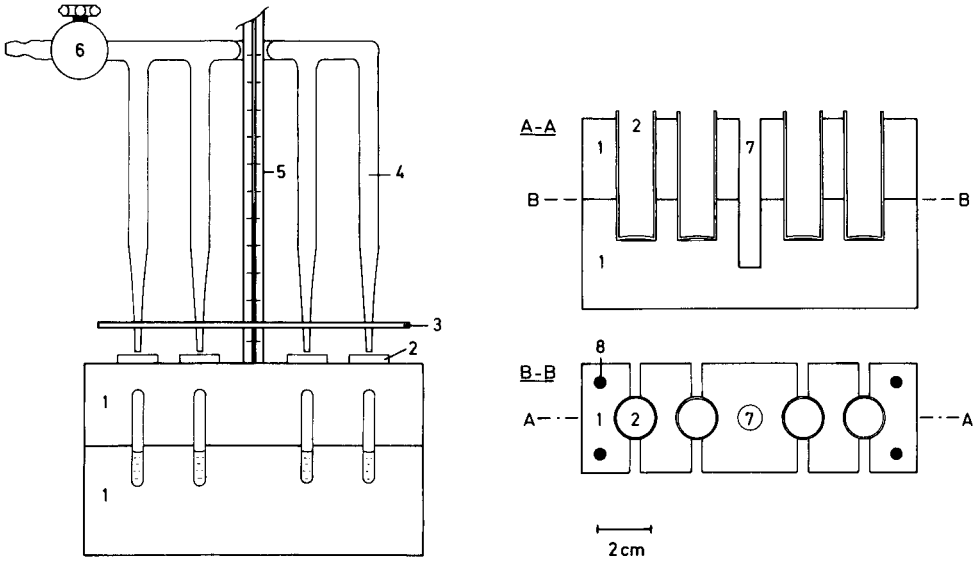

Fig. 1. Heating block and evaporation unit for wet ashing. (A-A) Longitudinal section of the heating block; (B-B) cross-section through the block. (1) Two-part aluminium heating block with observation slits; (2) Pyrex glass vessels; (3) Teflon plate for dust protection; (4) distribution unit made from Pyrex glass to blow highly purified nitrogen into the digestion vessels; (5) thermometer; (6) mounting of the evaporation unit; (7) hole for the thermometer; (8) pins for aligning the upper part of the block.

over the sample containers. This arrangement, which also serves to accelerate heating the sample to dryness after digestion, consists of a distribution unit with 4 Pyrex tubes and a Teflon plate which gives additional protection against dust particles (Fig. 1).

Procedure for wet digestion. Place the glass vessels with the sample and the digestion reagent in the lower part of the heating block on the hot plate. For the 5-ml vessels, the sample should not exceed 500 mg with the total solution volume of 1.5—2 ml. Mount the gas manifold above the openings of the vessels and pass a very small flow of highly purified nitrogen over the solutions. Then raise the temperature slowly and digest the sample at the desired temperature. This can be done under reflux-like conditions, since the upper part of the glass walls is not in contact with the heating block.

In the second step the remaining digestion reagents are evaporated and the sample is heated to dryness. For this purpose, place the upper segment of the heating block on the lower part and increase the nitrogen flow to accelerate the evaporation. Even sulphuric acid can be completely evaporated at 200°C in about 20 min in this way.

As an example, 0.4-ml blood samples can be digested completely with 0.85-ml aliquots of a mixture of HNO_3—$HClO_4$—H_2SO_4 (8 + 8 + 1) (Suprapur, Merck) at 200°C within 2 h. The samples are then heated to dryness, and each

residue is dissolved in 0.05 ml of concentrated hydrochloric acid (Suprapur, Merck) and 4 ml of water. The final solution can be analysed for trace metals for instance by means of differential pulse anodic stripping voltammetry; for details see [3, 4].

Results and discussion

Digestion in the unit described above gave considerably lower blank values (by about a factor of 4) than those obtained by using a heating block without any protection from the laboratory atmosphere. Typical blank values for the digestion of blood were $\leqslant$ 0.06 ppb for Cd and $\leqslant$ 0.4 ppb for Pb and Cu (cf. [5]).

It is also possible to use modified sample containers with a diameter of 20 mm directly as measuring cells for voltammetry (cf. [5]); this decreases the contamination risk further. No significant differences in blank values were found when quartz and Pyrex glass vessels were used. Increases in the blank values were not observed for Cd, Pb and Cu, when a high nitrogen flow was used over a period of 4 h.

The same principle can be used in the construction of heating blocks for larger quantities of samples.

This work was supported by a postdoctorate fellowship from the Norwegian Council for Scientific and Industrial Research. The author thanks Dr. W. Lund for valuable discussions and advice.

REFERENCES

1 R. Bock, Aufschußmethoden der anorganischen und organischen Chemie, Verlag Chemie, Weinheim, 1972.
2 O. G. Koch and G. A. Koch-Dedic, Handbuch der Spurenanalyse, 2. Aufl., Springer-, Verlag, Berlin, 1974.
3 M. Oehme, W. Lund and J. Jonsen, Anal. Chim. Acta, 100 (1978) 389.
4 M. Oehme and W. Lund, Fresenius Z. Anal. Chem., submitted.
5 J. Golimowski, P. Valenta, M. Stoeppler and H. W. Nürnberg, Fresenius Z. Anal. Chem., 290 (1978) 107.

Analytica Chimica Acta, 109 (1979) 199—203

Book Reviews

D. L. Massart, A. Dijkstra and L. Kaufman, *Evaluation and Optimization of Laboratory Methods and Analytical Procedures*, Elsevier, Amsterdam, 1978, xvi + 596 pp., price Dfl. 130.00, U.S. $57.75.

There are many excellent textbooks on statistical methods for the evaluation of analytical results. The problem of selecting the best procedure for solving a given analytical problem is, however, rarely discussed in depth. This book presents a survey of the various methods for evaluating the performance of an analytical method, and of strategies for selecting the optimal analytical procedure. In the first part, general concepts and methods for evaluating quantitative analytical methods are thoroughly discussed on a theoretical basis, with adequate emphasis on the various economic aspects. The second part is devoted to experimental optimization methods. The following section deals with combinatorial problems, including pattern recognition, cluster analysis, principal component analysis and related methods. In the last two sections, the requirements for analytical procedures are discussed, mainly in the context of process monitoring and control, and the systems approach to analytical chemistry is described.

The book includes some chapters on classical statistical methods and a series of mathematical sections where the topics are treated lucidly and are illustrated by many examples taken from chemical analysis. This saves the reader from having to consult specialized textbooks, where the subject is generally treated in a strictly formal manner. This, of course, sometimes results in duplication of material quite readily available elsewhere, but the lowering of the "activation energy" makes this worthwhile. The use of a coherent set of symbols throughout the book also helps to make the text easy to read.

Even though the price seems far too high, considering that it is a typescript reproduction, the book merits wide distribution in the analytical community. It would then help to move the selection of analytical procedures from today's mostly intuitive and empirical approach onto theoretically sound foundations.

J. T. Clerc

K. Venkataraman (Ed.), *The Analytical Chemistry of Synthetic Dyes*, J. Wiley, New York, 1977, xxiv + 591 pp., price £32.35.

In attempting to provide a comprehensive survey of the analytical techniques used in dyestuff chemistry, the editor and his associates have set themselves a difficult task. Their efforts have resulted in a useful reference volume, but the introductory chapter by Venkataraman is particularly disappointing. It fails to set the scene effectively for the other contributors and

does not provide a historical background to the evolution and importance of analysis in the dyestuffs industry, ancient and modern. The analytical classification of dyes, first by water solubility and then in terms of their use is sound enough but how much more useful this volume would be if the editor had persuaded the other contributors to use the same orderly approach in giving examples of the various techniques. The interrelated importance of chromatography and spectroscopy should have been emphasized at the outset and clearer reasons as to why some techniques are included and some excluded should have been given.

Chromatographic techniques are considered in Chapters 2—5. Elegantly simple but diagnostically powerful, thin-layer chromatography is perhaps rightly given pride of place as Chapter 2. This chapter is sound but, as its author admits, it is lacking in examples of disperse and reactive dyes, yet these classes perhaps command the greatest current research activity. Some details on the techniques and importance of quantitative t.l.c. are, however, a serious omission. The chapter on paper chromatography is excellent but redundant. The contribution on h.p.l.c. is good and comprehensive, although inevitably out of date because of its fashionable (and commercial) interest. The chapter on g.l.c. indicates its apparent lack of applicability to most dyes, but fails to emphasize its usefulness in rapid quantitative analysis for many intermediates used in dyestuff synthesis.

Spectroscopic methods are considered in the next five chapters. The first on visible "Solution Characteristics" is particularly readable and practical. The diagrams included give "colour" to the discussions, but a singular omission is one of log absorbance curves — a mode also forgotten by the u.v.-visible spectrophotometer manufacturers in their new microprocessor models. The possibilities of derivative-formation techniques are not discussed, nor is the Anlab colour space alternative to the CIE system considered. Although the other chapters on spectroscopic techniques are, in general, adequate, the chapter on x-rays is too long for a technique which is not always available, and the chapter on i.r. is too short for such a readily available technique in which further developments with computers and reflectance devices are being made.

The value of all these techniques is clearly brought out in the succeeding chapters on structure determination. These are good but all have individualistic approaches; a common, systematic, treatment would have been more illuminating.

There then follows an excellent chapter on the identification of dyes in textile fibres and a useful chapter on organic pigments. Chapters on food and hair dyes tend to be of specialized interest. The penultimate chapter, on Quantitative Analysis, is restricted to analysis for dyes on fibre. The volume concludes with a chapter on Ecological and Toxicological Monitoring and this contains a useful section on trace metal analysis.

In summary, this is a useful reference volume for all engaged in dyestuffs research, but only of limited value to those engaged in the production and use of dyestuffs. Although amply illustrated in some sections with figures, tables and structures, it contains no photographs. A few colour plates of some

thin layer chromatograms of a range of dyes and of the CIE chromaticity diagram would have enhanced the book enormously; after all, colour is an intrinsic dimension in all our lives.

G. H. Rettie

D. M. Hercules, G. M. Hieftje, L. R. Snyder and M. A. Evenson (Eds.), *Contemporary Topics in Analytical and Clinical Chemistry Vol. 2*, Plenum Press, New York, 1978, x + 286 pp., price $33.

Volume 2 of this series contains five articles: Wavelength Modulation Spectroscopy (28 pp.) by T. C. O'Haver; Apparatus and Methods for Laser Doppler Electrophoresis (26 pp.) by B. A. Smith and B. R. Ware; Detectors for Trace Organic Analysis by Liquid Chromatography, Principles and Applications (124 pp.) by P. T. Kissinger, L. J. Felice, D. J. Milner, C. R. Preddy and R. E. Shoup; Radioimmunoassay of Enzymes (21 pp.) by J. Landon, J. A. Carney and D. J. Langley; and Clinical Liquid Chromatography (80 pp.) by L. R. Snyder, B. L. Karger and R. W. Giese. Each article is informative and sufficiently detailed, and offers an up-to-date coverage of the field. It is a pleasant surprise to find 1978 references in a book published in the same year and, on the evidence of this volume, the editors are to be congratulated on producing a series of reviews which will be of considerable use to analytical chemists in clinical and other fields at this time.

Both radioimmunoassay and liquid chromatography have found increasingly significant applications in clinical analysis in the past few years, and the presentation of these three reviews in a single volume will contribute to the development and application of these techniques. The article on laser doppler electrophoresis is mainly concerned with principles and the design of experiments and apparatus. It will be useful to those workers who are already aware of the advantages and applications of the technique and wish to construct their own equipment. Those who wish to review the analytical possibilities of this technique will have to consult other recent reviews or references which are given. A review of wavelength modulation is also timely; the principle of this system has been known for many years but it is only now becoming increasingly used as a method of background correction in atomic emission, continuum-source atomic absorption and atomic fluorescence spectrometry and as a means of obtaining derivative spectra. O'Haver's article covers theory, experimental methods and applications in atomic and molecular spectroscopy and will be invaluable to many research groups and hopefully instrument manufacturers.

J. M. Ottaway

G. A. Webb (Ed.), *Annual Reports on N.M.R. Spectroscopy, Vol. 8*, Academic Press, London, 1978, x + 380 pp., price £28.00.

Volume 8 of Annual Reports contains four articles on diverse areas of n.m.r. spectroscopy. The opening report by T. A. Crabb updates a previous

review by the same author on the ^{1}H- and ^{13}C-n.m.r. of alkaloids, and covers the period 1972 until early 1977. The presentation is very clear, but this report is rather long and occupies about half of the book; considerable space might have been saved by reducing the size or number of the elaborate structural formulae. The second chapter by W. B. Smith on the ^{13}C-n.m.r. of steroids continues the natural products theme. Overlap with another recent review on the same topic has been minimized by concentrating on chemical shift reagents, substituent effects, stereochemistry and relaxation measurements. Previous tables of ^{13}C shifts in steroids are updated. The theory and practice of the analysis of exchange-modified bandshapes in dynamic n.m.r. spectra is considered by S. Szymanski, M. Witanowski and A. Gryff-Keller, who concentrate on the density matrix theory of bandshapes and on iterative least-squares procedures for deriving exchange rates. The final chapter by P. J. Smith and A. P. Tupciauskas is devoted to a survey of ^{119}Sn chemical shifts in organotin compounds from the first experimental measurement in 1960 until mid-1977.

All the reports are clearly presented and the reference lists are well up to date. This volume should be very useful for those working with alkaloids, steroids and organotin compounds. The report on exchange effects will be of some interest to n.m.r. specialists, but this subject has received considerable exposure in several other reviews. The price of this volume is rather high in comparison with Vol. 7, and it may be increasingly difficult for individual subscribers to continue collecting this useful series.

W. B. Jennings

L. Schriver, M. L. Jungfleisch and S. Tribalat. *Technétium et Rhénium. (Compléments au Nouveau Traité de Chimie Minérale, Vol. 10*, A. Pacault and G. Pannetier (Eds.)), Masson et Cie, Paris, 1978, 260 pp., price 220 FF.

The series of monographs, of which this is the tenth, is intended to replace an earlier treatise on inorganic chemistry, which appeared before the Second World War and which will eventually be completed when the programme of twenty books (30 volumes) has been published. Previously published monographs have dealt with ten elements (Rb, Cs, Pa, He, Mo, Sr, Se, Te, and Hg) and hydrogen peroxide and polyoxides of hydrogen. The necessity for monographs dealing with the less commonly used substances of inorganic chemistry is evident if ever one has the need to find up-to-date information. The literature is not necessarily large, but is exceedingly well dispersed.

This monograph deals with the chemistry of the two closely related elements, technetium and rhenium in two separate sections. Each section is sub-divided into two parts: one deals with the element, its properties, and the formation of alloys; the other deals with compounds of the elements. There is a separate section for each element dealing with the formation of organometallic compounds.

Although there are relatively few pages dealing with the separation and determination of these elements (10 pages and 18 pages, respectively), they

provide a useful starting point for anyone interested in the analytical chemistry of the two elements. The background of the chemistry provided by other sections of the book is extremely useful. Although there are only 4 or 5 pages dealing with the separation of technetium, formed either by the fission of uranium or the bombardment of molybdenum and occasionally ruthenium, the methods are well documented up to late 1976; there are over 120 references for these separation techniques alone. Whilst the determinations are not so extensively reviewed, the methods cover all those that are generally considered to be important. The actual presentation is not sufficiently critical and the reader must decide from the literature which method is appropriate for his own task, but there are sufficient references to enable one to do this with comparative ease.

The section dealing with rhenium is similar to that dealing with technetium although it is, of course, more extensive and covers a much wider range of methods. This monograph will form a useful addition to the literature of inorganic chemistry. It is not primarily concerned with analytical chemistry; indeed, the index lists only the names of the substances discussed and does not list any methods of identification or determination. The book will, however, be useful to analytical chemists; it is an excellent literature source and is to be recommended.

L. S. Bark

Analytica Chimica Acta, 109 (1979) 204—205

Federation of European Chemical Societies (FECS) — Working Party on Analytical Chemistry (WPAC)
European Analytical Column 2

As in 1978, when this European Analytical Column was first started in all major European broad-spectrum journals of analytical chemistry and outlets of the national member societies, the WPAC/FECS wants to inform the analytical community about recent activities.

In August 1978, the WPAC met twice during the Euroanalysis III conference in Dublin, Ireland. Prof. Dr. H. Malissa was reelected as chairman for a further period of 3 years. After the nomination of a Spanish representative, the WPAC now has 29 members representing 25 national societies in 19 European countries.

Euroanalysis III Conference (20—25 August, 1978, Dublin). This latest event in the series of European broad-spectrum Conferences on Analytical Chemistry was again very successful, and was attended by more than 700 delegates from 38 countries. The scientific programme consisted of 5 plenary, 11 keynote and 180 contributed papers and 150 posters. In addition, special sessions on Reference Materials and on Education in Analytical Chemistry were of great interest to the participants and provided an excellent survey over the respective fields in Europe. The contributions to the Special Session on Education will be published soon in Zeitschrift für Analytische Chemie; the plenary and the keynote lectures will appear as proceedings (edited by D. M. Carroll, Applied Science Publishers, London).

Discussons on the influence of recent copyright laws on the freedom and speed of publication are under way.

Euroanalysis IV (23—28 August, 1981, Helsinki). The next Euroanalysis Conference will again be organized on a wide subject basis, including the treatment of selected topics in special sessions. Topics such as "Information Extraction in Analytical Chemistry", "Analytical Chemistry, Legislation, Execution and Responsibility" are being considered, as well as a special joint session with IUPAC on "Harmonization of Collaborative Analytical Studies.

It was further decided to organize the *Euroanalysis V* Conference in 1984 in Krakow.

FECHEM-conference on Computer-Based Analytical Chemistry (COBAC). This 20th event of the FECS will be held in Pórtorož on 24—28 September, 1979, and is organized by Prof. Dr. D. Hadži, Ljubljana. This conference starts a new series that will pay particular attention to problems hitherto dispersed amongst various, more general meetings. The scope of the COBAC meetings is intended to be large and to include all aspects of computerization of analytical work, from mathematical and statistical fundamentals to practical solutions of analytical problems wherever computer-based philosophy and technology enter the scene.

FECHEM-conference on Education in Analytical Chemistry. This 21st event of the FECS will be held in Vienna on 10—12 December, 1979, and is organized by Prof. Dr. H. Malissa, Vienna, with the assistance of an international scientific committee. Based on the experiences of the Special Session in Dublin (1978) and the evaluation of the papers and posters discussed there, this conference will provide an unusual and important possibility of creating a new picture of education in modern analytical chemistry at university level. The main emphasis will be given to the scope and didactic aspects of computers in the teaching of analytical chemistry in plenary lectures and small group discussions.

Joint venture between WPAC and the Analytical Division of IUPAC. A joint study group was established in order to study possibilities for solving the problems connected with the increasing bulk of literature in analytical chemistry (e.g. by a symbolism language). The members are: Cserfalvi, Griepink, Kelker, Malissa, Simeonov (WPAC) Fresenius, Macdonald (Editors).

Feasibility of Standard Reference Materials (SRM). This discussion will continue. Experts in new fields of analytical chemistry are invited to present their opinions to Prof. Dr. R. Belcher, (Wolfson Clinical Chemistry Laboratories, The University, P.O. Box 363, Birmingham) who will act as a coordinator.

Colleagues who are interested in further details on any of the above topics are kindly requested to contact the Secretary of the WPAC:
Prof. Dr. R. Kellner, Institut für Analytische Chemie und Mikrochemie, Technische Universität Wien, Getreidemarkt 9, A-1060 Wien (Austria).

Analytica Chimica Acta, 109 (1979) 206—208

Announcements

International Winter Conference 1980 on Developments in Atomic Plasma Spectrochemical Analyses: Inductively Coupled, Microwave, and D.C. Plasma Discharges

An international conference featuring developments in atomic plasma spectrochemical analyses with inductively coupled, microwave, and d.c. plasma discharges will be held at the Hilton Condado Beach—La Concha Hotels and Convention Center in San Juan, Puerto Rico (U.S.A.) during January 7—11, 1980.

Papers describing original work on application, fundamentals, and instrumentation developments of atomic plasmas in spectrochemical analysis will be presented in general and invited symposia. Special application symposia organized and chaired by recognized experts will be held in topical areas. Other special symposia will feature recent developments in sample treatment and introduction; element-specific plasma detectors for chromatography, and new plasma generators, sources, and spectrometer systems.

A unique program has been arranged for manufacturers of atomic plasma spectrochemical instrumentation to present technical descriptions of their latest instrumentation developments, system design, and plasma system operation.

Plenary and invited lectures will be presented by S. Greenfield (England), P. W. J. M. Boumans (Netherlands), L. de Galan (Netherlands), R. L. Watters, Jr. (Washington), G. R. Kornblum (Netherlands), G. F. Kirkbright (England), K. Ohls (Germany), R. F. Browner (Atlanta), M. I. Boulos and R. M. Barnes (Sherbrooke/Amherst).

Authors of oral or poster papers for general and specialized symposia are requested to submit titles of their contributions and a 50—100 word preliminary abstract prior to July 1, 1979. Presentations will be minimally 15 minutes with 5 minutes of discussion, although longer times will be arranged on request. An extended abstract will be required by October 1, 1979.

Further information from: Winter Conference 1980, ICP Information Newsletter, Chemistry — GRC Tower I, University of Massachusetts, Amherst, Mass. 01003, U.S.A.

Fourth Australian National Conference and Schools on X-ray Analysis with Sessions on Surface Analysis

This conference will be held at the Australian National University, Canberra, A.C.T., on 4th—8th February, 1980, sponsored by the Australian X-ray Analytical Association. The following scientists will address the Conference and School Sessions: Dr. L. S. Birks (Washington, D.C.), Dr. K. Norrish (CSIRO Division of Soils, South Australia), Prof. N. C. Stephenson (NSW Institute of Technology).

Schools will be run in three concurrent groups for the first $2\frac{1}{2}$ days and will cover the theory and applications of x-ray fluorescence, x-ray diffraction, and surface analysis. A forum on computing techniques for x-ray analysts will lead into the conference sessions. Papers (20 min) and Posters to be presented at the conference sessions are now invited. A copy of the titles should be submitted to the AXAA Committee for consideration before 31st August 1979. Two copies of the detailed abstracts should reach the Conference Secretary no later than 30th November 1979. Further details from the Conference Secretary: Ms. D. Oliver, AXAA National Headquarters, c/— NSW Institute of Technology, P.O. Box 123, Broadway NSW 2007, Australia.

Third International Conference on the Organometallic and Coordination Chemistry of Germanium, Tin and Lead

The 2nd Conference was successfully conducted in Nottingham, England. The 3rd Conference will take place on July 21—25, 1980 in the Federal Republic of Germany at the University of Dortmund. The Conference will be prepared by an international committee in cooperation with Gesellschaft Deutscher Chemiker and under the sponsorship of the Federation of European Chemical Societies. The Conference will consider all aspects regarding organic compounds of germanium, tin and lead, including synthetic and mechanistic questions, spectroscopy, structural and coordination chemistry, technical applications and environmental problems. Further information from: Dr. W. Fritsche, GDCh-Geschäftsstelle, P.O. Box 90 04 40, D-6000 Frankfurt/M. 90, F.R.G.

8th International Microchemical Symposium

The Austrian Society of Microchemistry and Analytical Chemistry will organize the 8th International Microchemical Symposium in Graz on August 25th—30th, 1980. The aim of this symposium, to which about 600 participants from all over the world are expected, will be to deal with the most modern areas of microchemistry in theory, synthesis and analysis and intends to emphasize interdisciplinary relations between the different fields of chemistry, biochemistry, clinical chemistry, medical chemistry, pharmacy, physics and material sciences.

Further information from: Prof. Dr. A. Holasek, Institut für Medizinische Biochemie, Universität Graz, Harrachgasse 21, A-8010 Graz, Austria.

ISEC '80. International Solvent Extraction Conference

ISEC 80 will take place on 6—12th September, 1980 at the University of Liège on the new Sart-Tilman Campus. The University provides the convenience of modern conference rooms and of libraries in a woodland setting. The accommodation for delegates will be offered either on the Sart-Tilman Campus or in town. Liège is an historic city which will celebrate its 1000th anniversary in September 1980. It is situated 100 km east of Brussels and is within driving distance of the world famous Medieval cities of Bruges and Ghent.

The scientific programme will include invited plenary lectures and submitted research papers. Specialized papers will be presented in poster sessions in order to encourage direct contacts between those most interested. Poster sessions proved to be a real success at the ISEC conference in Toronto. A sightseeing tour is planned on Sunday, September 7th and technical tours to Belgian and near-by German plants and laboratories are planned on Wednesday, September 10th.

Further information from: Conference secreteriat, ISEC '80, Department of Chemistry, University of Liège, Sart-Tilman, B 4000, Liège, Belgium.

International Society of Electrochemistry

The 31st Meeting of the International Society of Electrochemistry will be held in Venice, Italy, on 22—26th September, 1980. Details from Prof. Enrico Vecchi, Secretary of the Organizing Committee, 31st Meeting of I.S.E., Coricerche-Lapelp, P.O. Box 1075, 35100 Padova, Italy.

(continued from outside of cover)

Naphthyldiazomethane as a derivatizing agent for the high-performance liquid chromatography of bile acids
D. P. Matthees (Washington, D.C., U.S.A.) and W. C. Purdy (Montreal, Quebec, Canada). . . 161
General dissolution procedure for the analysis of aluminium alloys by atomic absorption spectrometry
B. A. Milner, P. J. Whiteside and W. J. Price (Cambridge, Gt. Britain) 165
The determination of silver in silicate rocks by electrothermal atomic absorption spectrometry
P. J. Aruscavage and E. Y. Campbell (Reston, VI, U.S.A.) 171
Simple background monitoring device for atomic absorption spectrometry
R. F. M. Herber and J. L. M. de Boer (Amsterdam, The Netherlands) 177
Chemical analysis of manganese nodules. Part 5. Determination of gallium after anion-exchange separation
J. Korkisch, I. Steffan, J. Nonaka (Vienna, Austria) and G. Arrhenius (La Jolla, CA, U.S.A.) . 181
An accurate spectrophotometric method for determination of small amounts of water in acidic methanol
J. Toullec and M. El-Alaoui (Paris, France). 187
Extraction spectrophotometric determination of organic bases with some metallochromic indicators
M. Malát (Prague, Czechoslovakia) 191
Inexpensive wet ashing unit for routine trace analysis
M. Oehme (Oslo, Norway) 195

Book Reviews 199

Report: Federation of European Chemical Societies (FECS) – Working Party on Analytical Chemistry (WPAC) 204

Announcements 206

Printed in The Netherlands

VOL. 109 No. 1 ANALYTICA CHIMICA ACTA AUGUST 1, 1979

CONTENTS

Injection techniques in dynamic flow-through analysis with electroanalytical sensors
E. Pungor, Z. Fehér, G. Nagy, K. Tóth, G. Horvai and M. Gratzl (Budapest, Hungary) . . . 1
Potentiometric electrode measurement of serum antibodies based on the complement fixation test
P. D'Orazio and G. A. Rechnitz (Newark, DE, U.S.A.) 25
Amperometric determination of acetic acid with immobilized *Trichosporon brassicae*
M. Hikuma, T. Kubo, T. Yasuda (Kawasaki, Japan), I. Karube and S. Suzuki (Yokohama, Japan) 33
Microbioassay of nystatin with a yeast electrode
I. Karube, T. Matsunaga and S. Suzuki (Yokohama, Japan) 39
Isothermal distillation in flow injection analysis: determination of total nitrogen in plant material
E. A. G. Zagatto, B. F. Reis, H. Bergamin F° and F. J. Krug (Piracicaba, Brasil) 45
Biochemical cell for the determination of lactate
J. J. Kulys and G.-J. S. Švirmickas (Vilnius, U.S.S.R.) 55
Naphthyldiazoalkanes as derivatizing agents for the high-performance liquid chromatographic detection of fatty acids
D. P. Matthees (Washington, D.C., U.S.A.) and W.C. Purdy (Montreal, Quebec, Canada) . . . 61
Analytical applications of triethylenetetraminehexaacetic acid. Part 3. Amperometric determination of calcium in alkali metal salts
S. Rubel and M. Wojciechowski (Warsaw, Poland) 67
An injection method for the sequential determination of boron and several metals in waste-water samples by inductively-coupled plasma atomic emission spectrometry
J. A. C. Broekaert and F. Leis (Dortmund, W. Germany) 73
Multi-element analysis of geological samples by energy-dispersive x-ray fluorescence
P. Verbeke and F. Adams (Wilrijk, Belgium) 85
Signal depression in electrothermal atomic absorption spectrometry by nitrate and sulfate ions.
R. H. Eklund and J. A. Holcombe (Austin, TX, U.S.A.) 97
Spectrophotometric determination of trace amounts of silver(I) by formation of dicyanoargentate(I) and solvent extraction with methylene blue
T. Koh and M. Katoh (Kanagawa, Japan) 107
Spectrophotometric determination of boron in natural waters and rocks after specific adsorption on Sephadex gel
K. Yoshimura, R. Kariya and T. Tarutani (Fukuoka, Japan) 115
Extractive separation and spectrophotometric determination of osmium and ruthenium as thiocyanate complexes
Z. Marczenko and M. Balcerzak (Warsaw, Poland) 123
Determination of the acidity of petroleum bitumens by catalytic thermometric titrimetry
E. J. Greenhow and A. Nadjafi (London, Gt. Britain) 129
A search for losses of chromium and other trace elements during lyophilization of human liver tissue
J. J. M. de Goeij, K. J. Volkers and P. S. Tjioe (Delft, The Netherlands) 139

Short Communications

The ion-sensitive field effect transistor in rapid acid–base titrations
M. Bos, P. Bergveld and A. M. W. van Veen-Blaauw (Enschede, The Netherlands) 145
Potentiometric behaviour and surface composition of a prototype monohydrogenphosphate-selective electrode
A. C. Wilson and K. H. Pool (Pullman, WA, U.S.A.) 149
Determination of cobalt by anodic stripping voltammetry at a mercury film electrode
H. Bloom, B. N. Noller and D. E. Richardson (Hobart, Tasmania, Australia) 157

(continued on inside page of cover)